MODIFIED ROCK MASS RATING (M-RMR) SYSTEM

AND

ROOF BEHAVIOR MODEL

A THESIS SUBMITTED TO
THE GRADUATE SCHOOL OF NATURAL AND APPLIED SCIENCES
OF
THE MIDDLE EAST TECHNICAL UNIVERSITY

BY

İHSAN ÖZKAN

IN PARTIAL FULFILLMENT OF THE REQUIREMENTS FOR THE DEGREE OF

DOCTOR OF PHILOSOPHY

IN

MINING ENGINEERING

June, 1995

Approval of the Graduate School of Natural and Applied Sciences.

Prof.Dr. İsmail Tosun

Director

I certify that this thesis satisfies all the requirements as a thesis for the degree of Doctor of Philosopy.

Prof.Dr. A. Günhan Paşamehmetoğlu

Head of Department

This is to certify that we have read this thesis and that in our opinion it is fully adequate, in scope and quality, as a thesis for the degree of Doctor of Philosophy.

Assoc.Prof.Dr. Erdal Ünal

Supervisor

Examining Committee Members

Prof. Dr. A. Günhan Paşamehmetoğlu

Prof. Dr. Vedat Doyuran

Prof. Dr. Hasan Gerçek

Assoc. Prof. Dr. Reşat Ulusay

Assoc. Prof. Dr. Erdal Ünal

ABSTRACT

MODIFIED ROCK MASS RATING (M-RMR) SYSTEM

AND ROOF BEHAVIOR MODEL

ÖZKAN, İhsan

Ph.D., Department of Mining Engineering

Supervisor: Assoc.Prof.Dr. Erdal ÜNAL

June 1995, 370 pages

In this thesis, an extensive literature survey on rock mass classification systems and on behavior of mine roadways was carried out. Special attention was given to the most recent developments.

During studies carried out in a borax mine and two different coal mine regions, many difficulties were encountered in describing some of the joint related parameters, in determining the strength, and in evaluating the effect of groundwater. Therefore, a new classification system has been developed for weak, stratified and clay bearing rock mass. This classification system, called Modified Rock Mass Rating System (M-RMR System), is basically similar to Bieniawski's RMR System; however, it includes many modifications to prescribe real in situ conditions, and to accommodate new parameters for better characterization of the rock mass.

The rock masses in Bigadiç Underground Borax Mine, Çayırhan Underground Lignite Mine and Yatağan Surface Lignite Mine were classified based on the original and modified RMR systems and the results were compared. The impacts of the two different rating values (RMR and M-RMR) for the same rock mass was explained in terms of two engineering applications such as roadway support and slope stability. During classification studies, a computer program called "ROCK MASS" was also developed.

In order to investigate the roof behavior, a pilot study was carried out in a 300-meter section of the A-810 Gate-Road of Çayırhan Coal Mine. This gate road was divided into six support regions. Four of these sections were supported by rock bolts and the other two by rigid and yielding steel arches. Rock bolt types used consisted of Split-Set, Swellex, Sis-resin, and Fosroc-resin.

An extensive monitoring program was undertaken at A-810 gate road. A total of 18 convergence and 16 borehole extensometer stations were set-up in various supported regions.Consequently, a total of about 46,000 convergence and 110,000 borehole extensometer readings were taken during 15 months of monitoring period.

During stability analyses, time-dependent and face-advance dependent statistical analyses of convergence and roof strata movement were carried out. Based on further analyses of convergence, rate of convergence (velocity) and rate of convergence-velocity (acceleration), a roof behavior model was developed. The plots representing and comparing the behavior of different supported regions and the empirical equations developed were also presented.

Keywords: Rock mass classification, mine roadways, gate road, convergence, roof displacement, borehole extensometer readings, pull-out tests.

ÖZ

DÜZELTİLMİŞ RMR SINIFLAMA SİSTEMİ (M-RMR) VE TAVAN TABAKASI DAVRANIŞ MODELİ

ÖZKAN, İhsan
Doktora, Maden Mühendisliği Bölümü
Tez Yöneticisi: Doç.Dr. Erdal ÜNAL

Haziran 1995, 370 sayfa

Bu çalışmada, kaya kütlesi sınıflama sistemleri ve maden galerilerindeki tavan davranışının açıklanması üzerinde son yıllarda yapılan çalışmalar, geniş bir kaynak taraması ile belirlenmiştir.

Boraks ve iki farklı kömür ocağında yapılan kaya kütlesi sınıflama çalışmalarında; yeraltı suyunun etkisinin değerlendirilmesinde, sondajlardan elde edilen karotların dayanımlarının ve eklem takımlarına ait bazı parametrelerin belirlenmesinde çeşitli zorluklarla karşılaşılmıştır. Zayıf, tabakalı ve kil içeren kaya kütlelerinde karşılaşılan bu güçlükleri gidermek amacı ile yeni bir sınıflandırma sistemi geliştirilmiştir. Bu sınıflama sistemi (M-RMR) temelde orijinal RMR-Sistemi'ne benzemektedir. Ancak M-RMR sistemi, kaya kütlesinin daha iyi karakterize

edilmesinde kullanılan parametrelerin yeterli düzeydeki etkilerinin belirlenmesinde ve gerçek arazi koşullarının tanımlanmasında bir çok düzeltmeler ve yeni yaklaşımlar içermektedir.

Bigadiç yeraltı Boraks madeni, Çayırhan yeraltı linyit kömür madeni ve Yatağan açık kömür ocağında yapılan kaya kütlesi sınıflama çalışmalarında orijinal RMR sistemi ve M-RMR sistemi kullanılmıştır. Aynı kaya kütleleri üzerinde uygulanan bu iki sınıflama sisteminin mühendislik uygulamalarına yönelik etkileri, galerilerde tahkimat tasarımı ve açık ocakta şev duraylılığı analizleri ile açıklanmıştır. Bu çalışmaların sonucunda "ROCK MASS" adlı bir bilgisayar programı hazırlanmıştır.

Yeraltı maden galerilerinde tavan özelliklerini belirlemek amacıyla Çayırhan kömür ocağındaki A-810 taban yolunda yaklaşık 300 metrelik bir kesimde, altı ayrı tahkimat bölgesi oluşturulmuştur. Bu bölgelerden dört tanesi farklı kaya saplamaları ile, diğer iki tanesi de rijit ve kaymalı demir bağlar ile desteklenmiştir. Bu pilot uygulamada Split-Set, Uzayabilen Süper Swellex, Sis-reçineli ve Fosroc reçineli kaya saplamaları kullanılmıştır.

Bu pilot uygulama için A-810 galerisinde, ayrıntılı bir çalışma programı uygulanmıştır. Pilot uygulama esnasında değişik tahkimatlı bölgelerde 18 adet konverjans ve 16 adet delikiçi esktansometre istasyonu kurulmuştur. Sonuç olarak, yaklaşık 15 ay boyunca süren ölçümlerden 46,000 adet konverjans ve 110,000 adet delikiçi ekstansometre ölçüm değeri alınmıştır.

A-810 galerisindeki konverjans ve delikiçi esktansometre ölçümleri üzerindeki stabilite analizleri esnasında zamana ve galeri ilerlemesine bağlı istatistiksel analizler gerçekleştirilmiştir. Konverjans analizleri haricinde, konverjansın birim zamandaki değişimi (konverjans hızı) ile konverjans hızının yine birim zaman

içerisindeki değişiminin (konverjans ivmesi) analizleri ayrıca yapılmıştır. A-810 galerisinde oluşturulan farklı tahkimat bölgelerine ait konverjans grafikleri ile karşılaştırmalı analizler tamamlanmıştır. Ayrıca bu ölçüm sonuçlarını karakterize edecek ampirik bir eşitlik geliştirilmiştir.

Anahtar Kelimeler: Kaya kütlesi sınıflaması, maden galerileri, tavan-taban yolları, konverjans, tavan tabaka hareketleri, delikiçi ekstansometre ölçümleri, kaya saplamalarının yerinde çekme testleri.

ACKNOWLEDGEMENTS

I would like to express my appreciation to Assoc. Prof. Dr. Erdal Ünal for his kind supervision, valuable suggestions, discussions and friendship throughout this study.

I wish to express my gratitude to Prof. Dr. Hasan Gerçek for his guidance and valuable contributions.

Particular thanks are extended to examining committee members for serving on the Ph. D. Thesis committee.

I also wish to express my thanks to the research assistants Dr. Reha Özel, Taylan Bozdağ, gradute student Güray Çakmakçı from Middle East Technical University and Bülent Erdem from Cumhuriyet University for their help during different stages of this thesis.

This study is partially supported by Etibank, Turkish Coal Enterprises (TKİ), Technical Research Council of Turkey (TÜBİTAK). The support from the Project and Planning Department of TKİ Headquarters and assistance from management, engineers and workers of the Middle Anatolian Lignite Mines (OAL) are gratefully acknowledged.

Special thanks are also given to the research assistant Kemal M. Ergür who kindly provided help in all technical matters and typed patiently this thesis within a short period of time.

Finally, I wish to thank my wife Meltem Özkan and my son Onur Can Özkan for their understanding and patience throughout this study.

TABLE OF CONTENTS

APPENDIX

LIST OF TABLES

LIST OF FIGURES

CHAPTER I

INTRODUCTION

Roof falls in underground mines continue to be a major problem in terms of a safety factor and economy. Today vast majority of the fatalities occurring in underground mines are due to roof falls. Although loss of production due to strata control problems is very difficult to estimate, it is undoubtedly significant. Estimation of roof control costs for new areas is another major problem. Therefore, economics and safety demand the realization of mining conditions prior to and during any mining activity. This obviously requires more price assessment, particularly determination of rock mass conditions and proper design of underground mine openings excavated in these rock mass conditions.

Increasing depths and steeply dipping seams necessitate better ground control methods and in particular better prediction of unstable roof conditions. Unexpected changes in roof conditions are often encountered in underground mines. Intensive studies of the roof falls indicate that they can often be attributed to one, or a combination of the following parameters: i) lithology of the roof strata, ii) characteristics of discontinuities (bedding planes, joints, faults, etc.), iii) humidity, iv) ground water inflow, v) in-situ stresses, vi) stress relief due to surface erosion and stream channel, and vii) geological irregularities (clay, veins, fossils, concretions, etc).

Therefore, stability of underground mine openings can be best assessed by a through study of these parameters, and by classification of the rock mass.

1.1 Statement of the Problem

In underground mining today, safety and economical aspects demand a better understanding of the mining conditions, particularly for design of underground mine openings excavated in rock mass. The rock mass classification systems, in essence, are empirical approaches utilized during preliminary design stage. These systems have been developed for specific purposes and rock mass types, therefore, direct utilization of the rock mass classification systems, in their original form, for characterization of complex rock mass conditions is not always possible. For example, the most widely used rock mass classification systems, namely those proposed by Bieniawski (1973, 1979, 1984, 1989) and Barton et al. (1974) can not fully describe the specifications of weak, stratified and clay bearing rock masses. Thus, the engineering applications that would be carried out based on original RMR and Q ratings could be misleading in making design decision even during the preliminary design stage.

Although the rock mass classification systems have been used successfully in rock tunneling and hard-rock mining for many years, direct utilization of those systems for the purpose of roof stability assessment in weak and stratified rock masses is very rare. Consequently, there is a need for better characterization and classification of weak, stratified and clay bearing rock masses, and predict the behavior of roadways and/or tunnels driven in such grounds.

1.2 Scope of the Thesis

The main objectives of the present study are the followings:

i) to develop a Modified Rock Mass Rating (M-RMR) System, for better characterization of weak, stratified, and clay bearing rock mass. This is required for meaningful characterization of difficult rock mass conditions encountered in the field and for making better design decisions;

ii) to develop a computer program for evaluating classification input data and for obtaining classification logs. This is required for increasing the efficiency of classification process, for simplifying the long and tedious data processing work, and for saving time;

iii) to develop an empirical model for characterization of strata behavior in mine roadways. This is required for predicting the stability of unsupported or supported underground openings.

1.3 Outline of the Thesis

In order to meet the objectives stated in Section 1.2, a review of the literature associated with methods of mine roof stability assessment was conducted in Chapter II. The results of original classification system based on the rock units in three mining regions were presented in Chapter III. In Chapter IV, the difficulties encountered in determining the input parameters considered in RMR System were discussed. In addition, suggestions were given for modification of these parameters for better characterization of weak, stratified and clay bearing rock mass. "ROCK MASS" computer program based on M-RMR System was presented in Chapter V. Design analyses and pilot studies for A-810 gate road of Çayırhan Lignite Mine were

given in Chapter VI in detail. In Chapter VII, the results of statistical analyses based on the in situ convergence measurements, also, the results of the rate of convergence and rate of convergence-velocity were presented. In order to determine the mine roof behavior, a mathematical model which relies on time, face advance, Modified Rock Mass Rating, roof span, depth, support system stiffness and its installation time were developed by statistical analyses and the results of various parametric analyses on this model are evaluated. These studies were presented in Chapter VIII. Finally, the main conclusions associated with this study and the recommendations for future work were included in Chapter IX.

CHAPTER II

LITERATURE REVIEW

2.1 General

In this Chapter, a critical review of two main subjects, namely the rock mass classification systems and the roof behavior in mine roadways, has been presented based on an extensive review of the literature. The emphasis is given to the recent developments directly related to the topics of this thesis. In order to update the reader on these subjects, a detailed review is also given in Appendix A, included at the end of this thesis.

2.2 Discussions on the Current Status of Rock Mass Classification Systems

During review of the literature, twenty three classification systems were found in major basic books, conferences and symposia. In this section, the important input and output parameters for rock mass classification systems are briefly discussed, and secondly the approaches describing the rock mass behavior around tunnels are presented in tabulated and graphical form.

2.2.1 The Input Parameters of Rock Mass Classification Systems

The input parameters used in twenty three classification systems are given in Sections A.2.1 and A.2.2. These input parameters have been utilized in order to characterize the rock mass. Some of the parameters such as uniaxial compressive strength (UCS), RQD, joint spacing, groundwater, etc. have been considered by majority of the researchers. However, the parameters such as overburden thickness, height of roadway, cohesion, and support factor are not used in every system. Table 2.1 presents the input parameters used in each system.

The major input parameters based on rock mass classification systems as shown in Figure 2.1, are the uniaxial compressive strength or point load index, RQD, joint spacing (JS), fracture density (λ), weathering (W), roughness (R), aperture (A), persistence (C), filling thickness and its strength, groundwater (GW), orientation of discontinuities (O), weathering effect (WE), stress effect (SE), and span (B).

Figure 2.2 shows that the major input parameters used in RMR (Beniawski, 1979), MRMR (Laubscher, 1977), MBR (Cummings et al., 1982), RMS (Stille et al., 1982), Simplified RMR (Brook and Dharmaratne, 1985), RMR (Newman and Beniawski, 1985), CMRR (Molinda and Mark, 1993), Modified RMR (Sheorey, 1993), and Modified Q (Sheorey, 1993) Systems. Excluding the Modified Q system, the other classification systems could be considered as the extension of the original RMR system (Beniawski, 1993). In RMR system of Newman and Bieniawski (1985) suggests modifications for weathering effect and stress effect. The weathering effect in the R system of Venkateswarlu (1986) was determined by the slake durability test.

Table 2.1 Rock Mass Classification Systems and the associated input parameters

ROCK MASS CLASSIFICATION SYSTEM	FIELD DATA			EFFECT OF ROCK MASS PROPERTIES CONSIDERED IN DETAIL																		EFFECTS OF GW		EFFECTS OF ORIENTATION	EFFECTS OF WEATHERING		EFFECTS OF METHOD OF EXCAVATION		EFFECTS OF STRESS		EFFECTS SUPPORT
				EFFECT OF MECHANICAL PROPERTIES					EFFECT OF GEOLOGICAL PROPERTIES																							
									RELATIVE EFFECT		ABSOLUTE EFFECT																					
	B (m)	H (m)	Z (m)	RELATIVE EFFECT	σ_c (MPa)	PLT (MPa)	FRICTION OF	BIENIAWSKI HAMMER	STRUCTURE OF DISCONT.	JC	RQD %	JS mm	$\frac{\lambda}{m}$ mm	BS mm	JC W	JC R	JC A	JC C	JC F	JC CH		RELATIVE	ABSOLUTE		RELATIVE EFFECT	ABSOLUTE EFFECT	RELATIVE T M B	RELATIVE BLASTING	RELATIVE	ABSOLUTE	
ROCK LOAD *TERZAGHI, 1946*	✓																														
STAND-UP TIME LAUFFER, 1958	✓																														
NATM PACHER, ET AL., 1964	✓																														
RQD DEERE ET. AL., 1967											✓																				
RSR WICKHAM ET AL., 1972				✓					✓	✓		✓											✓	✓							
RMR - LAST MODIFIED RMR BIENIAWSKI, 1979					✓	✓			✓		✓	✓			✓	✓	✓	✓	✓				✓	✓				✓	✓		
Q BARTON ET AL., 1974					✓						✓		✓			✓	✓						✓						✓		
STRENG SIZE *FRANKLIN, 1975*					✓	✓	✓					✓																	✓		
BASIC GEOTECHNICAL DESCRIPTION - ISRM, 1981					✓	✓	✓					✓																			
MRMR LAUBSCHER, 1977					✓				✓		✓	✓				✓	✓		✓				✓	✓	✓			✓	✓		
MBR CUMMINGS ET AL., 1982					✓				✓		✓	✓			✓	✓	✓		✓				✓	✓				✓	✓		
RMS STILLE ET AL., 1982					✓	✓					✓	✓			✓	✓	✓	✓	✓				✓	✓							
SIMPLIFIED RMR BROOK AND DHARMARATNE, 1985					✓							✓				✓	✓	✓	✓			✓		✓	✓			✓	✓		
MODIFIED RMR NEWMAN AND BIENIAWSKI, 1985					✓						✓	✓			✓	✓	✓	✓	✓				✓	✓		✓			✓		
R VANKATESWARLU, 1986					✓							✓		✓									✓			✓			✓	✓	✓
BRZ DONG ET AL., 1988	✓		✓																							✓					
RTR INYANG, 1991		✓							✓			✓	✓									✓		✓							
SGDM MILNE AND POTVIN, 1992											✓		✓			✓	✓														
GC MENDES, 1993												✓					✓	✓	✓												
CMRR MOLINDA AND MARK, 1993								✓	✓			✓				✓	✓			✓	✓	✓		✓							
MODIFIED RMR SHEOREY, 1993					✓	✓					✓	✓			✓	✓	✓	✓	✓				✓	✓					✓		
LAST MODIFIED Q SHEOREY, 1991, 1993									✓		✓		✓			✓	✓						✓	✓					✓		
RFI SING ET AL., 1994									✓																						

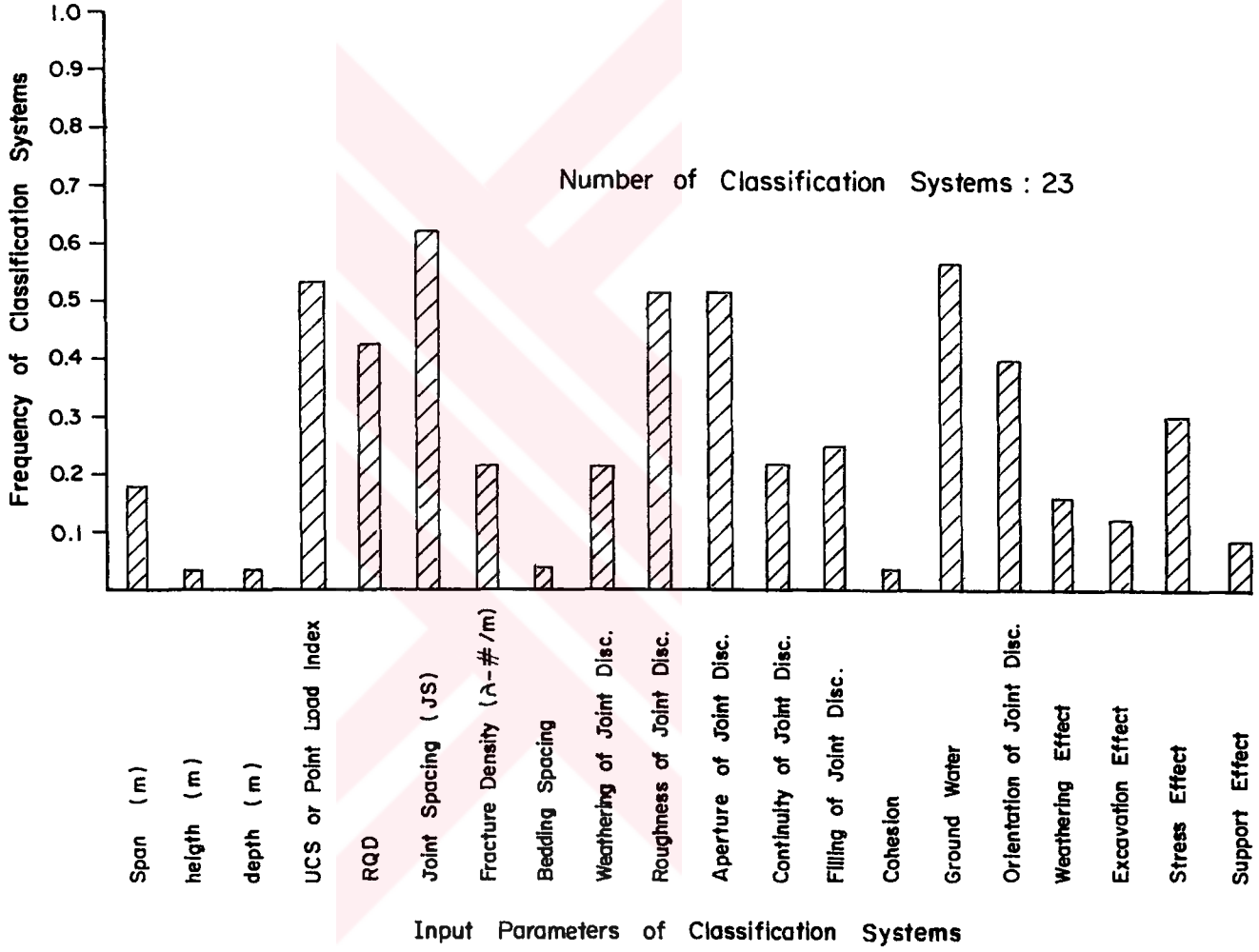

Figure 2.1 The frequency of used classifications versus input parameters of classification systems

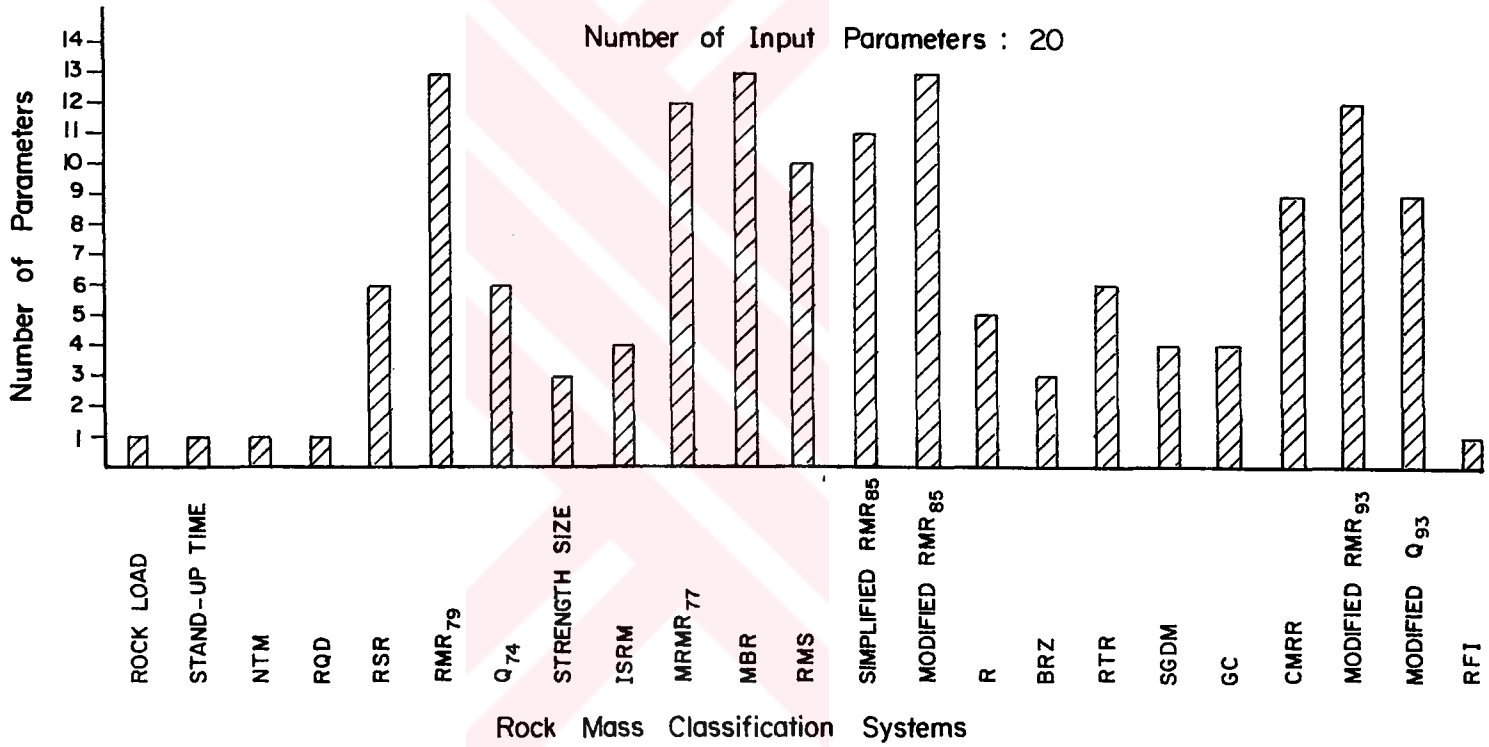

Figure 2.2 The number of parameters versus rock mass classification systems

2.2.2 The Outputs for Rock Mass Characterization of Rock Mass Classification Systems

Design oriented outputs of the classification systems are evaluated in Table 2.2. It includes information associated with the prediction of rock mass characteristics, rock mass behavior, and support requirements. The information associated with these predictions can be made in tabulated form or given by an equation. The RMR and Q systems provide 12 and 9 output parameters respectively.

An interesting graph presented in Figure 2.3 shows that the major output parameters given by the classification systems are friction angle, rock mass strength, stand-up time, unsupported span, support pressure, and support recommendations. Nevertheless, all of the outputs shown in abscissas, in Figure 2.3, are very important for rock mass characterization and support design. The most of these outputs are given by various RMR and Q systems (see Figure 2.4). However, the support recommendations are not adequately provided in most of these classification systems.

2.3 Discussion on Approaches Describing Rock Mass Behavior in and around Mine Roadways and Tunnels

Ladanyi (1974), Wilson (1980), Hoek and Brown (1980, 1988) and Brown et al. (1983) have developed theoretical design criteria, with a closed-form solutions, to calculate the radius of a fracture zone, the state of stresses, and tunnel closure. A comparative study of these theoretical solutions with in-situ measurement has been given by Whittaker et al. (1983). It has been shown that all closed-form solutions underestimate the tunnel closure.

Table 2.2 Design outputs based on rock mass classification systems

ROCK-MASS CLASSIFICATION SYSTEMS	PREDICTION OF ROCK-MASS CHARACTERISTIC		PREDICTION OF ROCK-MASS BEHAVIOR		PREDICTION OF SUPPORT REQUIREMENTS	
	BRIEFLY INFORMATION (WITH A CHART OR TABLE)	DETAILED INFORMATION (WITH A EQUATION)	BRIEFLY INFORMATION (WITH A CHART OR TABLE)	DETAILED INFORMATION (WITH A EQUATION)	BRIEFLY SUGGESTIONS (WITH A CHART OR TABLE)	DETAILED DESIGN (WITHS VARIOUS EQUATIONS)
ROCK LOAD TERZAGHI, 1946				1. ROCK LOAD HEIGTH 2. VERTICAL AND HORIZONTAL SUPPORT PRESSURE	3. TABLE	
STAND-UP TIME LAUFFER, 1958			1. STAND-UP TIME-TABLE		2. TABLE	
NATM PACHER ET. AL., 1964			1. STAND-UP TIME-TABLE		2. TABLE	
RQD DEERE ET. AL., 1967					1. TABLE	
RSR WICKHAM ET. AL., 1972					1. CHART	
RMR-LAST MODIFIED RMR BIENIAWSKI, 1979	1. COHESION-TABLE 2. FRICTION ANGLE-TABLE 3. ROCK MASS STRENGTH-TABLE	4. MODULUS OF ELASTICITY OF RMR 5. M,S CONSTANT VALUE 6. PRINCIPLE STRESS	7. STAND-UP TIME-CHART 8. MAX. UNSUPPORTED SPAN-CHART	9. ROCK LOAD HEIGTH SUPPORT PRESSURE 10. UNSUPPORTED OR SUPPORTED ROOF DEFORMATION	II. TABLE AND CHART	
Q BARTON ET. AL., 1974	1. M,S CONSTANT VALUE-CHART 2. FRICTION ANGLE-TABLE	3. BLOCK SIZE 5. ACTIVE STRESS 4. INTER BLOCK SHEAR	6. MAX. UNSUPPORTED SPAN-CHART	7. SUPPORT PRESSURE	8. CHART	9. BOLT LENGTH
STRENGTH-SIZE FRANKLIN, 1975	1. BLOCK SIZE-CHART				2. CHART	
BASIC GEOMECHANICS DESCRIPTION-ISRM, 1981						
MRMR LAUBSCHER, 1977		1. ROCK MASS STRENGTH 2. DESIGN ROCK MASS STRENGTH			3. TABLE	
MBR CUMMINGS ET. AL., 1982					1. CHART	
RMS STILLE ET. AL., 1982	1. ROCK MASS STRENGTH-TABLE 2. FRICTION ANGLE-TABLE 3. COHESION-TABLE					
SIMPLIFIED RMR BROOK AND DHARMARATNE, 1985					1. TABLE	
MODIFIED RMR NEWMAN AND BIENIAWSKI, 1985						
R VANKATESWARLU, 1986				1. SUPPORT PRESSURE		
BRZ DONG ET. AL., 1988				1. ROCK LOAD HEIGTH	2. TABLE	
RTR INYANG, 1991		1. ROCK MASS STRENGTH	2. SUITABILITY FOR TRENING TABLE			
SGOM MILNE AND POTVIN, 1992					1. CHART	
GC MENDES, 1993					1. TABLE	
CMRR MOLINDA AND MARK, 1993						
MODIFIED-RMR SHEOREY, 1993				1. SUPPORT PRESSURE		
LAST MODIFIED Q SHEOREY, 1993				1. SUPPORT		
RFI SING ET. AL,, 1994					1. TABLE	

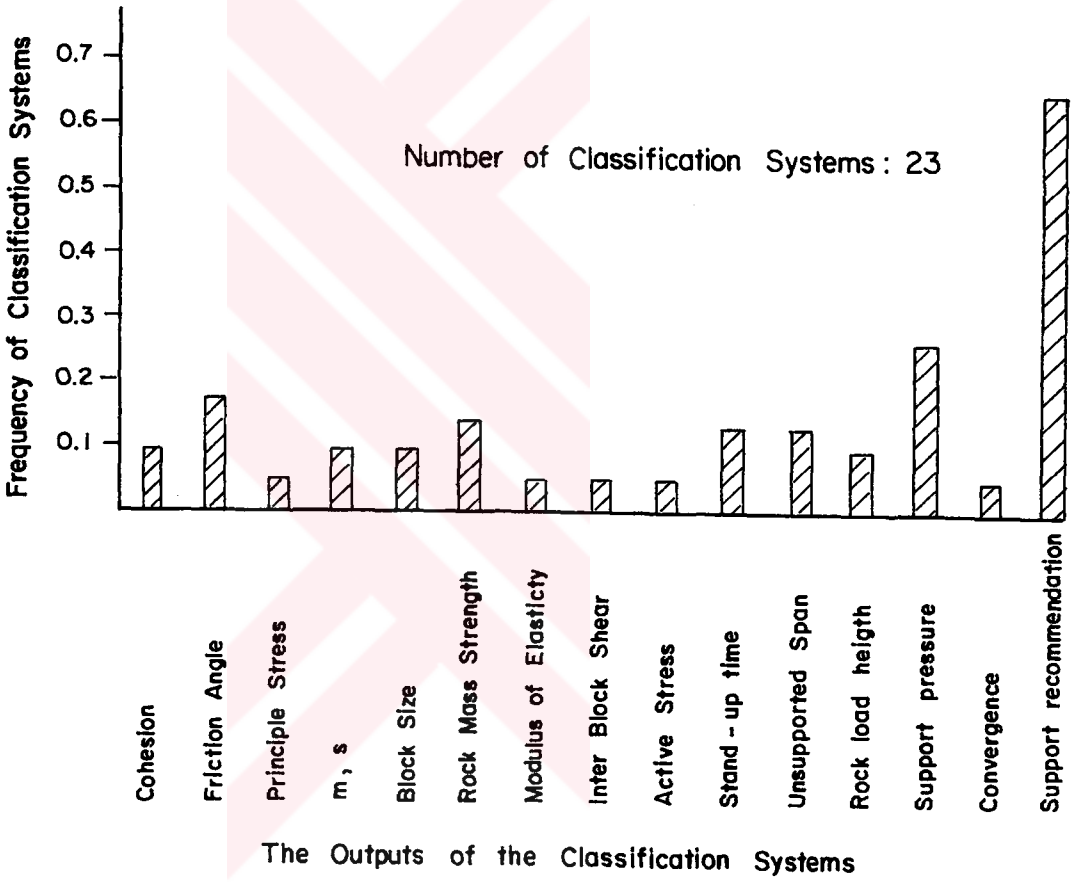

Figure 2.3 The frequency of classification systems versus the outputs of the classification systems

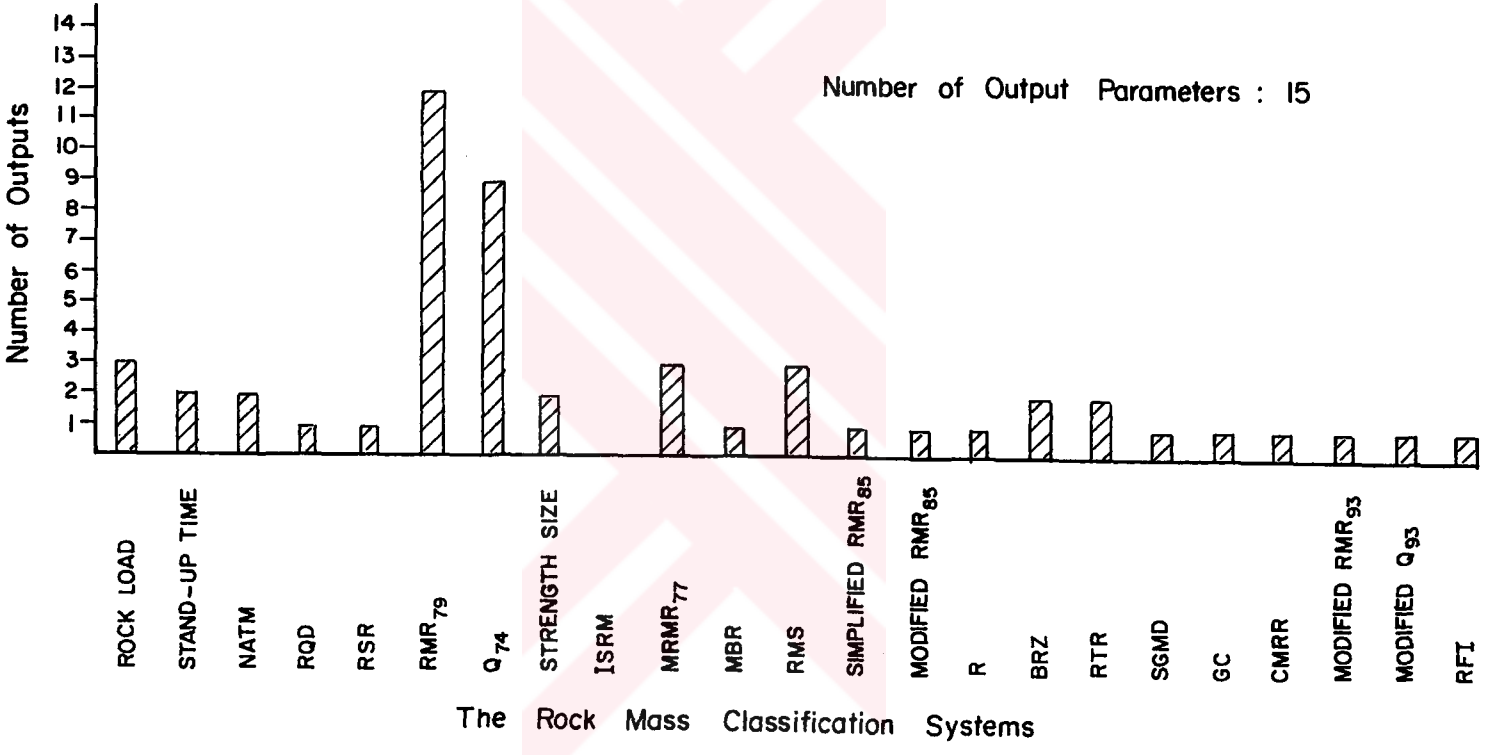

Figure 2.4 The number of outputs versus the rock mass classification systems

The most creep tests carried out on various rocks in laboratory scale have been evaluated by the rheological models (e.g. Dusseault and Fordham, 1993; Filcek and Kwasniewski, 1993) and the best fit curve to data points (e.g. Griggs, 1939, 1940; Parsons and Hedley, 1966; Hobbs, 1970; Amadei and Curran, 1980). However, experimental evidence shows that even very large samples are rarely representative of the full scale behavior of the rock mass around a tunnel (Ladanyi, 1993). This conclusion was also confirmed by Panet (1993).

In situ creep tests have also been evaluated by rheological models. The most serious disadvantages of in-situ creep testing are given by Dusseault and Fordham (1993). Despite the disadvantages, development of a large mine or civil engineering structure susceptible to creep requires in-situ tests, perhaps extended for several years into the construction phase.

The empirical approach proposed by Schwartz (in Tincelin, 1978), Panet (1979), Tallon (1982), Ünal (1983), Guenot et al. (1985), Wells and Singh (1985), Majdi et al. (1986), Sulem et al. (1987a), and Can (1987) provides plots of convergence as a function of distance from face and/or time. Recently, an empirical approach developed by Ghosh and Ghose (1992). It is interesting to note that this approach is not based on time and/or distance from face.

Ünal's empirical Integrated Approach (1983) considers rock mass index (i.e. in RMR system), excavation span (B), support reinforcement factor (RF), stand-up time, rock load height (h_t), rock density (γ) and time as input parameters, and provide total convergence and roof pressure as an output. Ghosh and Ghose's empirical approach (1992) considers the excavation span (B), rock density (γ), and rock mass properties (i.e. R-system)as an input and provides total convergence and roof pressure as output.

Majdi and Hassani (1989) made a series of analytical analyses considering Majdi et al.'s (1986) empirical function and Panet's empirical function (1993). In this approach, the effect of longwall extraction and in-situ structural defects were considered. In addition, a number of other approaches have been developed, such as by Pan and Dong (1991a, 1991b) who included analytical solutions based on rheological models and Sulem et al.'s (1987a, 1987b) empirical function.

Panet (1993) carried out studies on the rheological model and the empirical functions, and expressed the convergence as a function of time and distance from face.

Stresses and displacements developing in the rock mass due to excavation of tunnels depend on the rock mass properties, in situ initial stress field, stiffness of the lining or support and time of its installation (Panet, 1993). In addition, the size of the opening and time dependent stress redistribution were also mentioned by Ladanyi (1993).

In summary, tunnel deformation and rock pressure can be expressed as a function of the rock mass properties (i.e. RMR, Q etc.), the effect of depth (Z) or in situ stress (σ), the size effect of excavation (B), the rock load height (h_t), the type of excavation (E), the support stiffness (k), and its installation time (t), unit weight (γ), time (T) and face advance rate (X) as shown in Equation 2.1 and 2.2.

$$U = f(RMR, \sigma, B, E, \gamma, T, X) \tag{2.1}$$

$$P = f(RMR, \sigma, B, E, h_t, \gamma, k, t) \tag{2.2}$$

In this study, convergence in mine roadways is expressed as shown in Equation 2.3.

$$U = f(M - RMR, B, Z, k, t, T, X) \tag{2.3}$$

Details related to this function is given in Chapter VII and VIII.

CHAPTER III

ROCK MASS CLASSIFICATION STUDIES CARRIED OUT IN A BORAX MINE AND TWO COAL MINE REGIONS AND DIFFICULTIES ENCOUNTERED DURING THESE STUDIES

3.1 General

The input information needed for design purposes generally includes geological characterization of the rock masses, evaluation of the virgin ground stresses and the mechanical properties which characterize the rock mass in its natural state. Whatever procedures and techniques are employed to obtain input parameters, it is necessary to emphasize that any such procedures and techniques should only be used if they can be fully justified for the purposes of a given project. In other words, measurements and investigations should be carefully planned and matched with the purpose of a project, full justification being given for any investigations and tests performed. Furthermore, determination of the input parameters for design should be so planned that as much quantitative data as possible is obtained rather than relying on qualitative descriptions.

In essence, the following three important messages emerge (Rafia, 1980):

1. The eventual quality of engineering design is directly proportional to the quality of the input parameters.

2. Any procedures or methods employed in providing the input data should be fully justified and carefully planned.

3. Quantitative rather than qualitative information is required for design purposes.

The determination of the input data for design involving geological site characterization, ground stress conditions, ground water conditions and mechanical properties of rock masses are best considered by the original, modified and emerging rock mass classification systems (see Appendix A.2). In addition, most of the outputs for design are given by again these classification systems.

In this chapter, rock mass classification studies carried out, based on RMR and Q systems, in a borax mine and two coal mine regions are briefly described. The emphasis is given to the difficulties encountered during characterization of weak, stratified and clay-bearing rock masses and the ratings associated with input parameters utilized.

The studies described in this chapter had constituted a base for the development of a Modified RMR system (M-RMR) for weak, stratified and clay bearing rock mass.

3.2 Earlier Studies and Development of the Modified RMR System

3.2.1 General

The information presented in this section are based on evaluation of considerable amount of data obtained during four years of geotechnical investigations carried out in a borax mine and two coal mine regions in Turkey.

During classification process, carried out based on RMR and Q systems, serious difficulties were encountered in determining or describing some of the rock mass parameters such as compressive strength, effect of water, and condition and orientation of discontinuities.

3.2.2 Studies at Bigadiç Borax Mine

A considerable amount of rock mechanics studies and strata control investigations were carried out at Bigadiç Borax Mine located in the north-west of Turkey (Paşamehmetoğlu et al., 1988; Özel, 1988; Gökay, 1988; Özkan, 1989; and Paşamehmetoğlu et al., 1989).

The borax ore, consisting of ulexite and colemanite, and the surrounding strata were weak in nature, and contained clay which often existed in the form of bands and beds of varying thickness. The presence of water accelerated the strata control problems associated with clay-bearing strata.

The average seam inclination was 20°. In general, there were four borax seams with average thicknesses ranging between 3 - 8 meters. The strata between the borax seams generally consisted of laminated and bedded limestone with continuous beds and bands of consolidated clay, and their thicknesses ranging between 2 and 9 meters. Depth of the underground workings from the surface was between 100 - 150 meters. Seams were extracted by retreat longwall mining or retreat longwall mining with sublevel caving, and the four seams were fully extracted successively with no pillars left behind the upper level. In locations where the ore seams were closer to the surface, they were extracted by the surface mining methods.

The ore and rock units encountered in the borax mine region were classified based on RMR and Q Systems, considering both the original and modified input parameters and their intervals. A total of 830-meter long cores, obtained from five surface and two underground boreholes, were evaluated for classification purposes. A considerable number of difficulties were encountered in describing the stratified and clay-bearing formations during the classification process.

In order to characterize the rock material encountered in the borax mine region, a considerable number of laboratory tests were carried out on specimens representing different formations and ore zones. In performing these tests, the methods suggested by ISRM were followed. The results of the standard (ISRM) rock mechanics laboratory tests, relying on total of 1766 specimens, were utilized in this work. The main rock types encountered at Bigadiç borax mine are shown in Table 3.1.

Table 3.1 The main rock types at Borax mine region

Rock type cod no	**The names of rock types**
10a	Colemanite
10b	Ulexite
8	Limestone
4/8	Limestone alternating with claystone
5/8	Limestone with clay laminea
9a	Weathered limestone with claystone
9c	Highly weathered limestone
7	Tuffite
11	Tuff
12	Upper tuff
6a	Siltstone
13b	Claystone
14	Marl

On the other hand, the cores obtained from five surface and two underground boreholes were evaluated for rock mass classification purpose. The first step in the classification was to divide the rock mass into a number of structural regions. In most cases, and for borehole evaluations, each type of formation was considered as a new structural region in which the type of rock material and the nature of discontinuities were more or less uniform. In addition, any distinct zones (i.e. those containing clay, heavily fractured, or highly weathered) within each formation were treated as a new structural region. It was also assumed that the boundaries of structural regions also coincide with such major geological features as faults and shear zones.

Once the structural regions have been delineated, the ratings for input parameters were determined and the associated information was filled in the geotechnical and joint condition borehole log forms. A typical empty log form is given in Figure 3.1.

As a second step, RMR and Q values were determined for each structural region, within each borehole, based on original RMR (Bieniawski, 1989) and Q (Barton et al., 1974) systems. After that, the common structural regions were combined by taking the weighted average of the classification ratings (RMR and Q values). Finally, all of the boreholes were combined systematically within a single borehole - log representing the region. The results are listed in Table 3.2.

3.2.3 Studies at Çayırhan Lignite Mine

In Çayırhan lignite mine, a series of rock mechanics studies were carried out by METU, Mining Engineering Department (Ünal et al., 1994). These studies included the following:

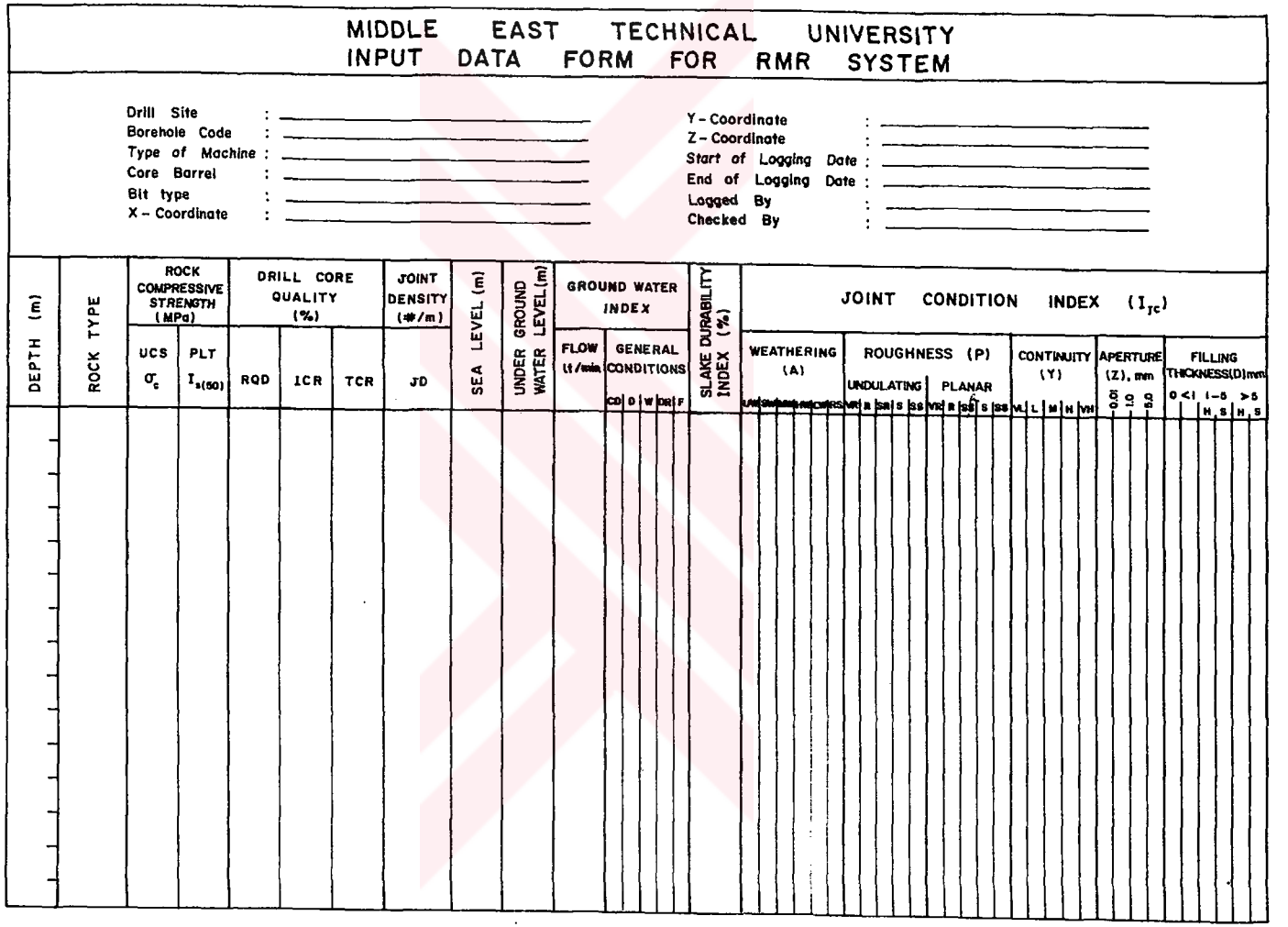

Figure 3.1 A typical log form for geological input data

Table 3.2 Summary of rock mass classification results obtained in Simav mine region (RMR, Q and RQD rating values represent the weighted average of ratings obtained from 9 boreholes) (after Özkan, 1989)

Rock Type Code	Thickness (m)	Original RMR		Original Q		RQD		Description of the Rock Units
Layer - 1	5.60	30		0.840		23		Alterated limestone interbedded with claystone and tuff
Layer - 2	1.90	24		0.233		2		Limestone laminated with claystone and repeated limestone
Layer - 3	0.90	28		0.374		10		Limestone interbedded with claystone and tuff
1st Seam	3.80	32		0.725		24		COLEMANITE
Layer - 4	3.45	24	16-46	0.213	0.15 0.98	7	0-39	Limestone alterated with claystone and tuff
Layer - 5			12-32		0.42 0.51		0-16	Limestone laminated with claystone and interbedded with tuff
Layer - 6			12-32		0.02 0.31		0-11	Limestone laminated with claystone and random colemanite
2nd Seam	5.60	33		1.097		24		COLEMANITE
Layer - 7	4.10	23	19-40	0.471	0.096 0.482	12	0-41	Limestone laminated with claystone and random colemanite
Layer - 8			13-40		0.016 0.202		0-36	Limestone interbedded and laminated claystone
Layer - 9			18-33		0.018 0.317		0-17	Claystone and limestone interbedded with tuff
3rd Seam	7.30	29		0.325		11		COLEMANITE
Layer - 10	5.00	28	13-24	0.341	0.013 0.457	16	0-18	Limestone laminated with claystone and randomly interbedded limestone and claystone
Layer - 11			13-30		0.015 0.450		0-17	Limestone laminated with claystone
Layer - 12			13-40		0.045 0.603		0-30	Limestone interbedded with hard claystone
4. Seam	5.00	31		0.978		22		ULEXITE
Layer - 13	4.37	30	18-44	0.692	0.032 1.390	29	0-75	Limestone laminated with claystone
Layer - 14			11-54		0.003 1.910	29	0-43	Claystone interbedded limestone

Table 3.2 (continued)

Rock Type Code	Thickness (m)	Original RMR	Original Q	RQD	Description of the Rock Units
5. Seam	3.20	35	0.267	8	COLEMANITE
Layer - 15	9.65	37	0.963	29	Tuff, limestone interbedded with claystone, limestone laminated with claystone
Intermediate Tuff	1.00	56	20.33	74	Intermediate tuff
Layer - 16	5.45	42	1.20	48	Tuff and alterated limestone interbedded with claystone
Upper Tuff	2.80	57	21.54	65	Upper tuff

i) identification of geological units,

ii) underground drilling studies,

iii) investigation of laboratory tests,

iv) classification of rock masses.

Drilling Investigations

In order to identify the geological structure of the roof rock, to determine the quality and characteristics of rock mass, and to obtain specimens for laboratory tests, necessary for rock mass classification process, a total of nine underground boreholes were drilled in A-510 gateroad and two borehole in A-810 gateroad. The boreholes were named as KM 510-1 through KM 510-7, and KM 810-1 and KM 810-2.

All of these boreholes were drilled perpendicular to the roof strata. The length of each borehole was about 10 meters. The rock layers were identified, by a naked eye, based on structural and color differences observed. The main rock layers identified at the roof are shown in Table 3.3.

Laboratory Tests

The specimens for laboratory tests were prepared by utilizing the cores obtained from various drill-holes. The specimens were prepared in the Rock Mechanics Laboratory of the Mining Engineering Department at METU, in accordance with the standards suggested by the International Society of Rock Mechanics, ISRM (1979, 1981). A total of 985 specimens were tested in the laboratory and utilized in this work.

Table 3.3 The main rock types at Çayırhan lignite mine

Rock type code no	The names of rock types
A0	Coal alternating with marl
A1	Fine grained sandstone alternating with siltstone
A2	Limestone with claystone laminea
A3	Siltstone alternating with clay and sandy claystone
A4	Limestone with claystone laminea
A5	Limestone with irregular thick claystone
A5-1	Thin limestone alternating with claystone
B	Limestone with claystone laminea
C1	Marl
C2	Marl alternating with gray clay
D	Marl
E	Marl with claystone
F	Claystone
G	Claystone with siltstone
H	Sandstone

Rock Mass Classification

Before the initiation of rock mass classification studies, the photographs of core boxes were taken as permanent records.

For better characterization of rock masses and easier communication, the rock units (layers) encountered in Çayırhan Mine were divided into three main groups based on their: (i) physical appearance, (ii) types, and (iii) condition as to whether they contain clay or incorporate other type of rocks in the same formation.

After determining the boundaries of structural regions and their thicknesses, the core boxes were prepared for investigations and logging. After this stage, the core logging process was completed for each borehole. A typical core log prepared for borehole KM - 1 is given in Figure 3.2. The core logs representing the other boreholes have been given elsewhere (Ünal et al., 1994). The core logs are the first output of the rock mass classification process.

The rock units encountered in Çayırhan Mine region were classified initially based on the original RMR and Q systems. A total of about 90-meter long cores, obtained from nine underground boreholes, were evaluated for classification purposes. A number of difficulties, as in the case of rock mass classification at Bigadiç borax mine region, were encountered in describing the weak, stratified and clay-bearing formations.

The structural regions, geological and geotechnical input parameter ratings, and the results of laboratory tests were recorded on the geological and geotechnical logging forms. After that, the common structural regions were combined by taking the weighted averages of the classification ratings for the original RMR and

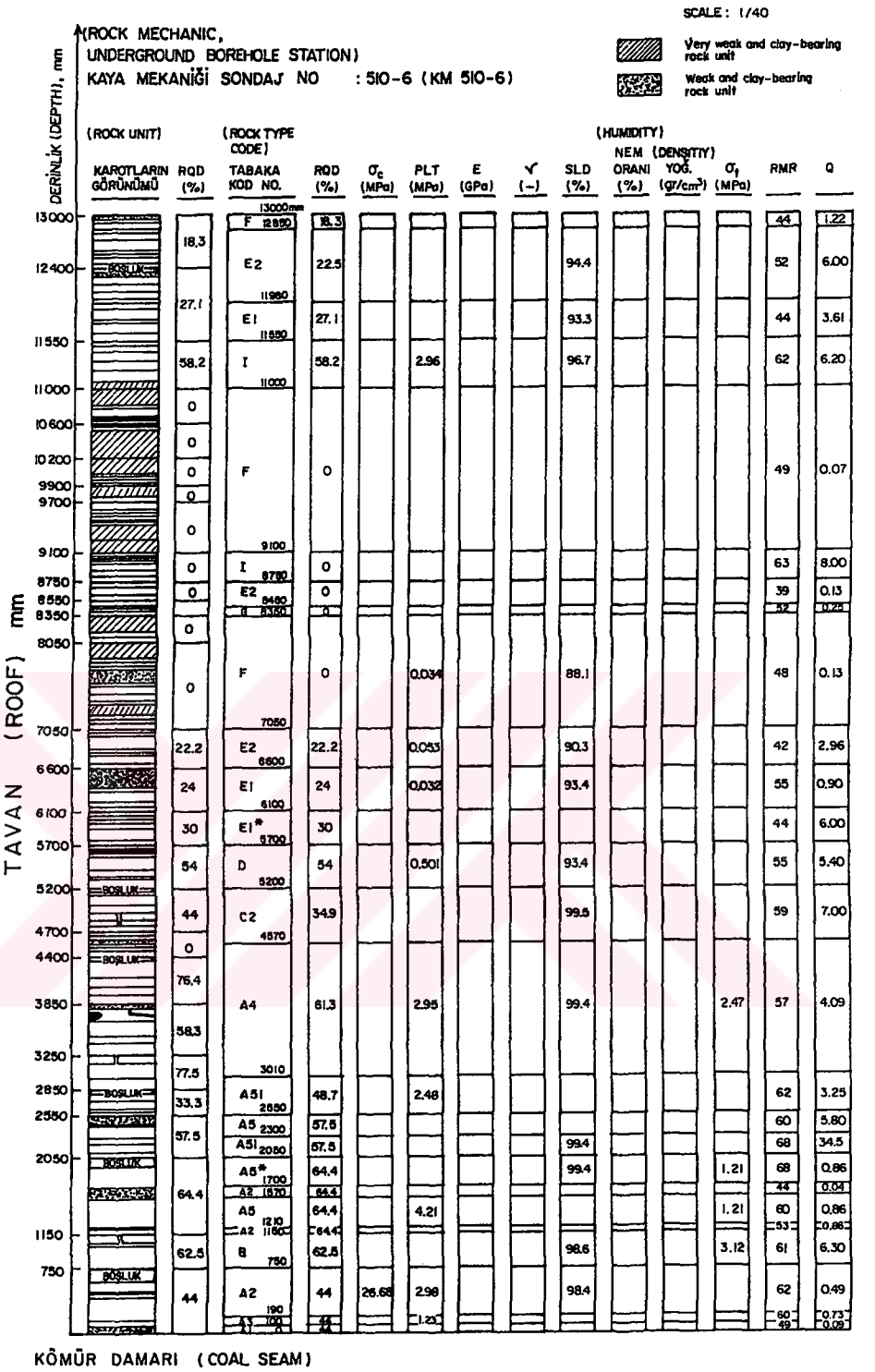

Figure 3.2 A typical core log for the borehole region: KM 510-6 (after Ünal et al., 1994)

Q systems. Consequently, all of the boreholes were combined as a single borehole-log representing that specific region. These results are listed in Table 3.4.

3.2.4 Studies at Yatağan Surface Coal Mine

In the surface-coal mine region, the major part of the overburden strata consists of alteration of clayey limestone, consolidated clay and laminated marl beds of thickness ranging between a few centimeters to 20 cm at the top, and medium to thick bedded compact marls at the bottom. In this mine, prime consideration was given to the weaker upper sequence and 102 individual sections (from nine boreholes with a total length of 530 meters) were evaluated. In addition, seven scanline sections on pitwall were investigated.

Geotechnical investigations in Yatağan surface coal mine region was evaluated by Ulusay (1991). During rock mass classification studies, the RMR index values were determined based on the original RMR System, in spite of the difficulties encountered in determining or describing some of the weak and clay bearing rock mass parameters during classification process. Determination of the index values was made possible only with the aid of a number of assumptions and engineering judgments. The Final RQD and RMR values determined during classification studies are presented in Table 3.5.

Table 3.4 Summary of classification results for Çayırhan lignite mine region with RMR, Q and RQD rating values representing the weighted average (after Ünal et al., 1994)

Rock Type Code	Thickness (m)	Original RMR	Original Q	RQD	Description of the Rock Units
A	0.96 (0.85-1.10)	48.30 (44.2-52.6)	2.31 (1.27-4.54)	44 (26.5-100)	Claystone interbedded with limestone with claystone laminea
B	0.34 (0.09-0.60)	54.10 (45.8-64.0)	4.62 (0.47-11.47)	69 (44.2-100)	Limestone with claystone laminea
A'	3.25 (2.88-3.42)	53.30 (42.7-62.8)	2.08 (1.59-2.90)	65 (22-90)	Claystone interbedded with limestone. Limestone with the irregular claystone
C	0.64 (0.28-0.89)	48.30 (41.5-59.6)	5.64 (0.33-14)	32 (4-72)	Marl interbedded with claystone
D	0.58 (0.15-0.94)	47.90 (41.8-54.5)	1.46 (0.48-2.4)	57 (19-87)	Marl
E	1.23 (0.95-1.40)	48.30 (42.6-57.9)	4.11 (2.09-8.72)	42 (23.9-85.4)	Marl with claystone
F	1.08 (0.94-1.60)	45.20 (39-55.5)	2.25 (0.67-3.60)	19 (0.0-55)	Claystone

Table 3.5 According to the Original RMR-System and RQD, Summary of Classification Results for Yatağan Strip Coal Mine (after Ulusay, 1991)

Description of the Rock Units	Thickness (m)	RQD (%)	Original RMR
Weak Marl	25.33 (13.95-56.55)	34 (0-100)	43 (34-57)
Compact Marl	9.82 (6.30-13.95)	69 (35-100)	56 (46-65)

3.3 Difficulties in Determining RMR and Q Values in Weak, Stratified and Clay-Bearing Rocks

As mentioned before, during classification process, serious difficulties were encountered in describing some of the rock-mass parameters. In this section, a number of these difficulties associated with the original RMR System will be explained in detail. The difficulties and problems associated with Q System have been given elsewhere (Ünal and Özkan, 1990).

3.3.1 Difficulties in Determining Compressive Strength

It became clear during investigations carried out in borax and coal mine regions that direct-determination of the uniaxial compressive strength of weak and stratified rocks through the full thickness of rock units was not always possible. This was due to the difficulties in obtaining suitable number of cores for preparation of standard specimens required for standard uniaxial compressive strength tests. In order to obtain a full strength-spectrum of each rock unit, point-load tests should be considered in addition to the direct compressive strength tests, because number of core pieces available in core boxes are usually adequate to carry out diametrical and axial point load tests through the full thickness of weak rock units. The question, however, is to find out a reliable relationship by which one can relate the strength index values, obtained from point load tests, to the results obtained from direct uniaxial strength tests. Classification systems should permit determination of the importance rating for strength, based on direct results of point load tests namely the point load index.

3.3.2 Difficulties in Determining RQD

As suggested by Deere et al. (1967), RQD is calculated as follows:

$$RQD = 100 \times \frac{\text{total length of core pieces} > 10 \text{ mm}}{\text{total length of a drill} - \text{run}} \qquad (3.1)$$

According to this expression, regardless of the number of rock units existing in a drill-run, only the total length of the run is suggested to be taken into account. However, as shown in Figure 3.3, if half of the drill-run contains solid cores (RQD=100) and the other half consists of fractured weak and laminated cores (RQD=0), the RQD of the total length would be 50%. If it is now assumed that this weak and laminated strata (RQD=0) constitutes the immediate roof of a roadway, taking the RQD as "50" could result in a considerable misinterpretation in engineering design analyses.

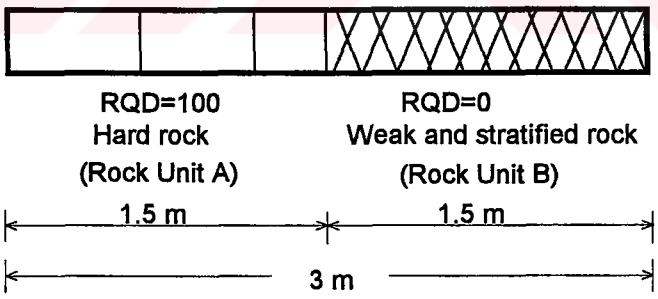

Figure 3.3 The positions of the rock units in drill-run

3.3.3 Difficulties in Determining the Effect of Water on Clay Bearing Rocks

The existence of water in the rock mass affects a number of other rock mass properties such as strength and joint conditions. The effect of water is even more pronounced in the existence of claystone or clay-bearing strata. In RMR system, Bieniawski (1979) recommends a ground water index without taking into account the damage caused in clay bearing strata due to the existence of groundwater. In this study, slake-durability tests were recommended to overcome this difficulty.

3.3.4 Difficulties in Describing the Condition of Joints

In calculation of "joint condition index", although the RMR system considers a number of parameters such as separation, continuity, roughness, alteration and filling of joints, these parameters were not weighed adequately to represent the joint conditions in stratified and clay-bearing strata. The details associated with joint condition index, also including the suggestion made, will be given in Chapter IV.

3.3.5 Difficulties in Describing the Joint Orientation

The information related to the influence of strike and dip orientation of discontinuities in adjusting the basic RMR has been reviewed in Section A.2.1. This step is treated separately because the influence of discontinuity orientations depends on the engineering applications, such as excavation of a tunnel, mine, slope, or foundation. It will be noted that the "value" of the parameter "discontinuity orientation" is not given in quantitative terms but by qualitative descriptions such as "favorable". During this study it was seen that determination of the orientation of

discontinuities from surface was very difficult. Consequently, the intact core recovery (ICR), is being considered as an additional parameter in describing joint orientation.

In summary, in order to better characterize the stratified and clay-bearing rock mass, interval limits of a number of the input parameters considered in RMR-System were modified, and/or new conditions and ratings were defined for these parameters. The total rating associated with each parameter, however, was not changed. The importance of ratings associated with modified and new conditions were also rearranged when it was necessary.

A number of recommendations to overcome the difficulties encountered in the original RMR system are given in the next chapter.

CHAPTER IV

THE MODIFIED RMR SYSTEM FOR WEAK, STRATIFIED AND CLAY-BEARING ROCK MASS

4.1 General

During the classification process, carried out based on original RMR System, serious difficulties were encountered in determining and/or describing some of the parameters in weak, stratified and clay bearing rock mass. Determination of modified RMR and Q values for weak, stratified and clay-bearing rock mass is necessary due to following reasons:

i) It is not always possible to obtain suitable cores, from weak rock, for preparation of standard specimens required for direct uniaxial compressive strength tests. Point load tests are not recommended for weak rocks by Bieniawski (1984). However, the actual uniaxial compressive strength value for these rocks could be determined with employing this method. According to Brook and Dharmaratne (1985), this type of test can be performed in the field with portable equipment with natural moisture content of the rock; an immediate assessment of rock mass strength can, therefore, be made.

ii) Some of the joint conditions physically observed on cores or observed in underground mines are either not adequately described or they are completely ignored in RMR and Q systems. Number of discontinuities per unit length of core, condition of joints, joint set number and joint alteration number are typical examples of these parameters.

iii) The effect of water on clay-bearing strata plays a major role in characterization of the rock mass. This effect, however, is not adequately described in RMR and Q systems.

iv) For meaningful interpretation of the input parameters and for providing a common basis for communication between engineers and designers, standard interval-limits for the classification parameters should be considered. The suggested ISRM standards seem to be the logical alternative for this purpose.

In this chapter, a number of recommendations are given to overcome these difficulties. In addition, development of the modified RMR-System is described in detail. The Modified RMR System relies on the experience gained in borax and coal mine regions explained in Chapter III.

4.2 Suggested Modifications in RMR System

In the following sections, recommendations are given to overcome the difficulties encountered during characterization of weak, stratified and clay bearing rock mass. Intervals used for parameters given in the M-RMR are based on ISRM suggestions.

4.2.1 Suggestions for Using Point Load Index Values in Determining Compressive Strength Index

During the laboratory studies carried out as part of this study, the direct uniaxial strength and point load tests were carried out in two series. In the first series, the direction of loading was parallel to the bedding planes in diametral tests, but perpendicular to the bedding planes in performing axial point load index tests. In performing uniaxial compressive strength tests, however, the direction of loading was perpendicular to the bedding planes. During second series, the direction of loading was parallel to bedding planes in case of direct uniaxial compressive strength tests, while it was perpendicular to bedding planes in diametral, but parallel to bedding planes in performing axial point load index tests. The final point load index values $(I_{s(50)})_{av}$ for each series were calculated by taking the arithmetical average of the point load index values obtained from axial and diametral tests.

Based on statistical evaluation of the results, the regression equations shown in Equations 4.1 and 4.2 were determined respectively for the first and second series of tests.

$$(\sigma_c)_V = 16.57 \cdot \left(I_{s_{(50)}}\right)_{av} + 2.127 \quad (r = 0.94) \tag{4.1}$$

$$(\sigma_c)_H = 19.60 \cdot \left(I_{s_{(50)}}\right)_{av} - 1.50 \quad (r = 0.95) \tag{4.2}$$

The results obtained from these analyses are presented in Figures 4.1a and 4.1b.

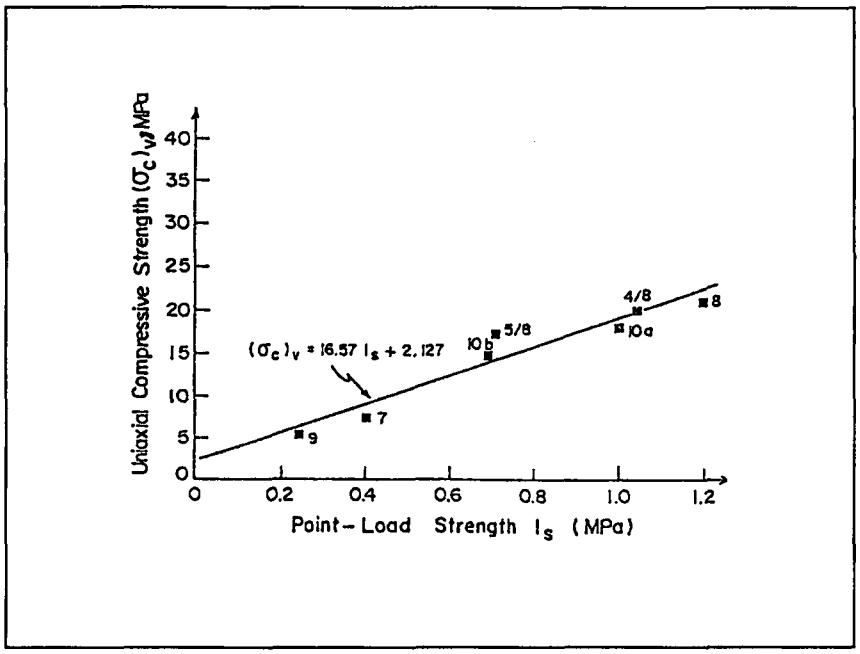

Figure 4.1a The relationship between the compressive strength $(\sigma_c)_V$ and point load index for first series (after Ünal and Özkan, 1990)

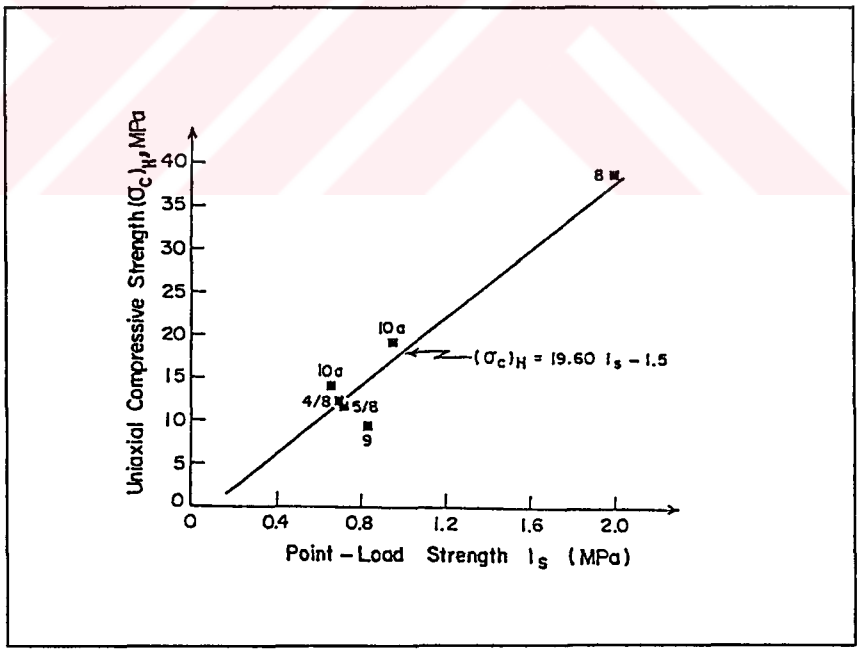

Figure 4.1b The relationship between the compressive strength $(\sigma_c)_H$ and point load index for second series (after Ünal and Özkan, 1990)

In the literature, a number of different statistical relationships have been determined between the unconfined compressive strength and point load strength index by various researchers such as Broch and Franklin (1972), Boisen (1977), Hassani et al. (1981), Singh et al. (1983), O'Rourke (1989) and Tsidzi (1991).

Based on the statistical evaluation of the results obtained from diametral and axial point load tests, carried out in this study, and considering the anisotropy index (I_a) as well as Young's Modulus and Poisson's Ratio of rocks the following regression equation (Figure 4.2) was obtained:

$$E/\nu = 732 \cdot I_a^{-5.54} \qquad (r^2 = 0.92) \qquad (4.3)$$

The suggested intervals and ratings associated with uniaxial compressive strength and point load index values are given in Figure 4.3 (Ünal and Özkan, 1990; Ünal et al., 1992; Ulusay et al., 1992).

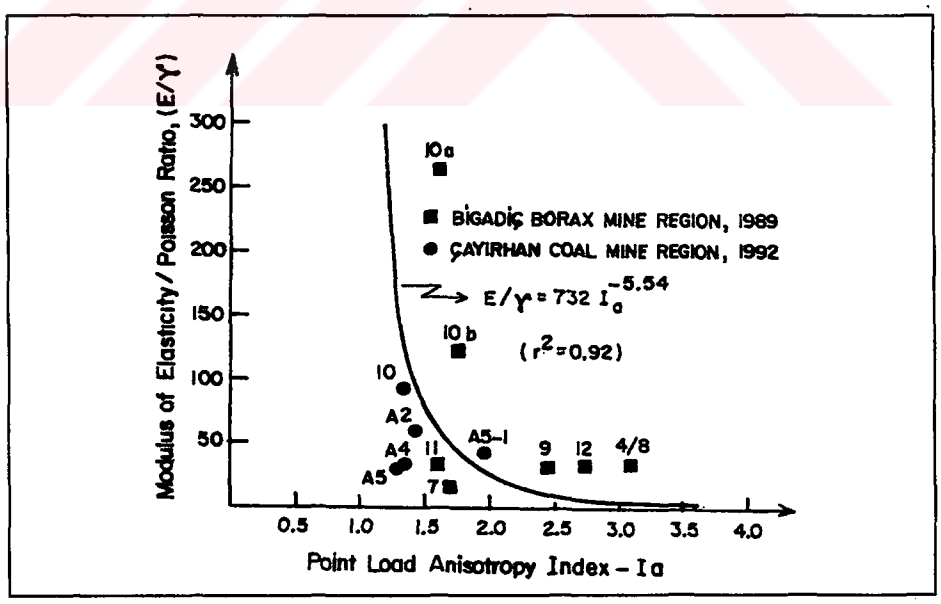

Figure 4.2 The relationship between the anisotropy index (I_a) and E/ν ratio

4.2.2 Rock Quality Designation (RQD)

In calculating RQD with the equation suggested by Deere et al. (1967), only the total length of drill-run is considered as explained in Section A.2.1. This could cause considerable misinterpretation in engineering analysis. For this reason, each information should be treated separately. In addition, RQD logging should be carried out soon after the cores obtained from boreholes. The standard procedures should be followed during borehole coring and in treating the cores until logging. The photographs of the core boxes should always be taken as permanent records.

According to Priest and Hudson (1976), the RQD value can be predicted by considering the number of joints per meter. The suggested equation is as follows:

$$RQD = 100 \cdot e^{-0.1\lambda} \cdot (0.1\lambda + 1) \qquad \text{(A.1)}$$

where, λ is mean number of discontinuities per meter.

The suggested intervals and ratings about RQD are given in Figure: 4.3.

4.2.3 Modifications for the Effect of Water in Clay Bearing Strata

Weathering is a time dependent factor. The influence of weathering must be taken into consideration in making decisions on size of the opening, in determining the stability of the opening and design of support. According to the findings in literature, the three parameters that are affected by weathering are uniaxial compressive strength (σ_c) or point load strength index ($I_{s(50)}$), RQD, and joint condition. RQD decreases if density of the fractures increases. Compressive strength decreases significantly as chemical changes take place. The joint condition is affected by alteration of the wallrock and the joint filling. Weathering data from borehole core

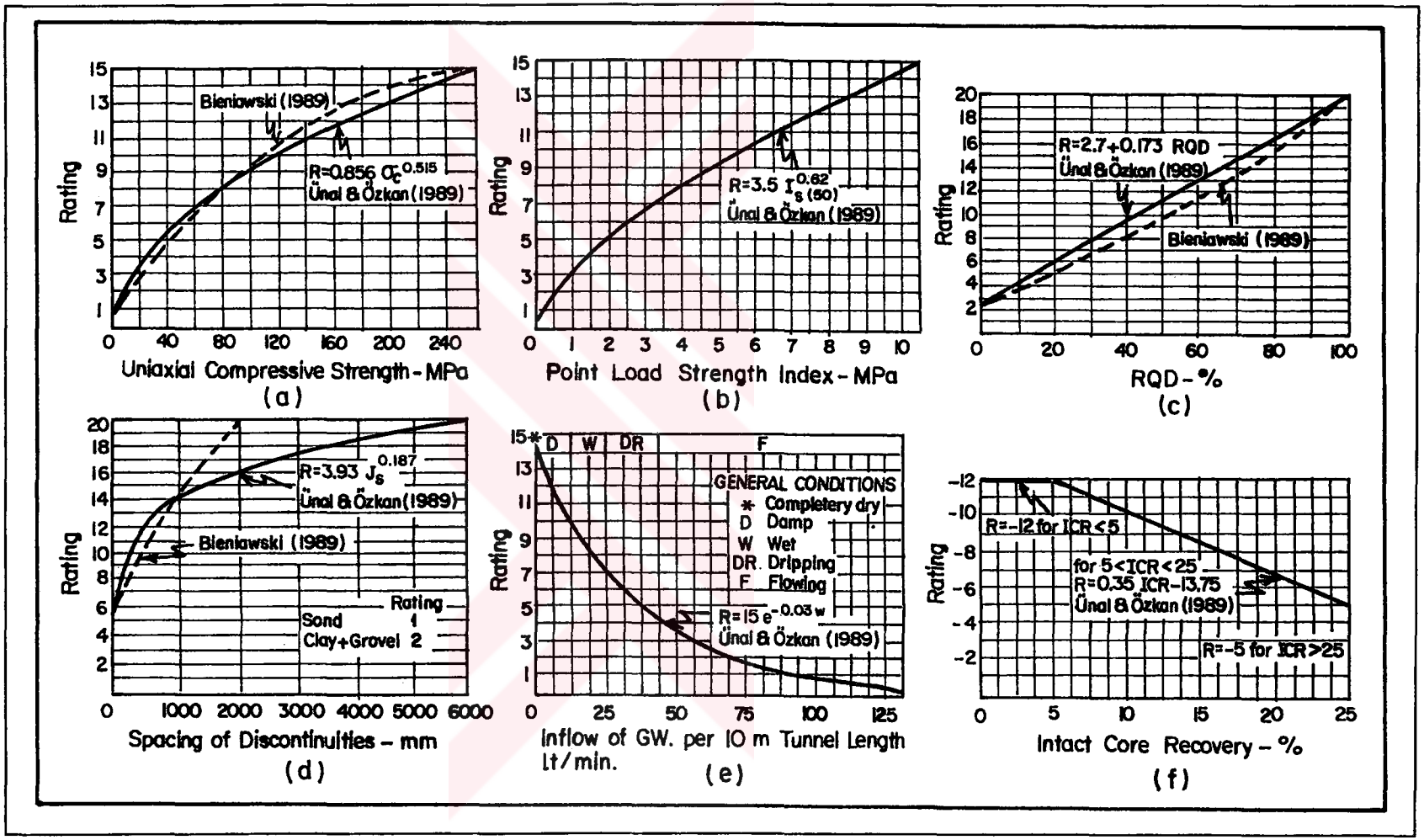

Figure 4.3 Suggested intervals and ratings for various input parameters (after Ünal and Özkan, 1990; and Ünal et al., 1992)

can be conservative owing to the large surface area of core relative to the volume-underground exposures will be more reliable.

The slake durability index has been developed for providing a quantitative measure of the relative breakdown from drying and wetting of argillaceous rocks. Durability test predicted the effects of weathering agents with short-term engineering significance. Of these, climatic slaking is undoubtedly the most widespread and therefore the most important. A slake durability test predicts deterioration due to climatic wetting and drying. The damage of clay-bearing rock due to effect of humidity can be expressed by the slake durability index.

Utilizing the slake durability test results, relationships between a number of input parameters and slake durability index (I_{d2}) have been investigated. A total of 125 specimens were tested during this study. Based on the statistical evaluation of the results, the equations and corresponding correlation coefficients presented in Table 4.1 were obtained.

Table 4.1 Regression equations and the associated correlation coefficients for slake durability index and input parameters considered in RMR System (after Özkan, 1989)

Regression Equation	Correlation Coefficient
$\sigma_c(\text{MPa}) = 0.232\, I_{d2} + 1.835$	r = 0.80
$RQD(\%) = 15.31 I_{d2}^{0.00835}$	r = 0.70
$JC(\text{Index}) = 0.068\, I_{d2} + 6.6$	r = 0.74
$JS(\text{mm}) = 5.78372\, I_{d2} + 45.6267$	r = 0.30

JC : Joint condition
JS : Joint spacing

Considering the results presented in Table 4.1 it can be concluded that, only the three input parameters are affected by weathering, namely the uniaxial compressive strength (σ_c), RQD, and condition of joints (JC). Effect of weathering on these parameters was also observed by Laubscher (1977, 1984, 1990, 1993), Rafia (1980), Newman and Bieniawski (1985), Brook and Dharmaratne (1985), Venkateswarlu (1986), and Ojo and Brook (1990). The slake durability index tests were suggested by Venkateswarlu (1986) and Ojo and Brook (1990) to determine the effect of weathering.

In this study, the rating values for RQD, JC and σ_c are added together and adjusted for weatherability by multiplying the sum of these ratings with the weathering coefficient. The suggested weathering coefficient is presented in Figure 4.4.

4.2.4 Condition of Discontinuities

In RMR system, the parameters associated with condition of joints (the separation, continuity, roughness, alteration, and filling) have not been weighed adequately to represent stratified and clay-bearing strata. Therefore, for evaluation of these parameters, the interval limits and ratings suggested by Ünal (1988) were utilized. In order to calculate the joint condition index (*JC*), for normal cases, the relationship given in Equation 4.4 was considered.

$$JC = A + P + (Y \times Z \times D) \tag{4.4}$$

where, A is the importance rating for weathering, P is for roughness, Y is for discontinuity, Z is for aperture, and D is for filling. For special cases, a set of new ratings were assigned to parameters Y, Z and D (Ünal, 1988). The total rating for "JC" is taken 30, as suggested by RMR system.

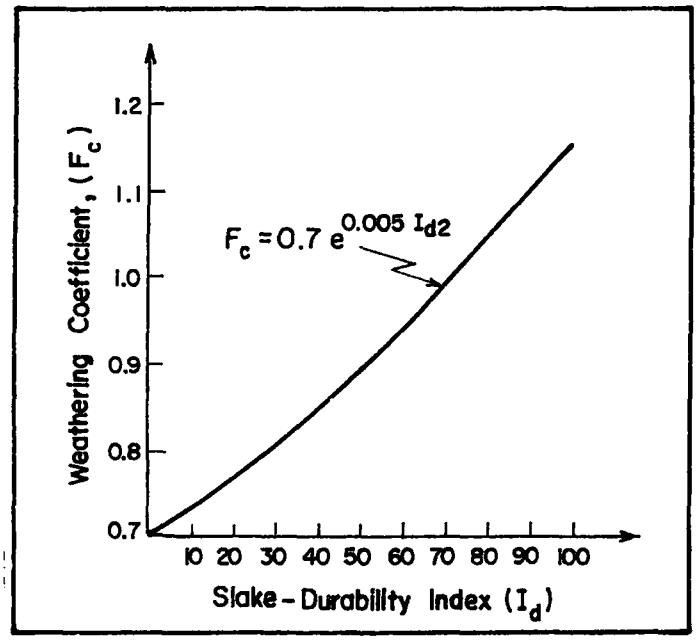

Figure 4.4 Slake durability index vs. weathering coefficient (after Ünal and Özkan, 1990)

4.2.5 Orientation of Discontinuities

The size, shape and orientation of the excavation will affect the behavior of the rock mass. The attitude of the joints and whether or not the bases of blocks are exposed has a significant bearing on the stability of the excavation and the ratings must be adjusted accordingly. The magnitude of the adjustment depends on the attitude of the joints with respect to the vertical axis of the block. As gravity is the most significant force to be considered, the instability of the block depends on the number of joints that dip away from the vertical axis.

To overcome the difficulties due to orientation of discontinuities in highly fractured or broken rock a new parameter, namely the intact core recovery (ICR), was introduced into evaluations (Ünal, 1988). The interval limits and the ratings associated with ICR is given in Figure 4.3f.

4.3 Modified RMR (M-RMR) System

The six input parameters considered in M-RMR system are; uniaxial compressive strength, RQD, spacing of discontinuities, condition of discontinuities, groundwater conditions and orientation of discontinuities. Some of the input parameters in M-RMR System, the suggested intervals and the associated ratings are presented in Figure 4.3. The conditions and the suggested intervals and ratings associated with joint condition parameters are provided in Table 4.2. For calculation of the joint condition index (I_{JC}), the guidelines given in Table 4.3 should be used. I_{JC} is dependent on intact core recovery (ICR), rock quality designation (RQD), filling thickness (f) and it's nature (hard or soft).

Figure 4.5 illustrates the process of calculating the Modified RMR (M-RMR). In order to calculate the M-RMR, geological and geotechnical data must be converted to numerical values. This can be accomplished by using Figure 4.3, and Tables 4.2 and 4.3. The calculation is done in four steps. Firstly, Unit Mass rating (UMR) is determined for each structural region. Secondly, Final Unit Mass Rating (FUMR) is calculated by multiplying the UMR with the weathering coefficient (F_c). Thirdly, the rating values for Final Unit Mass Rating (FUMR), Joint Spacing (JS) and Groundwater (GW) are added together in order to calculate Basic M-RMR. Final Modified Rock Mass rating (M-RMR) is calculated by adding Joint Orientation Index (I_{JO}) to Basic M-RMR:

Table 4.2 Intervals and ratings for "joint condition" index (after Ünal and Özkan, 1990)

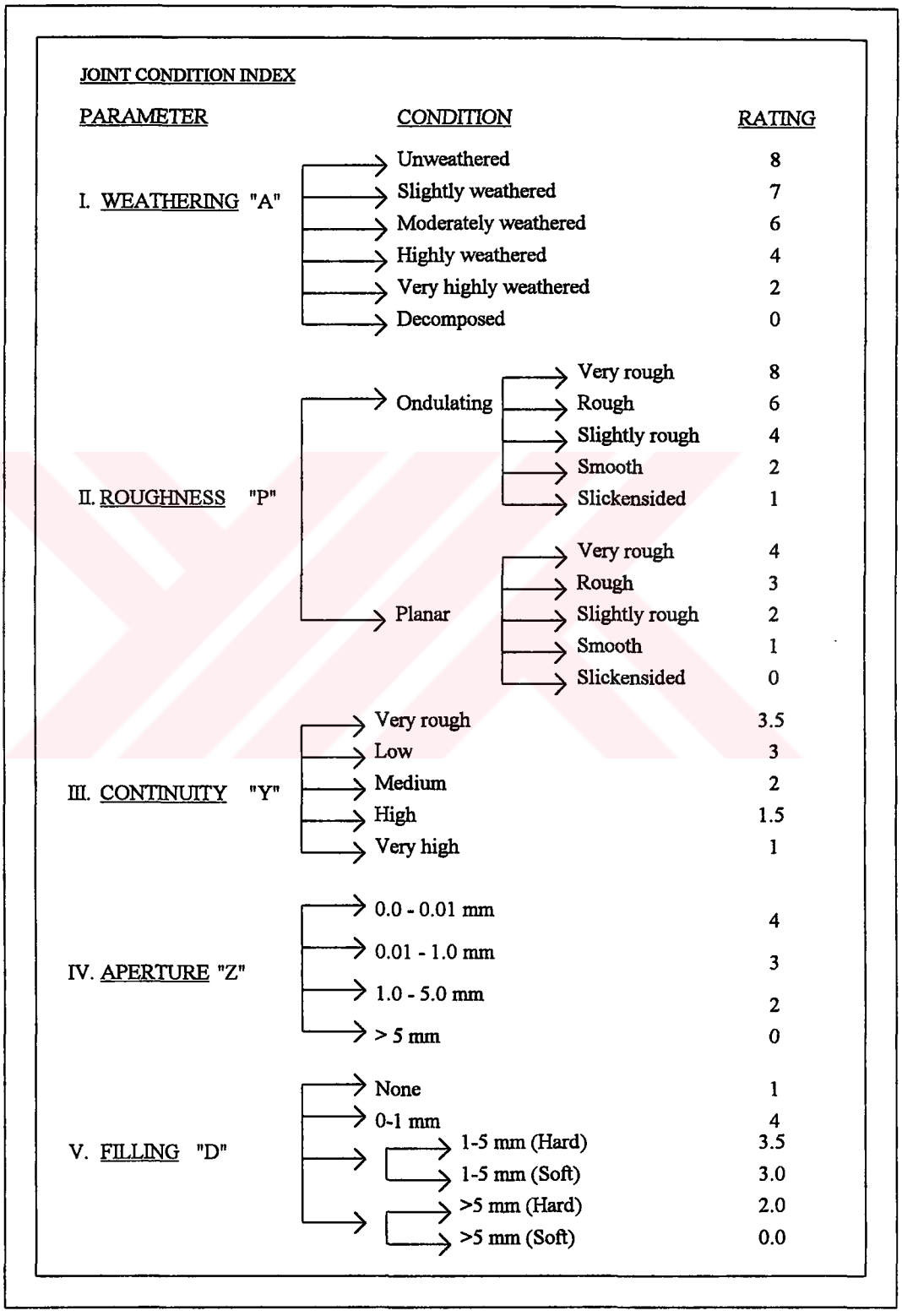

Table 4.3 Determination of joint condition index (I_{JC})

				I_{JC}
ICR < 5	D = 1 (without filling)			10
	D ≠ 1 (with filling)			0
5 ≤ ICR ≤ 25	D = 1	RQD = 0		13
		RQD < 10		17
		RQD > 10		22
	D ≠ 1	f > 5 mm	soft	0
			hard	4
		1 mm < f < 5 mm	soft	8
			hard	11
		f < 1mm		14
ICR > 25	D = 1	Use I_{JC} Index Table and Calculate I_{JC} from Equation: $I_{JC} = A + P + (YxZxD)$		
	D ≠ 1	f > 5 mm	soft	$I_{JC} = 0$
			hard	$I_{JC} = 2 + (YxD)$
		1 mm < f < 5 mm	soft	$I_{JC} = 4 + (YxD)$
			hard	$I_{JC} = 6 + (YxD)$
		f < 1 mm		$I_{JC} = 8 + (YxD)$

Note :
A : Alteration, P: Roughness, Y: Persistence, Z: Aperture, D: Filling

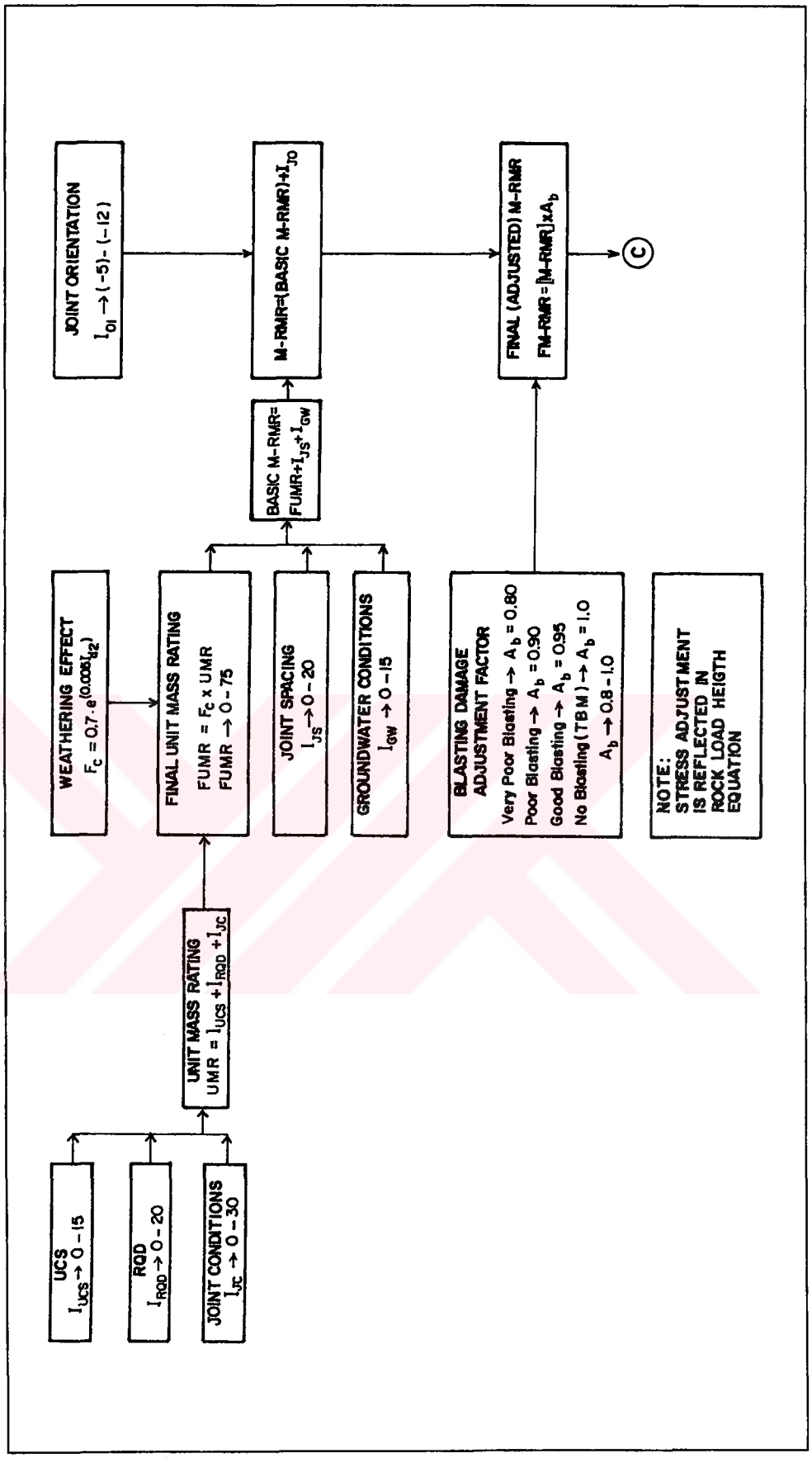

Figure 4.5 Modified RMR calculation and inputs for support recommendation

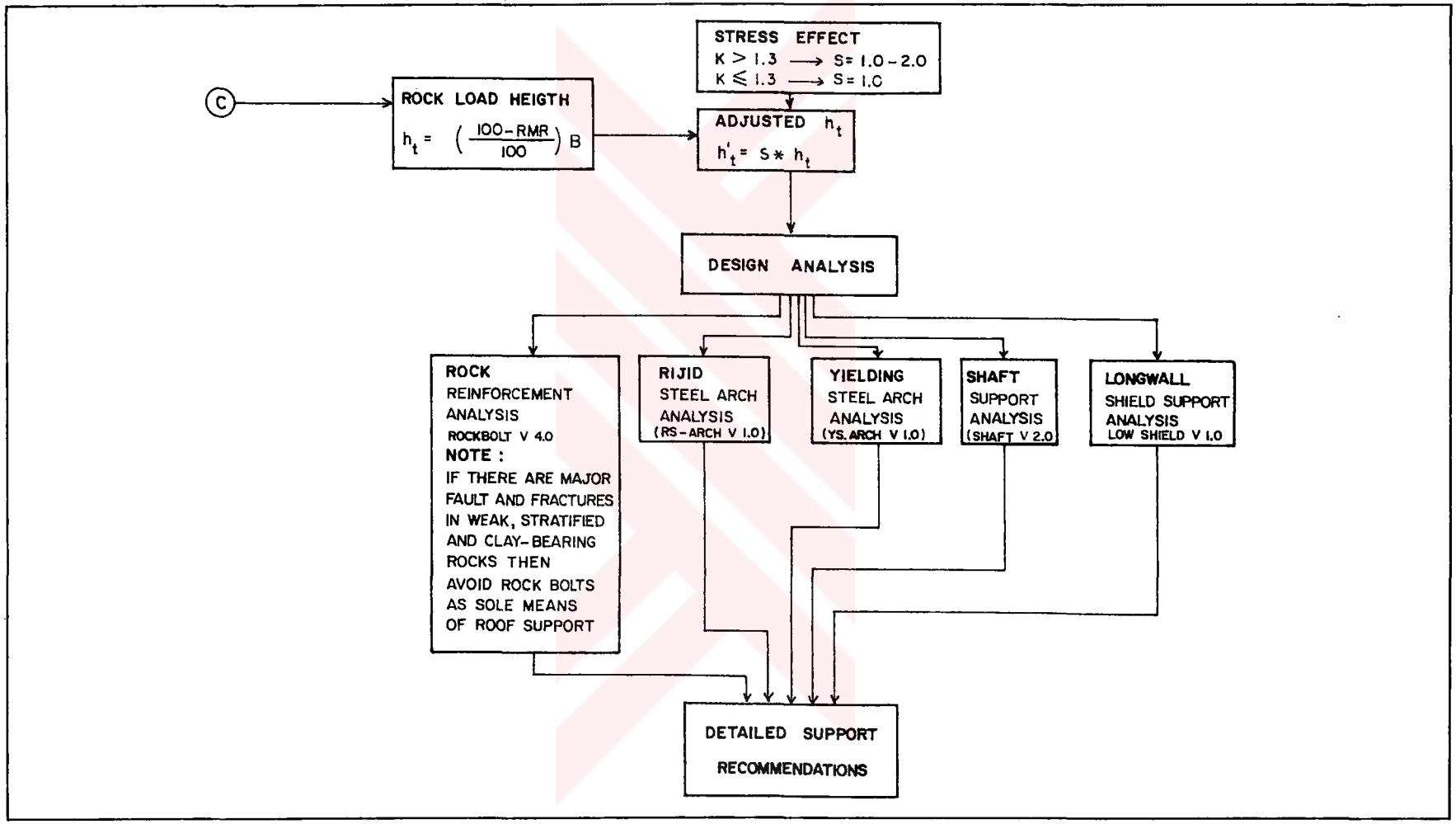

Figure 4.5 (continued)

The simplified equation of Final M-RMR Index can be defined as follows:

$$M-RMR = F_C \cdot \left[I_{PLT} + I_{RQD} + I_{JC}\right] + I_{JS} + I_{GW} + I_{JO} \qquad (4.5)$$

where, F_C is the weathering coefficient, I_{PLT} is point load strength index, I_{RQD} is rock quality designation index, I_{JC} is joint condition index, I_{JS} is joint spacing index, I_{GW} is ground water condition index and I_{JO} is orientation of discontinuity index.

The fourth and the final step is to determine adjusted M-RMR. Adjustment factors for blasting (A_b) can be determined from Figure 4.5. Adjustment for stress is reflected in rock load height equation suggested by Ünal and Ergür (1990).

The following examples illustrate the Modified Rock Mass Rating (M-RMR) classification system.

Example-1: Assume that the following data are given:

Uniaxial Compressive Strength	(σ_C)	: 100 MPa
Rock Quality Designation	(RQD)	: 80 %
Spacing of Discontinuity	(JS)	: 1000 mm
Condition of Discontinuity		
Weathering	(A)	: Unweathered
Roughness	(P)	: Ondulating-Rough
Persistency	(Y)	: Very Low
Aperture	(Z)	: < 0.01 mm
Filling Thickness	(D)	: None
Ground Water Condition	(GW)	: 10 lt/min

Intact Core Recovery (ICR) : 100 %

Slake Durability Index ($I_{d\text{-}2}$) : 95 %

Step - 1

The rating values for the uniaxial compressive strength, RQD, the spacing of discontinuities, the ground water condition could be found by Figure 4.3 as follows:

$$I_{UCS} = 0.856 \cdot \sigma_c^{0.515} = 9.17$$

$$I_{RQD} = 2.7 + 0.173 \cdot RQD = 16.54$$

$$I_{JS} = 3.93 \cdot J_S^{0.187} = 14.30$$

$$I_{GW} = 15 \cdot e^{-0.03W} = 11.11$$

The rating values for the weathering, the roughness, the persistency, the aperture and the filling thickness and its hardness could be found from Tables 4.2 and 4.3 in order to calculate the condition of discontinuities.

From Table 4.2:

W = 8 P = 6 Y = 3.5 Z = 4 D = 1

From Table 4.3:

There is not filling in this structural region, i.e. D = 1. Therefore,

$$I_{JC} = A + P + (Y \times Z \times D)$$

$$I_{JC} = 8 + 6 + (3.5 \times 4 \times 1)$$

$$I_{JC} = 28$$

Now, the Unit Mass Rating can be calculated as:

$$UMR = I_{UCS} + I_{RQD} + I_{JS} = 9.17 + 16.54 + 28 = 53.71$$

Step - 2:

In order to calculate the Final UMR, UMR is multiplied with F_C

From Figure 4.3, $F_C = 0.7 \cdot e^{(0.005 I_{d-2})} = 1.126$

Final UMR = $F_C \times UMR = 1.126 \times 53.71 = 60.48$

Step - 3:

Final M-RMR is calculated in this step as follows:

$$\text{Basic M} - \text{RMR} = \text{Final } UMR + I_{JS} + I_{GW} = 60.48 + 14.30 + 11.11 = 85.89$$

In order to calculate the M-RMR, Basic M-RMR is added to I_{JO}

where, $I_{JO} = -5$ (for ICR > 25%)

$$\text{M} - \text{RMR} = \left[\text{Basic M} - \text{RMR}\right] + I_{JO} = 85.89 - 5 = 80.89$$

Bieniawski's original RMR value with the same input parameters is about 73.

Step - 4:

Assuming that tunnel is driven with TBM (A_b=1), Adjusted M-RMR value will not change.

Example - 2: Assume that the following data are given:

Point Load Strength Index	(PLT)	: 1.5 MPa
Rock Quality Designation	(RQD)	: 45 %
Spacing of Discontinuity	(JS)	: 50 mm
Condition of Discontinuity		
Weathering	(A)	: Moderately Weathered
Roughness	(P)	: Planar-Slightly Rough
Persistency	(Y)	: High
Aperture	(Z)	: None
Filling Thickness	(D)	: > 5 mm, Hard
Ground Water Condition	(GW)	: 25 lt/min
Intact Core Recovery	(ICR)	: 50 %
Slake Durability Index	($I_{d\text{-}2}$)	: 50 %

Step - 1

The rating values for the uniaxial compressive strength, RQD, the spacing of discontinuities, the ground water condition could be found by Figure 4.3 as follows:

$$I_{PLT} = 3.5 \cdot I_{s(50)}^{0.62} = 4.50$$

$$I_{RQD} = 2.7 + 0.173 \cdot RQD = 10.49$$

$$I_{JS} = 3.93 \cdot J_s^{0.187} = 8.17$$

$$I_{GW} = 15 \cdot e^{-0.03W} = 7.09$$

The rating values for the weathering, the roughness, the persistency, the aperture and the filling thickness and its hardness could be found by Table 4.2 and 4.3 in order to calculate the condition of discontinuities.

From Table 4.2:

W = 6 P = 2 Y = 1.5 Z = 0 D = 2

From Table 4.3:

There is filling in this structural region, i.e. D = 2. Therefore,

$$I_{JC} = 2 + (Y \times Z)$$

$$I_{JC} = 2 + (1.5 \times 0)$$

$$I_{JC} = 2$$

$$UMR = I_{PLT} + I_{RQD} + I_{JS} = 4.50 + 10.49 + 2 = 16.99$$

Step - 2:

In order to calculate the Final UMR, UMR is multiplied with F_C

$$F_C = 0.7 \cdot e^{(0.005 I_{d-2})} = 0.89$$

Final UMR (FUMR) = $F_C \times UMR = 0.89 \times 16.99 = 15.12$

Step - 3:

$$\text{Basic M} - \text{RMR} = \text{Final } UMR + I_{JS} + I_{GW} = 15.12 + 8.17 + 7.09 = 30.38$$

In order to calculate the M-RMR, Basic M-RMR is added with I_{JO}

where, $I_{JO} = -5$ (for ICR > 25%)

$$M-RMR=[\text{Basic M}-RMR]+I_{JO}=30.38-5=25.38$$

Bieniawski's original RMR value with the same input parameters is about 34.50.

In design analyses, M-RMR should be adjusted for blasting damage and for stress conditions.

4.4 Comparison of Original and Modified RMR and Q Values

Based on the suggestions made in this study, the modified RMR and Q values were determined for various formations and compared with the original ratings.

The regression equations and the associated correlation coefficients obtained from statistical evaluations of data points obtained from five surface and nine underground boreholes carried out at Bigadiç Borax Mine are presented in Equations 4.6 and 4.7, respectively, for the original and the modified RMR and original Q ratings.

$$RMR=7.79\cdot\ln Q+36.70 \quad (r^2=0.81) \tag{4.6}$$

$$M-RMR=9.66\cdot\ln Q+37.90 \quad (r^2=0.84) \tag{4.7}$$

The relationship between the original and the modified RMR and Q ratings are presented in Figure 4.6. As can be seen from Figure 4.6, the data points obtained from modified values fall into a narrower band. The regression line representing the modified ratings is closer to the classical line ($RMR=9\cdot\ln Q+44$) when compared with the line representing the original ratings. The regression coefficient for the modified conditions ($r^2 = 0.84$) is higher than the original conditions ($r^2 = 0.81$).

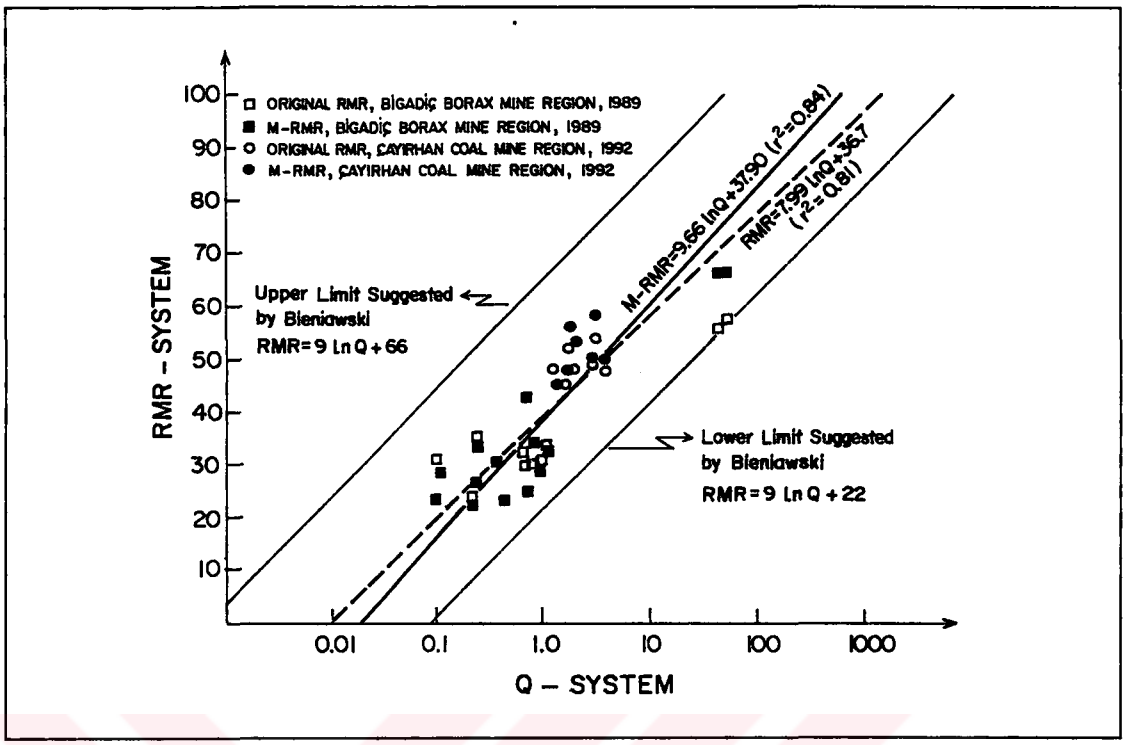

Figure 4.6 The relationship between the original and modified RMR and Q values (Note: Each data point in this graph represents a different structural region. Data points are obtained by the taking the average of the index values achieved in the same structural region.)

Earlier Studies Carried Out by the Author

The following results were found during the earlier studies carried out by the author (Özkan, 1989):

- The results of support pressures calculated based on RMR and Q systems indicate that, estimates of RMR system are less than the Q system. The support pressures calculated from modified Q values are more reasonable as compared with the original Q values.

- "m" and "s" material properties in original and modified RMR systems were determined as estimated by Priest and Brown (1983) and from Hoek and Brown's chart (Hoek and Brown, 1980). The results indicated that,

"m" values estimated by Priest and Brown are slightly greater than those estimated by Hoek and Brown. On the other hand, "s" values estimated by Priest and Brown were slightly less than the estimates of Hoek and Brown. It can be concluded that both methods provided similar results.

- Based on the international friction angles predicted from Q and RMR systems, and obtained from actual laboratory tests, it can be concluded that the internal friction angles estimated by modified RMR values are closer to actual peak friction angles determined from laboratory tests. On the other hand, the internal friction angles estimated by Q system are close to the residual friction angles determined from laboratory tests.

4.5 Comparison of Original and Modified RMR Values Based on Engineering Applications

In this section, the original and modified RMR values are being compared on the basis of their impacts on some engineering applications related to a borax and two coal mining regions considered in this study.

4.5.1 Underground Cases

One of the basic difference between the original and modified rating systems appears in characterization of the extreme ends (the stratigraphic regions representing the worst and the best rock mass conditions) of the weak, stratified and clay-bearing rock units. The results shown in Figure 4.7 indicate the upper and lower limits of RMR values, obtained from the three mining regions investigated in this study. In Çayırhan Coal Mine, for example, the RMR value of the same structural region was determined as 43 and 25 based on the original and modified rating

systems, respectively. On the other hand, another structural region at the same mine was rated as 66 based on the original, but as 73 based on the modified system.

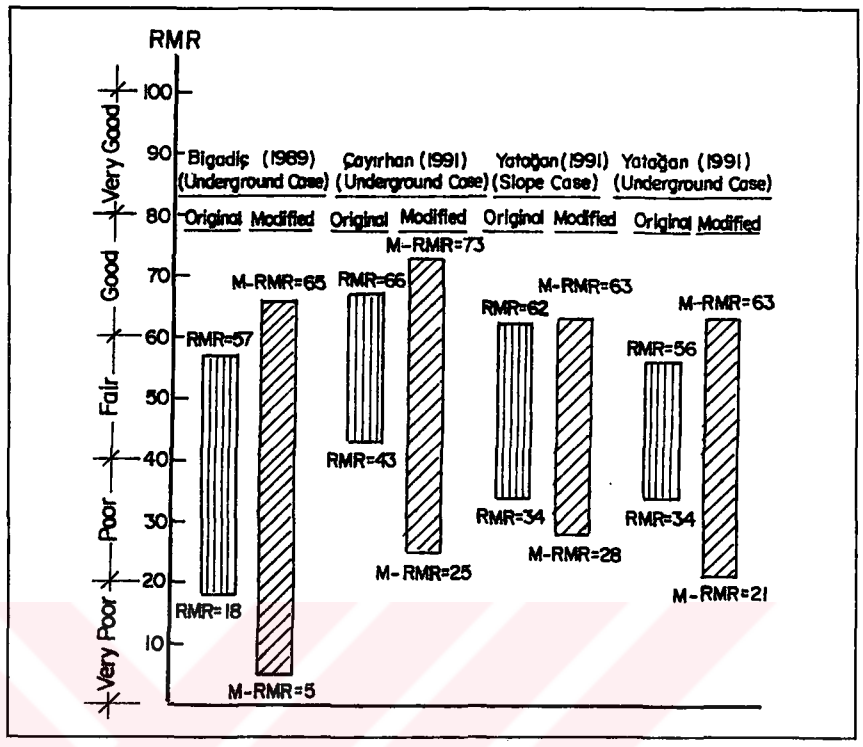

Figure 4.7 Typical results obtained from classification studies carried out in different mining areas (after Ünal et al., 1992)

Interpretation of the results presented in Figure 4.7 provides drastic examples in terms of engineering outputs. The critical maximum roof-spans above which immediate collapse occur determined based on lower limits of the original and modified RMR values, are presented in Table 4.4.

Table 4.4 Maximum roof spans above which an immediate collapse occur (after Ulusay et al., 1992)

Mine (Structural Region)	Original and Modified RMR Values	Critical Roof Span (m)
Bigadiç (Borax) (SR:BB-LL)	RMR original = 18 M-RMR = 5	2.6 0
Çayırhan (Coal) (SR:CC-LL)	RMR original = 43 M-RMR = 25	8.4 3.6
Yatağan (Coal) (SR:YC-LL)	RMR original = 34 M-RMR = 21	5.6 3.0

For the same structural region in a mine the maximum roof span determined based on the modified RMR values is much lower than the one predicted based on the original rating. In Çayırhan coal mine, for example, for a roof span of 6 m, while the stand-up time predicted by the original system is about one day, an immediate collapse occurs according to the prediction of the modified system which calls for a partial excavation.

In the following example, a similar argument can be extended to the critical width of the openings below which no support is required, considering the upper limits of the original and modified values determined for the same structural region. The results indicate that in all cases, the critical minimum- spans predicted based on two systems are not significantly different than each other.

The rock-load heights (h_t) or roof pressures (P_r) above the underground openings can be calculated considering Equation A.7 suggested by Ünal and Ergür (1990). In the existence of low horizontal stresses (S=1) and for a roof span of 6 meters the h_t and P_r expected in three mining regions, for weak, stratified and clay bearing rock mass (lower limits of RMR values), can be calculated as shown in Table 4.5. For the conditions considered, since M-RMR ratings are always lower than the original RMR ratings, the rock-load heights and the corresponding roof pressures predicted by modified ratings are always greater. Consequently, the modified rating system calls for more support. In the existence of high horizontal stresses ($S > 1$), the differences in (h_t) and (P_r) values become more pronounced and hence the support requirements.

Table 4.5 Rock load heights and roof pressures calculated based on original and modified RMR values (after Ulusay et al., 1992)

Mine	RMR Values	Rock Load Height, h_t (m)	Roof Pressure (kPa) $P_r = \gamma \cdot h_t$
Bigadiç (Borax)	RMR original = 18	4.92	123
	M-RMR = 5	5.70	142.5
Çayırhan (Coal)	RMR original = 43	3.42	85.5
	M-RMR = 25	4.50	112.5
Yatağan (Coal)	RMR original = 34	3.96	99
	M-RMR = 21	4.74	118.5

Based on the data obtained from geotechnical investigations and considering the original and modified RMR values, rock-reinforcement design analyses were carried out for Çayırhan underground mine.

The following input data were used during analyses:

Roof Span	: 6.0 m
Roof Type	: Marl
Overburden Thickness	: 200 m
Unit Weight	
Immediate roof	: 19 kN/m^3
Overburden rock	: 23 kN/m^3
Hor. to Ver. Stress Ratio	:1/3

The design summary shown in Figure 4.8 was obtained, for normal swellex bolts, considering the original (RMR=43) and modified (M-RMR = 25) ratings.

The estimated material costs, per meter of roadways advance, were determined as 61 and 83 US dollars for the original and modified systems, respectively. The important point here is that, for the same rock unit, the two rating system predicts different RMR values. If the real RMR value is 25, then the rock reinforcement design based on RMR value of 43 will result in a disaster (roof fall) although it looks economical.

4.5.2 Slope Case

In the strip coal-mine, weak, stratified and clay-bearing overburden rock units were evaluated based on the original and modified rock mass rating of RMR system. Moderately spaced joint systems showing negative exponential distribution and bedding planes are smooth-planar with apertures ranging between 0.1 mm to 0.5 mm and contains very thin coating of finest material. The bedding surfaces are easily separated when they are exposed to air possibly due to stress relaxation caused by

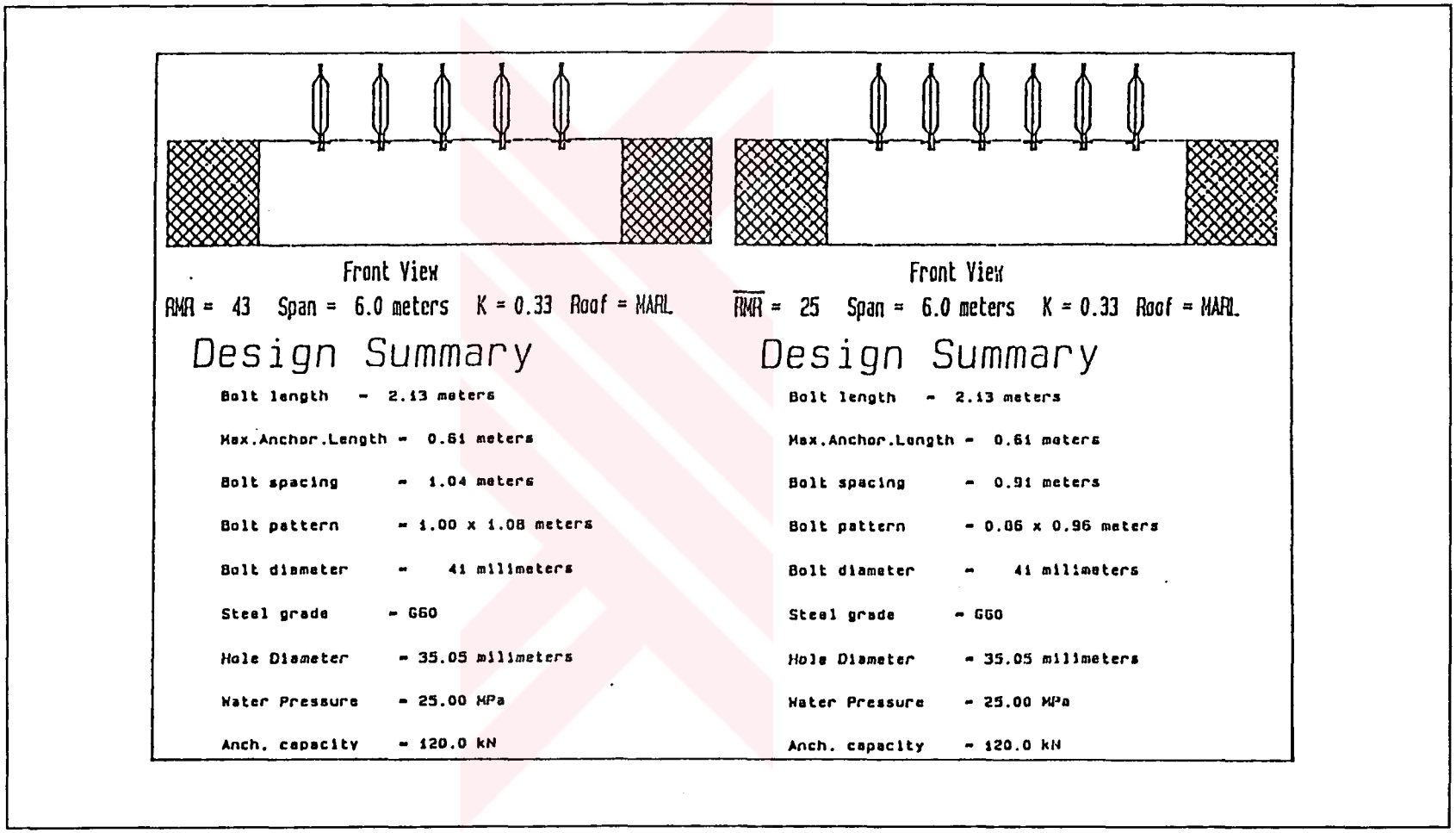

Figure 4.8 Design summary for swellex bolts determined based on original and modified RMR values (after Ünal and Ergür, 1990)

excavation. On the basis of site condition (Ulusay, 1991) only one possible mode of failure (circular type) was considered for joint orientation adjustment (-5).

A histogram of the 109 values of original RMR values (Figure 4.9a) has a bimodal form, which suggests that, from a geotechnical point of view, the overburden should be regarded as comprising two rock mass types. Based on examination of core loges and observations on pitwalls, the rock mass in the overburden was divided into "more fresh (compact marls)" and "weak upper sequence" according to depth. This application yielded average RMR values of 53 (original) and 52 (modified) for more fresh portion, and 43 (original) and 40 (modified) (Figure 4.9b) for weak sequence.

The RMR values obtained from both original and modified systems are very close to each other (for RMR>40) without any noticable difference in rock mass class. However, below the rating value of 40 modified values show a noticable variation and a wider band of RMR values as compared with the original RMR values.

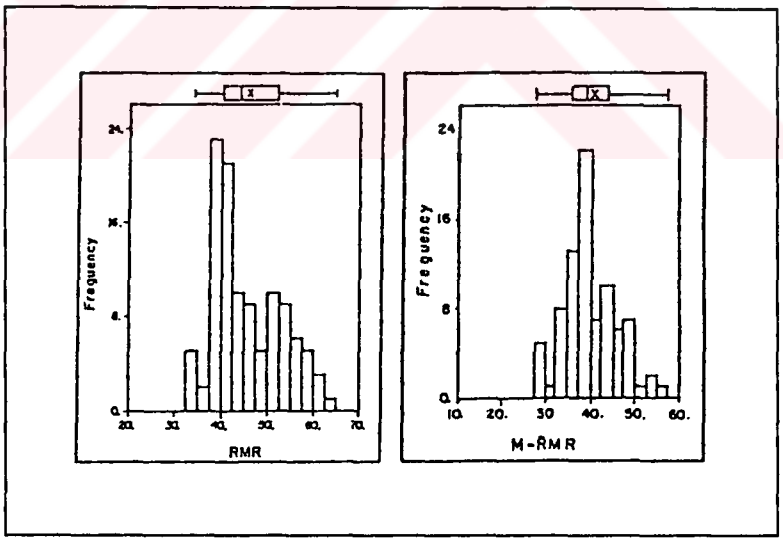

Figure 4.9 Histograms: (a) all RMR values for all samples based on original RMR system, (b) M-RMR values for weak sequence based on modified system (slope case) (after Ulusay et al., 1992)

In the weak sequence, lower limit of RMR values of 34 and 28 derived from original and modified systems, respectively, confirm this argument. Therefore, in stability assessments, prime consideration was given to the weak, stratified and clay-bearing sequence. (Figure 4.10).

In order to provide a rational basis for estimating the values of material constants and shear strength behavior of the weak rock mass, Hoek and Brown empirical failure criterion (Hoek and Brown, 1988) was used. Calculations were made by employing the measured triaxial data pairs from intact rock, and using the computer program HOBR written by Ulusay (1991).

The resulting curvilinear failure envelopes with rock mass constants, and variation of the shear strength parameters (c, ϕ) with normal stress for mean and lower bound values of original and modified RMR values are given in Figures 4.11 and 4.12

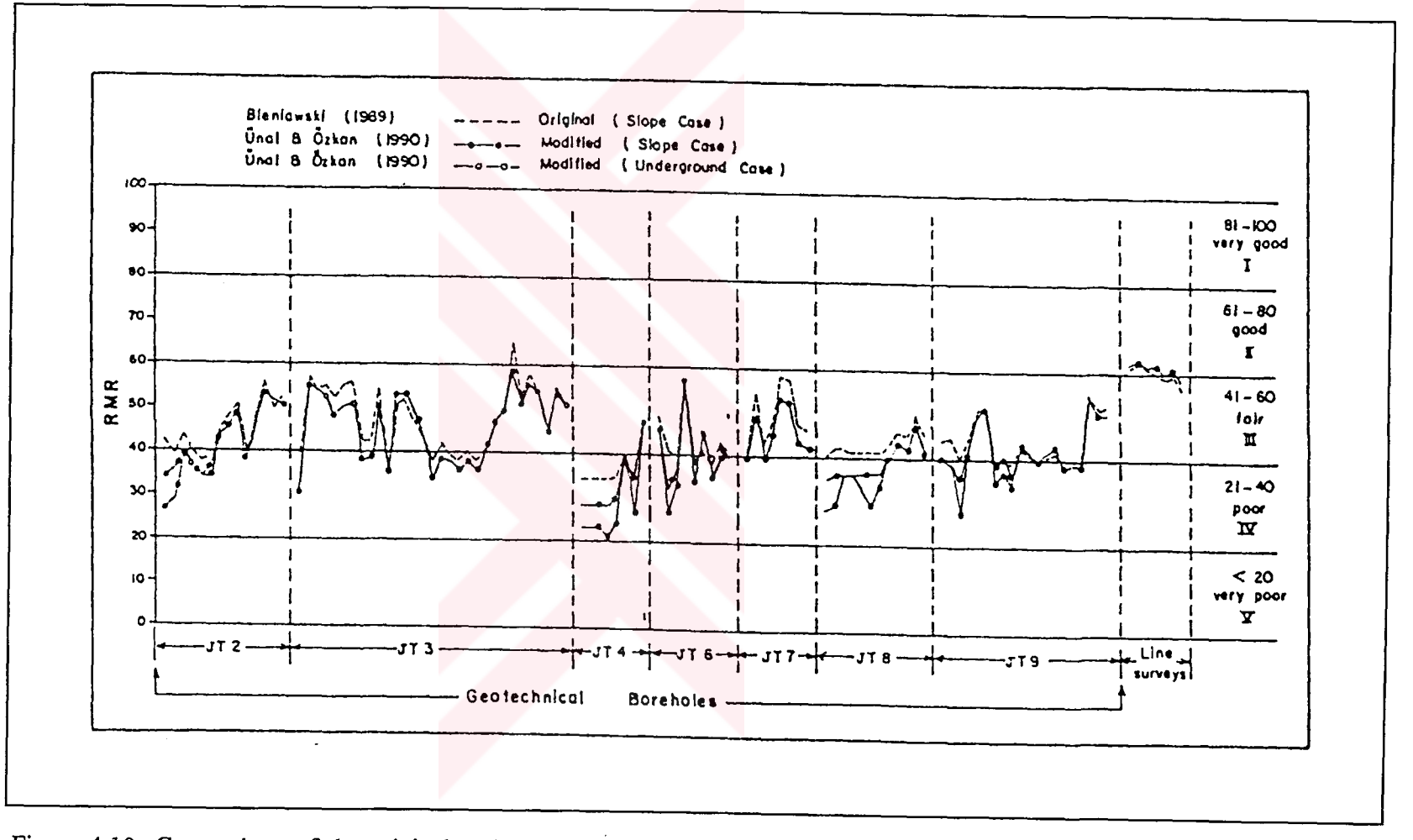

Figure 4.10 Comparison of the original and modified RMR values determined from geotechnical boreholes and scanline survey data in the coal mine (after Ünal et al., 1992)

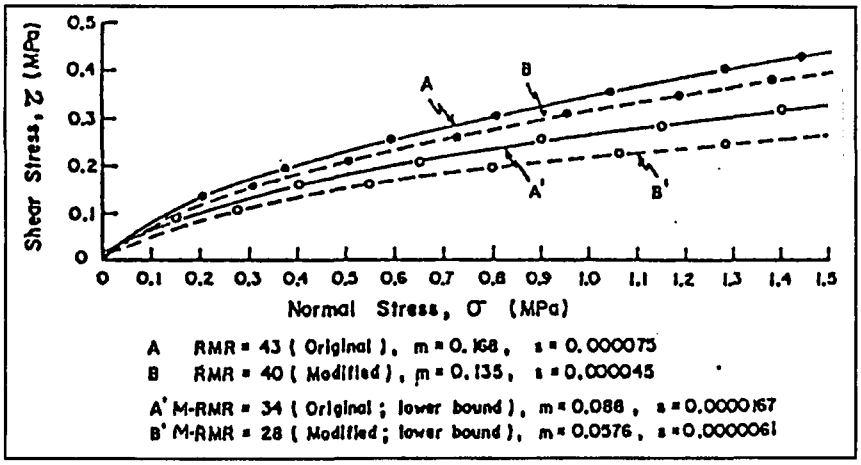

Figure 4.11 Failure envelopes based on empirical failure criterion for mean and lower bound RMR values (slope case) (after Ulusay et al., 1992)

Figure 4.11 suggests that failure envelopes based on mean original and modified ratings show negligible and/or slight differences. While, for lower bound ratings obtained from both systems the difference is noticeable. The same conclusions are also valid for c-ϕ curves shown in Figure 4.12b. This situation indicates that in the case of a slope to be excavated in a weak, stratified and clay-bearing rock mass with an RMR rating less than 40, prime consideration should be given to its shear strength parameters derived from modified system to be on the safe side, particularly at the initial design stage of a planned slope where the rock performance has not been observed yet.

The possibility of a mass failure along the SW sidewall slopes of the investigated pit planned to be excavated in the weak sequence was deterministically analyzed in conjunction with sensitivity approach to assess the effects of shear strength behavior of the rock mass based on both rating systems, on the stability of slope.

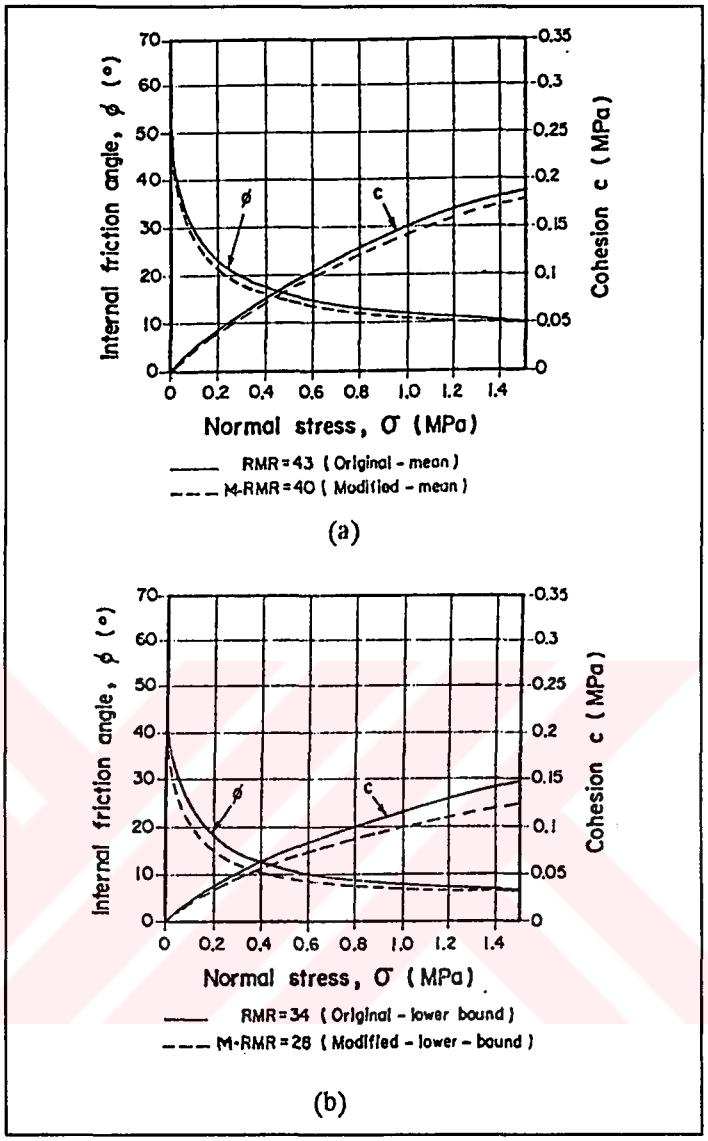

Figure 4.12 Variation of c and ϕ with normal stress for mean (a) and lower (b) bound RMR values obtained from the both systems (slope case) (after Ulusay et al., 1992)

A unit weight of 16.1 kN/m^3, a maximum slope height of 70 m, groundwater conditions prevailing in the pit (Ulusay, 1991) and values of c and ϕ determined from Figure 4.10, based on the normal stress level anticipated in the slope, were considered in two series of analysis. Considering the negligible difference between the strength parameters derived from both systems (Figure 4.12a), parameters associated with an RMR value of 43 (original mean) were employed in the first series of analyses. During second series, parameters from lower bounds of both systems (RMR=34 and 28) were considered. The analyses were carried out using a computer program MTASLP developed at MTA based on Bishop's method (Bishop, 1955). The critical slip surfaces for various overall slope angles are illustrated in Figure 4.13.

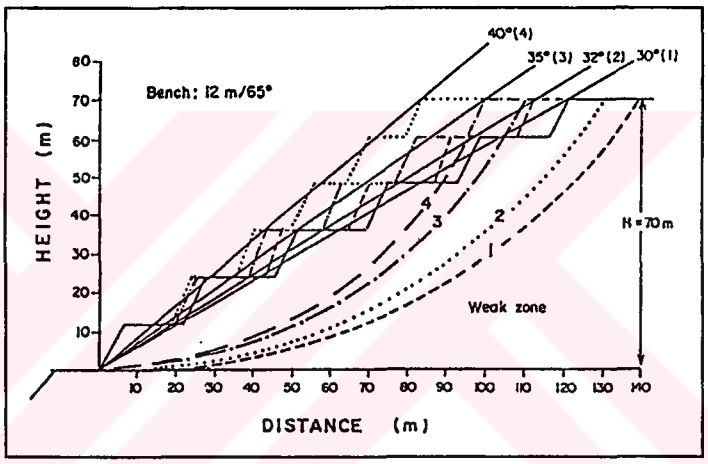

Figure 4.13 Slope configurations analyzed and most critical slip surfaces for a 70 m height slope in the strip coal mine (after Ulusay et al., 1992)

The results of the analyses, presented as a plot of factor of safety, against slope height (Figure 4.14), shows the effect of RMR ratings on the factor of safety. The curves in Figure 4.14 suggest that design of a slope cutting weak stratified and clay-bearing rock mass with an RMR rating lower than 40 based on modified system calls flatter overall slope angles than those of suggested by original RMR values. This

is due to a noticeable reduction recorded in rock mass shear strength parameters based on modified values.

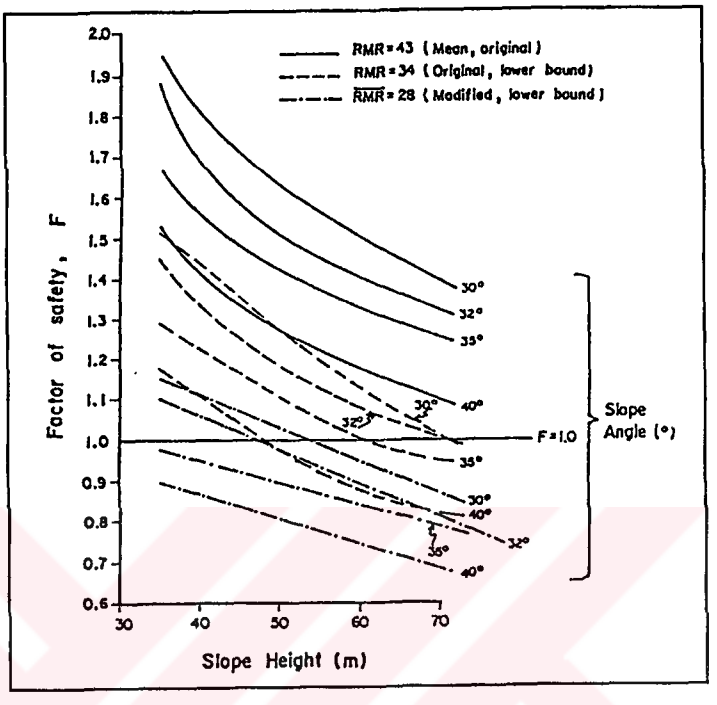

Figure 4.14 Influence of the shear strength parameters from various RMR values on factor of safety (slope case) (after Ulusay et al., 1992)

As a result of these analyses it was shown that a meaningful characterization of the rock mass is essential for optimum design of underground openings and surface slopes excavated in weak, stratified and clay-bearing rock mass. An accurate interpretation and utilization of the outputs of the classification systems are also required for providing stability and safety of these mining structures within economical limits.

CHAPTER V

COMPUTER PROGRAM "ROCK MASS" DEVELOPED BASED ON M-RMR SYSTEM

5.1 General

The three design methods available for assessing the stability of mines and tunnels, providing support recommendations are: (1) analytical, (2) observational and (3) empirical methods.

Empirical methods are based on statistical evaluation of underground observations. Engineering rock mass classification systems constitute the best known empirical approach for assessing the stability of underground openings in rock (Goodman, 1980; Hoek and Brown, 1980). According to Butler and Franklin (1990) empirical design methods have the singular advantage of improving with age.

In empirical design studies, the design engineers usually utilize tables and charts associated with the systems that they are using. They evaluate the input parameters for each structural region based on the information obtained from a lot of borehole cores or underground observations. In some projects, this process should be repeated hundreds of times. Consequently, rock mass classification is a difficult and time consuming process.

In order to decrease the processing time and to obtain the outputs of the RMR system, a computer program called ROCK MASS has been developed by Ünal and Özkan (1990).

Recently, a number of computer programs related to major engineering rock mass classification systems have also been developed, namely:

1. "RMR" (Santos and Bieniawski, in Bieniawski 1989)
2. "CLASSEX" (Butler and Franklin, 1990)
3. "Q" (Bhasin, 1994).

5.2 ROCKMASS Computer Program

The computer program "ROCK MASS" has been developed based on Modified RMR System (Ünal and Özkan, 1990) at the Middle East Technical University (METU). The original RMR and Q values may also be determined by using the program.

Figure 5.1 shows the general structure of the ROCK MASS. In order to use this program, the input data form, presented in Figure 3.1 in Chapter III, should be used.

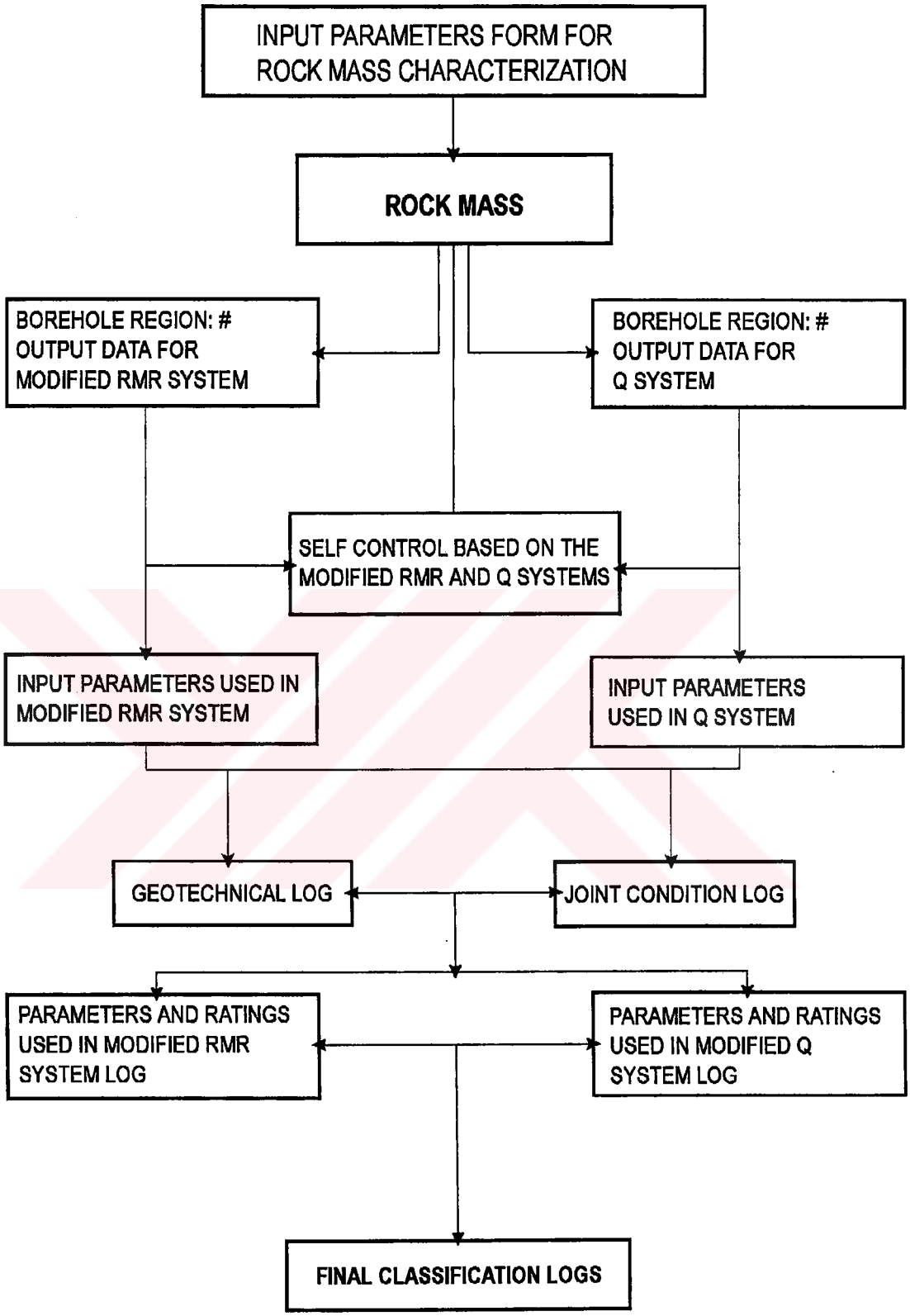

Figure 5.1 The structure of "ROCK MASS" program

As initial output of this program, a general drilling information provided and a tabulated summary of the input parameters can be obtained as shown in Figure 5.2 and 5.3.

ROCK MASS

LOGS FOR CLASSIFICATION SYTEMS

METU

Drill Site.....:OAL-ÇAYIRHAN	Number of Borehole....:KM 510-1
Type of Machine.....:TURMAK	Logged By.....:İhsan öZKAN
Core Barrel.....:B-86	Checked By.....:Dr. Erdal ÜNAL
Bit.....:DIAMOND	Start of Logging Date.:15.3.1991
X-Coordinate.....:42356.459	End of Logging Date...:30.10.1991
Y-Coordinate.....:89372.174	Z-Coordinate.....:585.850

Figure 5.2 The general drilling information for underground borehole KM 810-1

INPUT PARAMETERS USED IN MODIFIED RMR SYSTEM (KM 810-1)

INTERVAL	ROCK TYPE	STR	RQD	ICR	#J/m	GW	Id2	W	RD	RP	PRS	Ap	FT	FS
.0 - .03	A1	1	67	67	33	13	98	UW	U.	R	VL	0.0	1	S
.03 - .07	A2	2	67	67	25	13	99	UW	P.	S	M	0.0	1	H
.07 - .21	A3	2	67	67	14	13	98	UW	U.	SR	VL	0.0	1	S
.21 - .57	A2	2	66	78	22	13	99	UW	P.	SR	M	0.0	0	-
.57 - .63	B	3	65	100	17	13	99	UW	U.	S	VL	0.0	1	H
.63 - .97	A2	2	65	100	6	13	99	UW	P.	S	VH	0.0	5	H
.97 - 1.4	B	3	75	100	9	13	99	UW	P.	S	M	0.0	5	H
1.4 - 3.2	A5	1	85	93	6	13	98	UW	P.	SR	M	0.0	0	-
3.2 - 3.55	A5-1	2	83	100	9	13	99	UW	P.	S	M	0.0	8	H
3.55 - 4.55	A4	2	80	92	4	13	99	UW	P.	SR	VH	0.0	5	H
4.55 - 5.4	C2	2	72	85	33	13	99	UW	U.	S	M	0.0	2	H
5.4 - 5.92	D	0	87	100	25	13	97	UW	P.	SR	M	0.0	0	-
5.92 - 5.93	H	2	87	100	100	13	100	UW	U.	SR	VL	0.1	0	-
5.93 - 6.4	E1	0	56	66	9	13	95	UW	U.	S	VL	0.1	0	-
6.4 - 6.87	E2	0	67	81	17	13	95	UW	U.	S	VL	0.1	0	-
6.87 - 8.2	F	0	11	44	36	13	92	UW	U.	S	VL	1.0	0	-
8.2 - 8.25	H	2	0	54	20	13	100	UW	U.	SR	VL	0.0	10	S
8.25 - 8.37	G	1	0	54	8	13	99	UW	U.	SR	VL	1.0	0	-
8.37 - 8.7	H	2	0	54	9	13	100	UW	U.	SR	VL	0.0	10	S

Figure 5.3 The output form for input parameters of underground borehole KM 810-1

As an output, the importance ratings associated with the output parameters of the modified RMR and the original and modified Q systems may also be obtained together with the final rock mass classification index values as presented in Figure 5.4.

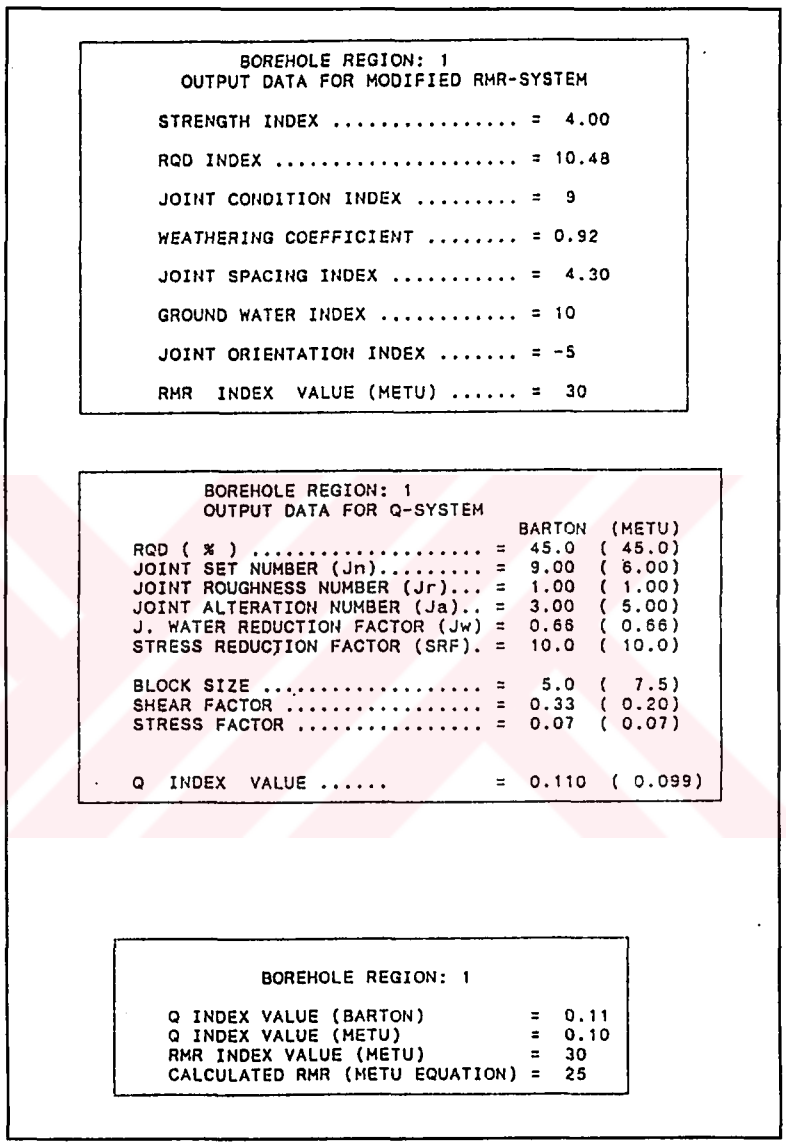

```
        BOREHOLE REGION: 1
   OUTPUT DATA FOR MODIFIED RMR-SYSTEM

  STRENGTH INDEX ..............  =  4.00

  RQD INDEX ...................  = 10.48

  JOINT CONDITION INDEX .......  =  9

  WEATHERING COEFFICIENT ......  = 0.92

  JOINT SPACING INDEX .........  =  4.30

  GROUND WATER INDEX ..........  = 10

  JOINT ORIENTATION INDEX .....  = -5

  RMR  INDEX  VALUE (METU) ....  =  30
```

```
        BOREHOLE REGION: 1
        OUTPUT DATA FOR Q-SYSTEM
                                          BARTON   (METU)
  RQD ( % ) ..................  =  45.0   ( 45.0)
  JOINT SET NUMBER (Jn).......  =  9.00   ( 6.00)
  JOINT ROUGHNESS NUMBER (Jr)...=  1.00   ( 1.00)
  JOINT ALTERATION NUMBER (Ja).. =  3.00   ( 5.00)
  J. WATER REDUCTION FACTOR (Jw) =  0.66   ( 0.66)
  STRESS REDUCTION FACTOR (SRF). =  10.0   ( 10.0)

  BLOCK SIZE .................  =   5.0   (  7.5)
  SHEAR FACTOR ...............  =  0.33   ( 0.20)
  STRESS FACTOR ..............  =  0.07   ( 0.07)


  Q  INDEX  VALUE ......        =  0.110  ( 0.099)
```

```
        BOREHOLE REGION: 1

  Q INDEX VALUE (BARTON)          =  0.11
  Q INDEX VALUE (METU)            =  0.10
  RMR INDEX VALUE (METU)          =  30
  CALCULATED RMR (METU EQUATION)  =  25
```

Figure 5.4 Output data for modified RMR and Q systems and comparison of Q and RMR values for borehole region 1

The geotechnical and joint condition logs, logs for modified RMR and Q parameters, and combined RQD, RMR and Q logs for a given borehole input data (Figures 5.5a and 5.5b). The presented Figures 5.2 through 5.5 are typical outputs of the ROCK MASS program. The outputs of ROCK MASS computer program prepared for all of borehole regions at Çayırhan Coal Mine have been given elsewhere (Ünal et al., 1994).

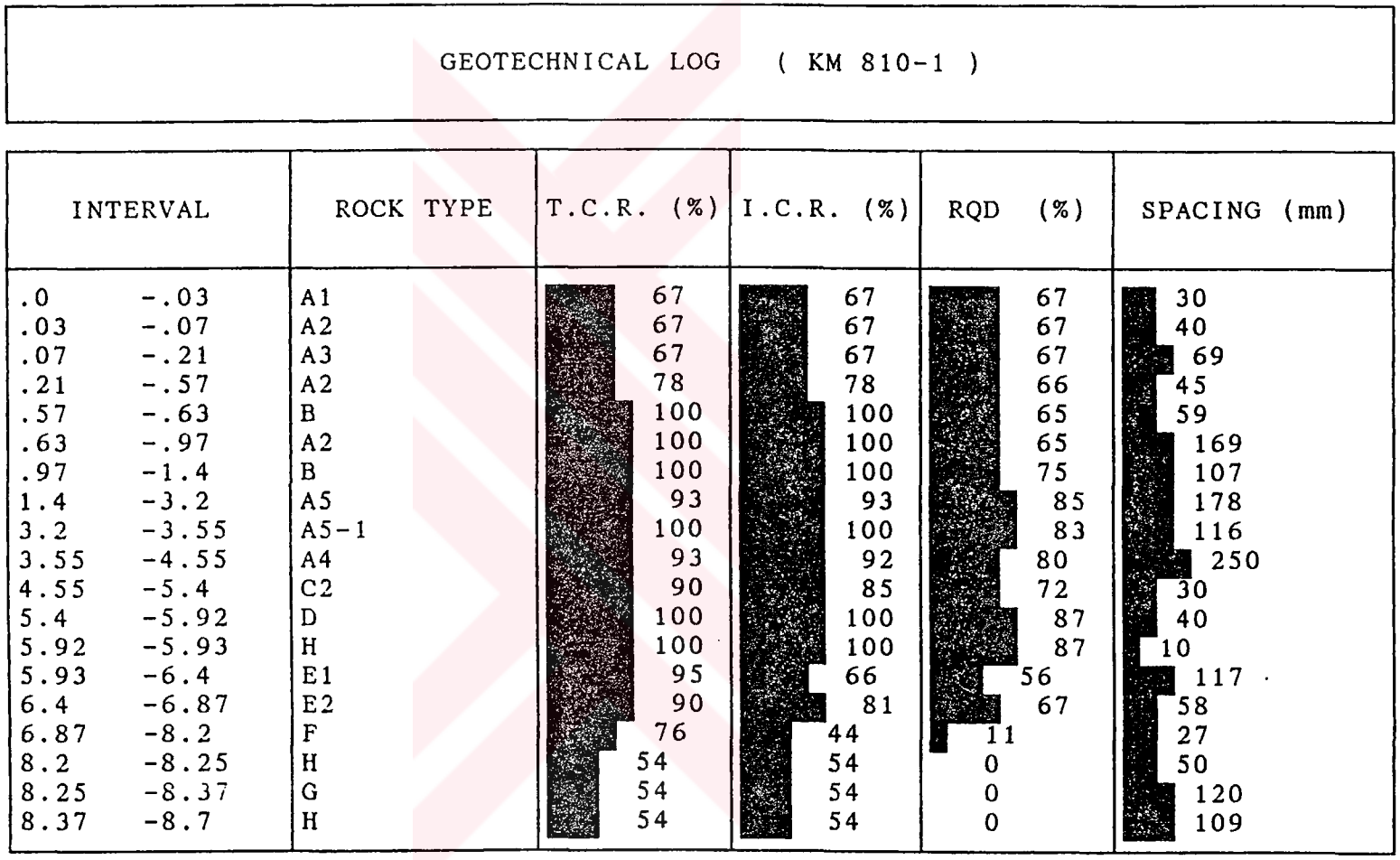

Figure 5.5a Output obtained from computer program ROCK MASS: input parameters used and geotechnical log for underground borehole KM 810-1

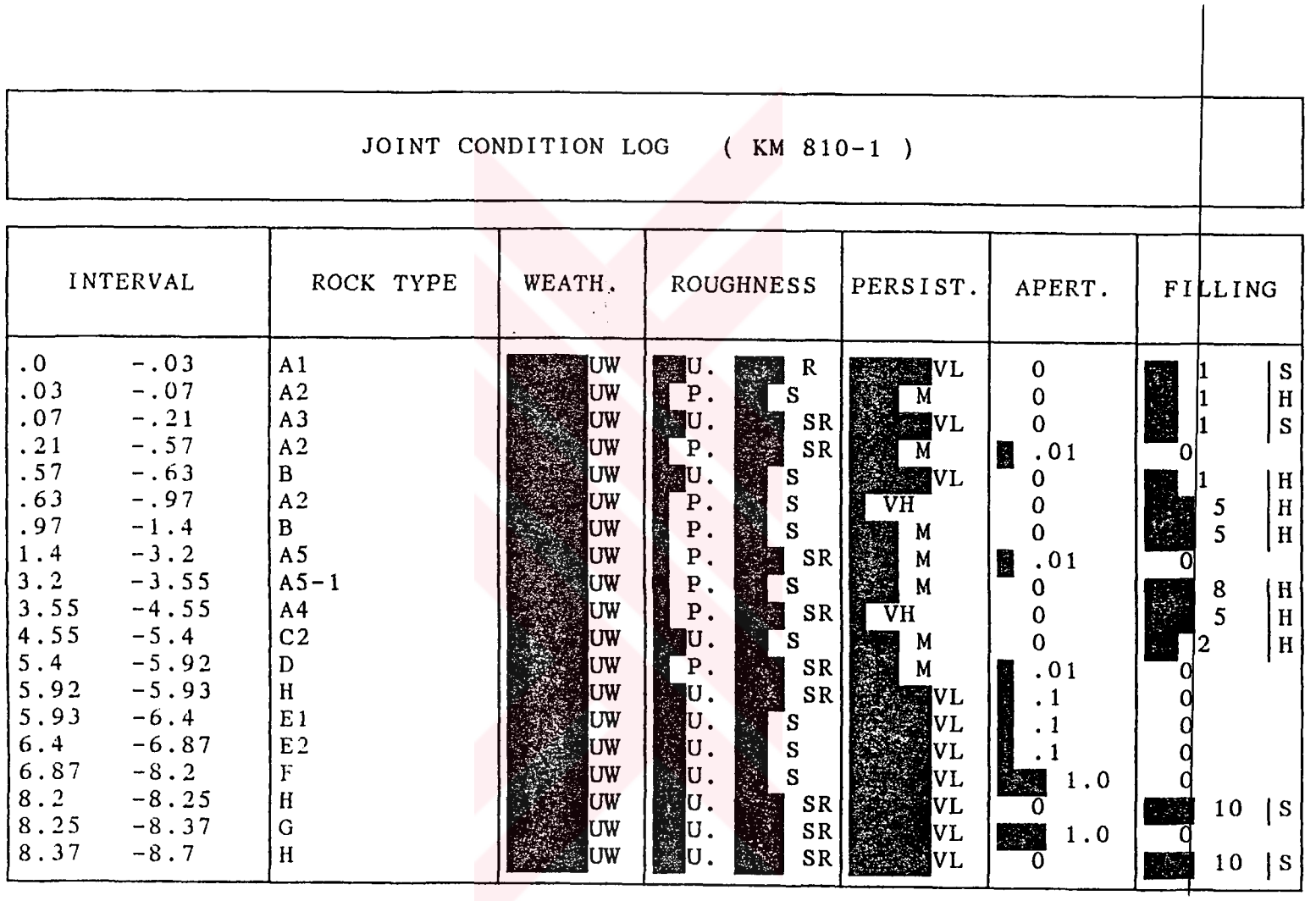

Figure 5.5b Output obtained from computer program ROCK MASS: input parameters used and joint condition log for underground borehole KM 810-1

PARAMETERS AND RATINGS USED IN MODIFIED RMR SYSTEM (KM 810-1)

INTERVAL	R.TYPE	STRI	RQDI	JSI	JCI	GWI	JOI	Fc
.0 -.03	A1	4	14	7	15	10	-5	1.14
.03 -.07	A2	5	14	8	13	10	-5	1.15
.07 -.21	A3	6	14	9	15	10	-5	1.14
.21 -.57	A2	5	14	8	18	10	-5	1.15
.57 -.63	B	8	14	8	18	10	-5	1.15
.63 -.97	A2	5	14	10	4	10	-5	1.15
.97 -1.4	B	8	16	9	6	10	-5	1.15
1.4 -3.2	A5	4	17	10	18	10	-5	1.14
3.2 -3.55	A5-1	5	17	10	6	10	-5	1.15
3.55 -4.55	A4	6	17	11	4	10	-5	1.15
4.55 -5.4	C2	6	15	7	13	10	-5	1.15
5.4 -5.92	D	2	18	8	18	10	-5	1.14
5.92 -5.93	H	5	18	1	26	10	-5	1.15
5.93 -6.4	E1	1	12	10	24	10	-5	1.12
6.4 -6.87	E2	1	14	8	24	10	-5	1.12
6.87 -8.2	F	2	5	7	24	10	-5	1.11
8.2 -8.25	H	5	3	8	0	10	-5	1.15
8.25 -8.37	G	4	3	10	26	10	-5	1.15
8.37 -8.7	H	5	3	9	0	10	-5	1.15

Figure 5.5c Output obtained from computer program ROCK MASS: parameters and ratings used in RMR system

PARAMETERS AND RATINGS USED IN MODIFIED Q SYSTEM (KM 810-1)

INTERVAL	R.TYPE	RQD	Jn	Jr	Ja	Jw	SRF
.0 -.03	A1	67	12	3	1	1	2.5
.03 -.07	A2	67	12	1.0	6	1	2.5
.07 -.21	A3	67	6	3	4	1	2.5
.21 -.57	A2	66	12	1.5	6	1	2.5
.57 -.63	B	65	6	2	3	1	2.5
.63 -.97	A2	65	2.0	1.0	6	1	2.5
.97 -1.4	B	75	3.0	1.0	6	1	2.5
1.4 -3.2	A5	85	2.0	1.5	8	1	2.5
3.2 -3.55	A5-1	83	3.0	1.0	6	1	2.5
3.55 -4.55	A4	80	2.0	1.5	6	1	2.5
4.55 -5.4	C2	72	12	2	1	1	5.0
5.4 -5.92	D	87	12	1.5	8	1	5.0
5.92 -5.93	H	87	15	3	5	1	5.0
5.93 -6.4	E1	56	3.0	2	4	1	2.5
6.4 -6.87	E2	67	6	2	4	1	2.5
6.87 -8.2	F	10	12	2	20	1	5.0
8.2 -8.25	H	10	12	3	20	1	5.0
8.25 -8.37	G	10	2.0	3	1	1	2.5
8.37 -8.7	H	10	3.0	3	1	1	2.5

Figure 5.5d Output obtained from computer program ROCK MASS: parameters and ratings used in Q system

FINAL CLASSIFICATION LOGS (KM 810-1)

INTERVAL	ROCK TYPE	R Q D	R M R	Q
.0 -.03	A1	67	50	6.7
.03 -.07	A2	67	50	0.37
.07 -.21	A3	67	54	3.35
.21 -.57	A2	66	56	0.55
.57 -.63	B	65	60	2.89
.63 -.97	A2	65	42	2.17
.97 -1.4	B	75	49	1.67
1.4 -3.2	A5	85	61	3.19
3.2 -3.55	A5-1	83	47	1.84
3.55 -4.55	A4	80	47	4.00
4.55 -5.4	C2	72	52	2.40
5.4 -5.92	D	87	56	0.27
5.92 -5.93	H	87	62	0.70
5.93 -6.4	E1	56	57	3.73
6.4 -6.87	E2	67	58	2.23
6.87 -8.2	F	11	47	0.02
8.2 -8.25	H	0	22	0.03
8.25 -8.37	G	0	52	6.0
8.37 -8.7	H	0	24	4.00

Figure 5.5e Output obtained from computer program ROCK MASS: parameters and ratings used in final classification logs

ROCK MASS computer program does not include the support recommendations; however, the final classification outputs of this program can use as input for the ROCKBOLT V5.0, STARCH V2.0, SHAFT V2.0 and LW-SHIELD V2.0 which were developed by Ünal and Ergür (1990), Ünal (1989), Ünal and Akçakoca (1989), Aghai (1990) and Özel (1995) respectively. The simplified structure for detailed support recommendations is as Figure 5.6.

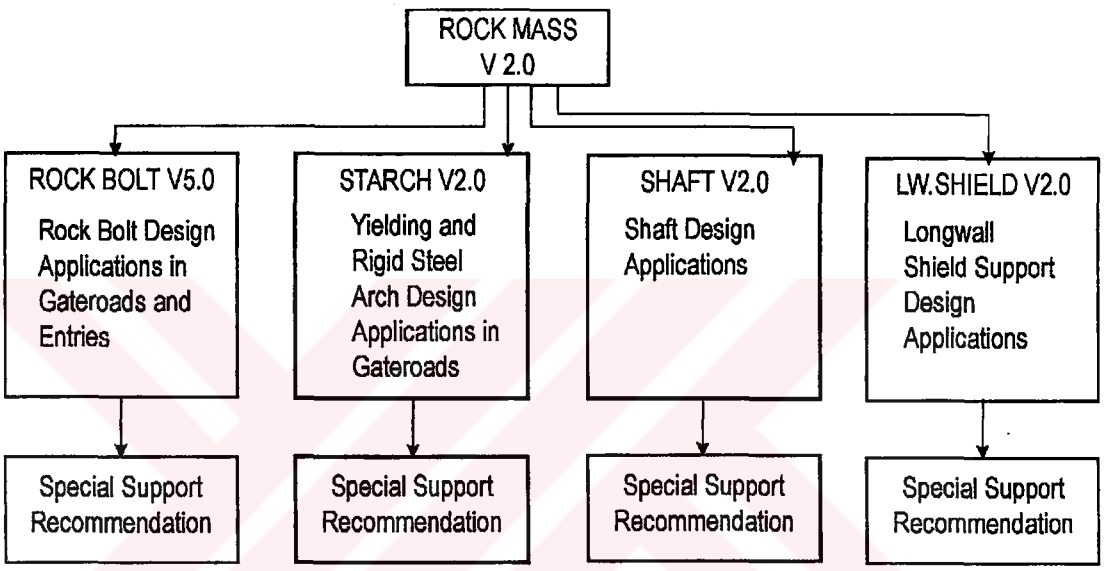

Figure 5.6 The simplified support recommendation structure

CHAPTER VI

ROOF BEHAVIOR AT A-810 GATE ROAD IN ÇAYIRHAN COAL MINE

6.1 General

The Middle Anatolian Lignite Mine (O.A.L.) lies in the western part of Ankara province, between the towns Beypazarı and Nallıhan, 123 km away from Ankara. The mine is operated by Turkish Coal Enterprises (T.K.İ.). As of 1995, the O.A.L. Mine (Çayırhan Lignite Mine) is the only fully mechanized underground coal (lignite) mine in Turkey.

Çayırhan formations are of Miocene age. There are two lignite seams separated by an intermediate marl layer having a thickness of approximately 80 cm. The upper seam has an average thickness of 150 cm and the lower seam is 170 cm. Roof rock of the upper seam is silisified limestone and floor rock of the lower seam is fairly strong claystone. At the working panels, the seam inclination ranges between 3 - 18 degrees, at depths of 150 - 250 meters. Stratigraphical section of Çayırhan region is illustrated in Figure 6.1.

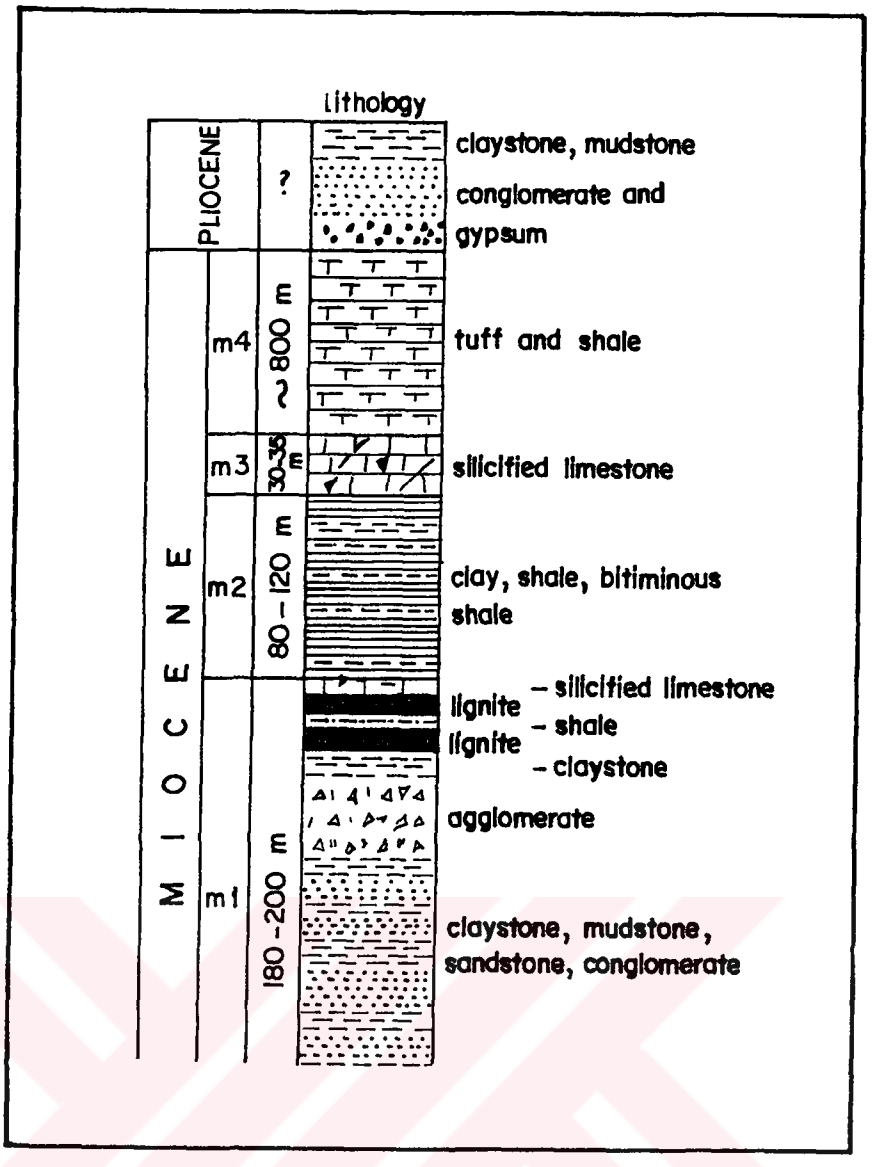

Figure 6.1 Stratigraphical section of Çayırhan region (after İstanbulluoğlu, 1995)

The total and proved reserves in coal basin are 430 and 345 million tons of lignite, respectively (İstanbulluoğlu, 1995). The chemical properties of the Çayırhan coal seams are presented in Table 6.1.

Table 6.1 Chemical properties of Çayırhan coal seams (after İstanbulluoğlu, 1995)

Property	Value
The average calorific value	2800 kcal/kg
Moisture content	30 %
Ash content	27.5 %
Sulphur content	4.65 %

Two main faults, namely the North and Davutoğlan, running in NE and SW direction divides the Çayırhan deposit into the mining fields; A and F (south of the fault), B and C (north of the fault), and D (east of the running out fault). A general plan view of the mine panels and the roadways are shown in Figure 6.2.

6.2 General Information About Gate-roads in Çayırhan Lignite Mine

6.2.1 Excavation and Support System

In Çayırhan lignite mine, retreating longwall mining is employed, and the coal seams in a panel are mined simultaneously with the upper face running about 20 - 30 meters ahead of the lower face. The longwall face lengths are 220 meters while the panel lengths vary between 800 and 1000 meters. The planned production rate is about 6,500 tons per day.

Coal in the face is cut by means of a double drum shearer each having an installation power of 230 kW. The face is supported by means of lemniscated type 2-leg shield supports having 240 ton capacity and consisting of three-stroke props. Double chain armored face conveyors are utilized to transport the coal from face to the stage loader chain conveyor at the main gate roadway. In gate roadways and main

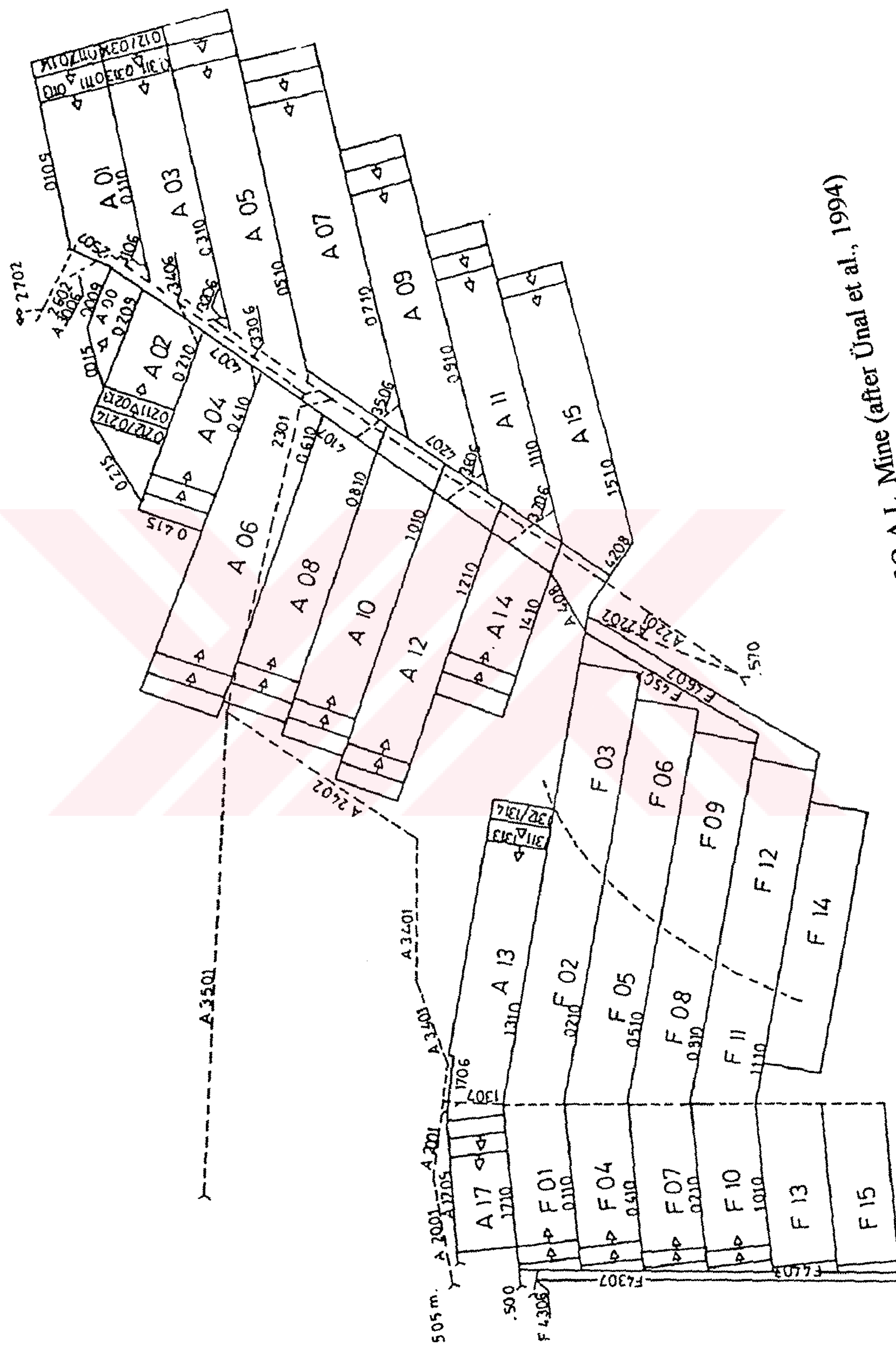

Figure 6.2 General plan view of O.A.L. Mine (after Ünal et al., 1994)

roadways lignite is continuously transported by belt conveyors of various capacities. The transportation of the mine personnel and the material are realized by monorails and floor-mounted transportation system.

6.2.2 Gate Roads

The gate roadways in the mine are enlarged to 16.8 m^2 in cross-section, to be simultaneously utilized by both the upper and the lower faces. No coal-pillar is left between the panel and the main gate. The main gate-road is protected by a concrete packing, 1.5 meters wide. A detailed information on packing is given by İstanbulluoğlu (1995). The gate roads are utilized twice. Initially, as the main gate of working panel, and for the second time as the tail gate of the adjacent panel. The gate road support is thus affected four times by the advance of the retreating faces, namely, two times by the upper and lower faces of the working panel (during the first use of the roadway as main gate), and two times by the other two faces of the adjacent panel (during second use of the roadway as a tail gate). A plan view of the longwall panels and position of the main and tail gate roadways are shown in Figure 6.3. Therefore, special attention should be given to stability of the roadways and the support systems used in these openings.

Currently, rigid type steel ribs with one-meter spacing are being used in gate roads; however, in the section of the main gate which is under the influence of the advancing longwall faces, sliding type of friction prop sets are used as a supplementary support. These sets consist of a cap and two GI 140 profile steel props. When the upper face approaches, face side and rib side rigid props, originally existing in the set are replaced by yielding type props and a middle hydraulic prop is added to the system (İstanbulluoğlu, 1995).

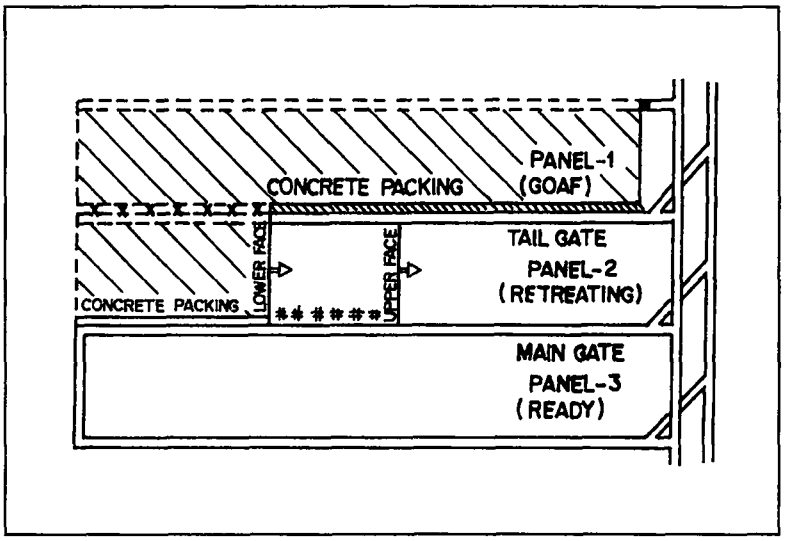

Figure 6.3 Plan view of longwall panel and position of gate roads in Çayırhan coal mine (after Ünal and Özkan, 1993)

After the lower face has been advanced, the concrete pack between the bottom and the top of gate road is constructed and in essence, support system is completed.

6.3 Field Studies and Characterization of Roof Strata

6.3.1 General

Basic site investigations, drilling nine boreholes in underground, characterization of roof strata, taking photographs of the core boxes, evaluation of the cores for classification purposes, and carrying out extensive rock mechanics tests were the main activities associated with field and laboratory studies in Çayırhan.

The original and modified RMR and Q values were determined by using a computer program called "ROCK MASS". Using this program, complete output data for each borehole were obtained including: input data provided; importance ratings

for the given input data; geotechnical log; log of input parameters used in modified RMR system; and final classification logs (RQD, RMR and Q).

After evaluating the data obtained from field and laboratory studies, the rock mass was classified based on modified RMR system. In classification process, computer program "ROCK MASS V2.0" was utilized.

In predicting the rock reinforcement requirements at Gate-Road A-810 four bolt types, namely, Split-Set, Swellex and two different resin bolts (German-Sis and British-Fosroc) were considered. The computer program called "ROCKBOLT V5.0" was utilized during design analyses. A typical input data used during design analysis are given in Table 6.2. The output specifications suggested for rock bolting applications are presented in Table 6.3.

Table 6.2 Input parameters used in design of A-810 gate road (after Ünal et al., 1994)

Input Parameters	Value
Rock Mass Rating (RMR)	50 (weighted average)
Roof Span	5.85 meters
Overburden Thickness	250 meters
Unit Weight of Immediate Roof	20 kN/m^3
Unit Weight of Overburden	23 kN/m^3
Horizontal-to-Vertical Stress Ratio	1/3
Type of Immediate Roof	Stratified Marl

Table 6.3 Typical design outputs associated with rock reinforcement applications in A-810 gate road (after Ünal et al., 1994)

Output Parameters	Split Set	Yielding Super Swellex
. Bolt Length ... vertical (L)	2.00 m	1.80 m
... inclined (L′)	2.80 m	3.00 m
. Bolt Diameter	39.0 mm	48.0 mm
. Hole Diameter	35.5 mm	54.0 mm
. Bolt Spacing	1.0 m	1.36 m
. Bolting Pattern	1.0 x 1.0 m	1.0 x 1.5 m
. Steel Grade	SS-39 (Standard)	G60 (ST 42, Min.)
. Anchorage Capacity	54 kN	180 kN
. Water Pressure	—	25 MPa

Output Parameters	Sis Resin Bolt	Fosroc Resin Bolt
. Bolt Length ... vertical (L)	2.20 m	1.80 m
... inclined (L′)	3.00 m	3.00 m
. Bolt Diameter	28.0 mm	25.0 mm
. Hole Diameter	32.0 mm	32.0 mm
. Bolt Spacing	1.20 m	1.20 m
. Bolting Pattern	1.0 x 1.5 m	1.0 x 1.5 m
. Steel Grade	G40 (ST 27, Min.)	G60 (ST 42, Min.)
. Anchorage Capacity	180 kN	180 kN

6.3.2 General Information About Pilot Study in A-810 Gate Road

Considering the result of design analysis obtained during preliminary design stage, each rockbolt type was installed systematically together with wire mesh in about every 50-meter section of the main gate A-810. Including a 50-meter long roadway supported by yielding steel ribs only, a total of 250-meter section of the gate road was currently under investigation. A plan view of the gate road showing the location of the supports used, and of the convergence and borehole extensometer stations is presented in Figure 6.4.

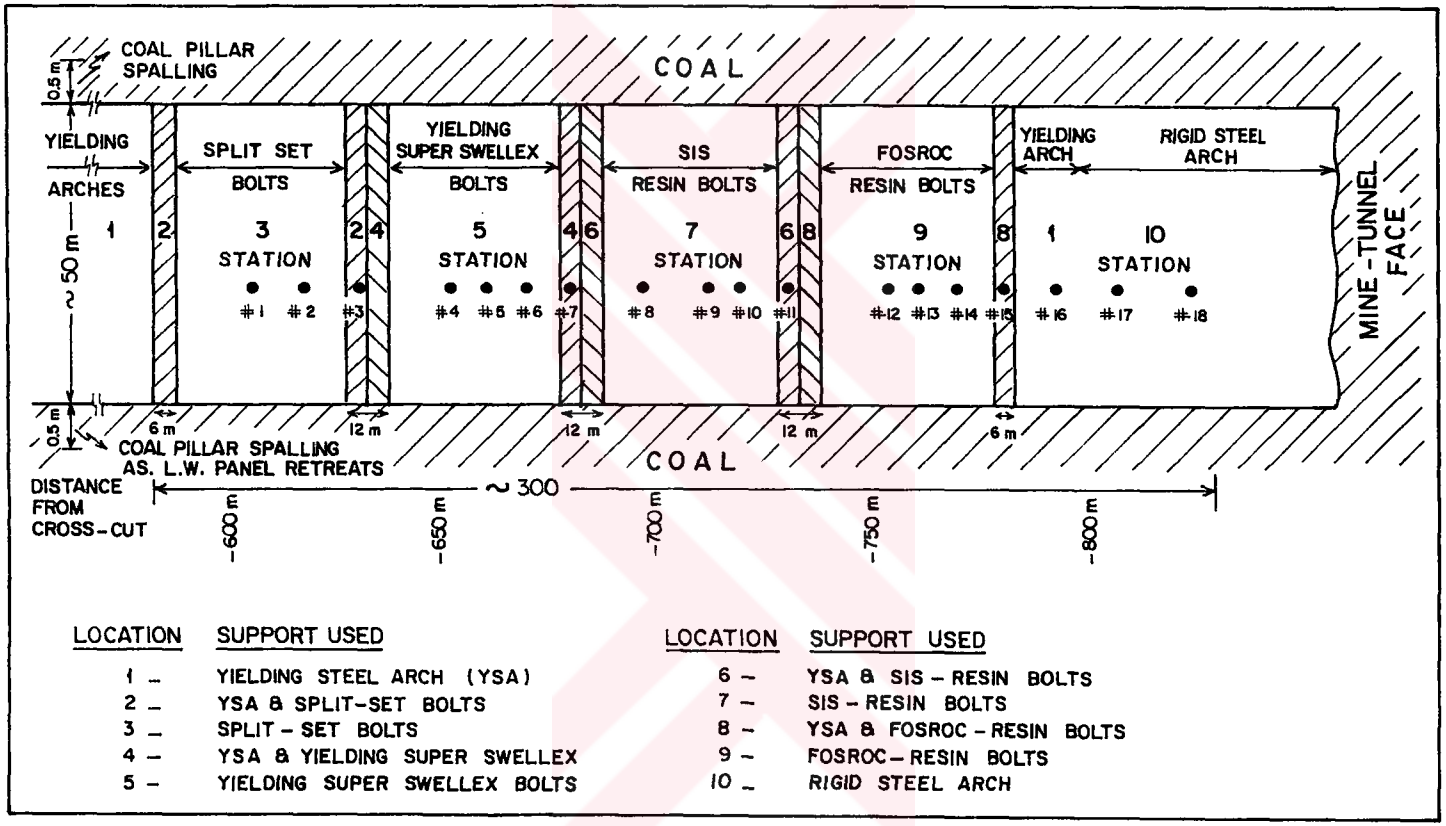

Figure 6.4 Plan view of A-810 Gate-Road, showing the locations of the supports used and of the convergence and borehole extensometer stations (after Ünal et al., 1994)

6.3.3 Specifications of Overall Monitoring System

The underground measurements in Çayırhan Lignite Mine were initiated in order to firstly the performances of the four different rock bolt types and the two different type of steel arches used in a gate road and to check the validity of the support design method used. These measurements were made in ten different support locations of the A-810 gate roadway.

The convergence and roof strata measuring systems and pull-out test system used during in situ measurements are explained in the following paragraphs.

Convergence Measuring System

In order to measure the in mine roadways a convergence recorder was designed in the Mining Engineering Department of Middle East Technical University. The original design of this instrument had been made by U.S. Bureau of Mines; however, the instrument used in this study was modified considering the local conditions in Çayırhan Lignite Mine region. A schematic diagram of home-made convergence recorder is given in Figure 6.5.

Basically the convergence recorder is made up of three telescopic steel tubes sliding within each other. The spring on the unit provides flexibility to the instrument when located between two fixed measuring points. As a result of the vertical closure, the lower and intermediate tubes move and compress the spring. A dial gauge, fixed to the lower tube, makes contact with a horizontal plate which is fixed to the intermediate tube. The movements between 0 - 50 mm can be read from this dial gauge with a resolution of 0.01 mm. Movements that are larger than 25 mm can be read from small holes by adjusting the position of these holes replaced with 25

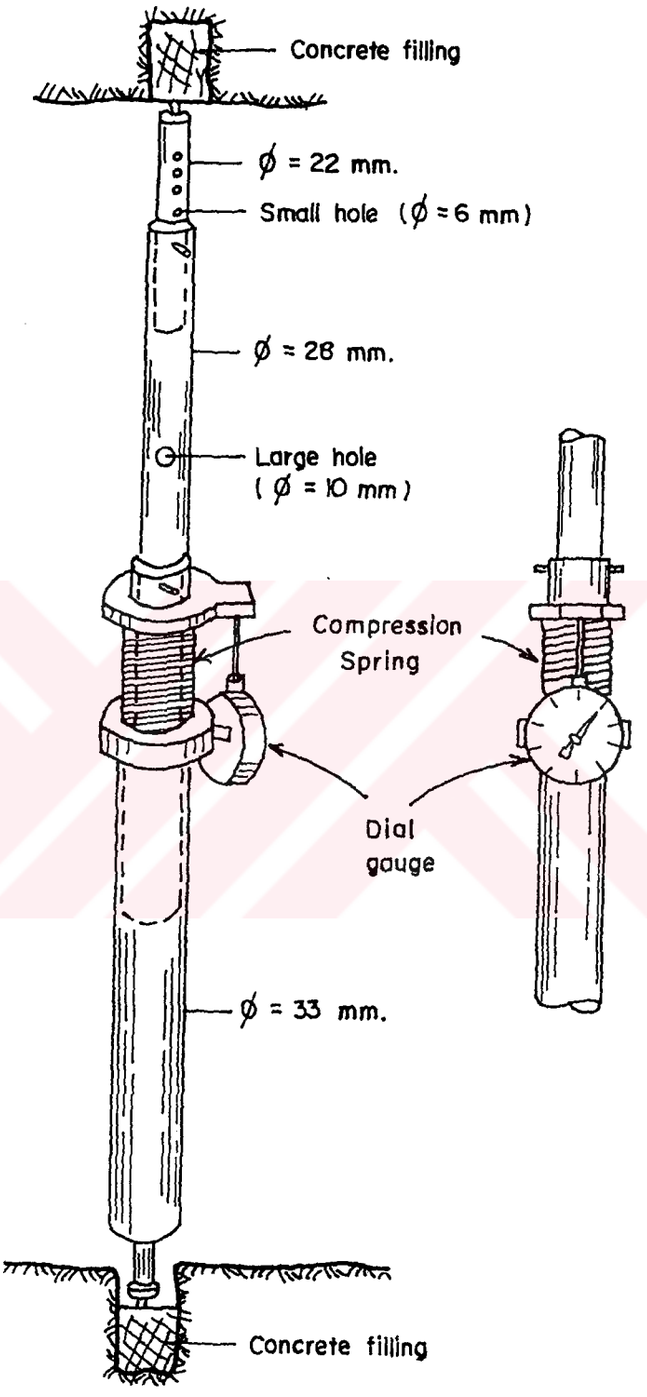

Figure 6.5 A typical convergence recorder

mm intervals on the upper tube. Thus, after each 25 mm movement, the upper tube should be adjusted to the next small hole and the reading in between should be made by dial gage. There are 21 small holes in the upper tube which provides reading range of 500 mm. When this range is not sufficient, then adjustment should be made by using the large holes made on the intermediate tube and the located with a 500 mm interval. The convergence recorder can be used within openings ranging between 2.60 and 4.50 meters.

Roof Strata Movement Measuring System

The differential sag (roof strata displacement) station provides an effective method of monitoring roof strata movement relative to an assumed stable rock horizon. The concept is simple: placing lengths stainless steel wire at various distances into the immediate roof and measuring the change in length of each wire at a common reference point. Through several formulae, the strata movement at the various locations as well as separations between points can easily be determined.

In order to determine the roof strata movement in A-810 gate road, a sag measuring system, as convergence recorder, was designed in Mining Engineering Department of METU. Figure 6.6 illustrates the components used in a typical sag station installation. Initially, a 41-mm diameter borehole is drilled to a depth where the rock mass is assumed relatively stable. The first 450 cm or so of the hole is overdrilled with a 30-cm bit in order that the copper tube can be grouted into the roof. The segments of stainless steel wire are attached to the anchoring springs and placed at various horizons in the borehole with a special setting tool. The free ends of each wire are fed through holes in the end cap and ferrules are crimped on each lead to allow insertion of a measuring device. A dial gage, capable of recording displacements to

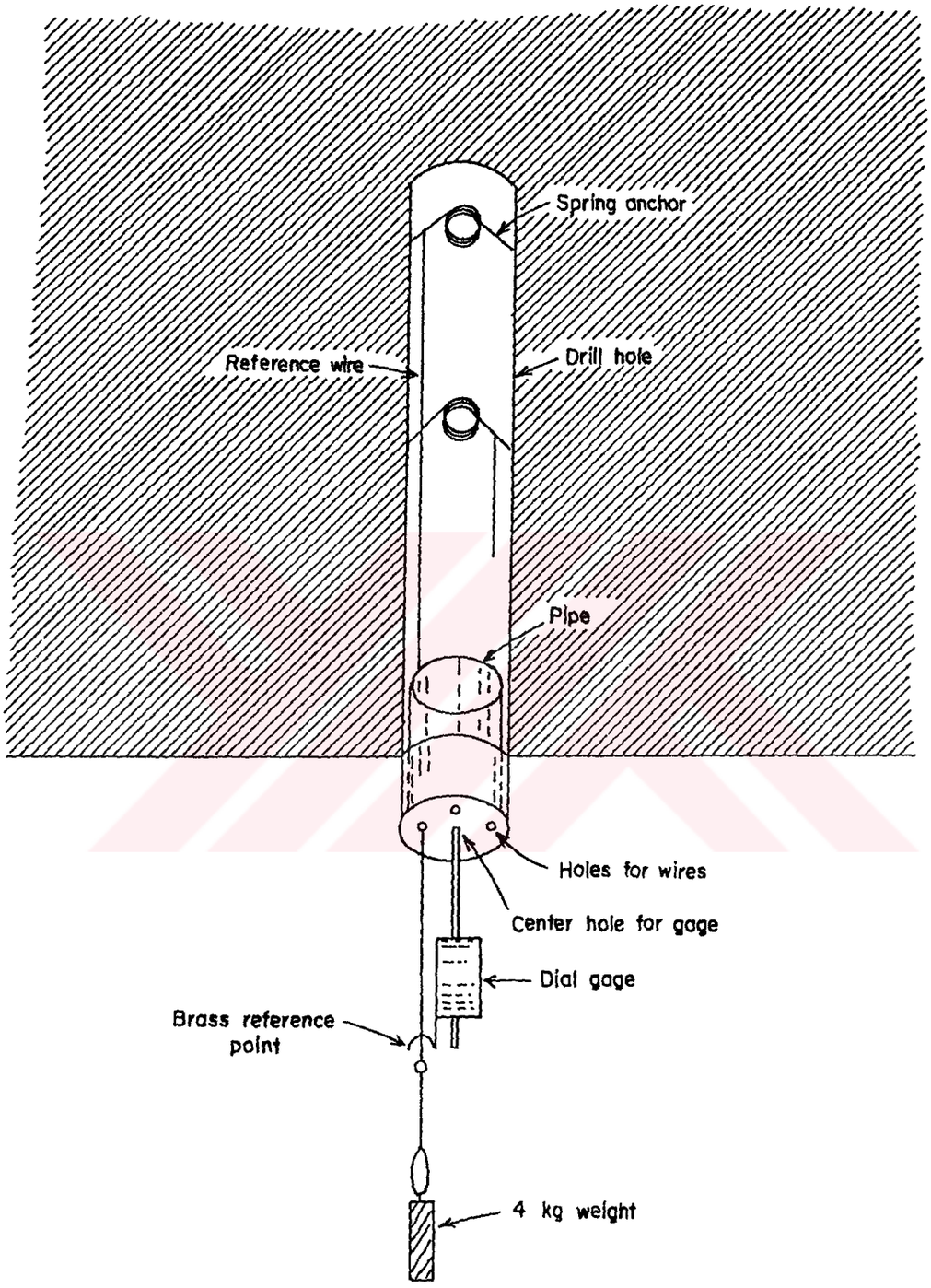

Figure 6.6 A typical roof sag station

the nearest 0.01 mm, with a 30-mm range is generally employed. To provide a uniform wire tension when readings are taken, a weight is hung from a loop in each lead, thus insuring consisting measurements.

Pull-Out Tests

This test is intended to measure the short term anchorage capacity of a rock bolt installed under field conditions. The equipment to test the efficiency (anchorage capacity) of different rock bolts were obtained from the manufacturer of the rock bolt. Anchorage capacity measured by a pull test in which bolt head displacements was measured as a function of the applied bolt load to give a load displacement curve.

6.3.4 Pilot Study in A-810 Gate Road

Field and laboratory studies carried out include: i) rock mass characterization, ii) rock mass classification, iii) design analysis, iv) pilot study, and v) performance monitoring.

During pilot studies certain sections of the gate road were supported by rigid steel arches, yielding steel arches and four different type of rock bolts, namely; split-set, yielding super swellex, sis-resin and fosroc-resin. The bolts were installed systematically together with wire mesh. The technical specifications and the pattern of bolts were determined based on the results of design analysis.

Each support type was installed to about 50-meter section of the A-810 main gate as shown in Figure 6.4. At the borders of the each rock bolt support section, called mixed regions, the bolts were used together with steel arches. The reason for this was to prevent a support section from the effect of the other. In mixed regions, bolting pattern used was not different than the ones used in other regions; however, the spacing of the steel arches was one meter. The technical specifications and the pattern of the rock bolts used during the pilot study are shown in Figures 6.7a, 6.7b, 6.8a and 6.8b.

6.3.5 Locations of In Situ Measuring Stations

In order to investigate the effectiveness of the support system used and to provide a feed back to the design method utilized 18 convergence and 16 borehole extensometer stations were installed in A-810 gate road.

The convergence measurement stations (K) in 10 different support locations are listed in Table 6.4.

The borehole extensometer stations (E) at 9 different support locations are given in Table 6.5.

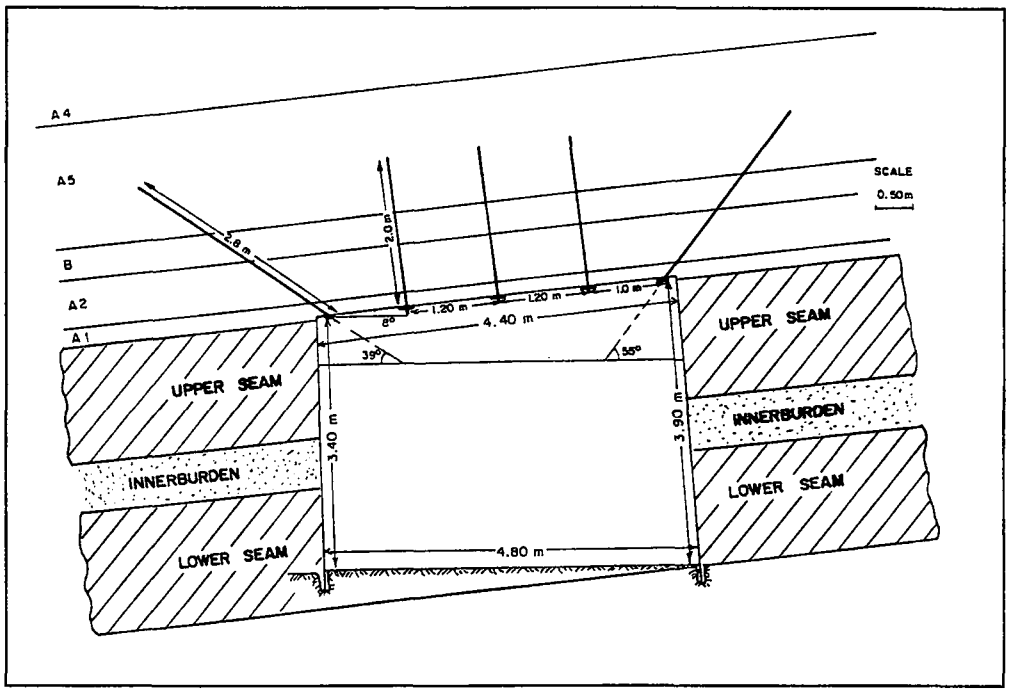

Figure 6.7a Cross section of bolted gate road with split-set at Çayırhan Lignite Mine

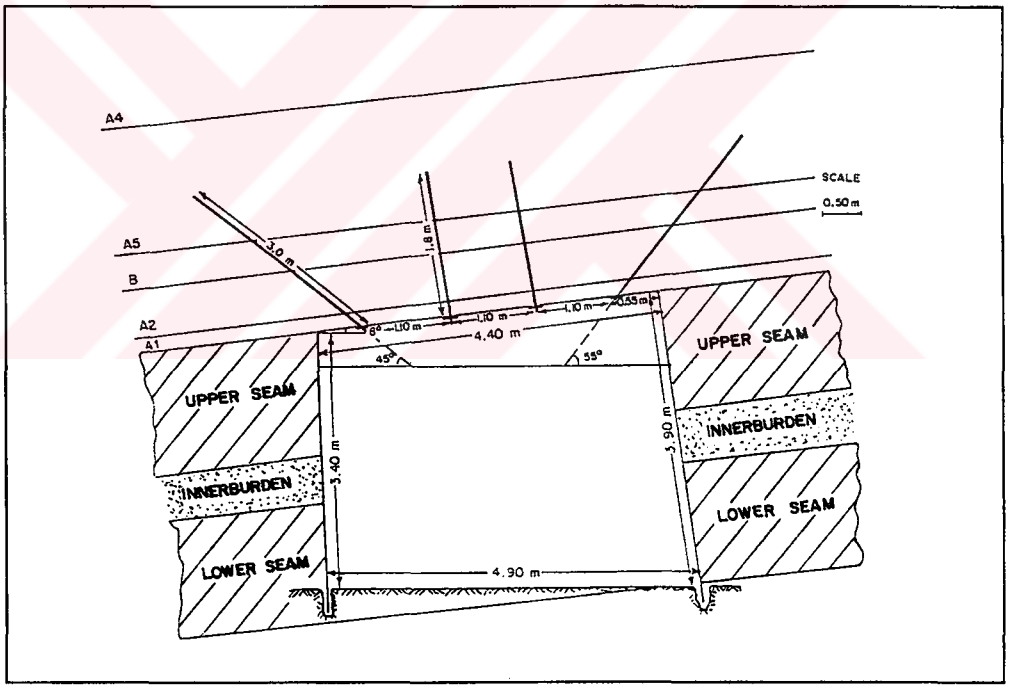

Figure 6.7b Cross section of bolted gate road with yielding super swellex at Çayırhan Lignite Mine

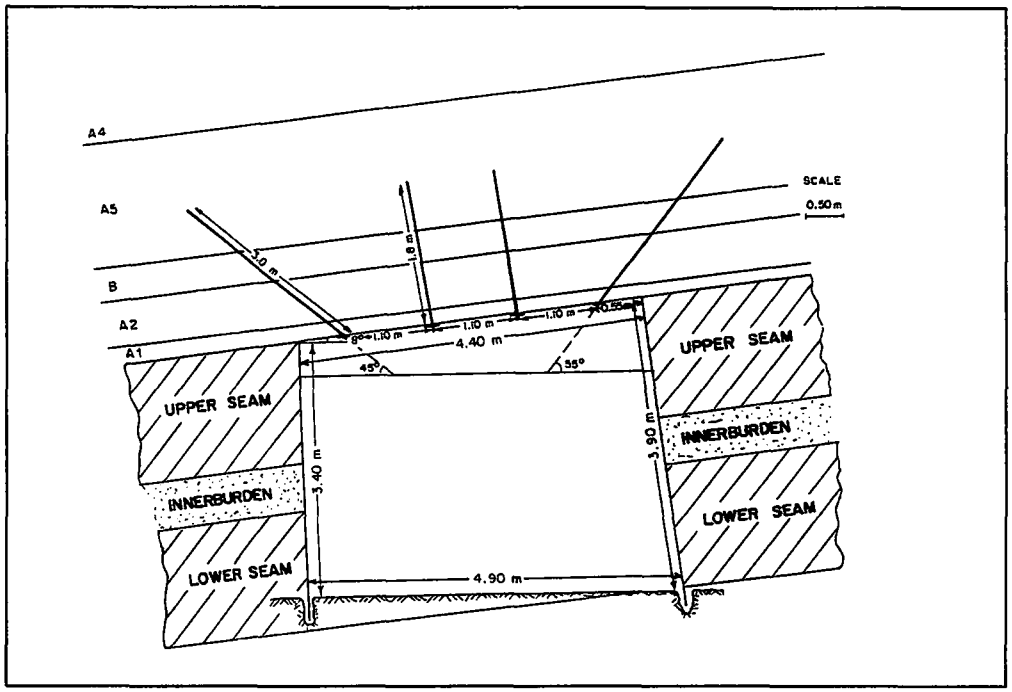

Figure 6.8a Cross section of bolted gate road with Fosroc resin bolt at Çayırhan Lignite Mine

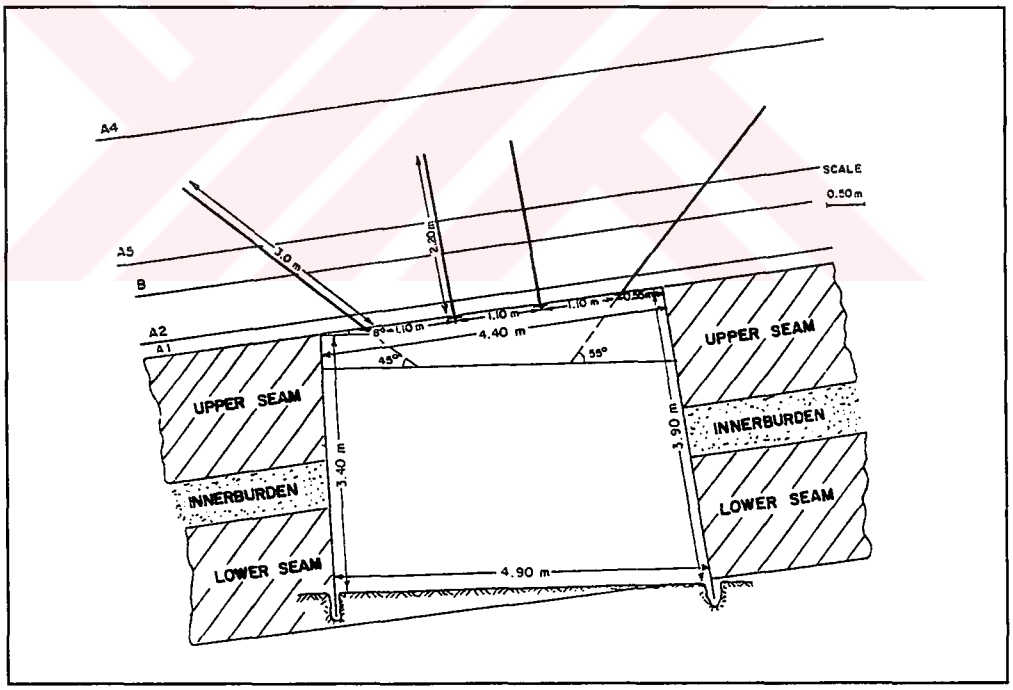

Figure 6.8b Cross section of bolted gate road with Sis resin bolt at Çayırhan Lignite Mine

Table 6.4 In-situ convergence measurement stations at A-810 gate road

Support Location	Code of the Convergence Station	Support Type
I	K1	Split-Set
	K2	Split-Set
II	K3	Split-Set & YSA
III	K4	Yielding Super Swellex
	K5	Yielding Super Swellex
	K6	Yielding Super Swellex
IV	K7	Yielding Super Swellex & YSA
V	K8	Sis-Resin
	K9	Sis-Resin
	K10	Sis-Resin
VI	K11	Sis-Resin & YSA
	K12	Fosroc-Resin
VII	K13	Fosroc-Resin
	K14	Fosroc-Resin
VIII	K15	Fosroc-Resin & YSA
IX	K16	Yielding Steel Arch (YSA)
X	K17	Rigid Steel Arch
	K18	Rigid Steel Arch

Table 6.5 In-situ borehole extensometer measurement stations at A-810 gate road

Support Location	Code of the Extensometer Station	Support Type
I	E1	Split-Set
	E2	Split-Set
II	E3	Split-Set & YSA
III	E4	Yielding Super Swellex
	E5	Yielding Super Swellex
	E6	Yielding Super Swellex
IV	E7	Yielding Super Swellex & YSA
V	E8	Sis-Resin
	E9	Sis-Resin
	E10	Sis-Resin
VI	E11	Sis-Resin & YSA
VII	E12	Fosroc-Resin
	E13	Fosroc-Resin
	E14	Fosroc-Resin
VIII	E15	Fosroc-Resin & YSA
IX	E16	Yielding Steel Arch (YSA)

Both the convergence and borehole extensometer stations were always installed at the same cross-section at the gate road. The plan view of A-810 gate road was presented earlier in Figure 6.4. A typical monitoring station in A-810 gate road is given in Figure 6.9.

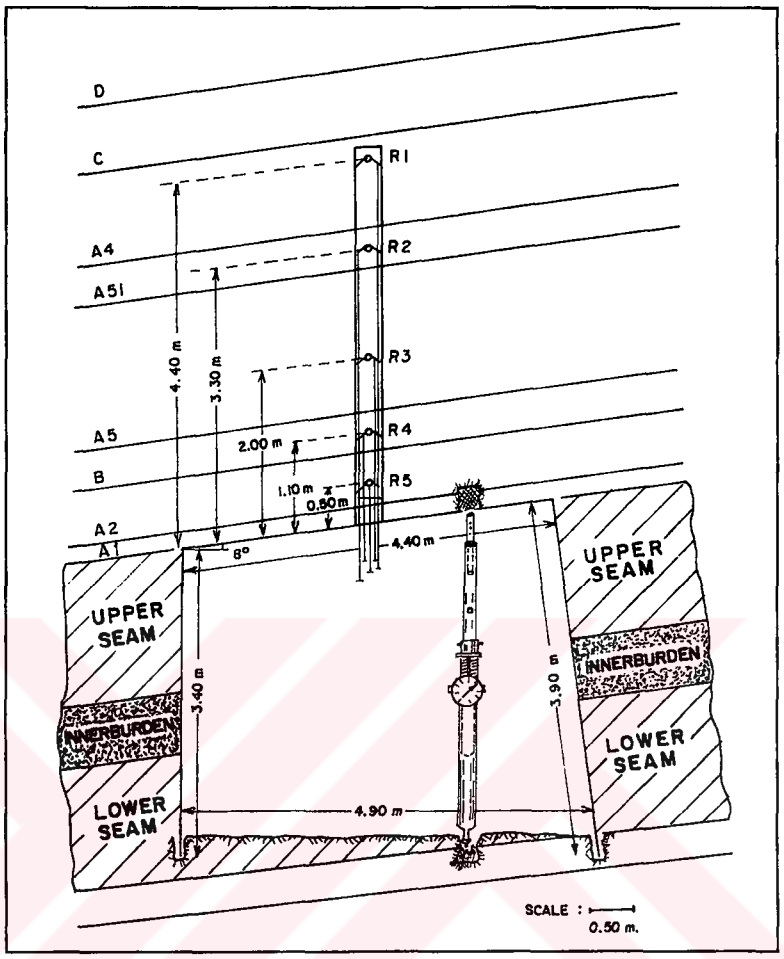

Figure 6.9 A typical convergence and borehole extensometer station in A-810 gate road

6.4 Results of In Situ Measurements

The convergence and displacement measurements were taken with four-hour intervals for the first 20-30 days and then increased to 8, 16, and 48 hours depending on the rate of convergence and roof strata displacement. As the interaction between the support and rock mass being completed, measuring intervals were further increased to 1, 2, and 4 weeks.

In each convergence and borehole extensometer station, six readings were taken at each time of the measurement. Later on, average value of these readings were taken to represent the amount of strata movement. About 46,000 convergence and 110,000 borehole extensometer readings were taken during 15 months of monitoring period. Consequently, a database was established for statistical analysis consisting of data obtained from 18 different convergence stations and 16 borehole extensometer stations. These data were installed to a personnel computer (PC) for further evaluations.

The plots of both convergence and roof strata movements were obtained as a function of time and distance from tunnel face by the aid of a commercially available software "Quattro Pro V5.0". The statistical analyses were carried out by a computer program known as STATGRAPH V5.0 (STSC Inc., 1991).

6.4.1 Results of Convergence Measurements

Based on the data obtained from 18 convergence stations located in different support regions, the graphs of "convergence versus time" and "convergence versus distance from tunnel face" were plotted for each support area. Then, a number of these plots were drawn on the same graph for comparison purposes. The maximum values of the total convergences obtained from each station are given in Table 6.6.

Table 6.6 The convergence stations and maximum values of the total convergence

Support Type Used	Code of the Convergence Station	Maximum Convergence (mm)
Split-Set	K1	10.50
Split-Set	K2	11.09
Split-Set & YSA	K3	9.00
Yielding Super Swellex	K4	6.25
Yielding Super Swellex	K5	6.50
Yielding Super Swellex	K6	5.34
Yielding Super Swellex & YSA	K7	4.62
Sis-Resin	K8	5.40
Sis-Resin	K9	7.00
Sis-Resin	K10	6.30
Sis-Resin & YSA	K11	6.00
Fosroc-Resin	K12	5.25
Fosroc-Resin	K13	6.30
Fosroc-Resin	K14	6.35
Fosroc-Resin & YSA	K15	4.80
Yielding Steel Arch (YSA)	K16	14.20
Yielding Steel Arch	K17	11.38
Rigid Steel Arch	K18	9.69

A total of 36 graphs was prepared during analyses. Two representative examples are given in Figures 6.10 and 6.11. A number of other examples are included in Appendix B.

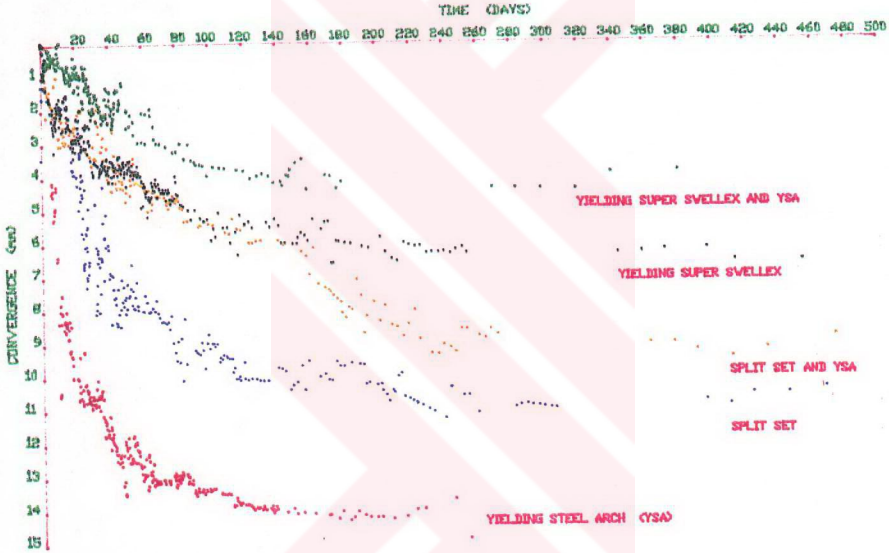

Figure 6.10 Convergence versus time plot for different support regions

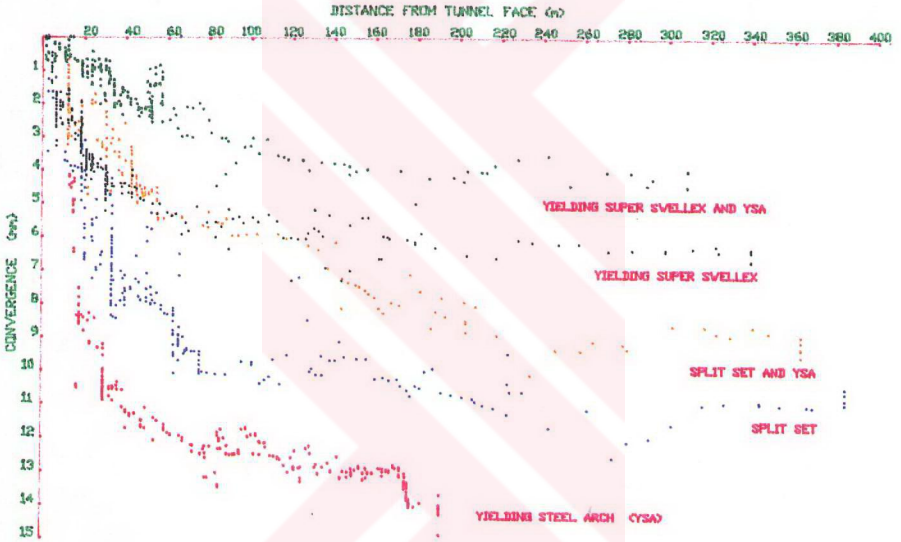

Figure 6.11 Convergence versus distance from tunnel face plot for different support regions

Evaluations based on the results of convergence measurements in different bolted regions indicate that the maximum and minimum convergences are 10.5 mm and 6.5 mm for split-set and yielding super swellex regions, respectively. The convergence in yielding steel arch region is 14.20 mm which is the maximum convergence obtained during the pilot study. On the other hand, the minimum convergence (4.62 mm) in A-810 gate road was obtained in the mix-support region of the yielding super swellex.

6.4.2 Results of Borehole Extensometer Measurements

Sixteen borehole extensometer stations at different support locations in A-810 gate road were installed. In essence, each borehole extensometer station consist of 5 sub-stations (fixed springs) R1 to R5 as shown earlier in Figure 6.9

A total of 160 graphs was drawn to represent the measurements. The maximum value of the roof strata movement obtained at each stations is given in Table 6.7. Two typical examples to these plots are given in Figures 6.12, 6.13, 6.14 and 6.15. The other examples are included in Appendix C.

According to measurement results, the maximum roof strata movements were obtained in yielding steel arch region as 12.10 mm and 7.07 mm for R5 and R1 sub-stations respectively. Moreover, the minimum values were obtained in mixed regions of yielding super swellex as 3.05 and 0.8 mm for R5 and R1 sub-stations, respectively.

Table 6.7 The borehole extensometer stations and maximum values of the total roof strata movement values

Support Type	Code of the stations	Maximum Roof Strata Movement (mm)
Split-Set	E1 - R1	6.50
	- R2	7.60
	- R3	9.50
	- R4	9.60
	- R5	10.00
Split-Set	E2 - R1	0.95
	- R2	-
	- R3	3.70
	- R4	-
	- R5	4.10
Split-Set and Yielding Steel Archs	E3 - R1	1.95
	- R2	2.00
	- R3	2.10
	- R4	3.30
	- R5	4.10
Yielding Super Swellex	E4 - R1	3.65
	- R2	3.70
	- R3	5.43
	- R4	5.50
	- R5	5.75

Table 6.7 (continued)

Support Type	Code of the stations	Maximum Roof Strata Movement (mm)
Yielding Super Swellex	E5 - R1	3.50
	- R2	4.00
	- R3	4.30
	- R4	4.70
	- R5	5.00
Yielding Super Swellex	E6 - R1	1.45
	- R2	1.84
	- R3	2.20
	- R4	4.20
	- R5	4.51
Yielding Super Swellex and Yielding Steel Archs	E7 - R1	0.80
	- R2	-
	- R3	2.40
	- R4	-
	- R5	3.05
SIS-Resin Bolt	E8 - R1	3.60
	- R2	3.80
	- R3	4.00
	- R4	4.00
	- R5	4.80

Table 6.7 (continued)

Support Type	Code of the stations	Maximum Roof Strata Movement (mm)
SIS-Resin Bolt	E9 - R1	2.03
	- R2	2.85
	- R3	2.93
	- R4	3.50
	- R5	4.20
SIS-Resin Bolt	E10 - R1	3.40
	- R2	3.45
	- R3	3.60
	- R4	5.34
	- R5	5.39
SIS-Resin Bolt and Yielding Steel Archs	E11 - R1	0.85
	- R2	-
	- R3	2.50
	- R4	-
	- R5	3.50
Fosroc-Resin Bolt	E12 - R1	3.55
	- R2	3.58
	- R3	3.60
	- R4	3.69
	- R5	4.35
Fosroc-Resin Bolt	E13 - R1	4.02
	- R2	4.11
	- R3	3.99
	- R4	4.50
	- R5	4.80

Table 6.7 (continued)

Support Type	Code of the stations	Maximum Roof Strata Movement (mm)
Fosroc-Resin Bolt	E14 - R1	2.92
	- R2	3.47
	- R3	4.13
	- R4	4.20
	- R5	4.25
Fosroc-Resin Bolt and Yielding Steel Archs	E15 - R1	0.90
	- R2	-
	- R3	3.20
	- R4	-
	- R5	3.75
Yielding Steel Archs	E16 - R1	7.07
	- R2	10.46
	- R3	-
	- R4	12.00
	- R5	12.10

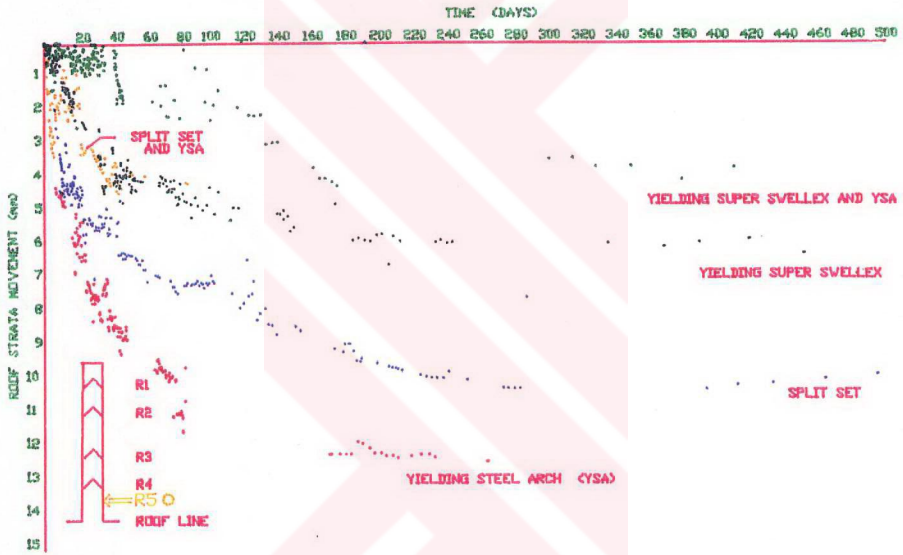

Figure 6.12 Roof strata movement versus time plot for sub-station R5

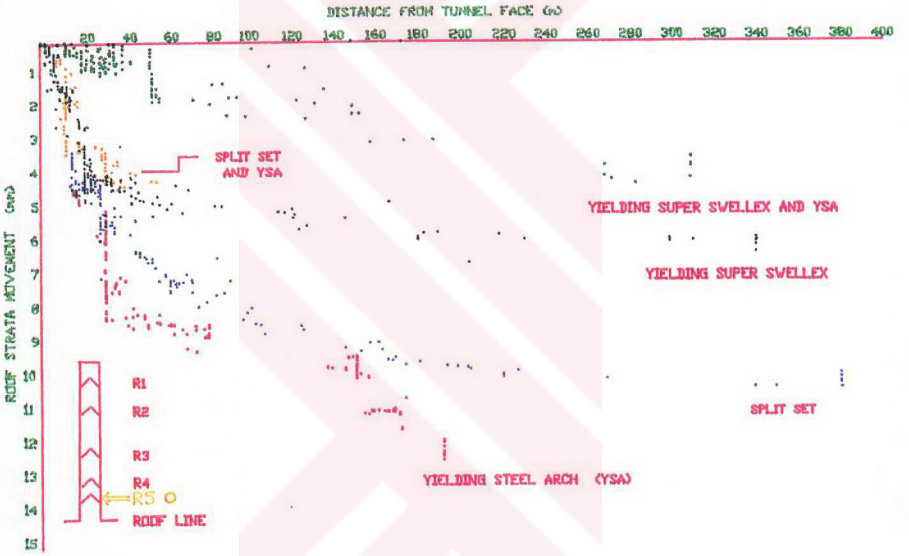

Figure 6.13 Roof strata movement versus distance from tunnel face plot for sub-station R5

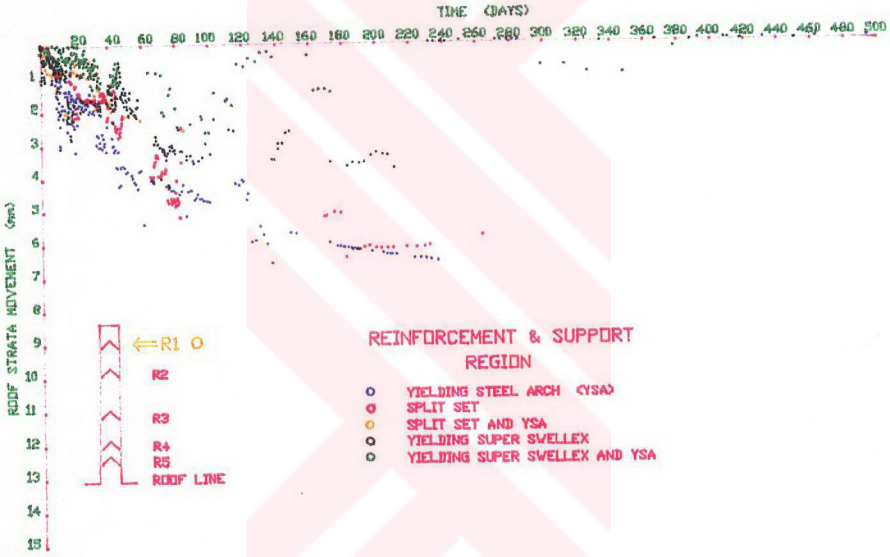

Figure 6.14 Roof strata movement versus time plot for sub-station R1

Figure 6.15 Roof strata movement versus distance from tunnel face plot for sub-station R1

Considering the regions where rock bolts were used as sole means of support, the maximum convergence value was obtained in Split-Set region as 10 mm and 6.5 mm for R5 and R1 sub-stations, respectively; whereas the minimum convergence value was obtained in yielding super swellex region as 5 mm and 3.5 mm for R5 and R1 sub-stations.

6.4.3 Results of Pull-Out Tests

Pull-out tests were carried out to determine the anchorage capacity of a rock bolt anchor installed into the rock mass. During the field investigations carried out in this study, pull-out tests were performed for all bolt types, and consequently the associated load-deformation relationships were determined. Typical results of pull-out tests are illustrated in Figures 6.16, 6.17, 6.18 and 6.19.

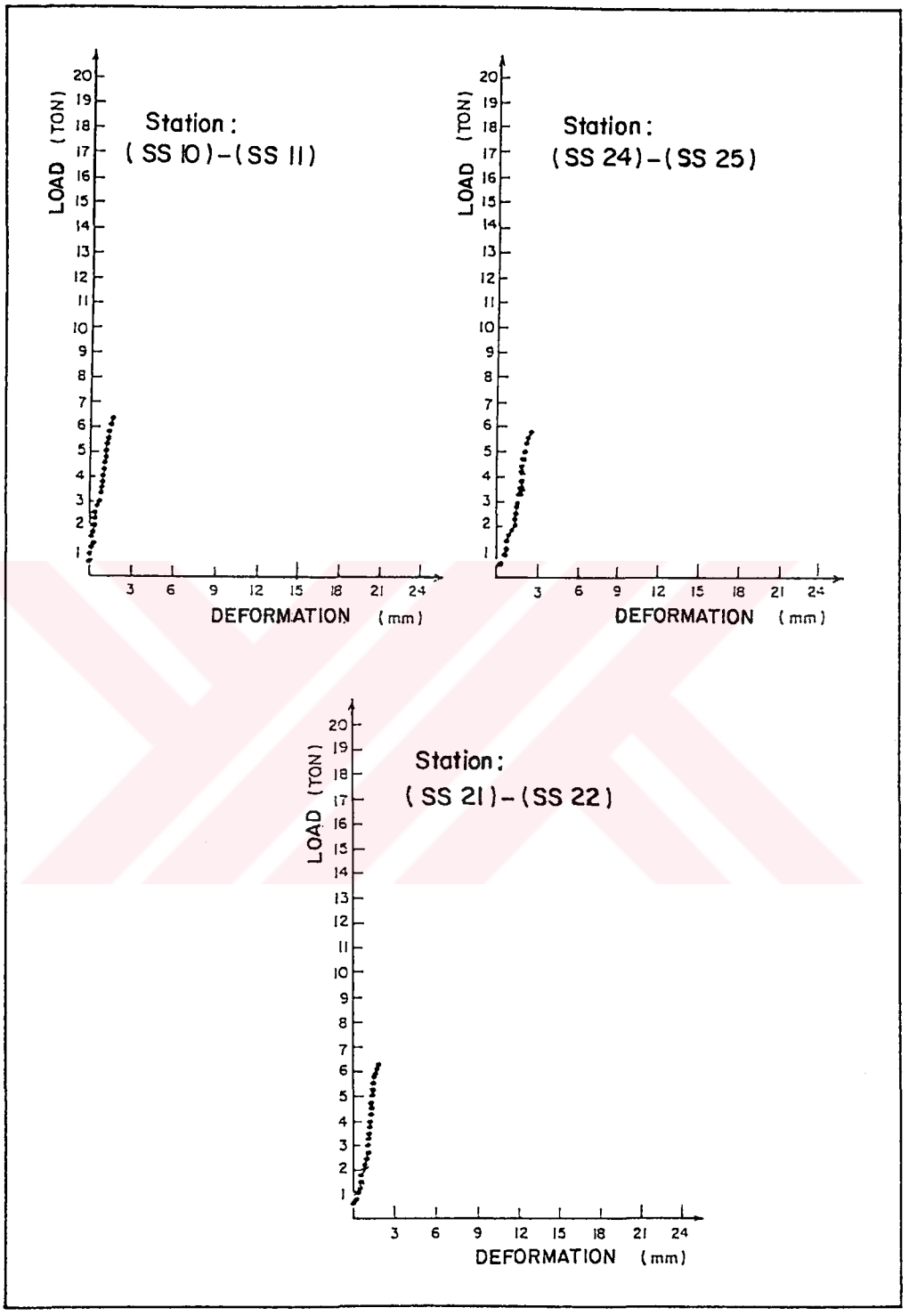

Figure 6.16 "Load-Deformation" characteristic curves of Split-Set under the field conditions

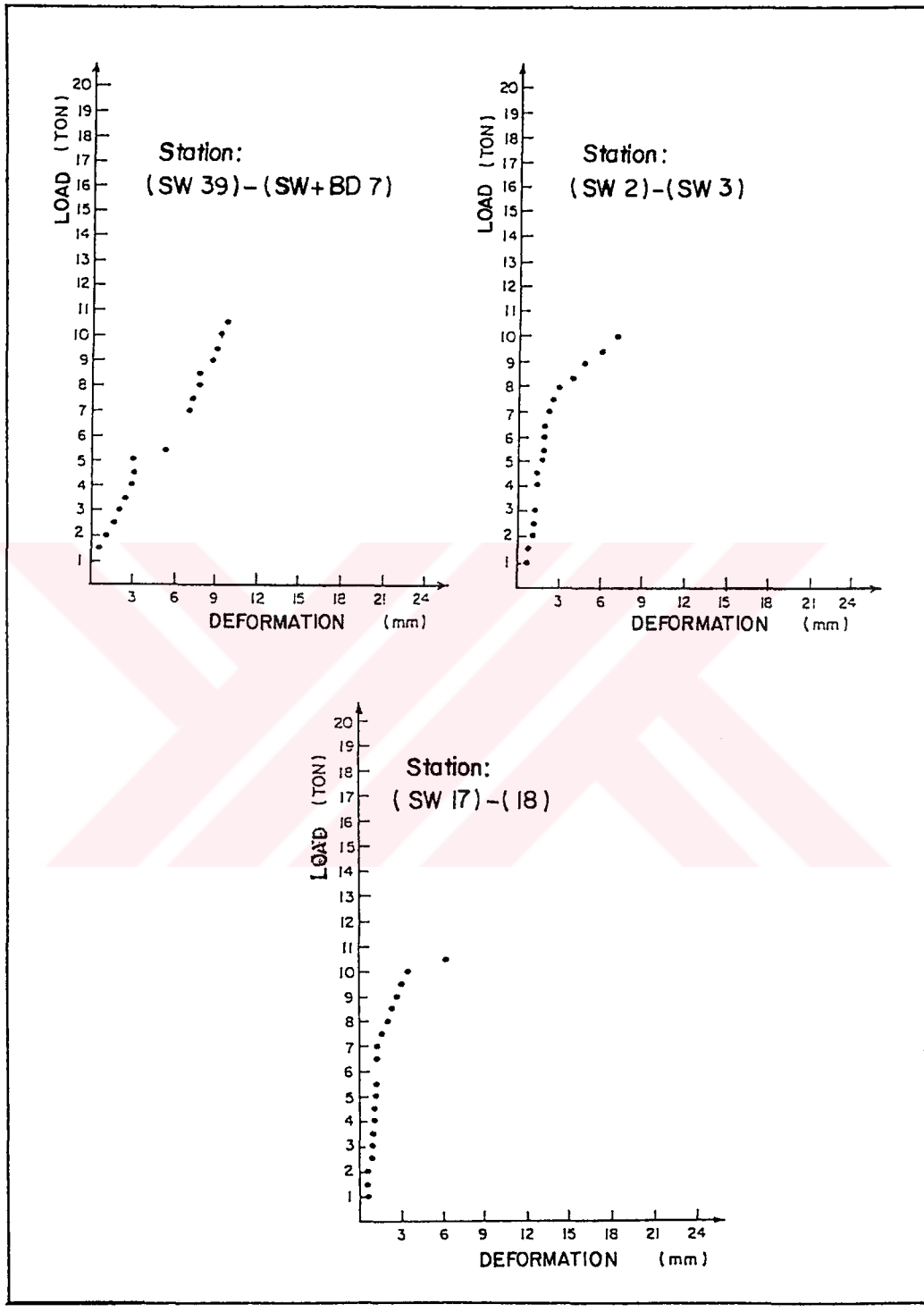

Figure 6.17 "Load-Deformation" characteristic curves of Yielding Super Swellex under the field conditions

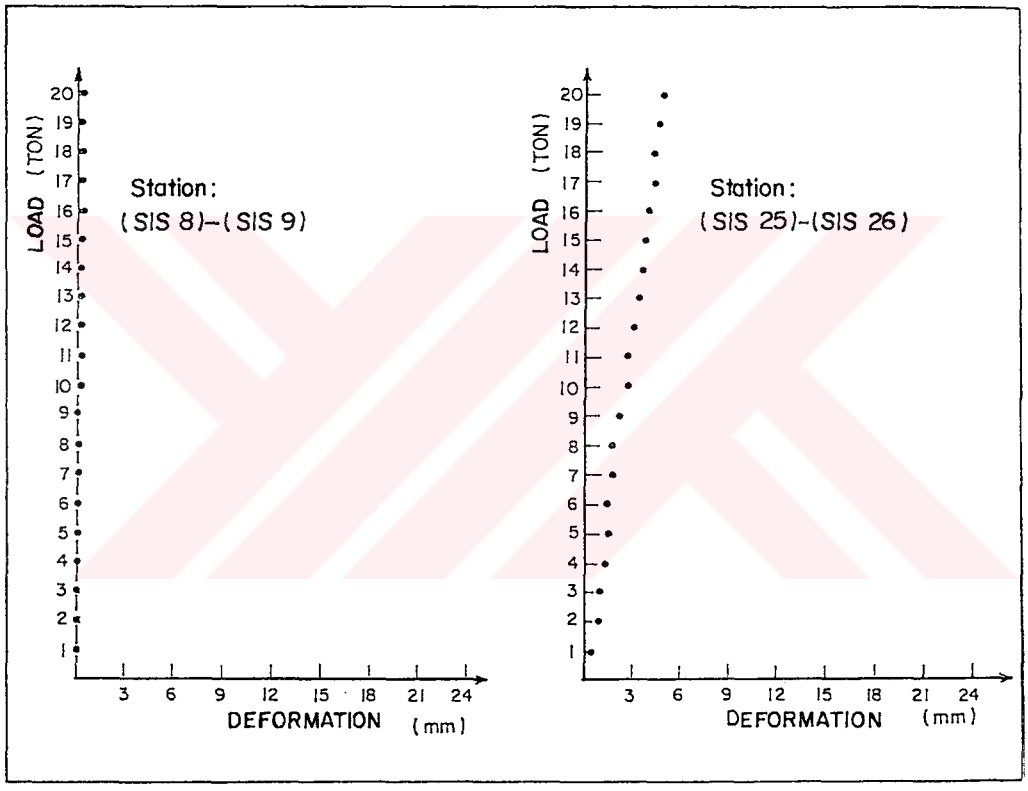

Figure 6.18 "Load-Deformation" characteristic curves of SIS-resin bolt under the field conditions

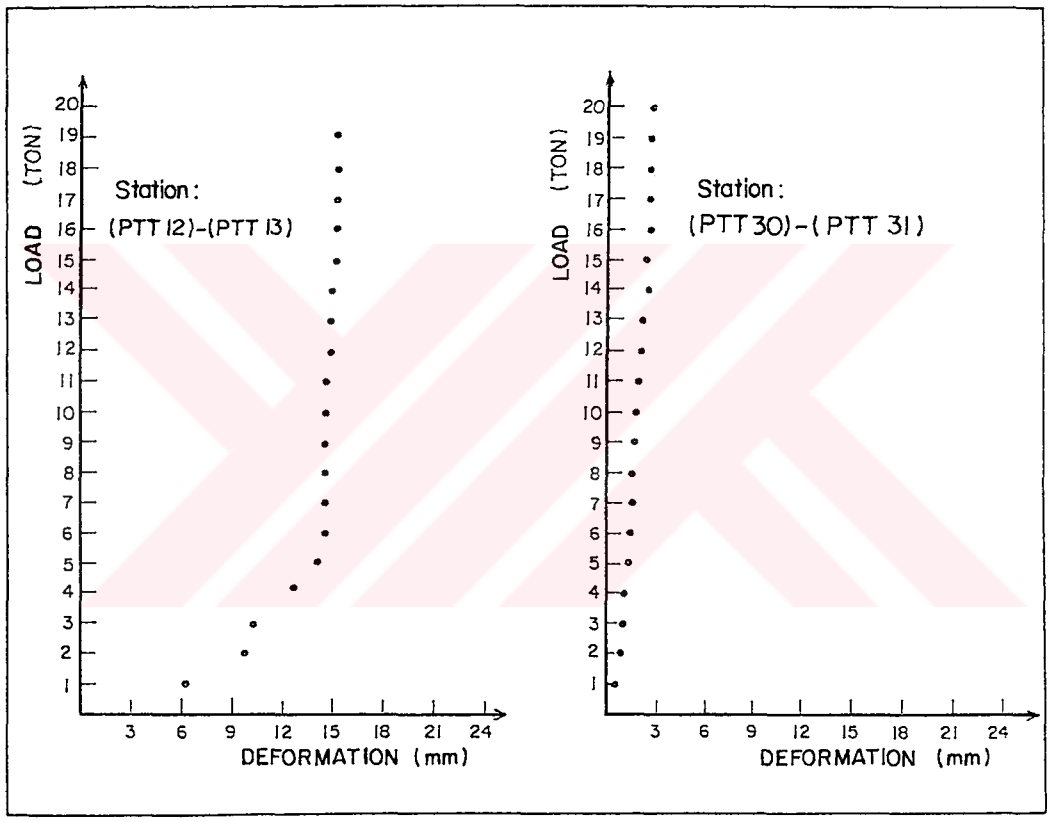

Figure 6.19 "Load-Deformation" characteristic curves of Fosroc-resin bolt under the field conditions

CHAPTER VII

ANALYSIS OF THE RESULTS OBTAINED FROM IN SITU MEASUREMENTS

7.1 General

Various specific formulations have been suggested in literature to express the behavior of the rocks tested in the laboratory, and the rock mass movements measured in underground roadways. Details related to above mentioned formulation were presented in Chapter II. In summary, the functions representing the behavior of the rock material and rock mass can be divided into two major categories: i) rheological time-dependent functions, derived based upon models composed of assemblages of linear springs and dashpots, and ii) empirical time dependent functions obtained based upon curve fitting to experimental data.

It was found that the rheological time dependent functions can represent the laboratory creep data only. The empirical time dependent functions, however, can represent the data obtained from both the laboratory and the field.

According to the findings presented in literature, the three function types, obtained by curve fitting, are logarithmic, exponential and power. The time dependent characteristic of the roof displacement in underground openings can be explained by a logarithmic as well as an exponential function.

Recently, in addition to time, the "distance from tunnel face" has been found important in expressing the roof displacement in underground openings. Consequently, it was suggested that the function representing the roadway or tunnel deformation should include parameters representing both the time and distance from tunnel face.

The statistical analyses carried out in this study are based on the data obtained from convergence and roof strata movement readings carried out at various stations located at A-810 gate road in Çayırhan Lignite Mine. The details associated with this study are presented in Chapter VI. In this chapter, the main consideration is given to instrumentation, measuring stations, types and location of various supports used, the plots of convergence and borehole extensometer measurements, and finally the discussions and conclusions derived based on these studies.

In order to derive statistical functions representing the characteristics of tunnel behavior in terms of convergence and roof strata movement in different support locations, the data obtained from underground measurements were evaluated by means of a computer package called STATGRAPH (STSC Inc., 1991). The statistical equations and their evaluations are presented in Sections 7.2, 7.3 and 7.4.

Based on empirical equations mentioned above, a mathematical model was developed for describing the behavior of the strata. In essence, this model is a mathematical expression of roadway convergence and roof strata displacement which are expressed in terms of time and/or distance from face advance. In this thesis, analyses carried out on both the rate of "convergence" and the rate of "convergence velocity" which rely on partial differential equations derived from convergence and roof displacement equations. Derivation of these partial differential equations and evaluations of their performances are presented in Sections 7.5 and 7.6.

7.2 Statistical Analysis of Convergence

The STATGRAPH computer program used during analyses is capable of performing ordinary as well as non-linear regression analysis. The non-linear regression is a flexible option because many function types can be tested by this program. As mentioned before, the real convergence and roof displacement data, obtained from underground measurements, are expressed as a function of time and distance from tunnel face. The data obtained from these measurements were analyzed by making use of STATGRAPH. The details of associated analyses and the results obtained are given in following sections.

All of the four basic statistical functions shown in Table 7.1 were considered in testing the original convergence and roof displacement data.

Table 7.1 The Basic statistical function considered during analyses

Statistical Function	The Mathematical Expression
Linear	$y = a + b\,x$
Logarithmic	$y = a + b \ln x$ or $y = a + b \ln(x+1)$
Exponential	$y = a\,e^{bx}$
Power	$y = a\,x^{b}$

7.2.1 Time Dependent Analysis of Convergence

The convergence data were initially analyzed as time dependent function. It was found that the results obtained based on basic linear and exponential models are not satisfactory. Typical results associated with station K1 (the first measuring station of split-set) are given in Table 7.2. In these statistical functions the units of the

independent (time) and dependent (convergence) variables are "day" and "mm", respectively.

Table 7.2 The results of regression analysis for Station No: K1 (roadway station supported by Split-Set)

The Statistical Function and The Associated Equation	Constant a	Constant b	Regression Coefficient, R^2
Linear $y = a + bT$	5.549	0.0209	0.517
Logarithmic $y = a + b\ln(T+1)$	-1.335	2.16	0.753
Exponential $y = a\,e^{bT}$	The result of analysis is infinite		
Power $y = a\,T^b$	2.218	0.289	0.742

As explained in literature survey (Chapter II and Appendix A), in case studies, the strata movement has been expressed by logarithmic, power and exponential functions as shown in Table 7.3.

Table 7.3 Suggested statistical functions in case studies

Statistical Function	The Mathematical Expression
Logarithmic	$y = a + b\ln T$ or $y = a + b\ln(T+1)$
Exponential	$y = a\,e^{bT}$
Power	$y = a\,T^b$

Note that in Table 7.3, a and b are constant values, T is independent variable and y is dependent variable.

The statistical analysis carried out based on logarithmic and power models are given in Tables 7.4 and 7.5 respectively.

Table 7.4 The results of logarithmic regression analysis based on the convergence data in A-810 gate road of OAL mine

Support Type	Station Code	Constant *a*	Constant *b*	Regression Coefficient, R^2
Split-Set	K1	-1.335	2.160	0.75
Split-Set	K2	-4.116	2.774	0.79
Split-Set & YSA	K3	-2.300	1.751	0.82
Yielding Super Swellex	K4	-1.009	1.284	0.89
Yielding Super Swellex	K5	-1.155	1.155	0.70
Yielding Super Swellex	K6	-2.329	1.359	0.81
Yielding Super Swellex & YSA	K7	-1.546	0.961	0.74
Sis-Resin	K8	-2.484	1.536	0.84
Sis-Resin	K9	-2.941	1.677	0.79
Sis-Resin	K10	-2.100	1.609	0.76
Sis-Resin & YSA	K11	-3.008	1.479	0.69
Fosroc-Resin	K12	-2.479	1.501	0.80
Fosroc-Resin	K13	-1.899	1.638	0.87
Fosroc-Resin	K14	-2.711	1.791	0.85
Fosroc-Resin & YSA	K15	-0.612	0.978	0.77
Yielding Steel Arch (YSA)	K16	+1.436	2.651	0.89
Rigid Steel Arch	K17	-2.231	2.804	0.97
Rigid Steel Arch	K18	-2.409	2.586	0.95

Table 7.5 Results of power regression analysis based on the convergence data, obtained in A-810 gate road of OAL mine

Support Type	Station Code	Constant *a*	Constant *b*	Regression Coefficient, R^2
Split-Set	K1	2.218	0.289	0.74
Split-Set	K2	0.444	0.697	0.87
Split-Set & YSA	K3	0.721	0.444	0.93
Yielding Super Swellex	K4	1.025	0.338	0.89
Yielding Super Swellex	K5	0.509	0.463	0.83
Yielding Super Swellex	K6	0.341	0.529	0.79
Yielding Super Swellex & YSA	K7	0.236	0.552	0.81
Sis-Resin	K8	0.547	0.462	0.79
Sis-Resin	K9	0.287	0.635	0.82
Sis-Resin	K10	0.753	0.429	0.75
Sis-Resin & YSA	K11	0.213	0.636	0.73
Fosroc-Resin	K12	0.559	0.438	0.74
Fosroc-Resin	K13	0.847	0.406	0.80
Fosroc-Resin	K14	0.757	0.429	0.78
Fosroc-Resin & YSA	K15	0.791	0.349	0.76
Yielding Steel Arch (YSA)	K16	5.128	0.212	0.84
Rigid Steel Arch	K17	2.286	0.336	0.91
Rigid Steel Arch	K18	1.649	0.381	0.88

The basic and suggested model for exponential function takes infinite values in non-linear statistical analysis. However, during statistical analysis, it has been found that the exponential function presented in Equation 7.1, realistically fits to in-situ data.

$$U = f(X) \tag{7.1a}$$

$$U = a\left(1 - e^{-X/b}\right) \tag{7.1b}$$

where, a and b are constant values, X and U are independent and dependent variables, respectively. The performance of this function is much better than the logarithmic and power type statistical functions as shown in Table 7.6.

Consequently, the best fit characterizing the roof in terms of time dependent behavior was defined empirically by an exponential function. This function can be rewritten as shown in Equations 7.2.

$$U = f(T) \text{ or} \tag{7.2a}$$

$$U = a\left(1 - e^{-T/b}\right) \tag{7.2b}$$

where, a and b are constant values, T is time (independent variable) in days, and U is convergence (dependent variable) in mm.

Table 7.6 Results of exponential regression obtained based on treatment of data associated with convergence measurements carried out in A-810 gate road of OAL mines

Support Type	Station Code	Constant *a*	Constant *b*	Regression Coefficient, R^2
Split-Set	K1	10.80	44.408	0.79
Split-Set	K2	11.704	55.181	0.87
Split-Set & YSA	K3	8.852	86.419	0.85
Yielding Super Swellex	K4	6.250	45.230	0.81
Yielding Super Swellex	K5	6.481	76.344	0.76
Yielding Super Swellex	K6	5.473	61.611	0.89
Yielding Super Swellex & YSA	K7	4.743	78.536	0.87
Sis-Resin	K8	5.500	45.472	0.92
Sis-Resin	K9	7.538	72.441	0.90
Sis-Resin	K10	6.072	40.436	0.82
Sis-Resin & YSA	K11	5.400	72.103	0.80
Fosroc-Resin	K12	5.400	43.734	0.88
Fosroc-Resin	K13	6.434	33.089	0.95
Fosroc-Resin	K14	6.383	40.799	0.90
Fosroc-Resin & YSA	K15	4.800	38.711	0.67
Yielding Steel Arch (YSA)	K16	14.200	20.234	0.81
Rigid Steel Arch	K17	11.200	26.164	0.95
Rigid Steel Arch	K18	9.584	23.866	0.98

A typical example for this model is given in Figure 7.1 where convergence measurement associated with station K1 are presented. The typical graphs for logarithmic and power functions for the same station are also given in Figures 7.2 and 7.3.

7.2.2 Face Advance Dependent Analysis of Convergence

Time is an important parameter in occurrence of convergence in roadways and gate roads; however, convergence does not only depend on time, but also depends on the distance from tunnel face.

In order to investigate the effect of the tunnel face advance only, the data were evaluated by utilizing the basic statistical function mentioned in Table 7.1. A typical example obtained in such analyses are presented in Table 7.7.

Table 7.7 The Results of statistical regression analysis for Station K1 located in A-810 gate road supported by Split-Set

The Statistical Function and The Associated Equation	Constant a	Constant b	Regression Coefficient, R^2
Linear $y = a + bX$	5.874	0.0206	0.447
Logarithmic $y = a + b\ln(X+1)$	-1.926	2.396	0.769
Exponential $y = a\,e^{bX}$	The result of analysis is infinite		
Power $y = a\,X^b$	2.481	0.275	0.700

According to the results shown in Table 7.7, it can be concluded that the logarithmic and power functions characterize the roof behavior better than the linear and exponential functions. The results representing all other measurements are given in Tables 7.8 and 7.9.

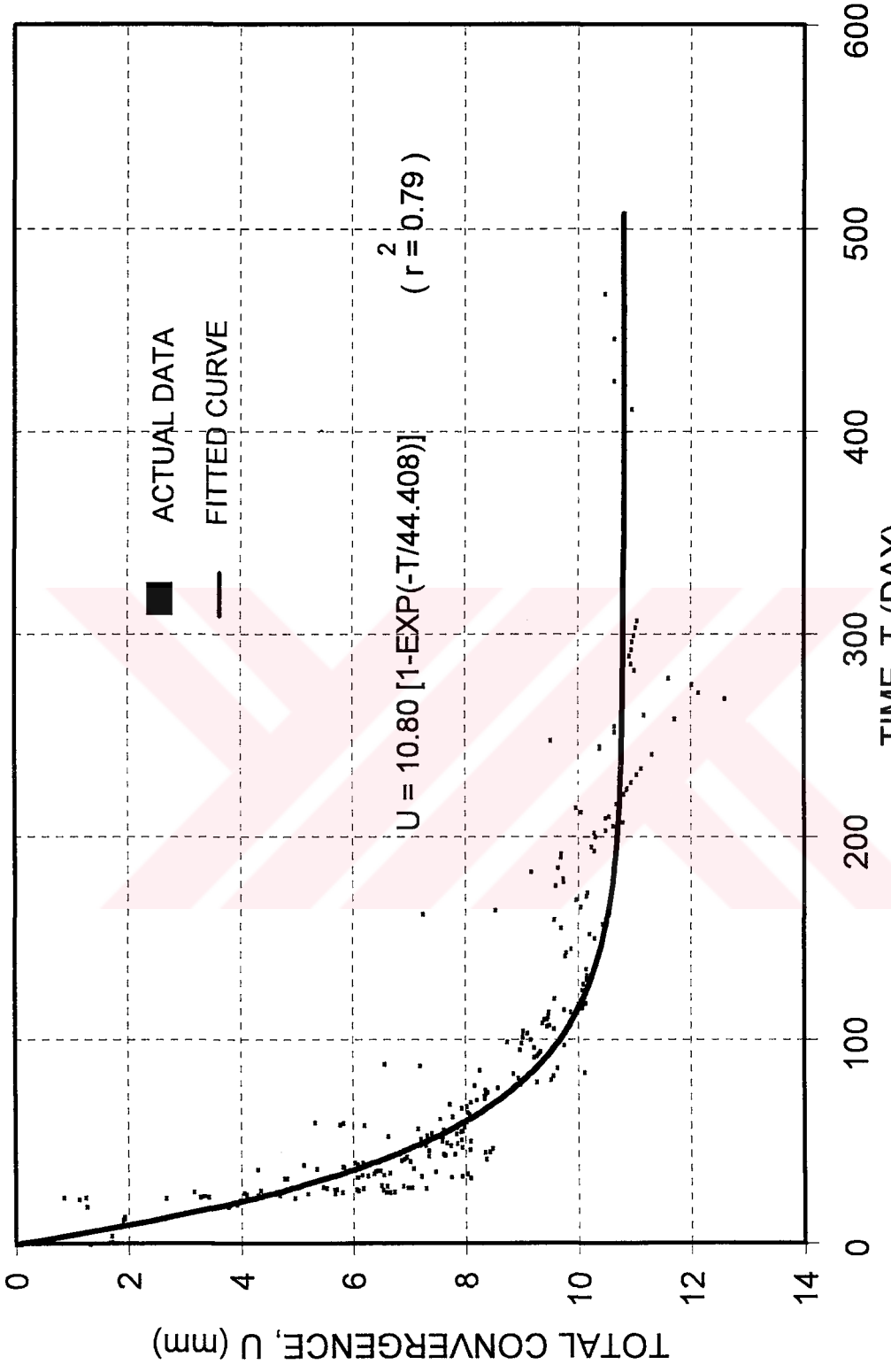

Figure 7.1 An exponential function for time dependent convergence for station K1

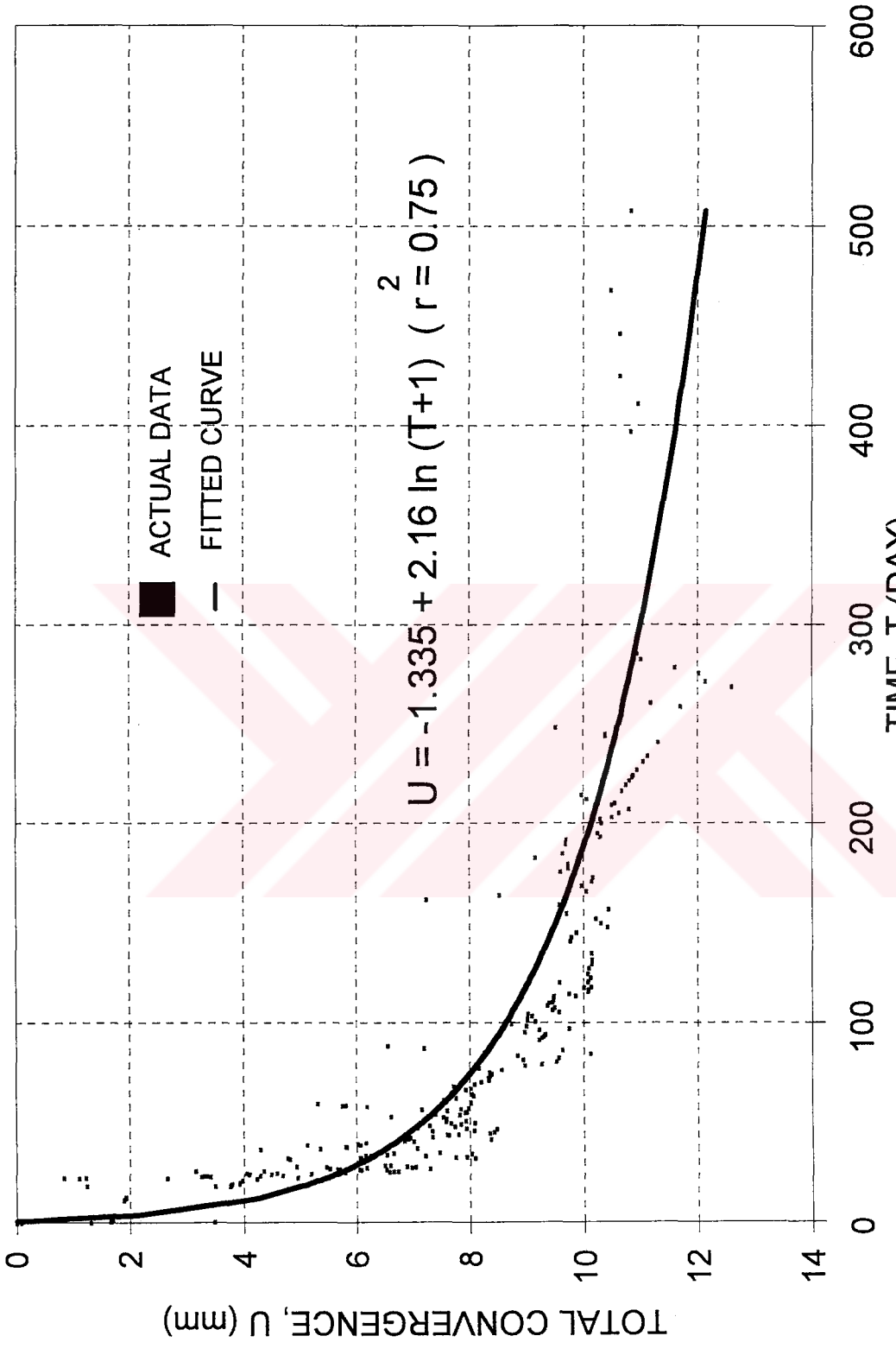

Figure 7.2 A logarithmic function for time dependent convergence for station K1

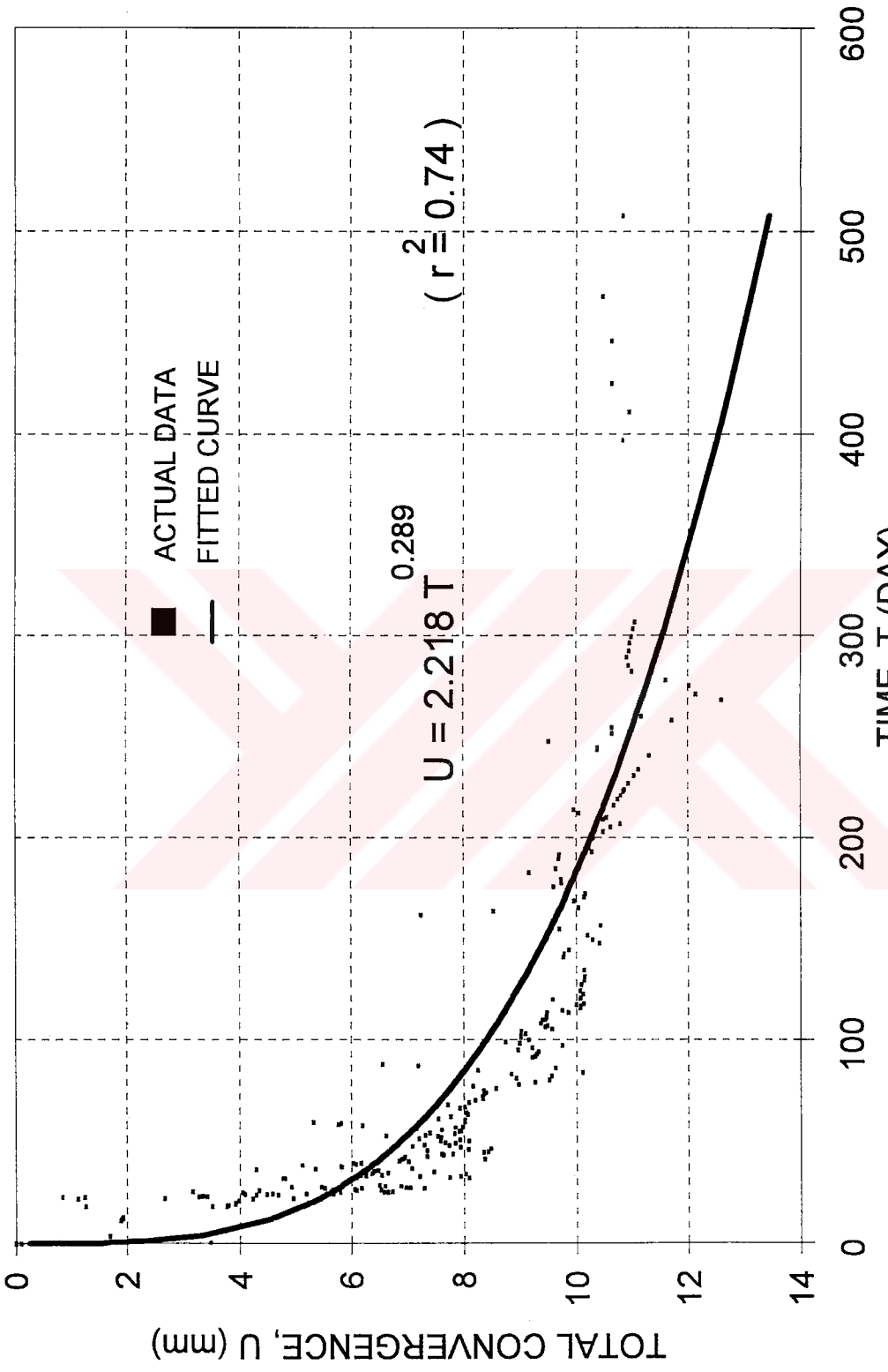

Figure 7.3 A power function for time dependent convergence for station K1

Table 7.8 Results of logarithmic regression based on data representing "Convergence" and "Distance from Tunnel Face"

Support Type	Station Code	Constant *a*	Constant *b*	Regression Coefficient, R^2
Split-Set	K1	-1.926	2.396	0.77
Split-Set	K2	-7.102	3.418	0.81
Split-Set & YSA	K3	-4.251	2.280	0.93
Yielding Super Swellex	K4	-0.952	1.405	0.86
Yielding Super Swellex	K5	-1.314	1.362	0.83
Yielding Super Swellex	K6	-2.715	1.498	0.88
Yielding Super Swellex & YSA	K7	-1.907	1.005	0.77
Sis-Resin	K8	-3.595	1.714	0.85
Sis-Resin	K9	-6.969	2.501	0.89
Sis-Resin	K10	-3.864	1.929	0.82
Sis-Resin & YSA	K11	-4.471	1.734	0.78
Fosroc-Resin	K12	-4.033	1.755	0.84
Fosroc-Resin	K13	-5.331	2.226	0.92
Fosroc-Resin	K14	-5.259	2.184	0.89
Fosroc-Resin & YSA	K15	-2.648	1.325	0.75
Yielding Steel Arch (YSA)	K16	1.446	2.376	0.83
Rigid Steel Arch	K17	-13.275	4.548	0.92
Rigid Steel Arch	K18	-9.00	3.699	0.89

Table 7.9 Results of power regression based on data representing "Convergence" and "Distance from Tunnel Face"

Support Type	Station Code	Constant *a*	Constant *b*	Regression Coefficient, R^2
Split-Set	K1	2.481	0.275	0.70
Split-Set	K2	0.608	0.579	0.76
Split-Set & YSA	K3	0.812	0.429	0.92
Yielding Super Swellex	K4	1.369	0.292	0.79
Yielding Super Swellex	K5	0.871	0.371	0.83
Yielding Super Swellex	K6	0.428	0.475	0.77
Yielding Super Swellex & YSA	K7	0.194	0.571	0.83
Sis-Resin	K8	0.448	0.479	0.77
Sis-Resin	K9	0.197	0.657	0.76
Sis-Resin	K10	0.539	0.478	0.78
Sis-Resin & YSA	K11	0.115	0.734	0.78
Fosroc-Resin	K12	0.311	0.542	0.78
Fosroc-Resin	K13	0.353	0.551	0.83
Fosroc-Resin	K14	0.406	0.523	0.81
Fosroc-Resin & YSA	K15	0.448	0.434	0.70
Yielding Steel Arch (YSA)	K16	4.874	0.201	0.80
Rigid Steel Arch	K17	0.245	0.738	0.94
Rigid Steel Arch	K18	0.109	0.942	0.97

Since the basic exponential function takes infinite values, non-linear exponential functions have been tried as in the case of time dependent statistical analysis. The results indicate that, in terms of distance from the face, the roof is better characterized by exponential function (Table 7.10) compared to logarithmic and power functions.

The governing equation showing the effect of the distance from tunnel face on convergence can be rewritten as shown in Equation 7.3.

$$U = f(X) \quad \text{or} \tag{7.3a}$$

$$U = a\left(1 - e^{-X/b}\right) \tag{7.3b}$$

where, a and b are constants values, X is distance from tunnel face in meters (independent variable), U is the convergence in mm (dependent variable).

A typical example for this model is given in Figure 7.4 where convergence is plotted as a function of distance from the face for station no: K1. The graphs for logarithmic and power models are also presented in Figures 7.5 and 7.6.

Table 7.10 Results of exponential regression obtained based on data representing the "Convergence" and "Distance from Tunnel Face"

Support Type	Station Code	Constant *a*	Constant *b*	Regression Coefficient, R^2
Split-Set	K1	10.80	36.523	0.80
Split-Set	K2	10.736	56.091	0.82
Split-Set & YSA	K3	8.717	65.890	0.92
Yielding Super Swellex	K4	6.006	24.833	0.89
Yielding Super Swellex	K5	5.600	30.158	0.76
Yielding Super Swellex	K6	5.065	46.721	0.88
Yielding Super Swellex & YSA	K7	4.620	92.396	0.87
Sis-Resin	K8	5.817	64.448	0.90
Sis-Resin	K9	7.626	111.861	0.85
Sis-Resin	K10	6.495	60.262	0.85
Sis-Resin & YSA	K11	7.367	148.538	0.83
Fosroc-Resin	K12	5.721	73.762	0.87
Fosroc-Resin	K13	6.693	69.915	0.92
Fosroc-Resin	K14	6.536	70.385	0.89
Fosroc-Resin & YSA	K15	4.212	50.465	0.73
Yielding Steel Arch (YSA)	K16	13.077	20.498	0.89
Rigid Steel Arch	K17	16.580	167.337	0.94
Rigid Steel Arch	K18	121.352	1395.469	0.96

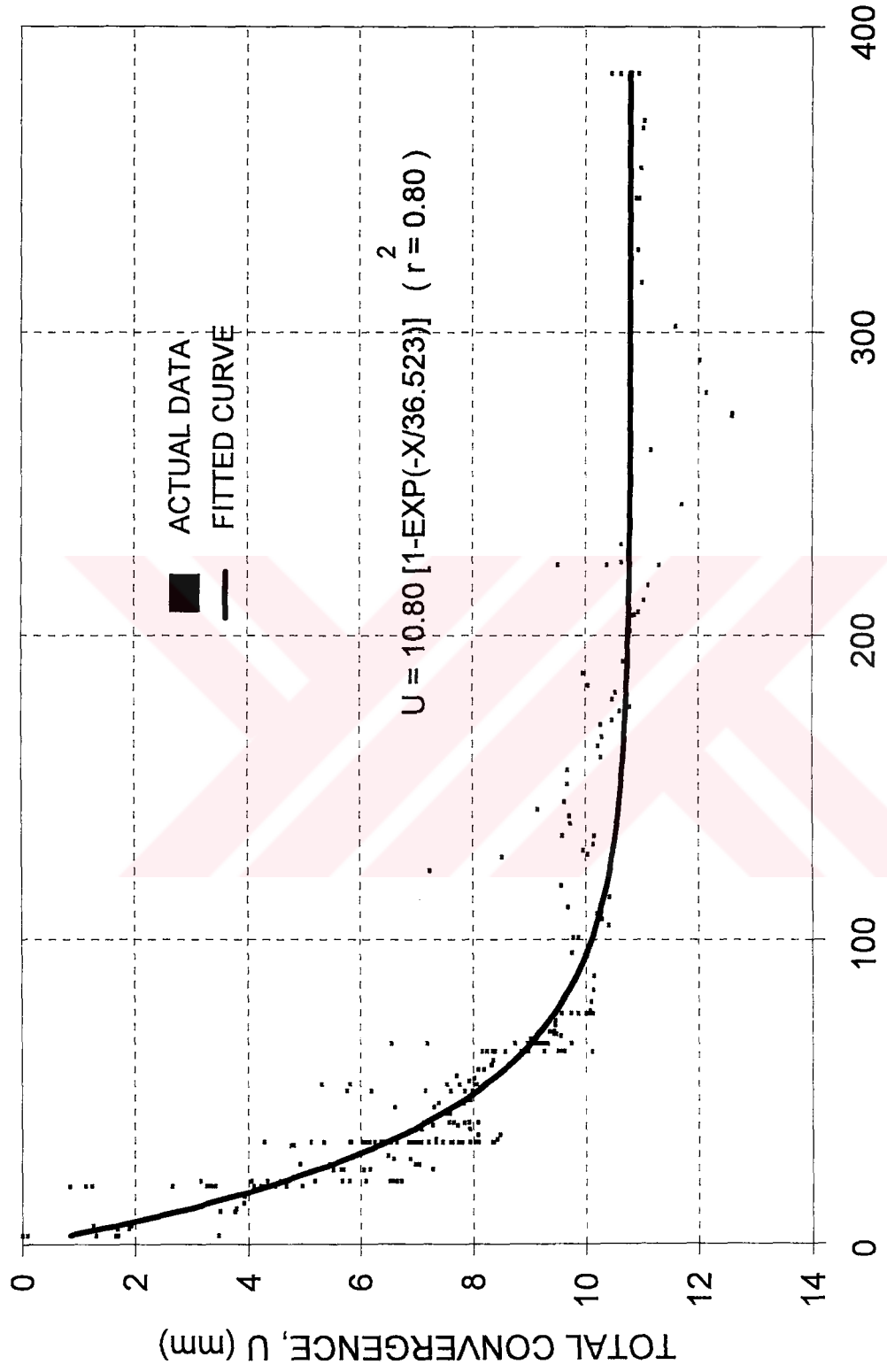

Figure 7.4 An exponential function for distance from tunnel face-dependent convergence for station K1

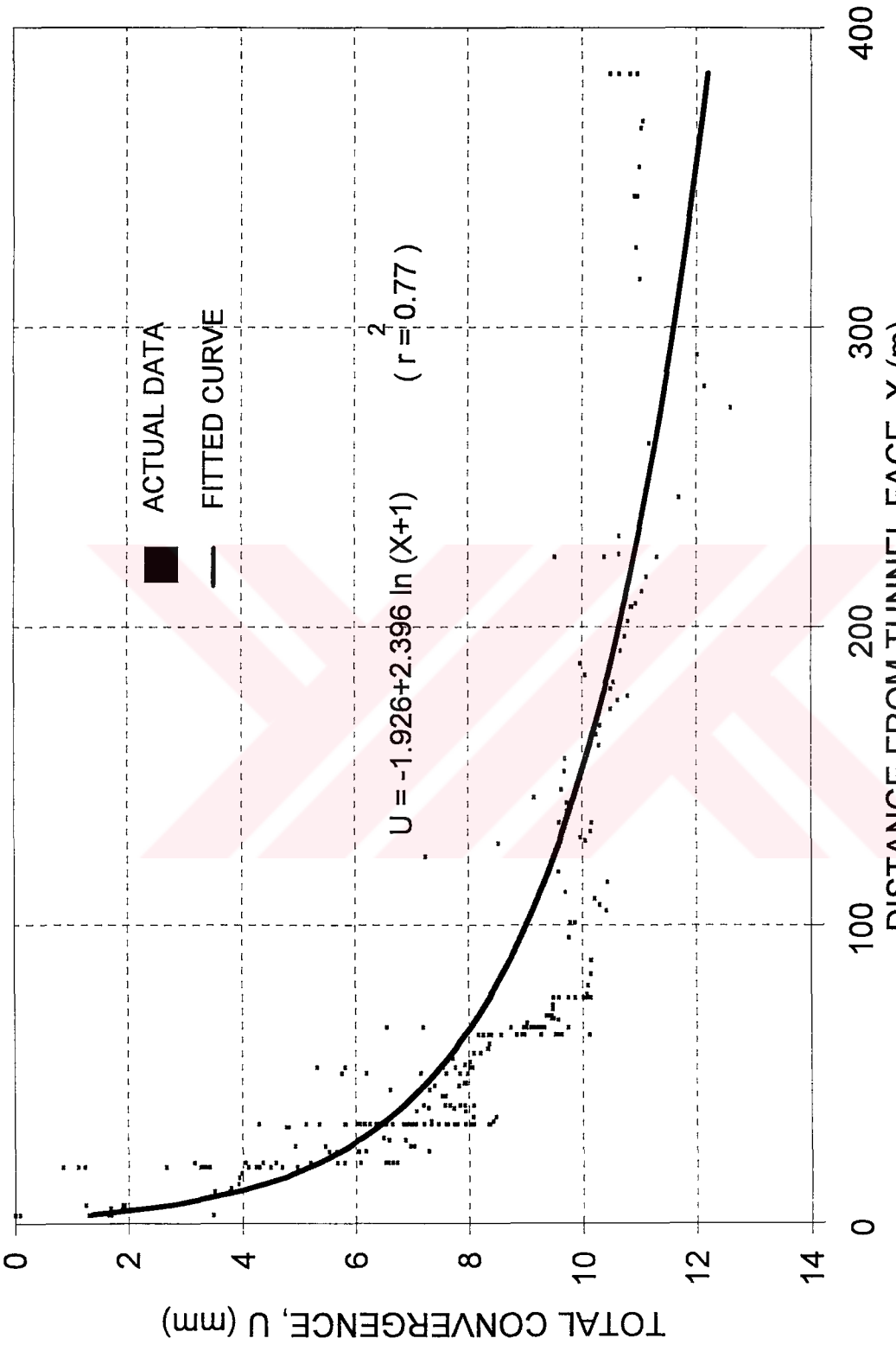

Figure 7.5 A logarithmic function for distance from tunnel face advance convergence for station K1

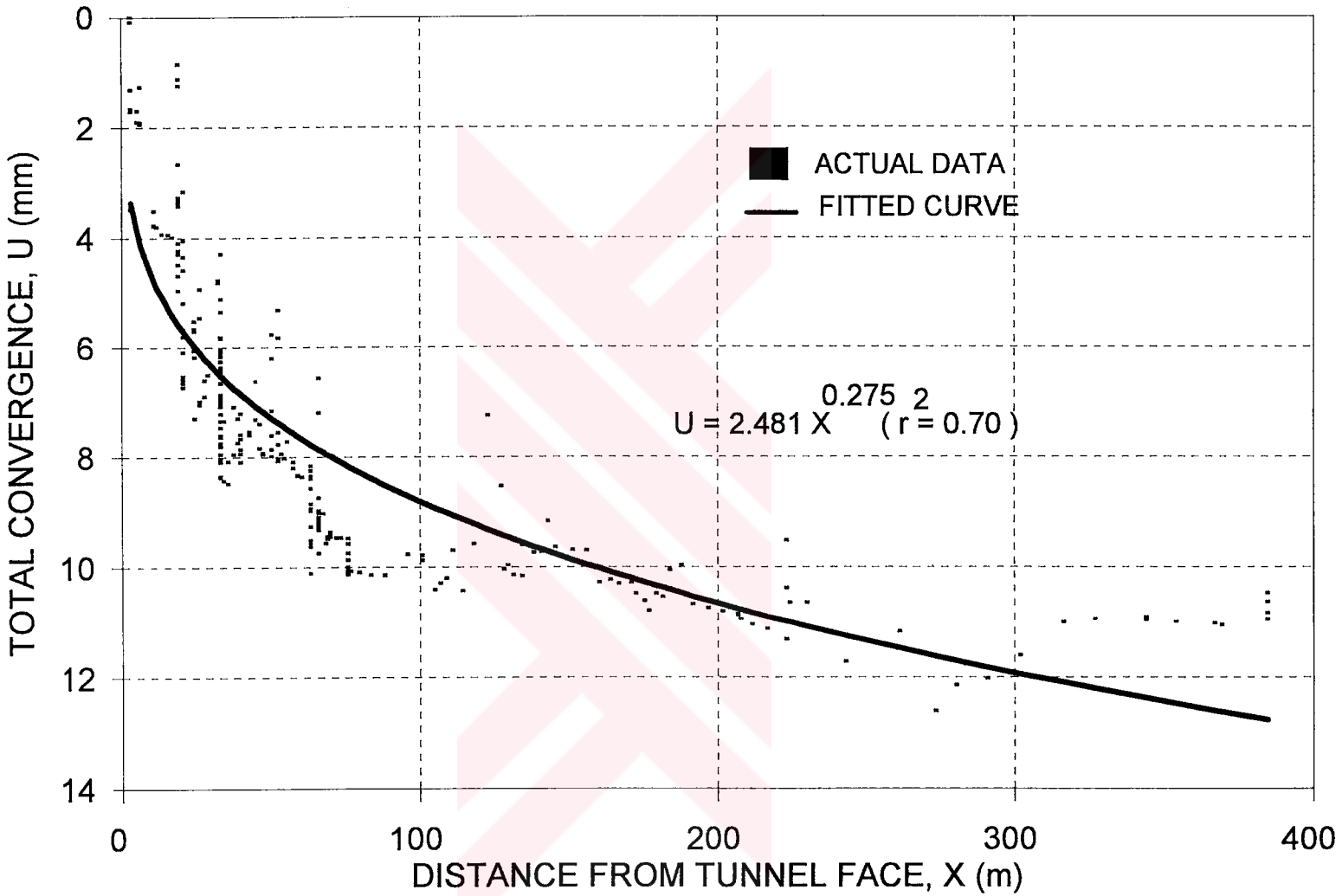

Figure 7.6 A power function for distance from tunnel face-dependent convergence for station K1

7.2.3 Statistical Analysis Based on Both Time and Distance from Tunnel Face

Panet (1993) essentially indicated that the convergence in gate roads depends on both the time and the distance from tunnel face. He suggested the following general functions given in Equations 7.4 and 7.5.

$$U = f(X,T) \quad \text{or} \tag{7.4}$$

$$U = f(X) + f(T) \tag{7.5}$$

where, X is the face advance, T is time and U is the convergence.

As a result of statistical analyses of underground measurements, it has been found that the convergence can be expressed best by functions similar to Equations 7.2 which represent the time dependent component and by functions similar to Equations 7.3 which represent the distance from tunnel face component.

Initially, the expressions given in Equations 7.6 and 7.7 have been evaluated:

$$U = a\left\{\left[1-e^{-X/b_1}\right]+\left[1-e^{-T/b_2}\right]\right\} \tag{7.6}$$

$$U = a\left\{\left[1-e^{-X/b_1}\right]\times\left[1-e^{-T/b_2}\right]\right\} \tag{7.7}$$

where, a, b_1, b_2 are constant values, X is the distance from tunnel face in meters, T is the time in days; and U is the convergence in millimeters.

Although the expression found in Equation 7.5 is more meaningful, the exponential function given in Equation 7.8 represents the roof behavior much better with higher coefficient of regression:

$$U = a\left[1 - e^{-X/b}\right]\left[1 - e^{-T/b}\right] \tag{7.8}$$

The results of the regression analysis obtained based on Equation 7.8 for various stations and also the associated support type at each station are given in Table 7.11.

Two typical examples showing "time" and "face advance" dependent convergence relationships are given in Figures 7.7 and 7.8 for station K1.

Convergence versus distance from tunnel face graph shows that, convergence approaches to an asymptotical value after 120 meters. In other words, the opening becomes fully stable at a distance twenty times of the roof span upon completion of the interaction between the support and the rock mass. The initiation and completion of the interaction at various stations are critical in stability and performance analyses.

Further statistical analyses were carried out based on the data obtained from different support locations. Consequently, the function given in Equation 7.9 was derived:

$$U = a\left[e^{0.025 - B/\left(B^2 + X\right)}\right]\left[1 - e^{-T/b}\right] \tag{7.9}$$

where, a and b are constants, B is the roof span (m), and X is the distance from tunnel face (m), T is the time (day).

Table 7.11 Results of Statistical Analysis Obtained Based on Data Representing "Convergence", "Time" and "Distance from Tunnel Face" (from Equation 7.8)

Support Type	Station Code	Constant *a*	Constant *b*	Regression Coefficient, R^2
Split-Set	K1	9.896	20.579	0.77
Split-Set	K2	8.735	21.416	0.84
Split-Set & YSA	K3	7.966	36.534	0.78
Yielding Super Swellex	K4	5.566	16.134	0.78
Yielding Super Swellex	K5	4.928	16.860	0.63
Yielding Super Swellex	K6	4.657	23.759	0.91
Yielding Super Swellex & YSA	K7	4.073	37.316	0.85
Sis-Resin	K8	5.289	28.544	0.92
Sis-Resin	K9	6.571	38.508	0.94
Sis-Resin	K10	5.839	26.636	0.79
Sis-Resin & YSA	K11	5.924	49.034	0.87
Fosroc-Resin	K12	5.332	29.661	0.91
Fosroc-Resin	K13	6.192	23.345	0.96
Fosroc-Resin	K14	6.082	28.198	0.91
Fosroc-Resin & YSA	K15	3.822	17.896	0.66
Yielding Steel Arch (YSA)	K16	12.871	10.823	0.86
Rigid Steel Arch	K17	10.227	20.166	0.94
Rigid Steel Arch	K18	9.337	19.945	0.97

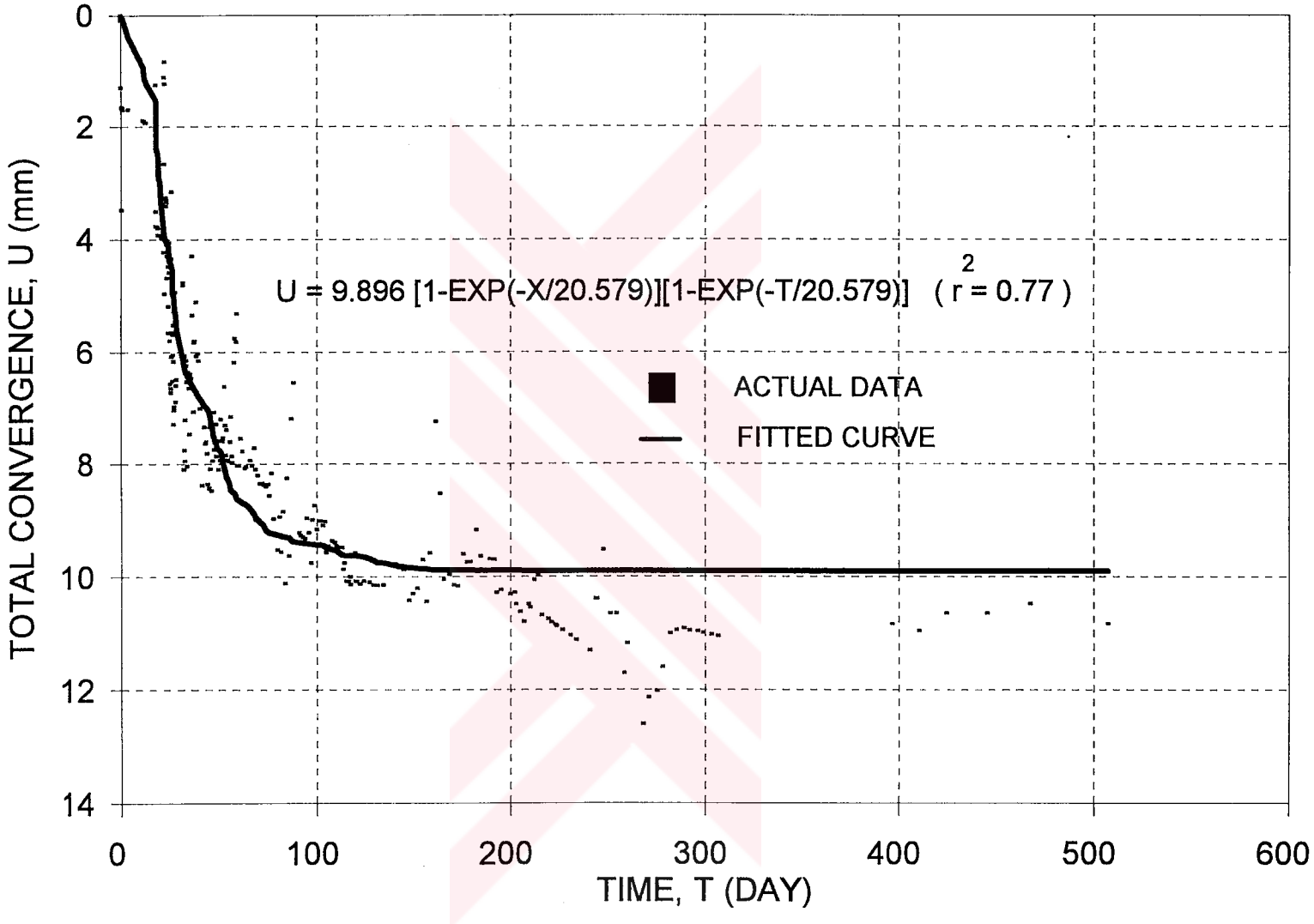

Figure 7.7 Total convergence versus time relationship obtained from the exponential model for station K1

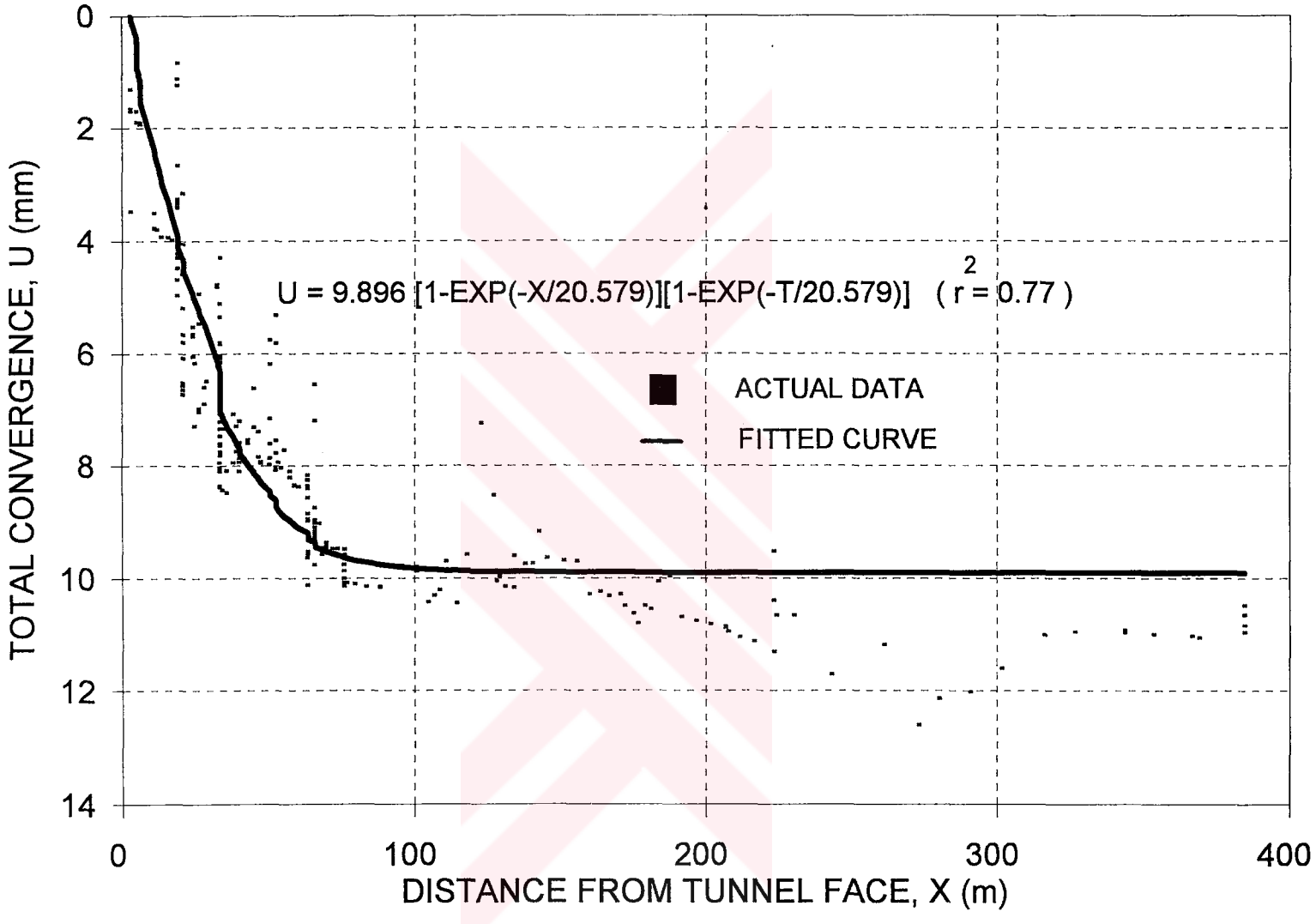

Figure 7.8 Total convergence versus distance from tunnel face relationship obtained from the exponential model for station K1

The results of statistical analysis derived based on empirical Equation 7.9 are given in Table 7.12. Two typical examples for station K1 are presented in Figures 7.9 and 7.10. The plots obtained from other stations are given in Appendix D.

In summary, the roof behavior in A-810 gate road, can be characterized by the statistical function given in Equation 7.9 which takes the following general form:

$$U = a\left[e^{0.025-B/(B^2+X)}\right]\left[1-e^{-T/b}\right] \tag{7.9}$$

where,

$$U = f\left(x = f(T), T\right) \tag{7.9a}$$

$$U = f\left(x = f(T)\right) \times f(T) \tag{7.9b}$$

7.3 Statistical Analysis of Roof Strata Movement

As mentioned in Section 7.2, borehole extensometer readings were evaluated by STATGRAPH, the statistical computer program. The results of statistical analysis for roof strata movement matches to the selected model developed for convergence.

7.3.1 The Time-Dependent Analysis of Roof Strata Movement

Similar to the results of convergence analysis, the results obtained from analysis of roof strata movement can also be characterized by three types of mathematical model shown in Table 7.13.

Table 7.12 Results of statistical analysis obtained based on Equation 7.9 for a 6-meter roof span

Support Type	Station Code	Constant a^*	Constant b	Regression Coefficient, R^2
Split-Set	K1	10.50	37.038	0.79
Split-Set	K2	11.096	46.867	0.87
Split-Set & YSA	K3	9.000	83.688	0.85
Yielding Super Swellex	K4	6.25	39.066	0.82
Yielding Super Swellex	K5	6.50	69.643	0.76
Yielding Super Swellex	K6	5.344	54.266	0.89
Yielding Super Swellex & YSA	K7	4.622	71.360	0.87
Sis-Resin	K8	5.400	40.195	0.92
Sis-Resin	K9	7.00	59.484	0.90
Sis-Resin	K10	6.30	38.431	0.82
Sis-Resin & YSA	K11	6.00	74.722	0.82
Fosroc-Resin	K12	5.25	38.594	0.88
Fosroc-Resin	K13	6.30	28.417	0.95
Fosroc-Resin	K14	6.35	36.284	0.90
Fosroc-Resin & YSA	K15	4.80	34.069	0.66
Yielding Steel Arch (YSA)	K16	14.20	17.166	0.81
Rigid Steel Arch	K17	11.30	25.669	0.94
Rigid Steel Arch	K18	9.689	22.897	0.98

* $a=U$, as $T\rightarrow\infty$ and $X\rightarrow\infty$

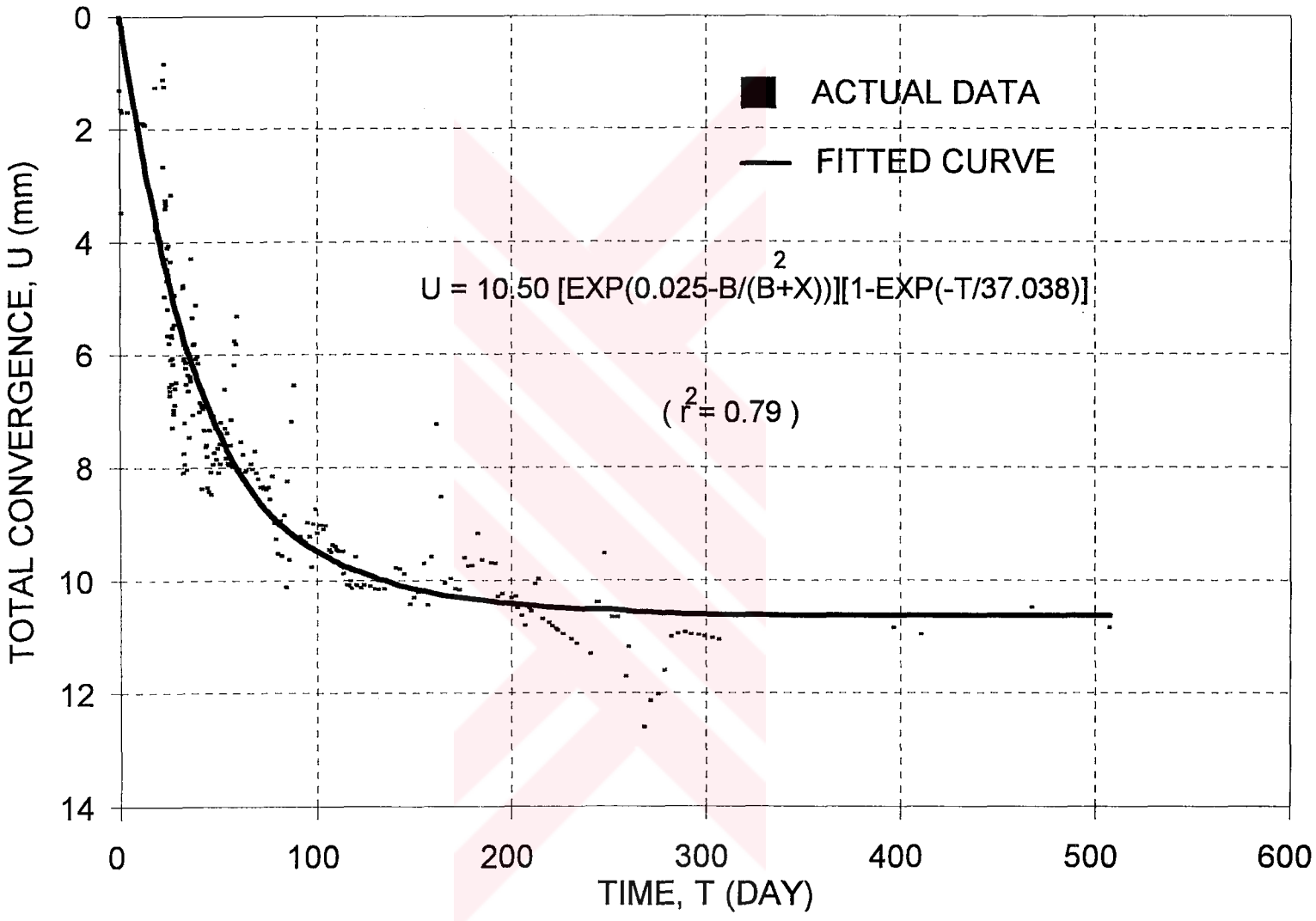

Figure 7.9 Statistical equation describing rock mass behavior around a roadway in "Time versus Total Convergence" for station K1

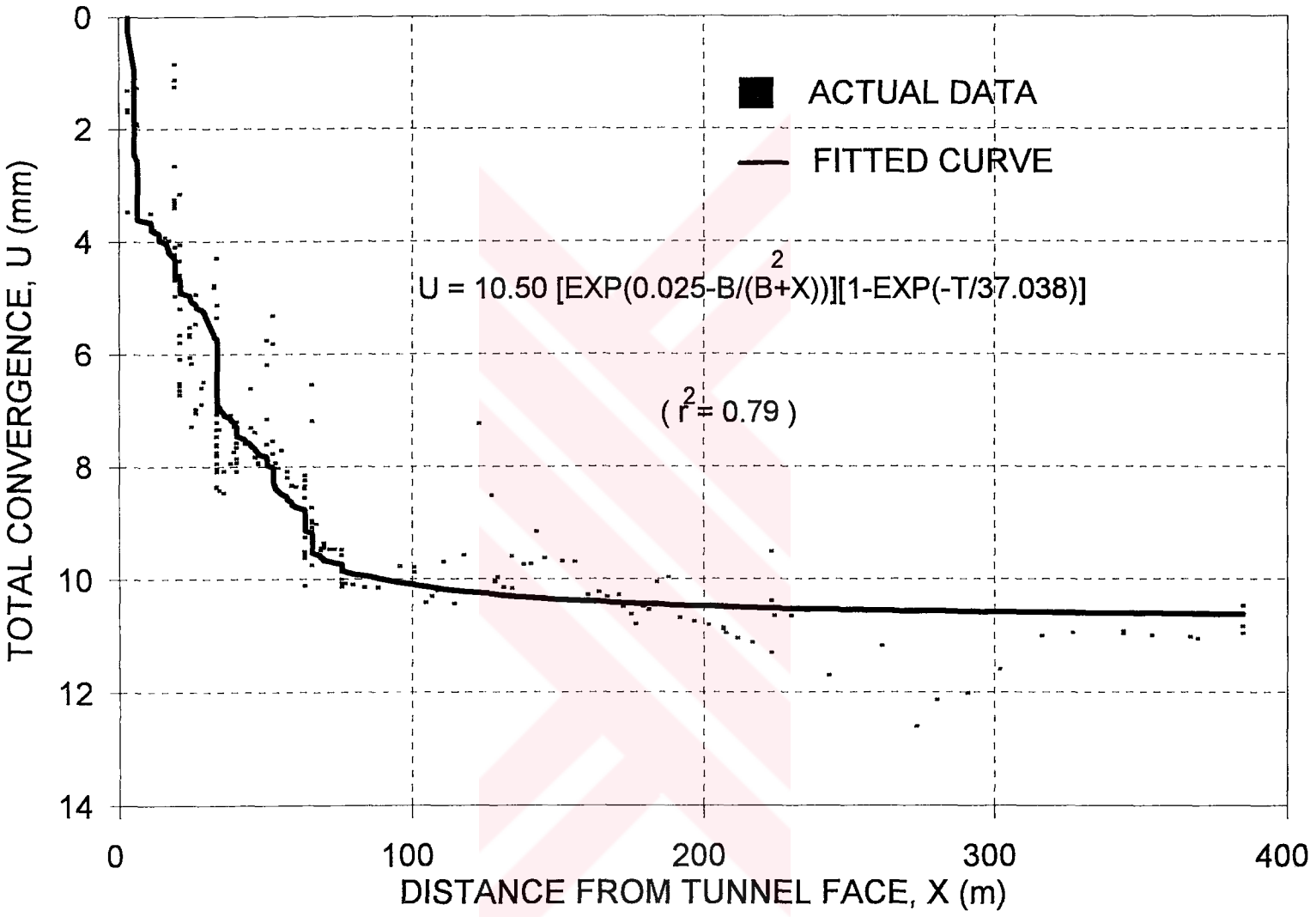

Figure 7.10 Statistical equation describing rock mass behavior around a roadway in "Distance from tunnel face vs Total Convergence" for station K1

Table 7.13 Mathematical models characterizing the roof behavior

Statistical Function	The Mathematical Expression
Logarithmic	$U = a + b \ln T$ or $U = a + b \ln(T+1)$
Exponential	$U = a\left(1 - e^{-T/b}\right)$
Power	$U = a\,T^{b}$

According to the results of statistical analysis, the best function characterizing the roof strata movement is also an exponential function (Equation 7.2). which was developed during time dependent convergence analyses (Section 7.2.1):

$$U = f(T) \quad \text{or} \tag{7.2a}$$

$$U = a\left(1 - e^{-T/b}\right) \tag{7.2b}$$

where, a and b are constant values, T is time in days, and U is the roof displacements in mm.

7.3.2 Analyses of Face-Advance Dependent Roof Strata Movement

The best fit to the data obtained from borehole extensometer measurements is an exponential function similar to the equations presented earlier as in Equations 7.3a and 7.3b:

$$U = f(X) \tag{7.3a}$$

$$U = a\left[1 - e^{-X/b}\right] \tag{7.3b}$$

where, a and b are constant values, X is the distance from tunnel face in meters, and U is the roof strata movement for each sub-station in an extensometer borehole in mm.

7.3.3 Statistical Analyses Based on Time and Distance from Tunnel Face

The roof strata displacements in different levels above the roof line can be determined by two functions as shown in Equations 7.8 and 7.9.

$$U = a\left[1 - e^{-X/b}\right]\left[1 - e^{-T/b}\right] \tag{7.8}$$

$$U = a\left[e^{0.025 - B/(B^2+X)}\right]\left[1 - e^{-T/b}\right] \tag{7.9}$$

A typical example for split-set E1 station is given in Table 7.14 and Figures 7.11 and 7.12. As a result of the analyses summarized in this section, Equation 7.9 has been selected for characterization of roof strata movement.

Detailed analysis of roof strata movement will not be given in this thesis.

Table 7.14 Results of Statistical Analyses Based on Equation 7.9 for Station E1

Support Type	Sub-Station Code	Constant a	Constant b	Regression Coefficient, R^2
Split-Set	R1	6.5	61.44	0.90
Split-Set	R2	7.6	55.19	0.77
Split-Set	R3	9.5	77.81	0.76
Split-Set	R4	9.6	47.54	0.67
Split-Set	R5	10.0	37.10	0.70

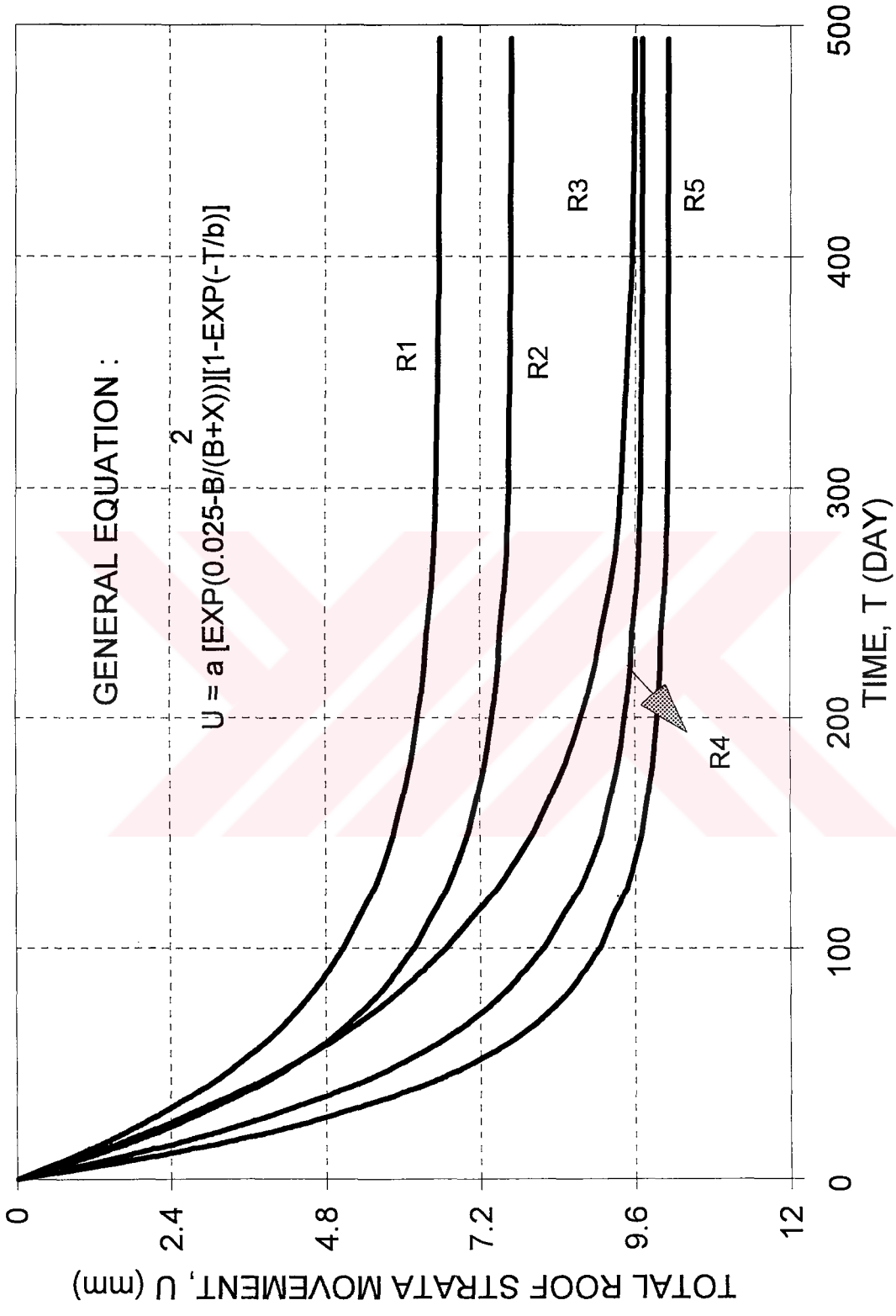

Figure 7.11 Total of the roof strata displacement versus time relationship obtained from the exponential model for station E1

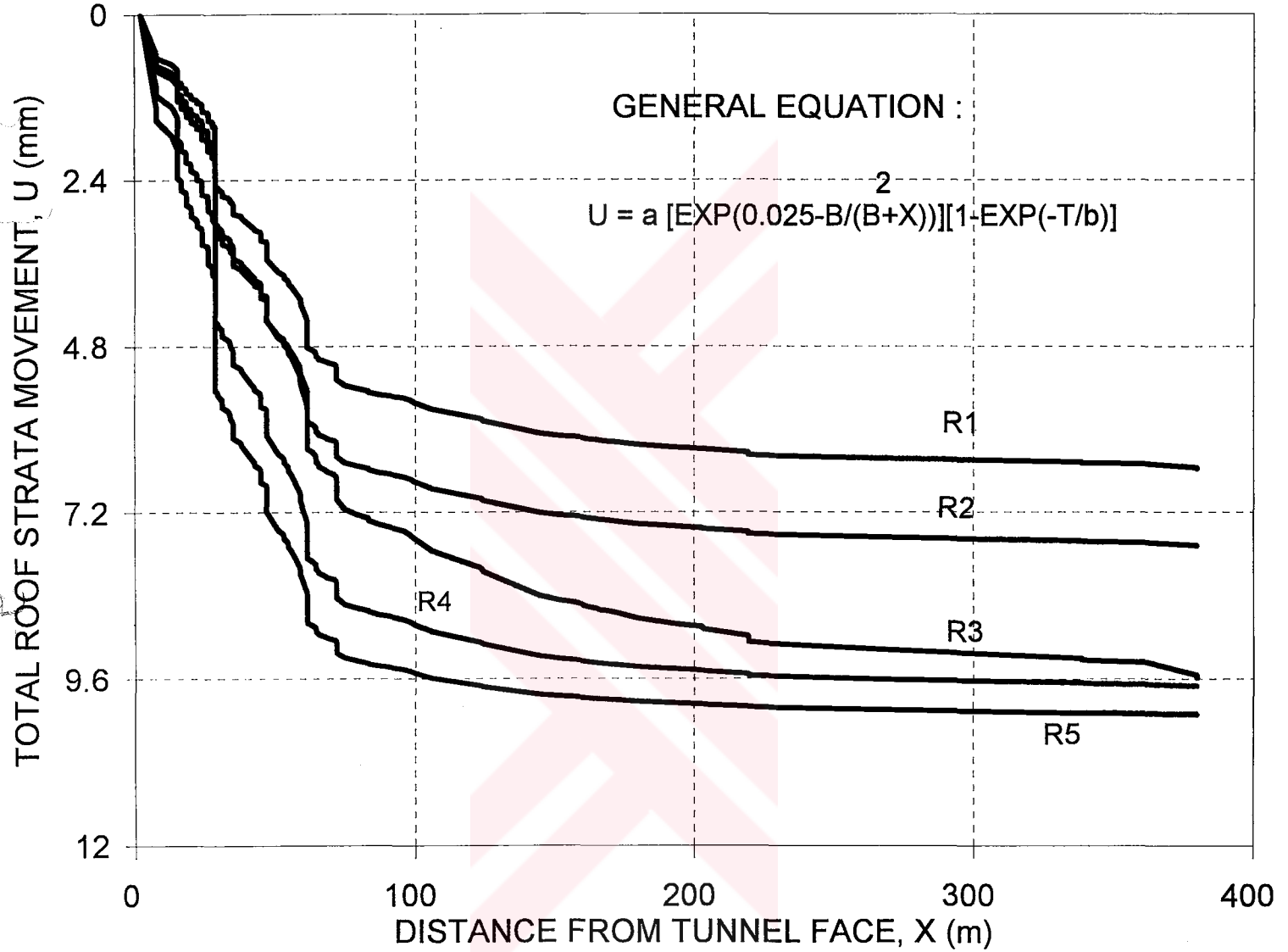

Figure 7.12 Total of the roof strata displacement versus distance from tunnel face relationship obtained from the exponential model for station E1

7.4 Results of Mathematical Analysis

Equation 7.9 derived in Section 7.2 and 7.3 to determine convergence and roof strata displacement, are functions having exactly the same structure. Both "time" and "face advance" dependent equations have been obtained by statistical evaluation of field data. These equations can be utilized not only to investigate the strata displacements, but also to interpret support and rock mass interaction and to compare the performance of underground roadways stabilize by different support types. In the cases of interaction and performance analysis; however, it is more meaningful to manipulate the functions provide "rate of convergence" and "rate of convergence-velocity". In Sections 7.4.1, 7.4.2 and 7.4.3 the results obtained from mathematical analysis are a general evaluation of the results and presented in Section 7.4.4. Comparison of the interaction and performances in various supported regions are given.

7.4.1 Analyses Based on Convergence Equation

In order to simulate the strata behavior of various supported sections in A-810 gate road, to investigate the stability of these sections, and to study the support and the rock mass interaction mechanism, a mathematical model was developed in this study. This model actually is a differential equation, developed based on statistical best fit to the field data consisting of 45,904 convergence readings obtained from 18 convergence stations for a period of 15 months.

Using the equation developed, initially the plots of total convergence versus time, were obtained for each supported region as shown in Figure 7.13 to 7.17. The actual values of the rate of face advance were used, in the Equations, for each

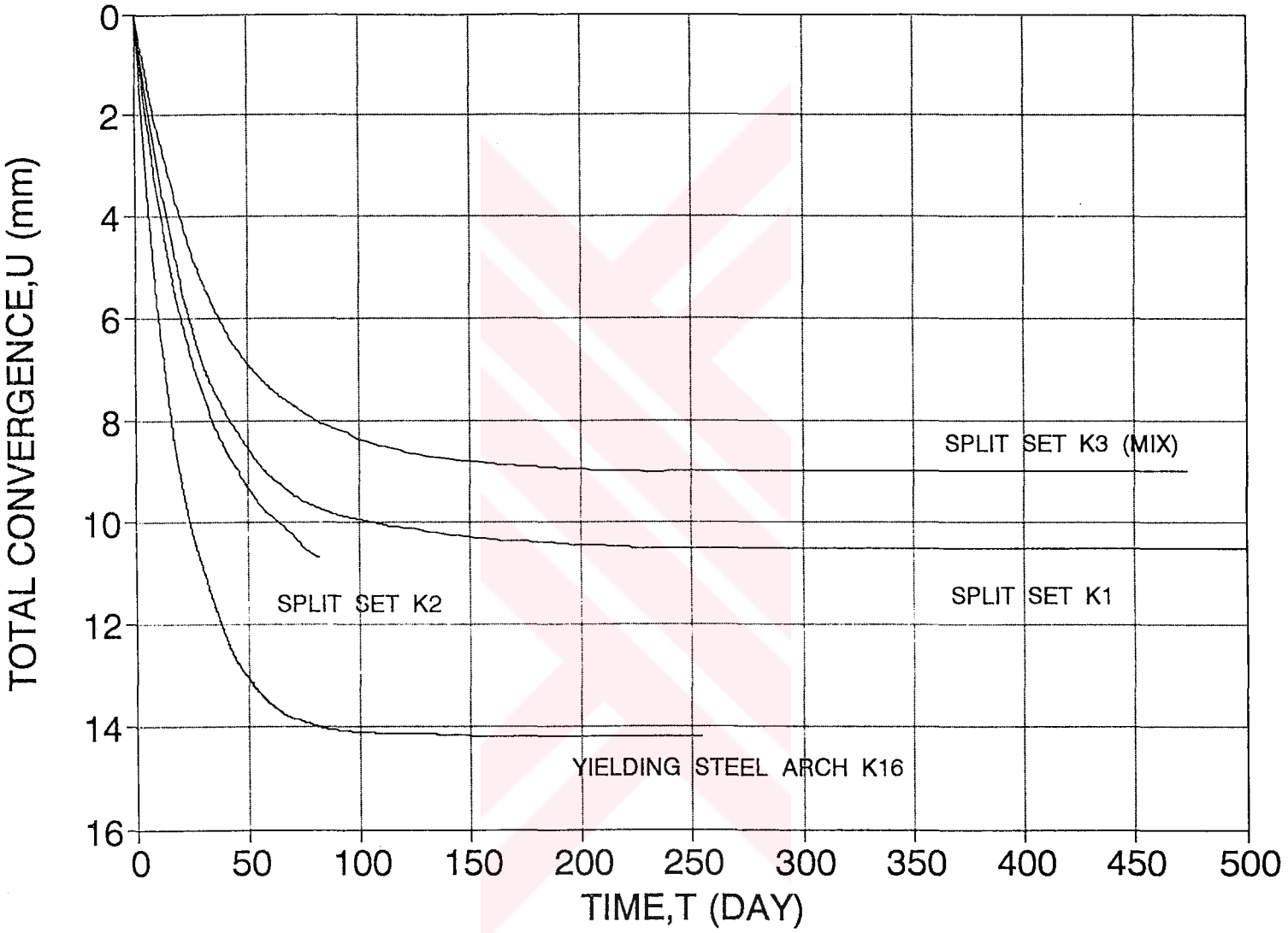

Figure 7.13 The characteristic curves for split-set bolts obtained from Equation 7.9 based on the in situ measurements

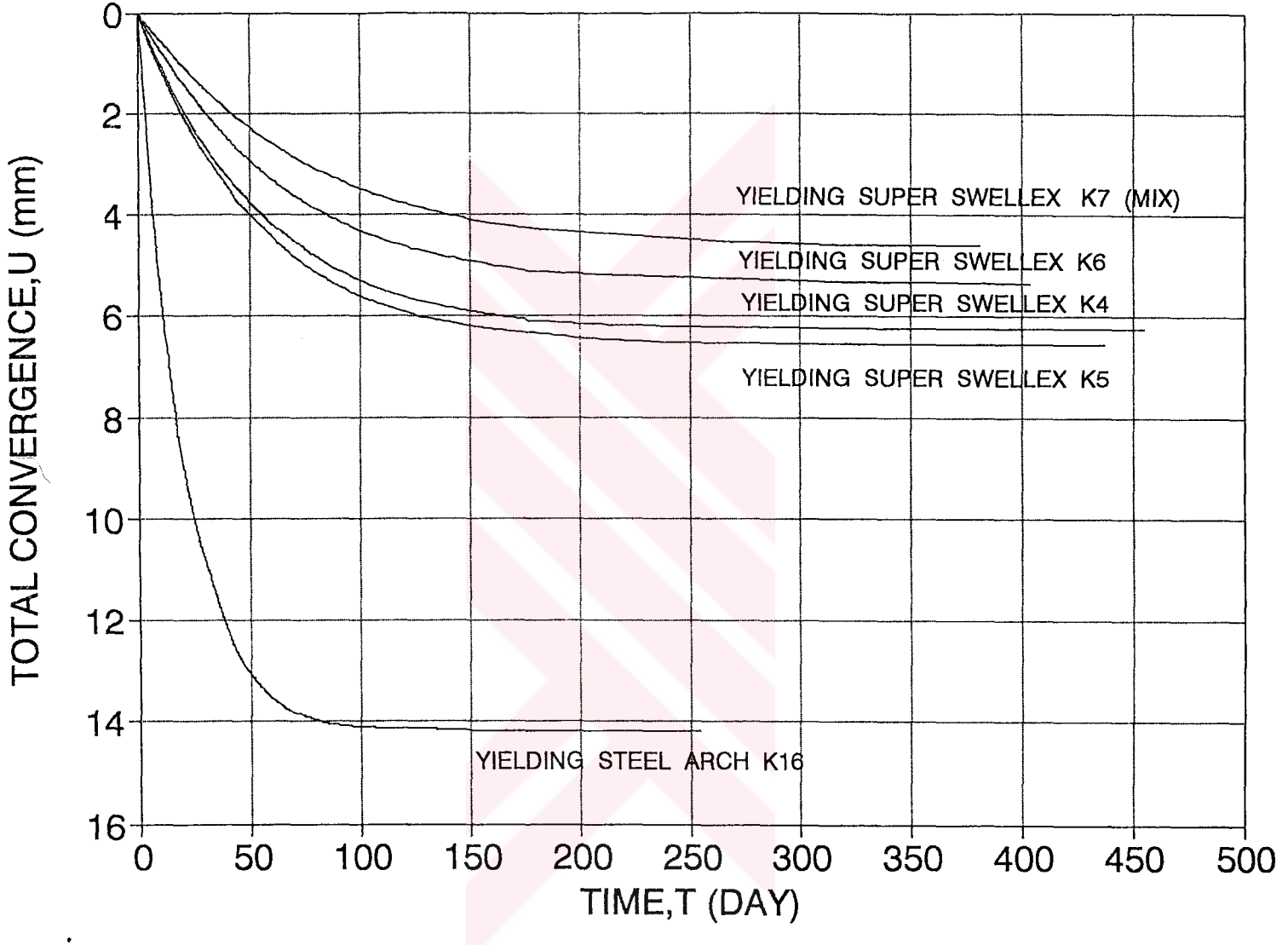

Figure 7.14 The characteristic curves for yielding super swellex bolts obtained from Equation 7.9 based on the in situ measurements

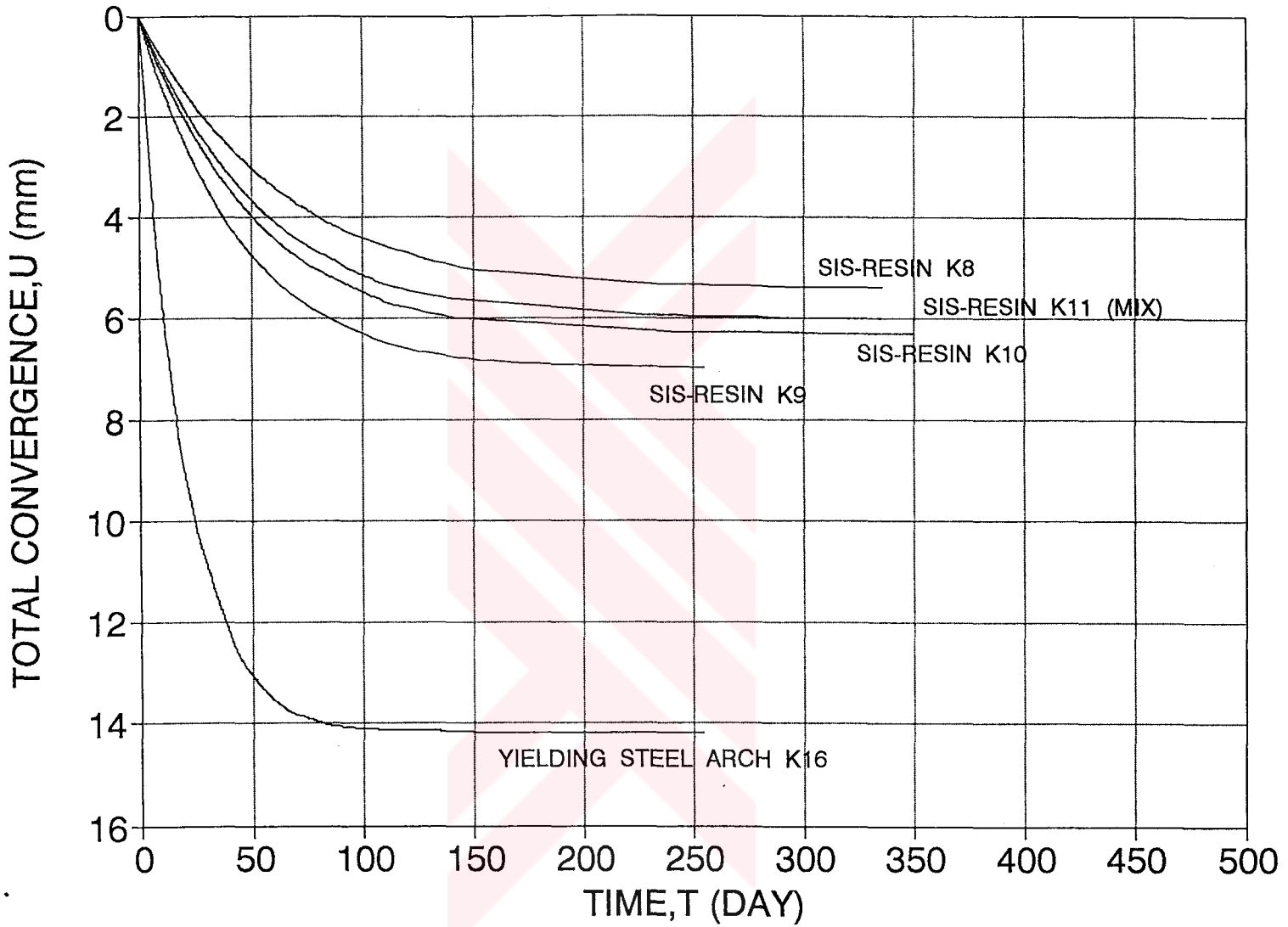

Figure 7.15 The characteristic curves for SIS-resin bolts obtained from Equation 7.9 based on the in situ measurements

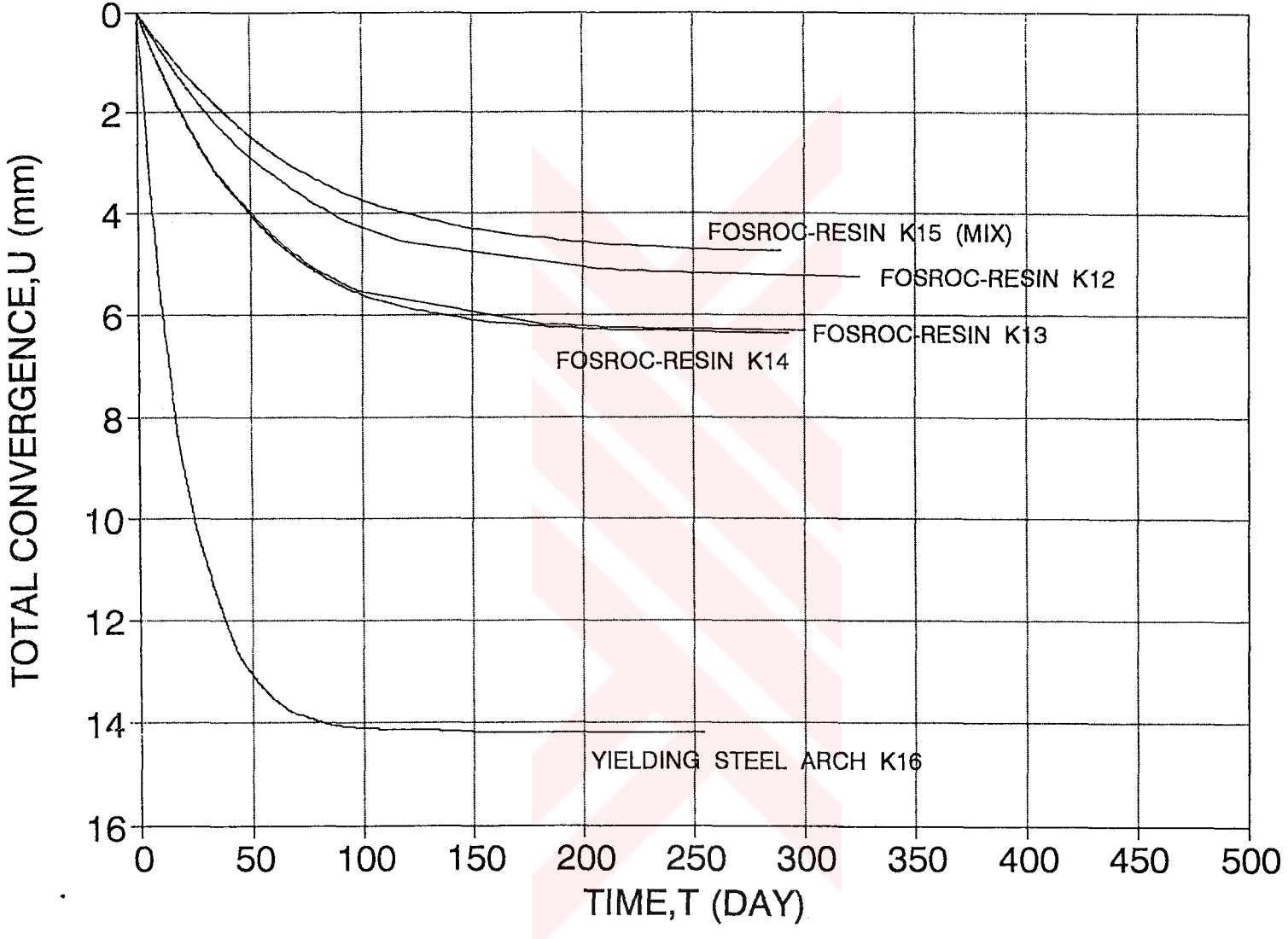

Figure 7.16 The characteristic curves for Fosroc-resin bolts obtained from Equation 7.9 based on the in situ measurements

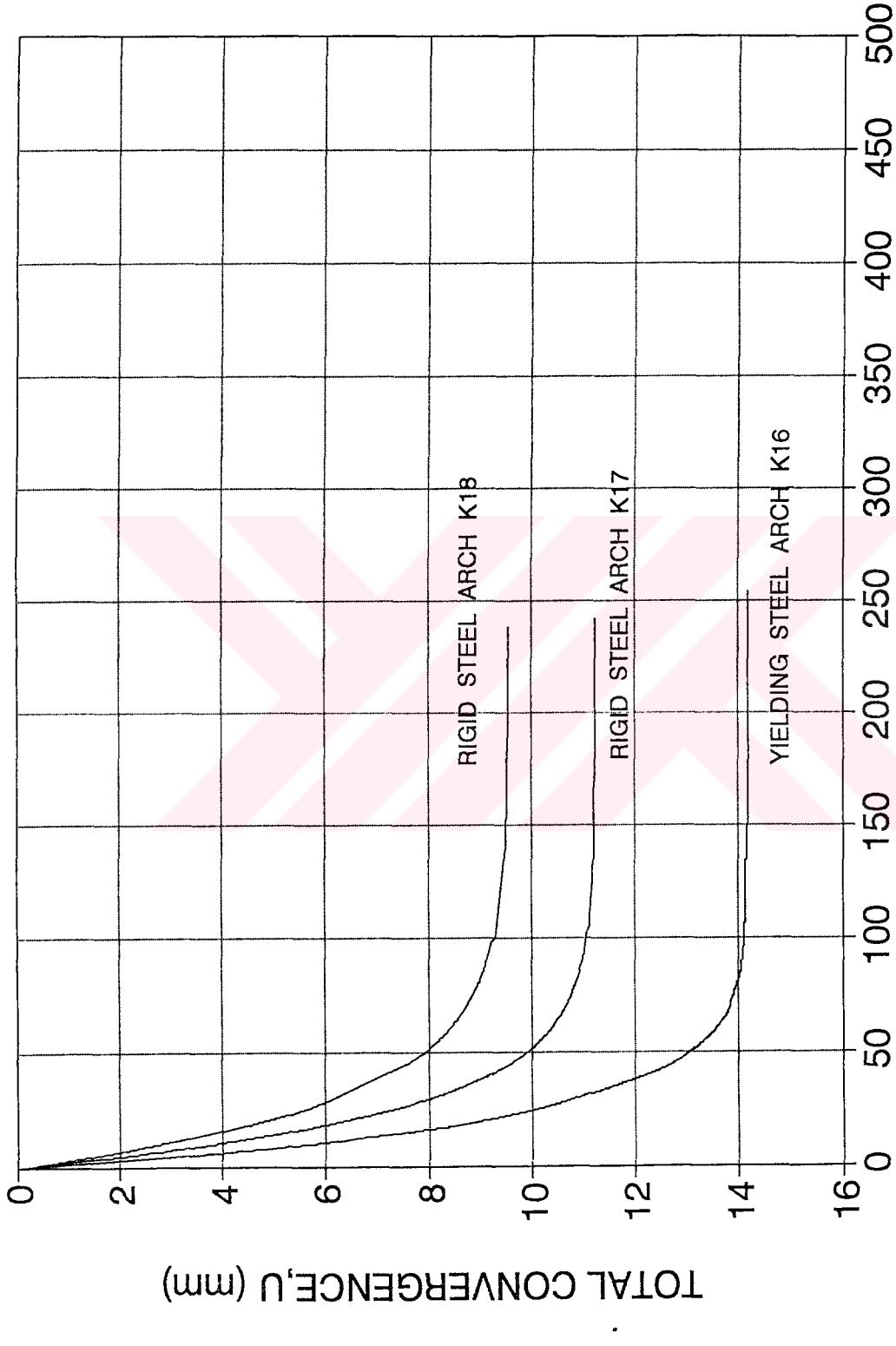

Figure 7.17 The characteristic curves for yielding and rigid steel arches obtained from Equation 7.9 based on the in situ measurements

supported region. As it can be seen, the plots representing the yielding steel arch (station K16) and the mixed region support (area supported by both the same rock bolt and steel arches) are also included into each figure for comparison purposes. The mixed region support represents an overdesign. It is obvious from these graphs that in general the maximum convergence occurs in the area supported by yielding steel arches and the minimum in the regions supported by mixed supports. It is also possible to observe that in the region where the maximum total convergence is higher, the convergence rate is also higher and the convergence curve reaches to an asymptotical value earlier (if the strata is stable) compared to the regions where maximum total convergence is relatively lower (see Figures 7.13 through 7.17). Comparison of the behavior of the strata supported by different units will be given in Section 7.4.4.

During interpretation of the convergence (U) versus time (T) graphs, it was realized that these graphs (U-T) were not adequate for explaining the support and rock mass interaction sufficiently. For this reason, convergence rate and convergence-velocity rate graphs were obtained by taking the first and second partial derivatives of the convergence equation.

Analysis associated with convergence rate is given in the next section.

7.4.2 Analysis of Rate of Convergence

The rate of convergence values were obtained by taking the derivative of the convergence-time (U-T) equation as follows.

General form of the (U-T) equation can be expressed as shown in Equation 7.9 presented earlier in Section 7.2.

$$U = a\left[e^{0.025-B/(B^2+X)}\right]\left[1-e^{-T/b}\right] \tag{7.9}$$

Rearranging this equation:

$$U = \left\{\frac{1.025a}{e^{\left(\frac{B}{B^2+X}\right)}}\right\} - \left\{\frac{1.025a}{e^{\left(\frac{B}{B^2+X}\right)}e^{T/b}}\right\} \tag{7.10}$$

If the partial derivative of this function is taken with respect to time (T), such as:

$$\frac{dU}{dT} = \frac{\partial U}{\partial x}\cdot\frac{dx}{dT} + \frac{\partial U}{\partial T} \tag{7.11}$$

then

$$\frac{\partial U}{\partial X} = \left\{\frac{-\left[-\frac{B}{(B^2+X)^2}\right]e^{\left\lceil\left(\frac{B}{B^2+X}\right)\right\rceil}1.025a}{\left[e^{\left(\frac{B}{B^2+X}\right)}\right]^2}\right\} - \left\{\frac{-\left[-\frac{B}{(B^2+X)^2}\right]e^{\left\lceil\left(\frac{B}{B^2+X}\right)\right\rceil}e^{T/b}\,1.025a}{\left[e^{\left(\frac{B}{B^2+X}\right)}e^{T/b}\right]^2}\right\}$$

$$\frac{\partial U}{\partial X} = \frac{1.025aB}{(B^2+X)^2 e^{\left(\frac{B}{B^2+X}\right)}e^{T/b}}\left[e^{T/b}-1\right] \tag{7.12}$$

$$\frac{\partial U}{\partial T} = \left[-\frac{-\frac{1}{b}e^{T/b}e^{\left(\frac{B}{B^2+X}\right)}1.025a}{\left[e^{\left(\frac{B}{B^2+X}\right)}e^{T/b}\right]^2}\right]$$

$$\frac{\partial U}{\partial T} = \left[\frac{1.025a}{be^{\left(\frac{B}{B^2+X}\right)}e^{T/b}}\right] \tag{7.13}$$

Putting Equations 7.12 and 7.13 into Equation 7.11 we obtain:

$$\frac{dU}{dT}=\frac{1.025aB}{\left(B^2+X\right)^2 e^{\left[\frac{B}{\left(B^2+X\right)}\right]} e^{T/b}}\left[e^{T/b}-1\right]\frac{dX}{dT}+\left[\frac{1.025a}{be^{\left(\frac{B}{B^2+X}\right)} e^{T/b}}\right] \qquad (7.14)$$

Rearranging this equation:

$$\frac{dU}{dT}=\frac{1.025a}{b\left(B^2+X\right)^2 e^{\left[\frac{B}{\left(B^2+X\right)}\right]} e^{T/b}}\left[b\cdot B\cdot\left(e^{T/b}-1\right)\frac{dX}{dT}+\left(B^2+X\right)^2\right] \qquad (7.15)$$

Using Equation 7.15, variation of both the instant and total rate of convergence $\left(\frac{dU}{dT}\right)$ were analyzed as a function of time (T). Typical examples of instant $\left(\frac{dU}{dT}\right)$ versus (T) graphs representing various stations are given in Figures 7.18 to 7.23. The plots obtained from other stations are given in Appendix E. From the results of analysis of these graphs, the following conclusions can be drawn:

i) The rate of strata convergence is different in each area stabilized by different type of support and decreases with time.

ii) When the value of total convergence is high, then the initial rate of convergence is also high. However, in these cases, rate of convergence reaches to zero (an indication of stability) earlier (i.e. yielding arch, Figure 7.18), then when the initial rate of convergence is low (i.e. yielding super swellex, Figure 7.19). These results can also be seen in Table 7.15.

Table 7.15 The results obtained from analysis of rate of convergence

Support Type	Station Code	Max Conv. (mm)	Initial Rate of Conv. (mm/day)	Time, when rate approaches to zero (days)
Split-Set	K1	10.50	0.690	225
Split-Set	K2	11.10	0.810	?*
Split-Set & YSA	K3	9.00	0.510	240
Yielding Super Swellex	K4	6.25	0.225	232.5
Yielding Super Swellex	K5	6.50	0.245	233.75
Yielding Super Swellex	K6	5.34	0.160	226.25
Yielding Sup. Swellex & YSA	K7	4.62	0.1133	345*
Sis-Resin	K8	5.40	0.162	295*
Sis-Resin	K9	7.00	0.300	207.5
Sis-Resin	K10	6.30	0.231	221.25
Sis-Resin & YSA	K11	6.00	0.207	238.75
Fosroc-Resin	K12	5.25	0.155	280*
Fosroc-Resin	K13	6.30	0.238	226.25*
Fosroc-Resin	K14	6.35	0.238	226.50*
Fosroc-Resin & YSA	K15	4.80	0.129	250*
Yielding Steel Arch (YSA)	K16	14.20	1.246	118.75
Rigid Steel Arch	K17	11.30	0.835	143.75
Rigid Steel Arch	K18	9.69	0.589	160.0

* rate of convergence had not reached to zero yet when the measurements terminated

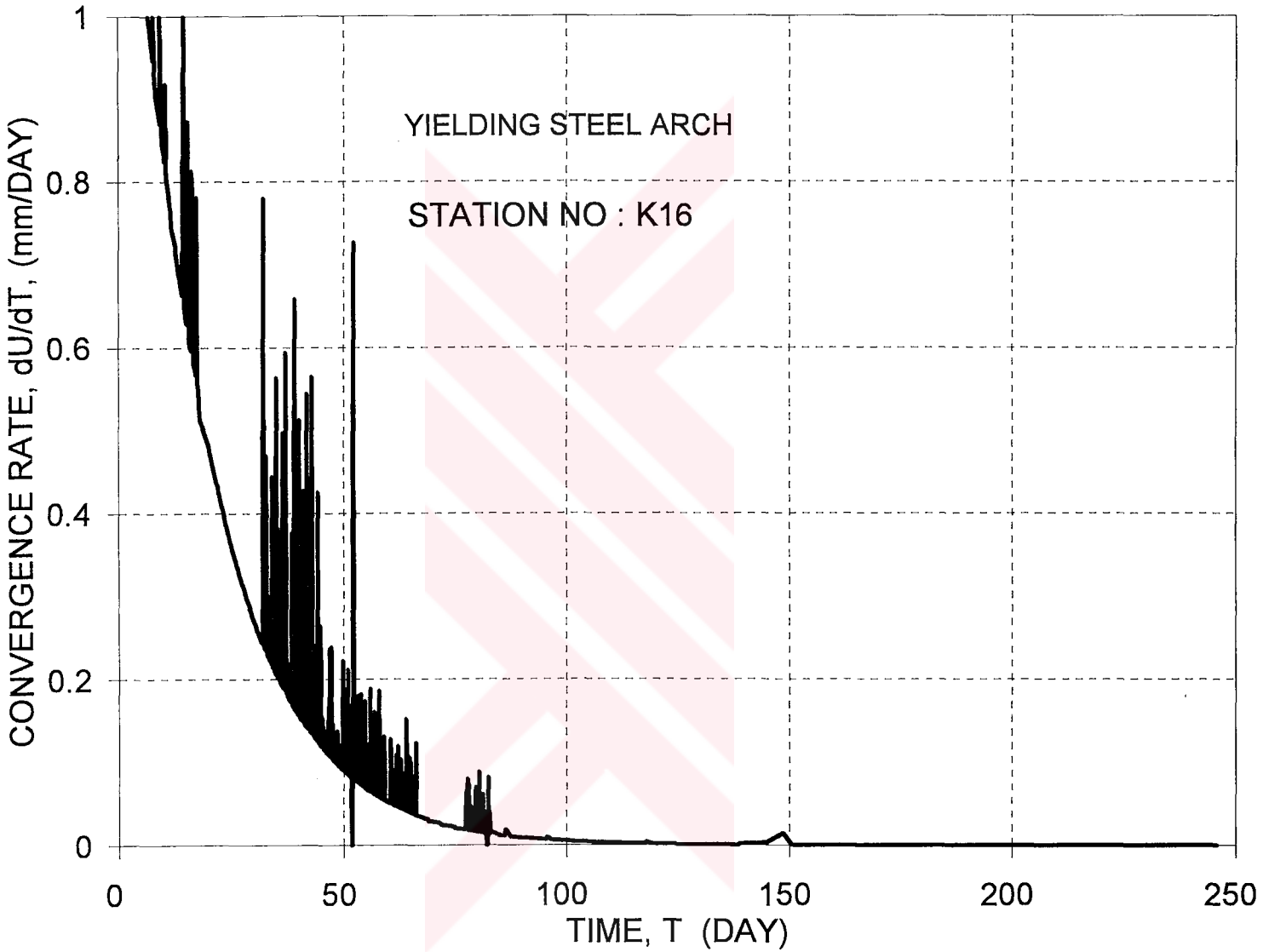

Figure 7.18 The characteristics of the instant convergence rate for the region supported by yielding steel arches

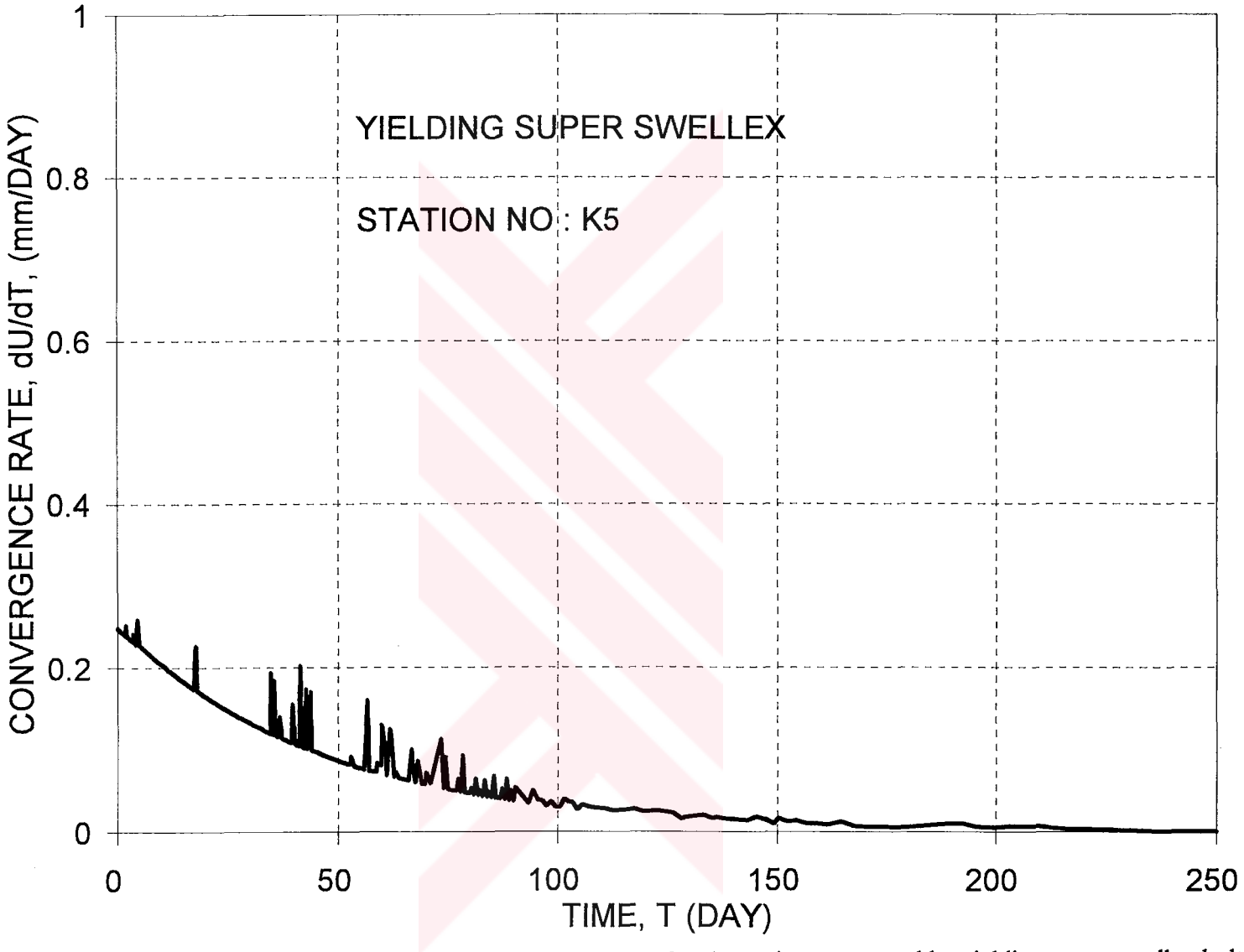

Figure 7.19 The characteristics of the instant convergence rate for the region supported by yielding super swellex bolts

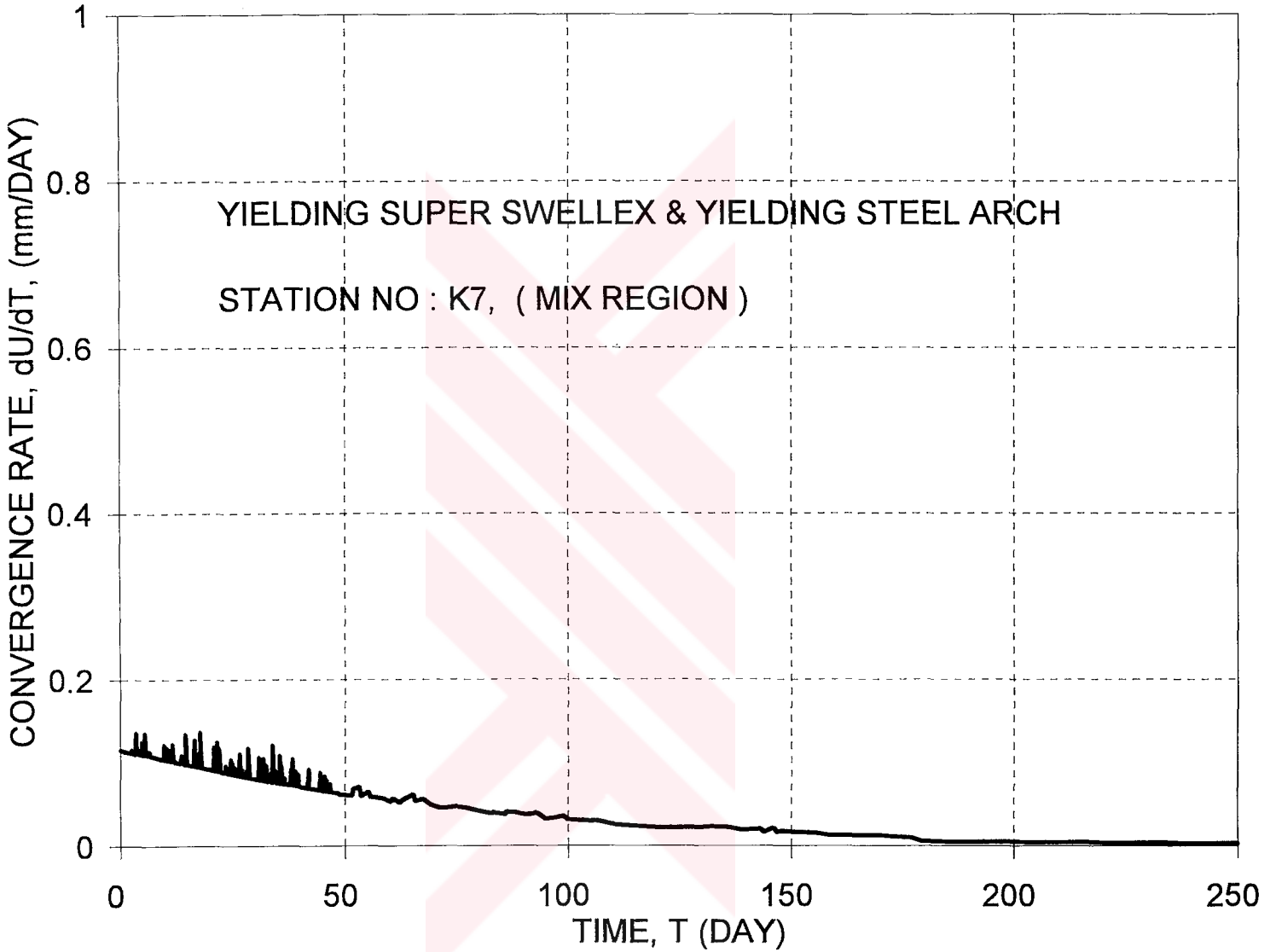

Figure 7.20 The characteristics of the instant convergence rate for supported mix region

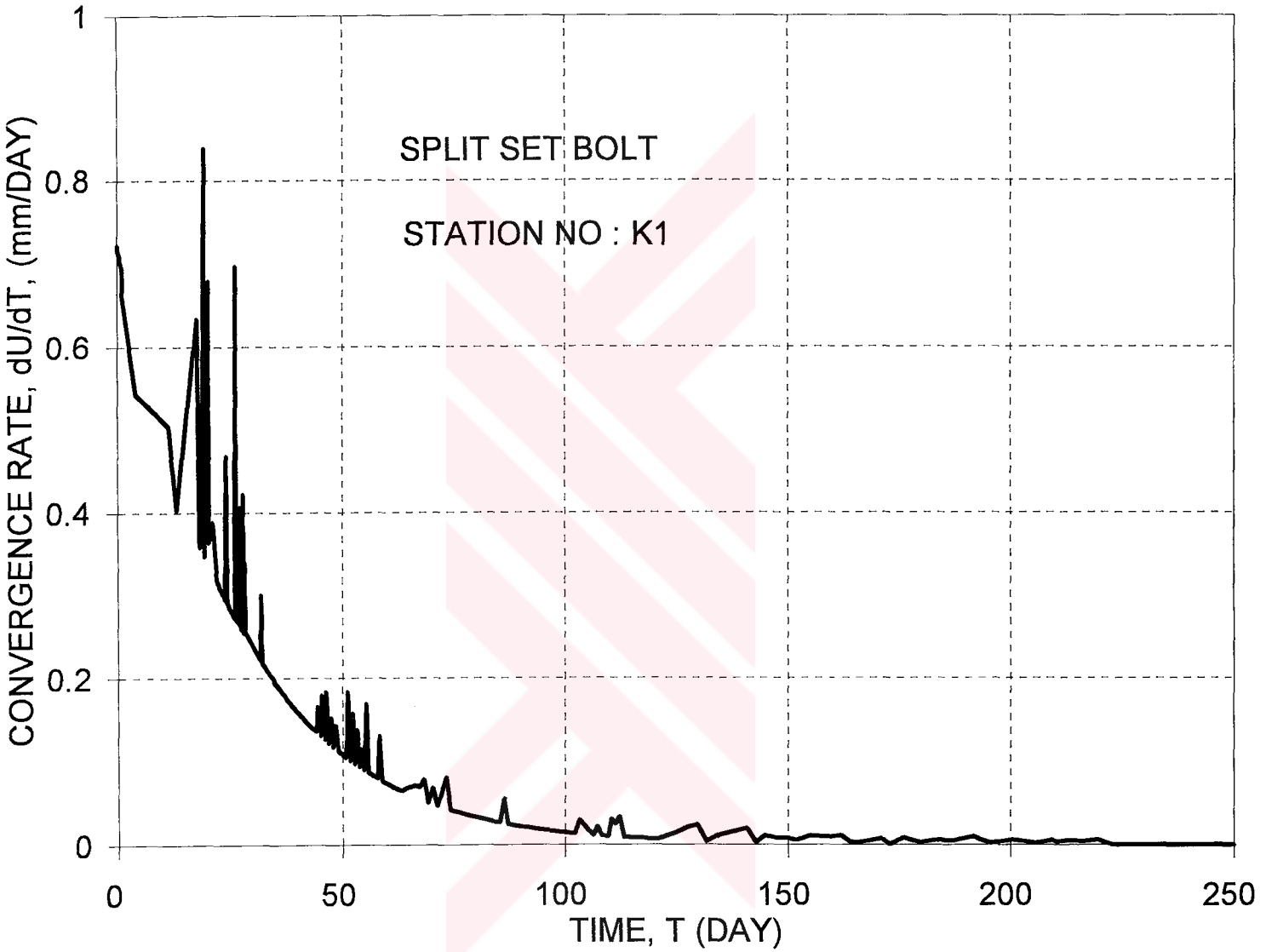

Figure 7.21 The characteristics of the instant convergence rate for the region supported by split-set bolts

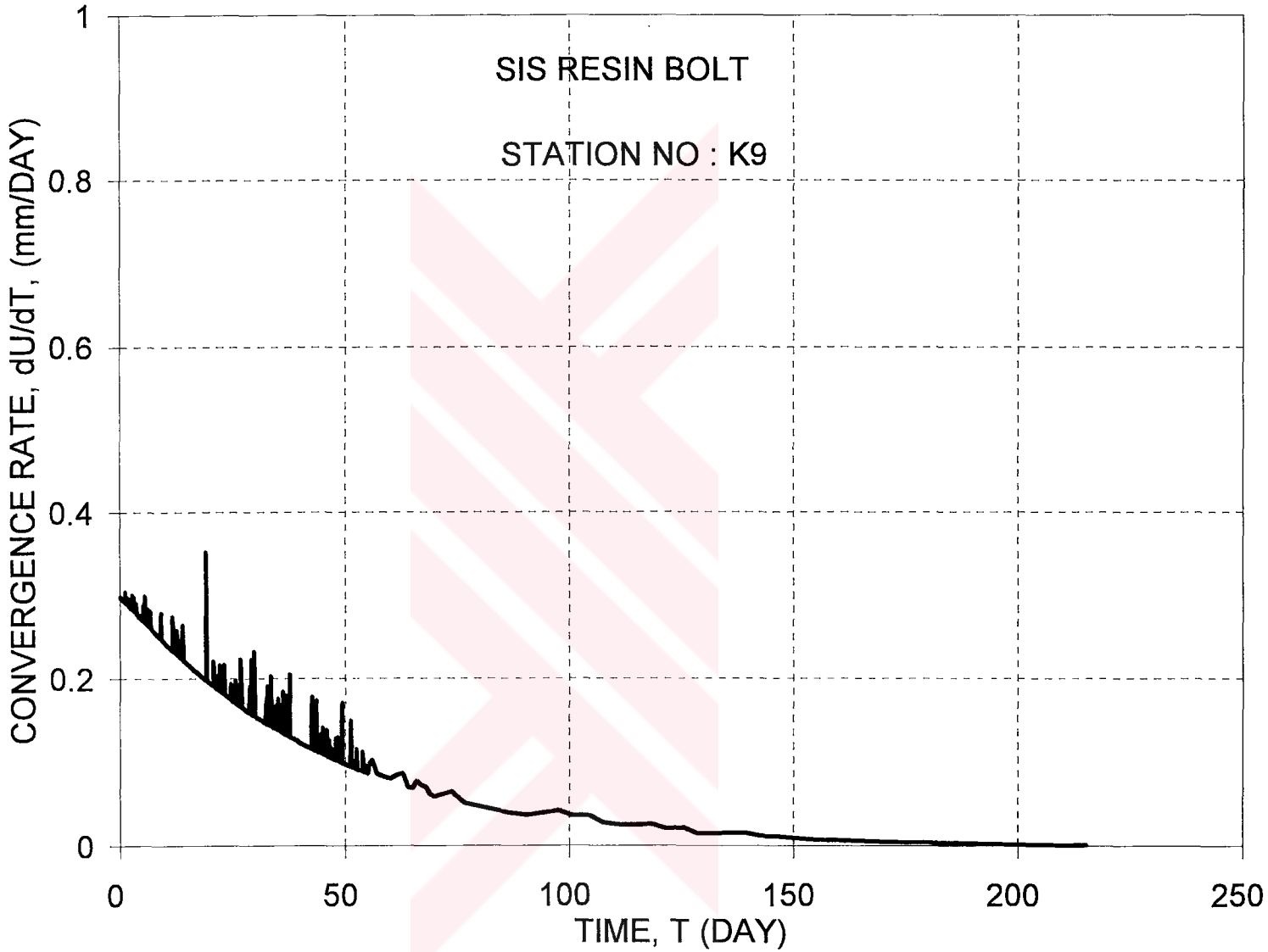

Figure 7.22 The characteristics of the instant convergence rate for the region supported by SIS-resin bolts

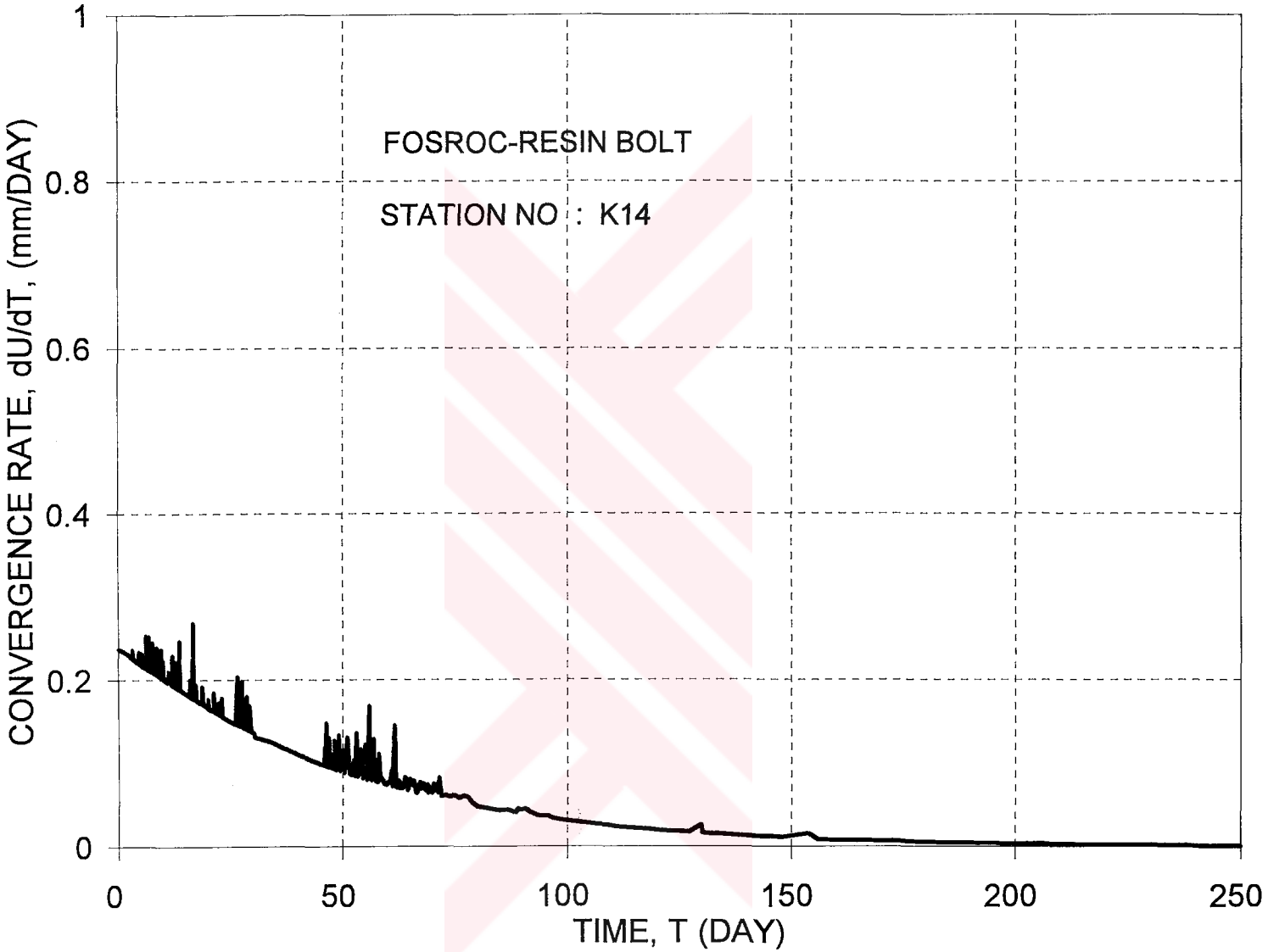

Figure 7.23 The characteristics of the instant convergence rate for the region supported by Fosroc-resin bolts

iii) In the graphs of "rate of convergence versus time", sudden increases and decreases in rates can easily be observed. This may be due to irregular rate of tunnel face advance. When excavation starts to advance after a stop, convergence increases suddenly reaching to a maximum value then drops down to its initial rates.

iv) The other important phenomena observed in these analysis is that this sudden increase and decreases in instant convergence rates (i.e. amplitudes) are high when the tunnel face is close to the station and decreases gradually and disappears finally when stability is fully reached. Frequency of the rate changes also reduces with time.

v) Lower amplitudes and frequencies in rate of convergence is an indication of better control of strata and better interaction between support and rock mass (Figure 7.19). It should be noticed however that this situation could be an indication of an overdesign (Figure 7.20). The importance of amplitude and frequencies will be more pronounced as will be seen in Section 7.4.3.

The total rate of convergence versus time analyses were also carried out in this study. The following conclusions were derived:

i) The total rate of convergence is the highest in the area supported by yielding steel arches. On the other hand, the total rate is lowest in the areas supported by rock bolts and steel arches together.

ii) the total rate of convergence is between curves representing yielding steel arches and mix support.

7.4.3 Analysis of Rate of Convergence-Velocity

The ratio of convergence-velocity values were obtained by testing the second partial derivative of the convergence equation (U) in the following form:

$$\frac{d^2U}{dT^2} = \frac{\partial\left(\frac{dU}{dT}\right)}{\partial X}\frac{dX}{dT} + \frac{\partial\left(\frac{dU}{dT}\right)}{\partial T} \tag{7.16}$$

Starting from Equation 7.9, given earlier, and taking the first and second partial derivatives:

$$U = a\left[e^{0.025 - B/\left(B^2+X\right)}\right]\left[1 - e^{-T/b}\right] \tag{7.9}$$

$$\frac{\partial\left(\frac{dU}{dT}\right)}{\partial X} = \left\{\frac{\left[-b\,2\left(B^2+X\right)\left(-\frac{B}{\left(B^2+X\right)^2}\right)e^{\left(B/B^2+X\right)}e^{T/b}\right] + \left[1.025\,a\,b\,B\left(e^{T/b}-1\right)\frac{dX}{dT}\right]}{\left[b\left(B^2+X\right)^2 e^{\left(B/B^2+X\right)}e^{T/b}\right]^2}\right\}$$

$$+\left\{\frac{\left[1.025\,a\,2\left(B^2+X\right)\right]\left[b\left(B^2+X\right)^2 e^{\left(B/B^2+X\right)}e^{T/b}\right]}{\left[b\left(B^2+X\right)^2 e^{\left(B/B^2+X\right)}e^{T/b}\right]^2}\right\}$$

$$-\left\{\frac{\left[b\,2\left(B^2+X\right)\left(-\frac{B}{\left(B^2+X\right)^2}\right)e^{\left(B/B^2+X\right)}e^{T/b}\right]\left[1.025\,a\left(B^2+X\right)^2\right]}{\left[b\left(B^2+X\right)^2 e^{\left(B/B^2+X\right)}e^{T/b}\right]^2}\right\}$$

$$\frac{\partial\left(\frac{dU}{dT}\right)}{\partial X} = \left\{\frac{2\,a\,B\,1.025\left(e^{T/b}-1\right)\left(\frac{B}{\left(B^2+X\right)^2}\right)\frac{dX}{dT}}{\left(B^2+X\right)^3 e^{\left(B/B^2+X\right)}e^{T/b}}\right\} + \left\{\frac{2\,a\,1.025\left(B^2+X\right)\left[1+\left(\frac{B}{\left(B^2+X\right)^2}\right)\right]}{b\left(B^2+X\right)^2 e^{\left(B/B^2+X\right)}e^{T/b}}\right\} \tag{7.17}$$

$$\frac{\partial\left(\frac{dU}{dT}\right)}{\partial T}=\left\{\frac{\left[1.025abB\frac{1}{b}e^{T/b}\frac{dX}{dT}\right]\left[b\left(B^2+X\right)^2e^{\left(\frac{B}{B^2+X}\right)}e^{T/b}\right]}{\left[b\left(B^2+X\right)^2e^{\left(\frac{B}{B^2+X}\right)}e^{T/b}\right]^2}\right\}$$

$$-\left\{\frac{\left[\frac{b}{b}\left(B^2+X\right)^2e^{\left(\frac{B}{B^2+X}\right)}e^{T/b}\right]\left[1.025abB\left(e^{T/b}-1\right)\frac{dX}{dT}\right]}{\left[b\left(B^2+X\right)^2e^{\left(\frac{B}{B^2+X}\right)}e^{T/b}\right]^2}\right\}$$

$$+\left\{\frac{-\left[\frac{b}{b}\left(B^2+X\right)^2e^{\left(\frac{B}{B^2+X}\right)}e^{T/b}\right]\left[1.025a\left(B^2+X\right)^2\right]}{\left[b\left(B^2+X\right)^2e^{\left(\frac{B}{B^2+X}\right)}e^{T/b}\right]^2}\right\}$$

$$\frac{\partial\left(\frac{dU}{dT}\right)}{\partial T}=\left\{\frac{1.025aB\frac{dX}{dT}}{b\left(B^2+X\right)^2e^{\left(\frac{B}{B^2+X}\right)}e^{T/b}}\right\}-\left\{\frac{1.025a}{b^2e^{\left(\frac{B}{B^2+X}\right)}e^{T/b}}\right\} \tag{7.18}$$

If Equations 7.17 and 7.18 are put into Equation 7.16

$$\frac{d^2U}{dT^2}=\left\{\left[\frac{2aB1.025\left(e^{T/b}-1\right)\left(\frac{B}{\left(B^2+X\right)^2}\right)\frac{dX}{dT}}{\left(B^2+X\right)^3e^{\left(B/B^2+X\right)}e^{T/b}}\right]+\left[\frac{2a1.025\left(B^2+X\right)\left[1+\left(\frac{B}{\left(B^2+X\right)^2}\right)\right]}{b\left(B^2+X\right)^2e^{\left(B/B^2+X\right)}e^{T/b}}\right]\right\}\frac{dX}{dT} \tag{7.19}$$

$$+\left\{\left[\frac{1.025aB\frac{dX}{dT}}{b\left(B^2+X\right)^2e^{\left(\frac{B}{B^2+X}\right)}e^{T/b}}\right]-\left[\frac{1.025a}{b^2e^{\left(\frac{B}{B^2+X}\right)}e^{T/b}}\right]\right\}$$

Rearranging this equation:

$$\frac{d^2U}{dT^2} = \left\{\frac{2ab^2 B\,1.025\left(e^{T/b}-1\right)\left(\frac{B}{\left(B^2+X\right)^2}\right)\frac{dX}{dT}\frac{dX}{dT}}{b^2\left(B^2+X\right)^3 e^{\left(B/B^2+X\right)}e^{T/b}}\right\}$$
$$+\left\{\frac{2ab\,1.025\left(B^2+X\right)^2\left[1+\left(\frac{B}{\left(B^2+X\right)^2}\right)\right]\frac{dX}{dT}}{b^2\left(B^2+X\right)^3 e^{\left(B/B^2+X\right)}e^{T/b}}\right\} \qquad (7.20)$$
$$+\left\{\frac{1.025ab\,B\left(B^2+X\right)\frac{dX}{dT}}{b^2\left(B^2+X\right)^3 e^{\left(B/B^2+X\right)}e^{T/b}}\right\}-\left\{\frac{1.025a\left(B^2+X\right)^3}{b^2\left(B^2+X\right)^3 e^{\left(B/B^2+X\right)}e^{T/b}}\right\}$$

where, T is the independent variable, a and b are constants, B is the roof span and X is the distance of the tunnel face.

The analysis of rate of convergence-velocity provides information much clear in terms of interpretation of the interaction mechanism and the performances of supported roadway sections. The rate of convergence-velocity (d^2U/dT^2) versus time (T) plots of the areas stabilized by different support types are illustrated in Figures 7.24 to 7.29. The plots obtained from other stations are given in Appendix F. Based on analysis of these plots, the following conclusions can be drawn:

i) The rate of convergence-velocity (acceleration) is different in each area stabilized by different type of supports and decreases with time.

ii) The point where rate of convergence-velocity approaches to zero, in other words the time at which full interaction is achieved, is different at each supported section as shown in Table 7.16.

Table 7.16 The results obtained from analysis of rate of convergence

Support Type	Station Code	Time, when rate approaches to zero (days)
Split-Set	K1	58
Split-Set	K2	80
Split-Set & YSA	K3	45/80
Yielding Super Swellex	K4	75
Yielding Super Swellex	K5	80/85
Yielding Super Swellex	K6	58
Yielding Super Swellex & YSA	K7	47
Sis-Resin	K8	55
Sis-Resin	K9	55
Sis-Resin	K10	68
Sis-Resin & YSA	K11	58
Fosroc-Resin	K12	35
Fosroc-Resin	K13	23
Fosroc-Resin	K14	30/(62-72)
Fosroc-Resin & YSA	K15	20/61
Yielding Steel Arch (YSA)	K16	83
Rigid Steel Arch	K17	43
Rigid Steel Arch	K18	29

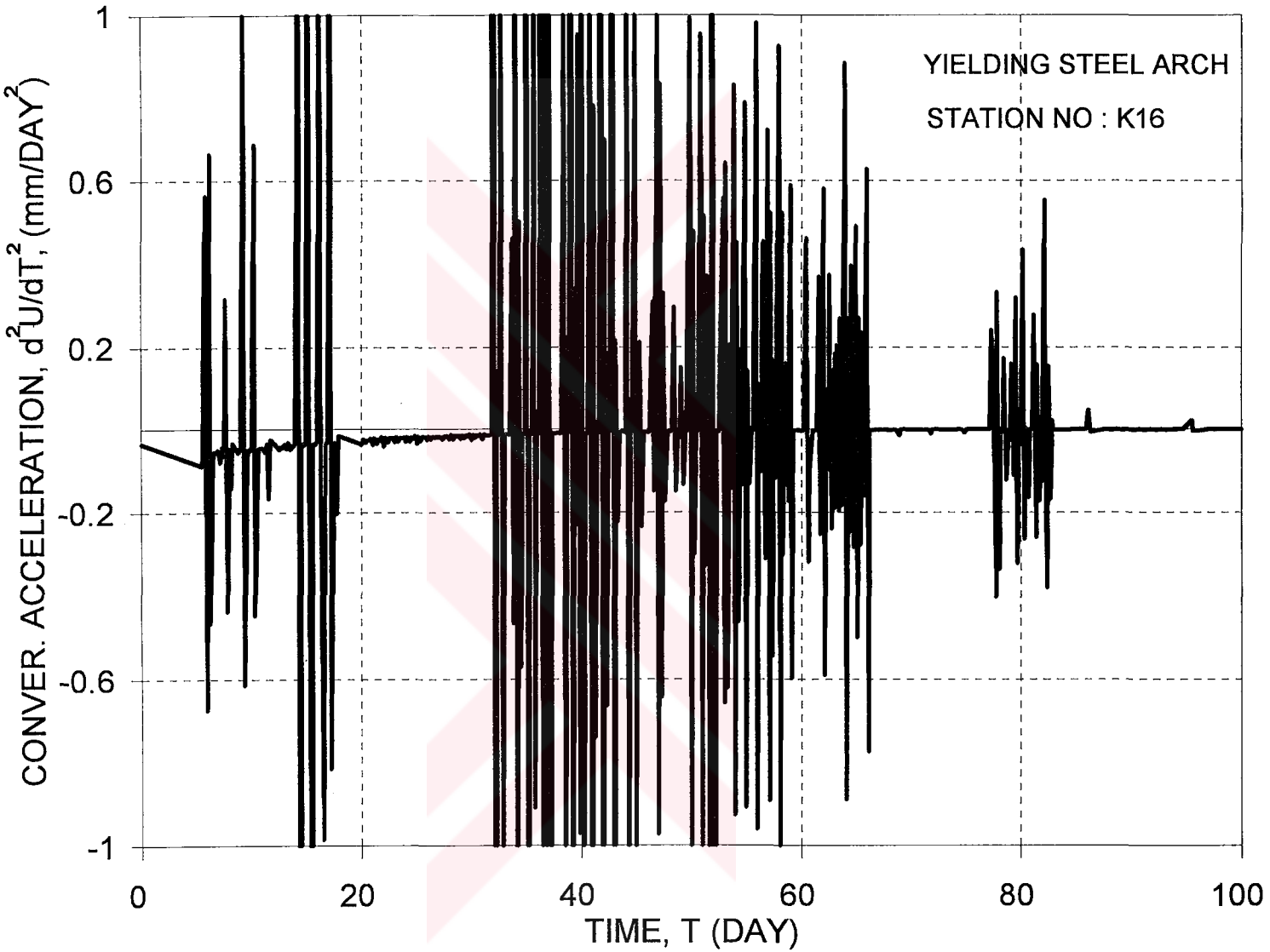

Figure 7.24 Characterization of instant convergence acceleration for the region supported by yielding steel arches

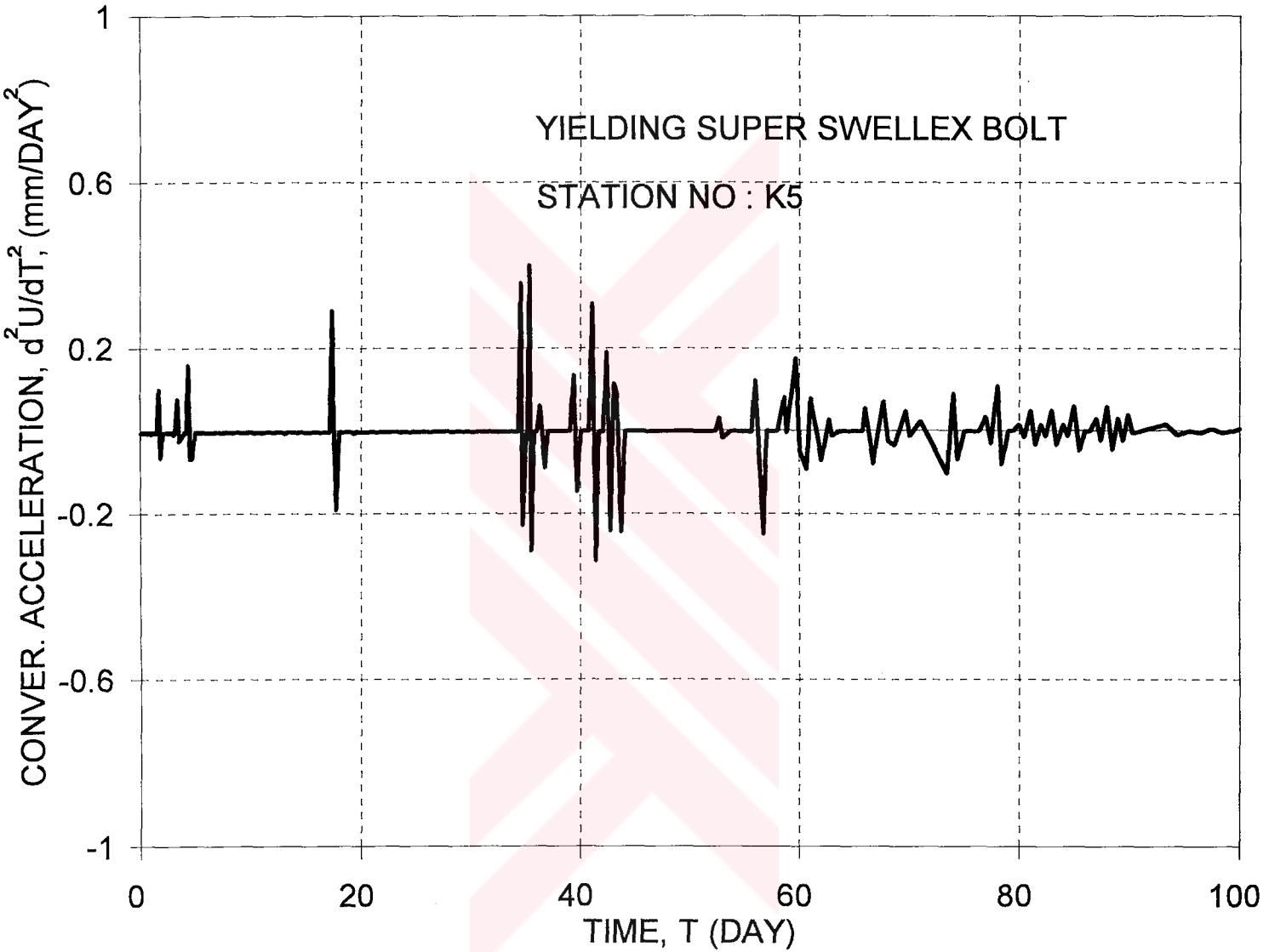

Figure 7.25 Characterization of instant convergence acceleration for the region supported by yielding super swellex bolts

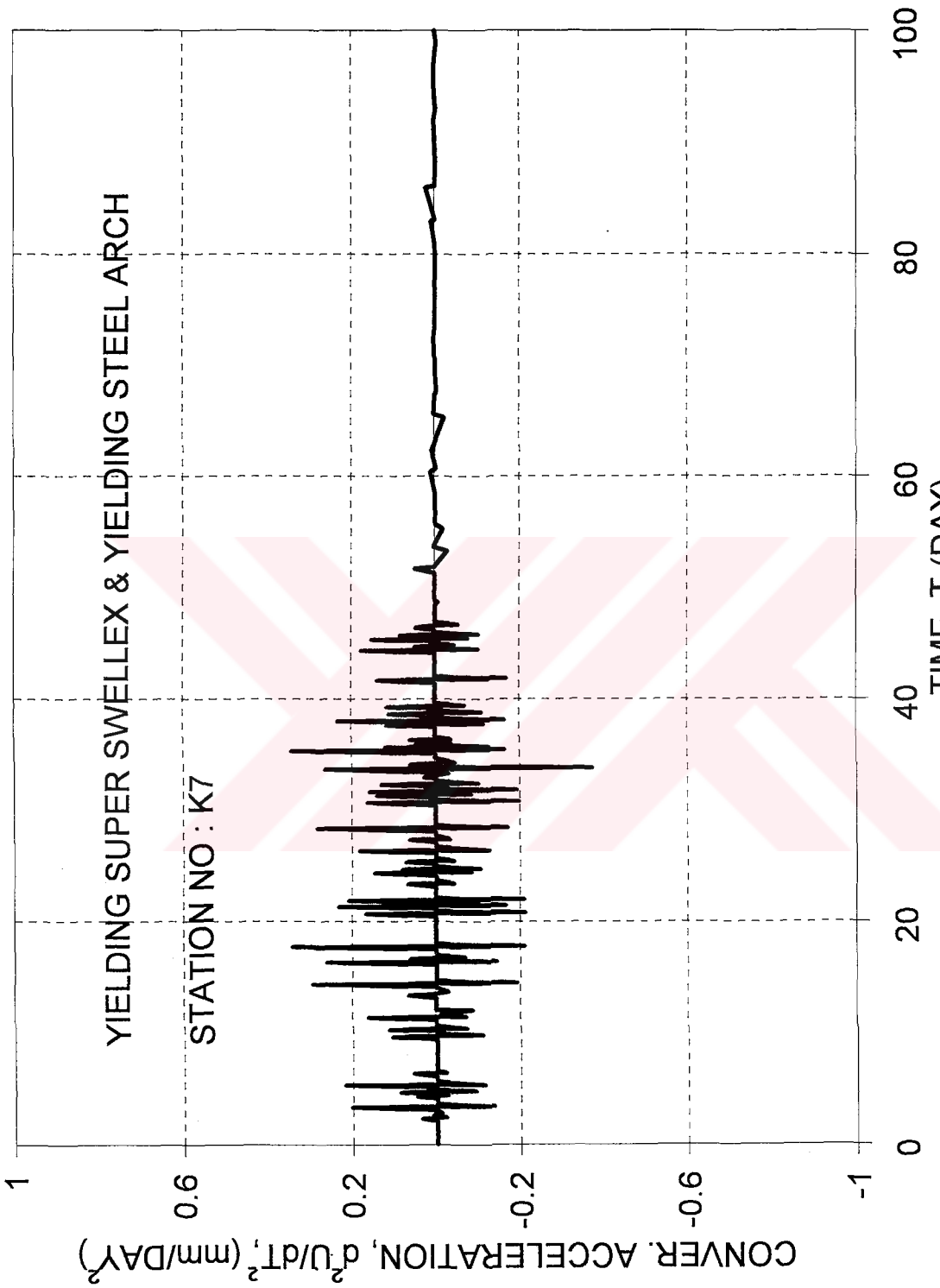

Figure 7.26 Characterization of instant convergence acceleration for supported mix region

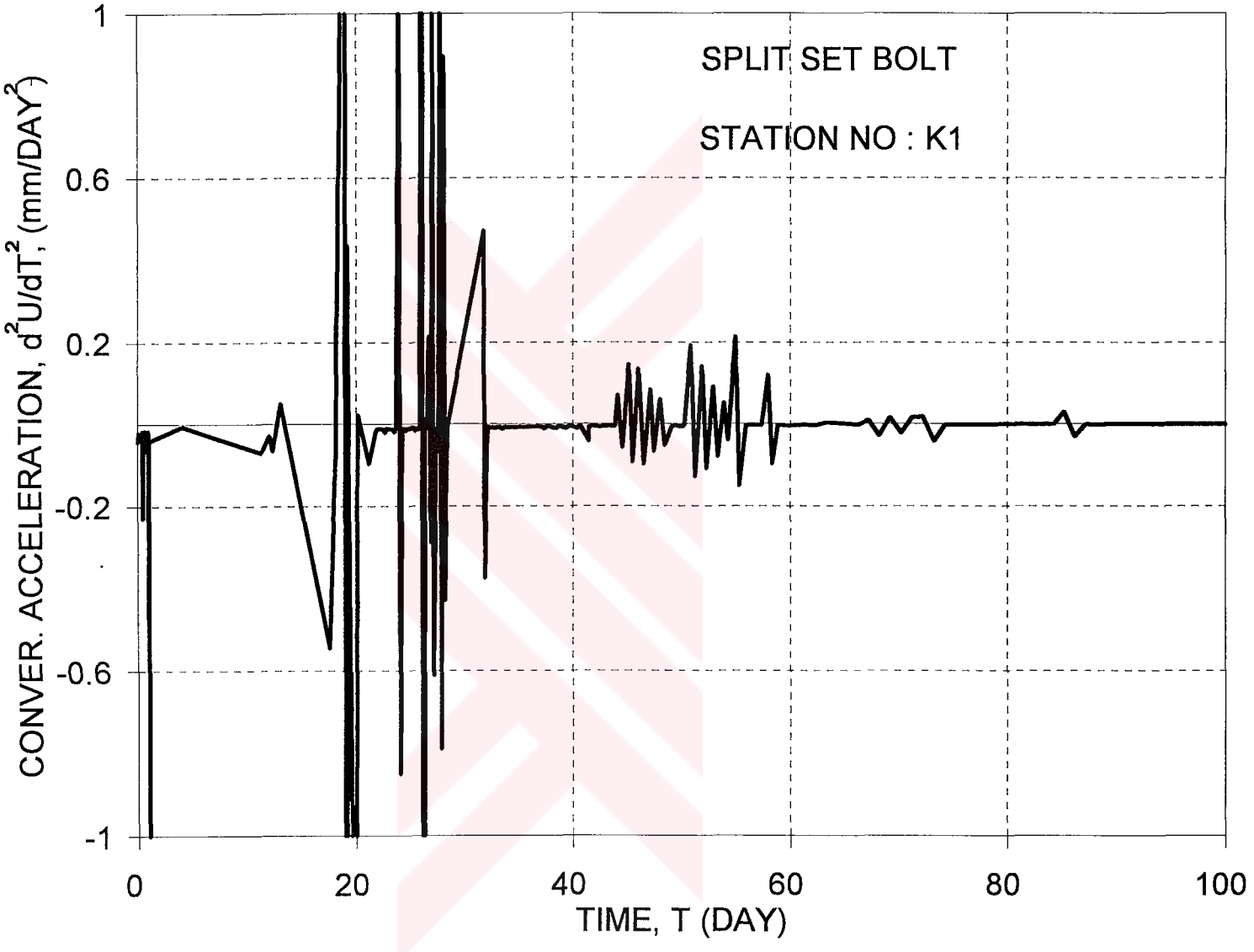

Figure 7.27 Characterization of instant convergence acceleration for the region supported by split-set bolts

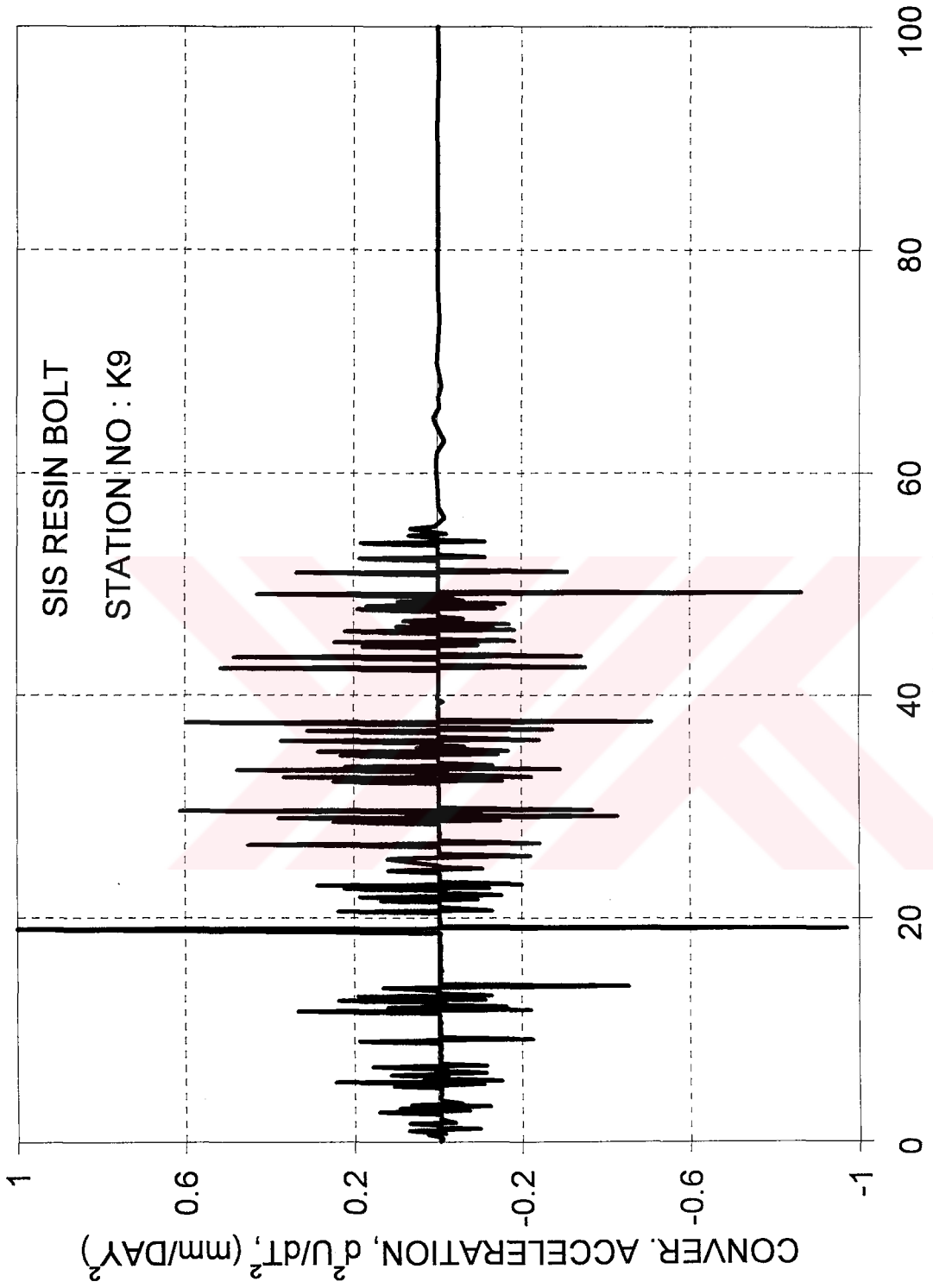

Figure 7.28 Characterization of instant convergence acceleration for the region supported by SIS-resin bolts

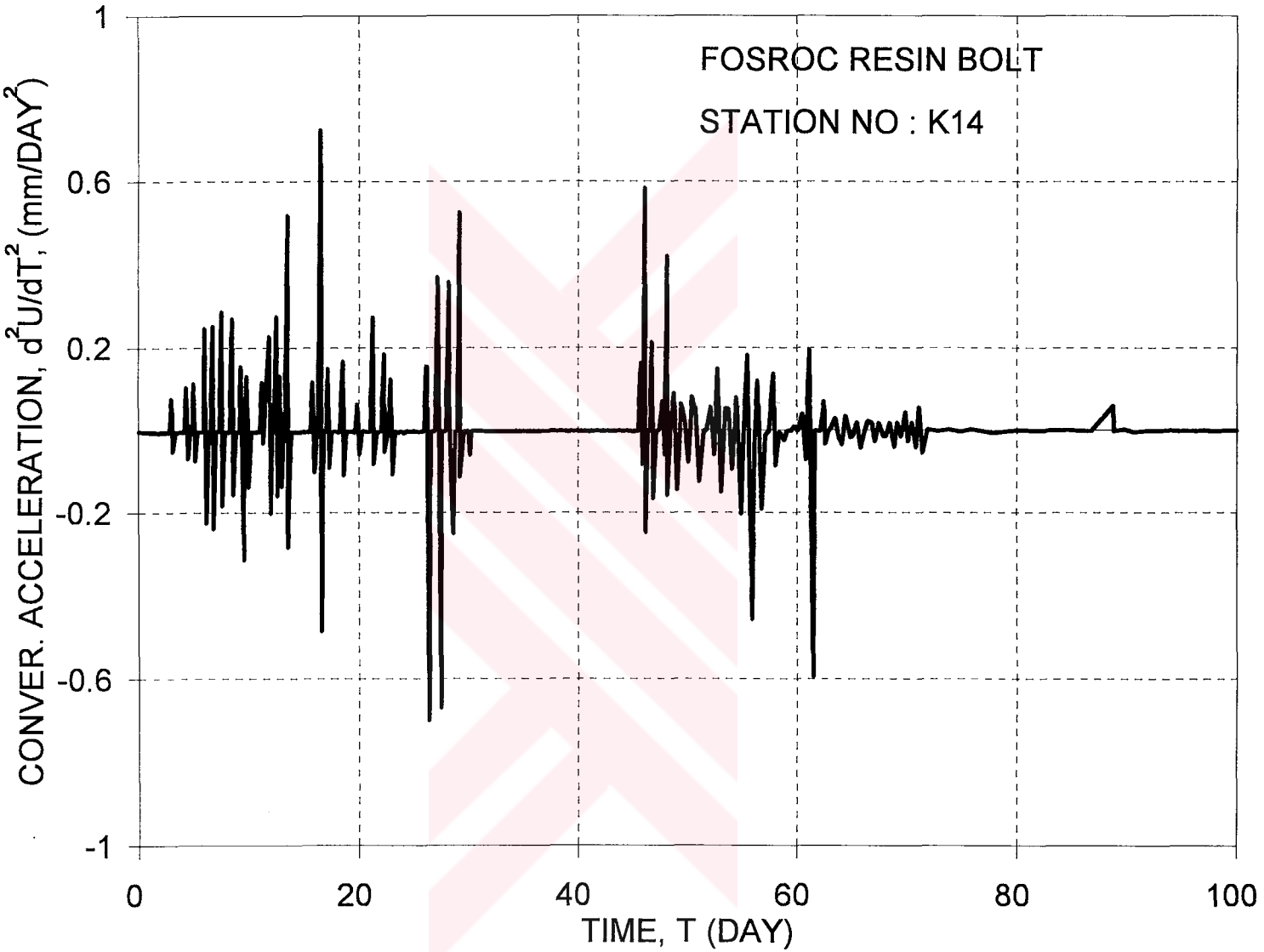

Figure 7.29 Characterization of instant convergence acceleration for the region supported by Fosroc-resin bolts

iii) As the acceleration approaches to zero, it fluctuates up and down between positive and negative values depending on the rate of face advance. The amplitude and frequency of those fluctuations are high when the area is close to the tunnel face; however, they fade as the tunnel face goes away.

iv) If the interaction is not sufficiently adequate or the rate of tunnel face advance is irregular, initially the acceleration is negative, and the amplitude and frequency of the activity (fluctuation) is high (Figure 7.24). If the interaction is better then the initial values of the acceleration is closer to zero and fluctuations of the acceleration will be relatively low as in the case of Figure 7.25.

7.4.4 Comparative Evaluation of the Results

In Sections 7.4.1, 7.4.2 and 7.4.3, the model equations representing the strata convergence, rate of convergence (velocity) and rate of convergence-velocity (acceleration) were presented. Strata behavior, rock mass and support interaction and performances of supports were analyzed in each roadway section stabilized by different support types. In this section, general evaluation of analyses are made by comparing the results obtained from different supported areas.

Convergence versus Time (Convergence Curves)

Convergence-time plots obtained from different supported areas are presented in Figure 7.30. The conclusions reached as a result of analyzing these plots are as follows:

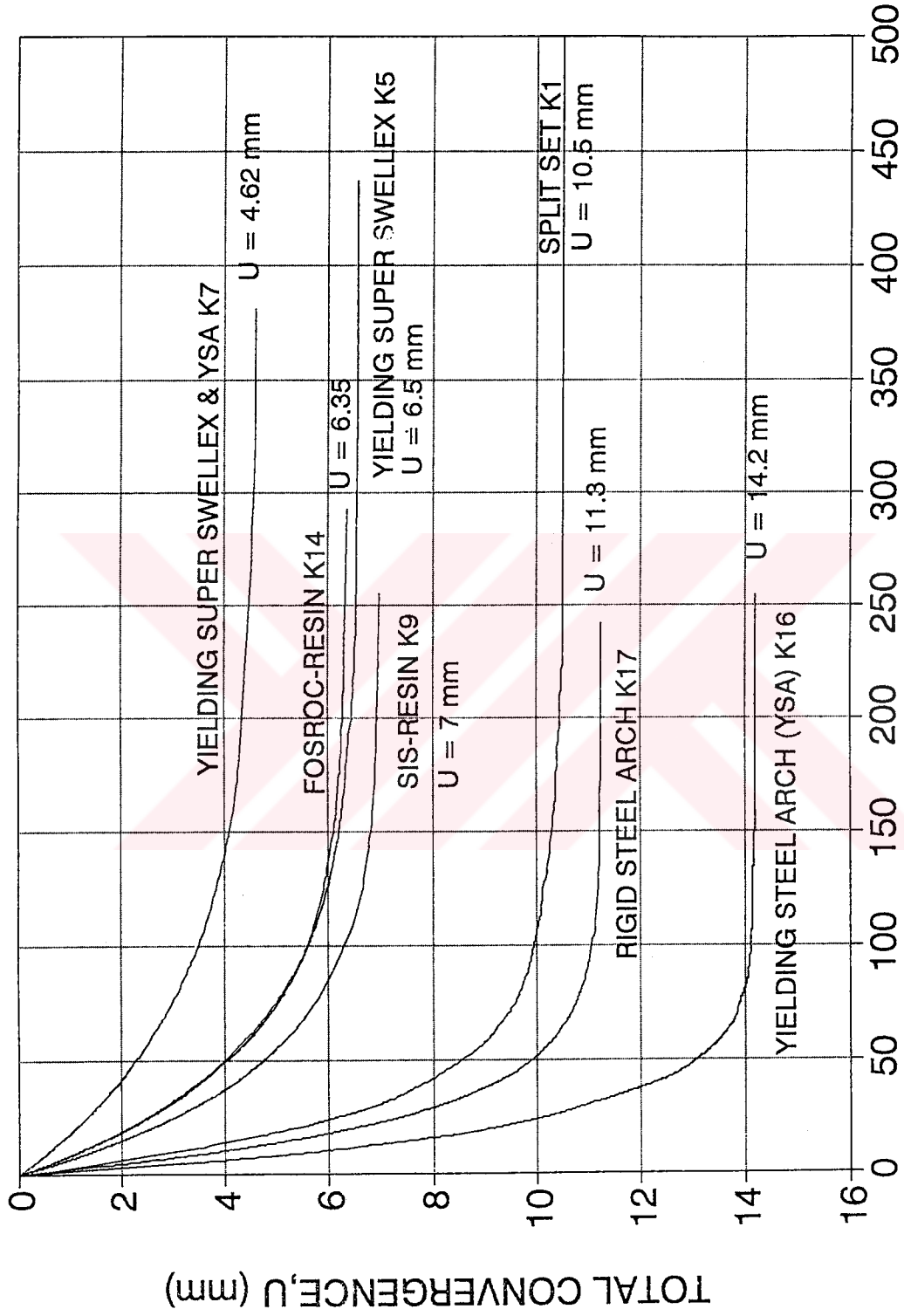

Figure 7.30 Characterization of total convergence in different supported regions

i) In all cases, convergence curve reaches to an asymptotical value indicating that the opening has been stabilized in all of the supported sections. This can also be interpreted as the success of the support design method used.

ii) According to Figure 7.30, the maximum total convergence occurs in the yielding steel arch region where station K16 is located. In other regions the maximum total convergence reduces with the following order: Split-Set (K1), Sis-resin (K9), yielding super swellex (K5), Fosroc-resin (K14) and the mixed support region (K7) in which yielding super swellex and yielding steel arches were used together.

iii) The lowest maximum convergence obtained in almost all regions with mixed support may reflect an overdesign but it is an indication of proper design in regions where rock bolts are used as the sole means of support.

iv) In the region supported by yielding steel arches (K16 in Figure 7.30), the total maximum convergence has the highest value but this asymptotical value is reached much earlier than the other types. The opposite fact is true for the mixed support region (K7 in Figure 7.30).

v) The slopes of the convergence curves also show the relative quality of the interaction or performance of the supported area. The lower the slope, the better the interaction performance is.

vi) The decrease in slope of a convergence curve reflects initiation of an interaction. When the convergence curve reaches to an asymptotical

value, this is an indication of the full stability or completion of the interaction between rock mass and support.

vii) It is difficult to determine the time when interaction starts and ends. However, it is possible to obtain this information from rate of convergence and rate of convergence-velocity graphs.

Rate of Convergence versus Time (Velocity Curves)

The following conclusions can be drawn by analyzing the rate of convergence (velocity) versus time plots shown in Figure 7.31:

i) In all stations (K7, K5, K14, K9, K1, K7 and K16) rate of convergence curve reaches to an asymptotical value (velocity becomes zero) indicating stability as in the case of velocity curves.

ii) The plots associated with the maximum total convergence rates follow the same pattern for all supported sections as in the case of the maximum total convergence plots. Therefore the same interpretation can be made for convergence rates.

iii) The first change in the slope of the velocity curve indicates the initiation of strata interaction. Each noticeable decrease in slope is a sign reaching towards stability. These points (green arrows in Figure 7.31) can be further detected easily from instant acceleration curves.

iv) The time when interaction is completed (red arrows in Figure 7.31) can be determined easily from instant velocity curves or instant acceleration curves. These significant points are plotted in Table 7.17.

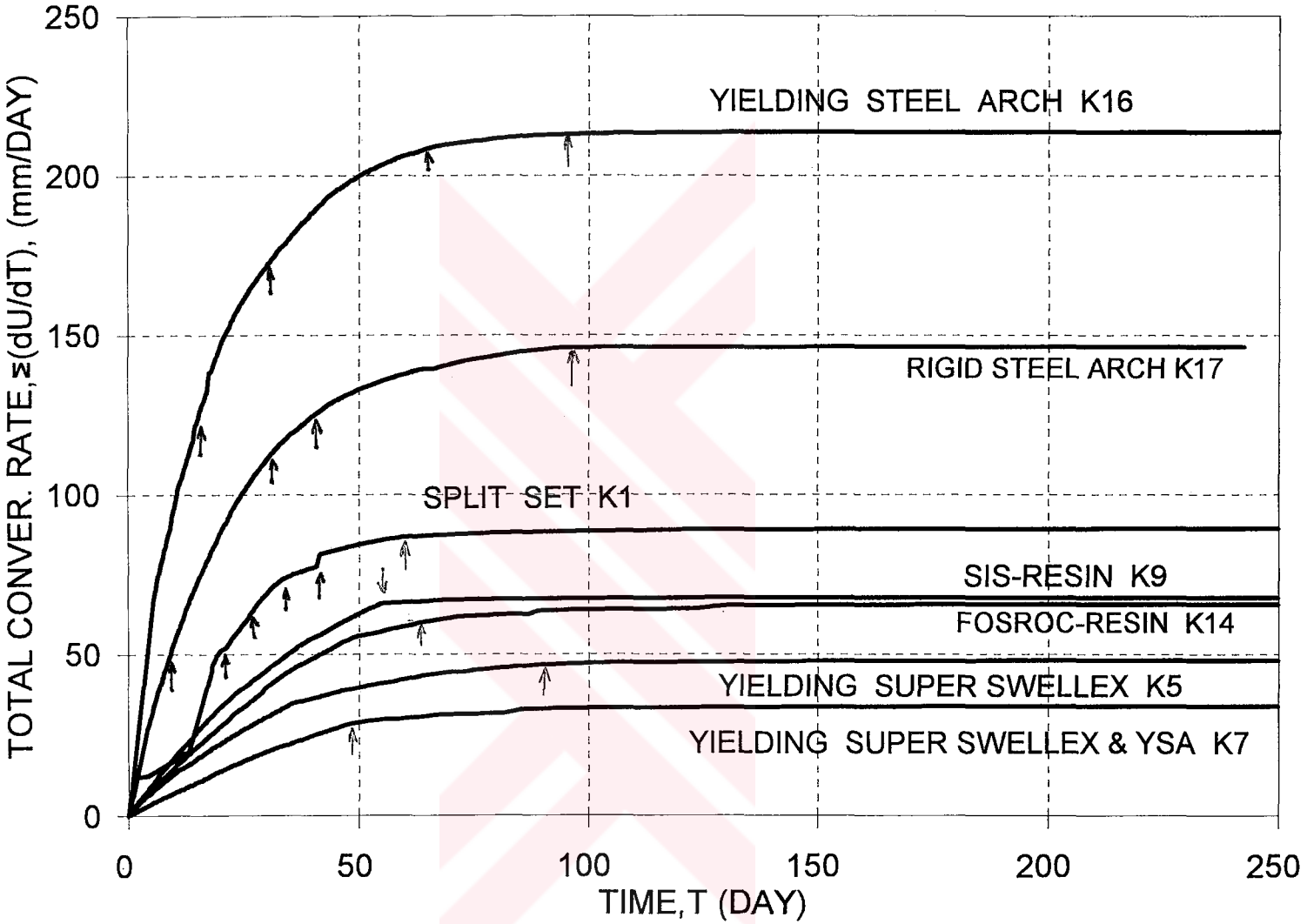

Figure 7.31 Characterization of total rate of convergence in different supported regions (One should not be confused with (dU/dT) axis which indicates the sum of the velocities as a function of time)

Table 7.17 The results of analysis showing the time of completion of interaction obtained from instant velocity curves

Support Type	Station Code	Time, when interaction is completed (days)	Max. Rate of	
			Convergence (mm/day)	Convergence -Velocity (mm/day^2)
Split-Set	K1	59	0.10	0.6
Yielding Super Swellex	K5	90	0.05	0.2
Sis-Resin	K9	57	0.05	0.3
Fosroc-Resin	K14	72	0.02	0.25
Yielding Steel Arch (YSA)	K16	83	0.20	> 1
Yielding Super Swellex & YSA	K7	47	0.02	0.2

Rate of Convergence-Velocity versus Time (Acceleration Curves)

The following conclusions can be drawn by analyzing the total rate of convergence-velocity versus time plots (Figures 7.24 to 7.29):

i) The acceleration curves reach to an asymptotical value in all stations (K7, K5, K14, K9, K1, K7 and K16) when convergence acceleration becomes zero.

ii) The stabilization time in each area by different type of supports can be determined easily from instant acceleration curves (Figures 7.24 to 7.29).

iii) The amplitude and frequency of the activity (fluctuation) differs according to the type of support used as shown in Figure 7.32.

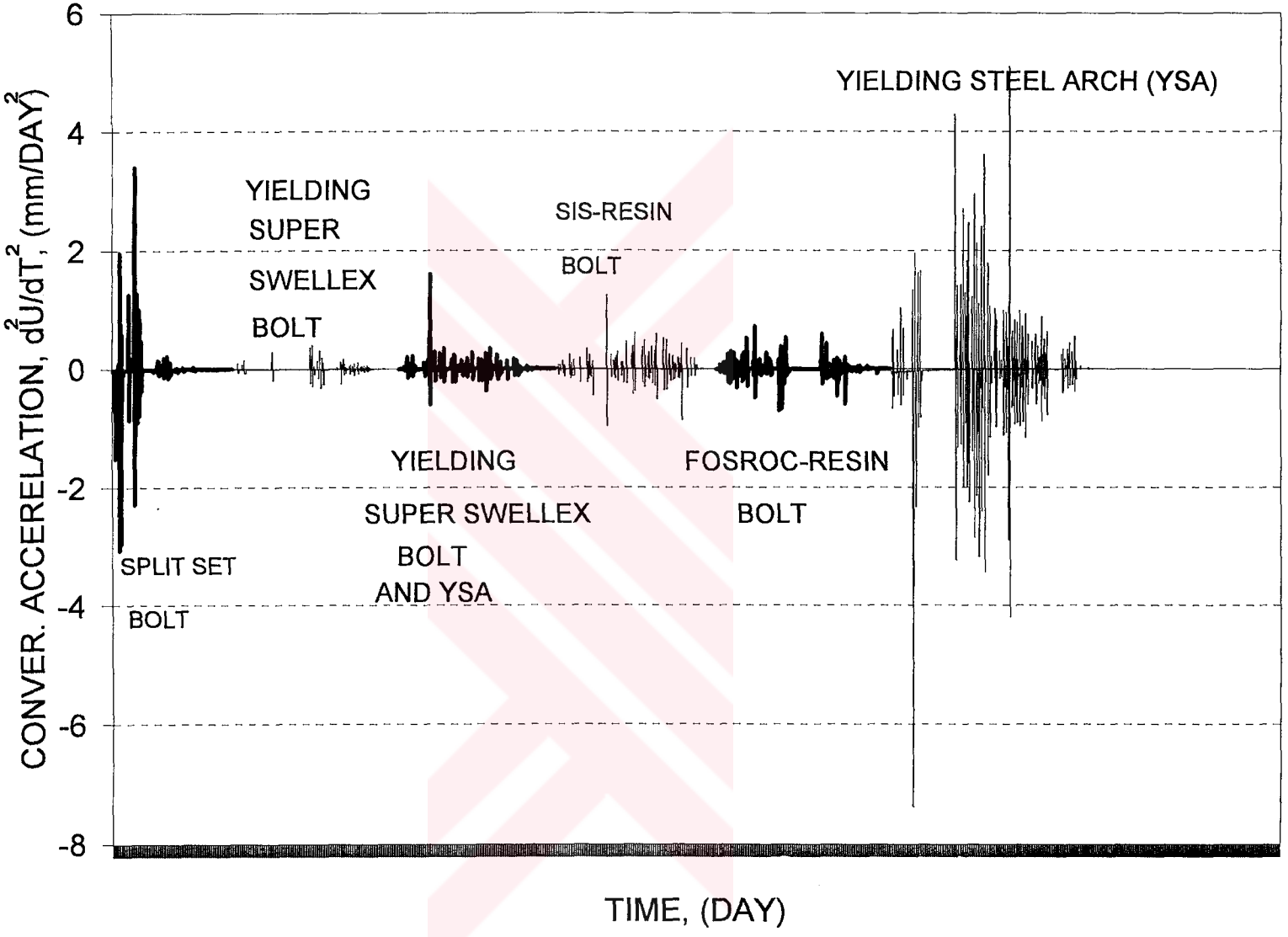

Figure 7.32 Characterization of rate of convergence velocity in different supported regions

CHAPTER VIII

DEVELOPMENT OF A ROOF BEHAVIOR MODEL: MODIFIED INTEGRATED APPROACH

8.1 General

The studies for determining roof mine behavior in underground openings have been continuing for the last fifty years. The associated models developed based on these studies can be categorized in three main groups as:

i) mathematical models based on closed-form solutions including rheological models;

ii) numerical models based on FEM, BEM, DEM, and FDM;

iii) empirical models based on statistical evaluation of underground measurements, case studies and engineering judgment.

A critical review for roof mine behavior is given in Chapter II of this thesis. Some critical points associated with these studies are as follows:

Ladanyi (1980, 1993) stated that:

"Important differences that have often been found between the predicted and observed behavior of underground openings and mine pillars are

considered to be due mainly to size effect and stress redistribution with time."

According to him, there is still question as to how data would apply to field situations.

Stresses and displacements developing in the rock mass due to excavation of tunnels depend on the rock mass properties, in situ stress field, stiffness of the lining or support and time of its installation (Panet, 1993). In addition, the size effect and time dependent stress distribution were also mentioned by Ladanyi (1993). However, the effect of parameters such as, rock mass properties, in situ stress, stiffness of support, and support installation time were not considered by majority of the empirical approaches which try to characterize the roof behavior in underground openings.

8.2 Modified Integrated Approach

Ünal proposed an integrated approach (Ünal, 1983; Ünal, 1986b; Bieniawski, 1989) in order to determine strata displacements and support pressures developing in tunnels. In his approach Ünal considers the following parameters as input; time, roof span, RMR, and support efficiency. The integrated approach relies on combination of different empirical facts, suggested by various investigators, into a single approach consisting of four steps. Ünal's approach, however, has not been supported by field studies yet. In this study, a modified integrated approach is introduced. The modified integrated approach is based on actual underground measurements as well as suggestions made in literature based on case studies.

8.2.1 Development of the Integrated Approach

The engineering geological description of roof strata which are necessary to identify the geological structures, and other features affecting the stability of the mine openings are the basic information used as an input data. The modified integrated approach consists of the following four steps:

Step - 1

This step includes determination of support pressure, as a function of roof span (B) and rock mass rating (RMR), by using Equation A.7b given in Section A.2.

$$P = S \cdot \left(\frac{100 - RMR}{100} \right) \cdot B \cdot \gamma \qquad \text{(A.7b)}$$

where, γ is the unit weight of the rock in kN/m³. The term $\left(\frac{100 - RMR}{100} \right) \cdot B$ describes the rock load height (h_t) in meters. A detailed explanation of Equation A.7b can be found elsewhere (Ünal and Ergür, 1990).

Step - 2

The second design step consists of developing the output of the Geomechanics Classification System, in terms of the stand-up times of the unsupported and the active spans. In Figure 8.1, an up-to-date plot of the output of the Geomechanics Classification System is presented. The figure includes cases for mining and tunneling.

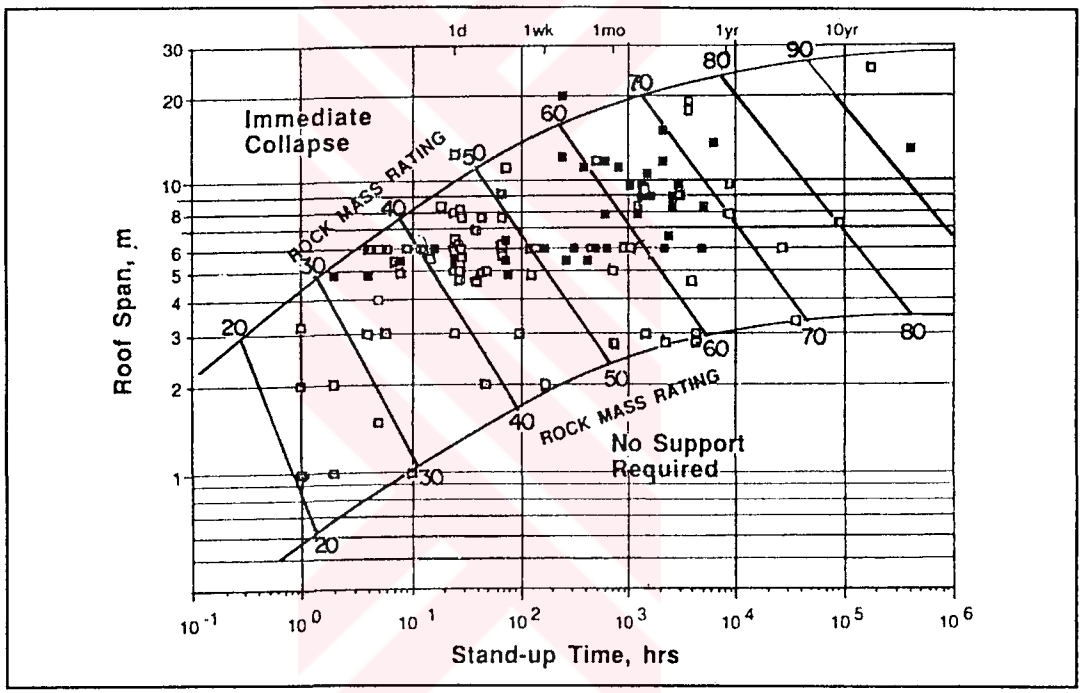

Figure 8.1 Geomechanics Classification of rock masses: output for mining and tunneling (after Bieniawski, 1989)

Step - 3

Once the stand-up time of the roof is determined, the ground behavior can be analyzed utilizing the observational and empirical methods. In order to develop a relationship between the output of the Geomechanics Classification System (stand-up time versus roof span) and the ground behavior (deformation versus time), it is necessary to express the deformation (U) as a function of time (T), distance from tunnel face (X), Modified Rock Mass Rating (M-RMR), roof span (B), the thickness of overburden (H), the support system stiffness (k), and its installation time (t). The effects of each of these parameters on deformation will further be discussed in Section 8.3. The general form of the equation of deformation which includes the above mentioned parameters is as follows:

$$U = \left[e^{(C+R+Z)-\ln\left(\frac{k^{0.25}}{t^{0.60}}+1\right)} \right] \left[e^{0.025-\frac{B}{(B^2+X)}} \right] \left[1-e^{-T/b} \right] \qquad (8.1)$$

where, U : deformation, mm

$$C = \frac{100-(M-RMR)}{(M-RMR)}$$

$$R = \frac{B_{\min}}{B_{\max}} B \quad (B_{min} \text{ and } B_{max} \text{ for the selected M-RMR value})$$

$$Z = 0.06\gamma H$$

k : support system stiffness per meter square, kPa/mm

t : support installation time, hours

B : roof span, meters

X : distance from tunnel face, meters

T : time, days

Step - 4

The fourth step provides information on rock loads as a function of allowable deformation. As stated by Ünal (1983, 1986b), the significance of this output information lies on the fact that the adequate support systems hence the guidelines for reinforcement of the roof strata can be prescribed based on this information. To do this the relative stiffness of the ground and that of the roof support should be analyzed through these respective characteristic curves because these two variables influence the equilibrium support loads. It is therefore important to understand the behavior of the unsupported ground, the behavior of the support, and the interaction between the two.

In underground coal mines, it is not always possible to observe the behavior of the unsupported roof spans because leaving an unsupported area is usually against the mining regulations. The best alternative is to make use of the analytical or empirical methods and, if possible, to cross check the findings with underground measurements (Ünal, 1983 and 1986b). Therefore at this stage, the support characteristic curves can be introduced to the analysis and they can be compared with the rock loads allowable deformations, which constitutes the output of the fourth step of the Integrated Approach. This step was not included in this thesis.

8.3 Ground Behavior Characteristics

In order to provide the required information for the third step of the Integrated Approach, the following basic procedures were followed:

i) Based on the results of the statistical analysis of in situ convergence measurements carried out in Çayırhan Lignite Mine, deformation (U) was defined by an exponential function which is a function of time (T)

and distance from tunnel face (X), in the following form as shown in Equation 8.2.

$$U = f(T, X) \tag{8.2}$$

ii) Equation 8.2 was further improved to include the effect of Modified Rock Mass Rating (M-RMR), the effect of roof span (B), the effect of stress (Z), the effect of support system stiffness (k), and the effect of support installation time (t) in the following general form given in Equation 8.3.

$$U = f(M\text{-}RMR, B, Z, k, t, T, X) \tag{8.3}$$

The effects of the factors included in Equation 8.3 will be discussed in the following sections.

8.3.1 Time and Face Advance Dependent Deformation in Roadways

As explained in Section 7.2 of Chapter VII, deformation (U) in roadways was expressed, initially, as shown in Equation 7.9.

$$U = a\left[e^{0.025-B/(B^2+X)}\right]\left[1-e^{-T/b}\right] \tag{7.9}$$

If T and X goes to infinity in Equation 7.9, the deformation (U) will be equal to a constant as given in Equation 8.4.

$$U = a \tag{8.4}$$

As a result, the maximum convergence of roof displacement becomes equal to the constant value a which is in mm. The effects of time and distance from tunnel face in Equation 7.9 can be analyzed in two parts namely:

i) $\left[1-e^{-\frac{x}{b}}\right]$, and (8.5)

ii) $\left[e^{0.025-\frac{B}{\left(B^2+X\right)}}\right]$ (8.6)

Based on statistical analysis carried out on data obtained from different support regions, the a and b constants given in Equation 7.9 were determined as presented in Table 8.1.

During statistical analysis the relationship given in Equation 8.7 was found between a and b constants.

$$b=\sqrt[-0.45]{\frac{a^{0.55}}{15.65}} \quad (R^2=0.80) \tag{8.7a}$$

or,

$$b=\frac{a^{-1.222}}{222\times10^{-5}} \quad (R^2=0.80) \tag{8.7b}$$

In this study, Equation 8.7 is very significant because, if a (Equation 8.4) is known, b can be calculated by Equation 8.7 and the characteristic "convergence versus time" and "convergence versus distance from tunnel face" graphs can be plotted by Equation 7.9 as shown in Figure 8.2.

Table 8.1 Constants *a* and *b* determined by statistical analyses

Support Type	Station Code	Constant *a*	Constant *b*
Split-Set	K1	10.50	37.037
Split-Set	K2	11.09	46.87
Split-Set & YSA	K3	9.00	83.69
Yielding Super Swellex	K4	6.25	39.07
Yielding Super Swellex	K5	6.50	69.64
Yielding Super Swellex	K6	5.34	54.27
Yielding Super Swellex & YSA	K7	4.62	71.36
Sis-Resin	K8	5.40	40.92
Sis-Resin	K9	7.00	59.48
Sis-Resin	K10	6.30	38.43
Sis-Resin & YSA	K11	6.00	74.72
Fosroc-Resin	K12	5.25	38.59
Fosroc-Resin	K13	6.30	28.42
Fosroc-Resin	K14	6.35	36.28
Fosroc-Resin & YSA	K15	4.80	34.07
Yielding Steel Arch (YSA)	K16	14.20	17.17
Rigid Steel Arch	K17	11.30	25.69
Rigid Steel Arch	K18	9.69	22.89

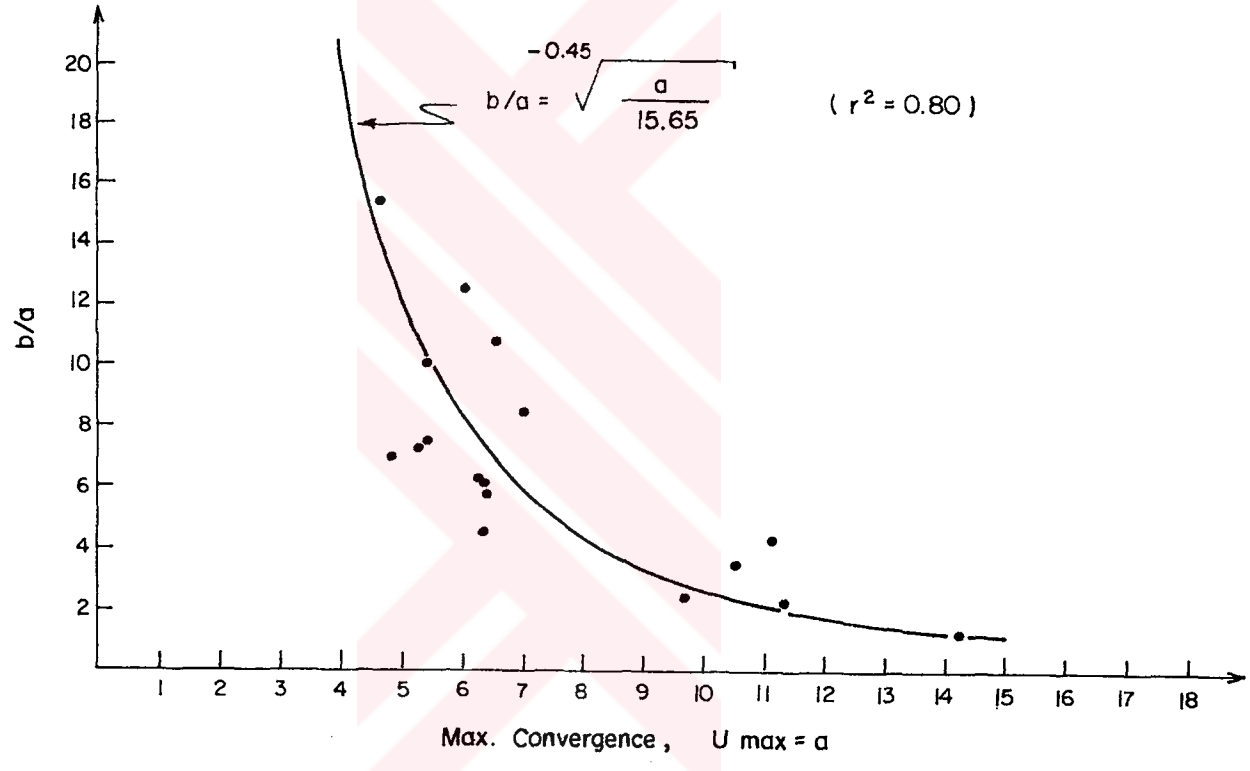

Figure 8.2 The relationship between constants *a* and *b*

8.3.2 Effects of Support Stiffness and Installation Time

During investigations, the effect of the support system stiffness (k) and the support installation time (t) were also tested by statistical analysis. The relationship between maximum convergence and support stiffness obtained from in situ results is shown in Equation 8.8 and Figure 8.3.

$$a = e^{2.875-\ln\left[\frac{k^{0.25}}{t^{0.60}}+1\right]} \quad (R^2 = 0.92) \tag{8.8}$$

where, $e^{2.875}$ is a constant for Çayırhan Lignite Mine. If k, the support system stiffness, is equal to zero, Equation 8.8 becomes as follows:

$$a = e^{2.875} \tag{8.9}$$

Equation 8.9 means that if a roadway is unsupported, then the maximum deformation for this unsupported span (in Çayırhan Lignite Mine) will be equal to $e^{2.875}$.

If Equation 8.8 is put into Equation 7.9, the maximum convergence for different supported regions in Çayırhan Lignite Mine would be obtained as shown in Equation 8.10.

$$U = \left[e^{2.875-\ln\left(\frac{k^{0.25}}{t^{0.60}}+1\right)}\right]\left[e^{0.025-\frac{B}{\left(B^2+X\right)}}\right]\left[1-e^{-\frac{T}{6}}\right] \tag{8.10}$$

As mentioned before, if T and X go to infinity in Equation 8.8 and k becomes equal to zero (i.e. unsupported span) then the maximum convergence will be equal to $e^{2.875}$. This value was found by statistical analysis which is a specific value representing Çayırhan Lignite Mine. If this constant value is defined as e^A then this equation can be rewritten as shown in Equation 8.11.

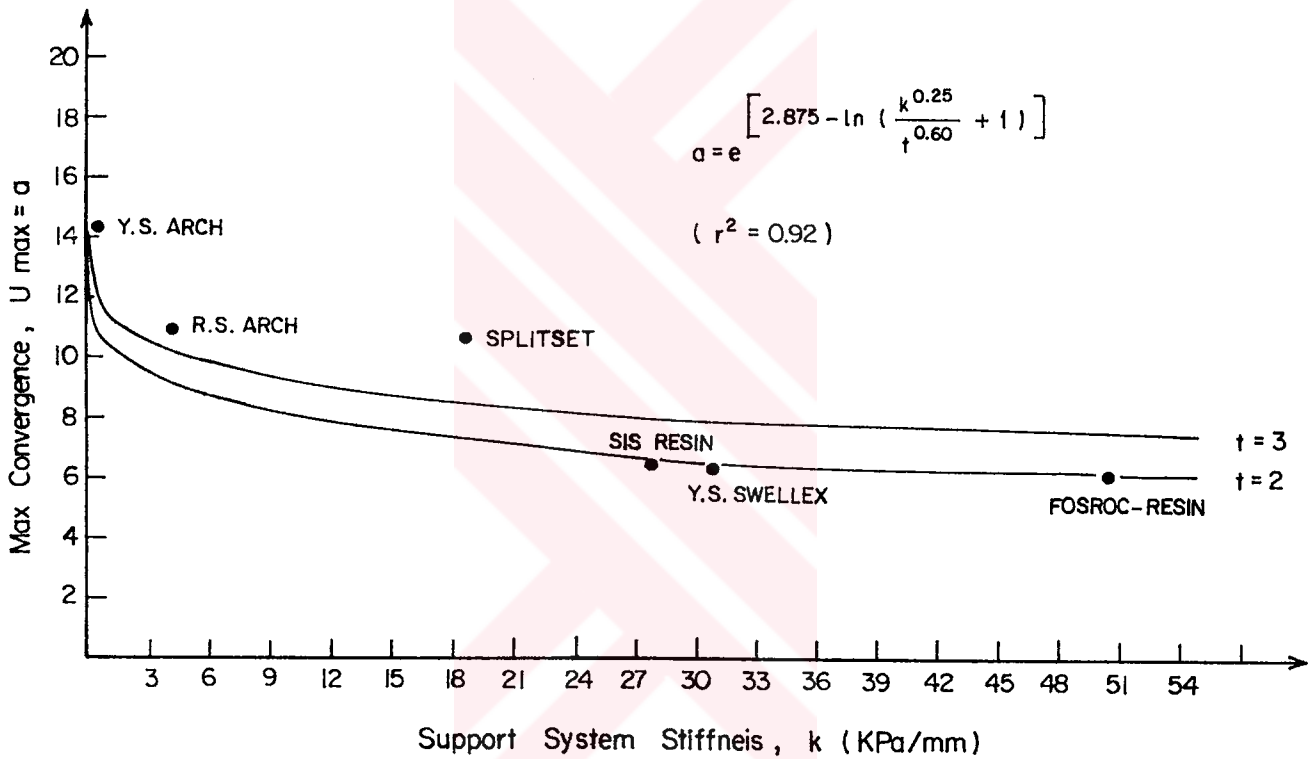

Figure 8.3 The relationship between the maximum convergence and the support system stiffness and its installation time

$$U = \left[e^{A - \ln\left(\frac{k^{0.25}}{0.60}+1\right)} \right] \left[e^{0.025 - B/(B^2+X)} \right] \left[1 - e^{-7/b} \right] \qquad (8.11)$$

Effect of Support System Stiffness (k)

It is very difficult to collect roof fall data for unsupported roof spans, since leaving an unsupported span is, in most cases, against the mining regulations. On the other hand, mine records are usually full of roof fall occurrences caused by inadequately applied support systems. In order to express the behavior of the inadequately supported roof span mathematically, a new term, support system stiffness (k) is introduced. The support system stiffness can be determined from the results of "deformation-load" based on pull-out (anchorage capacity) tests explained in Chapter VI. The unit of k is kPa/mm and gives the force per unit length of the bolt subjected to deformation normalized by the area.

In order to determine the effect of this parameter, the total convergence for various M-RMR values were calculated by Equation 8.13 which will be presented in Section 8.3.3 and the results were plotted as shown in Figure 8.4.

The effect of support system stiffness (k) is more pronounced in weak rock mass compared to good ones.

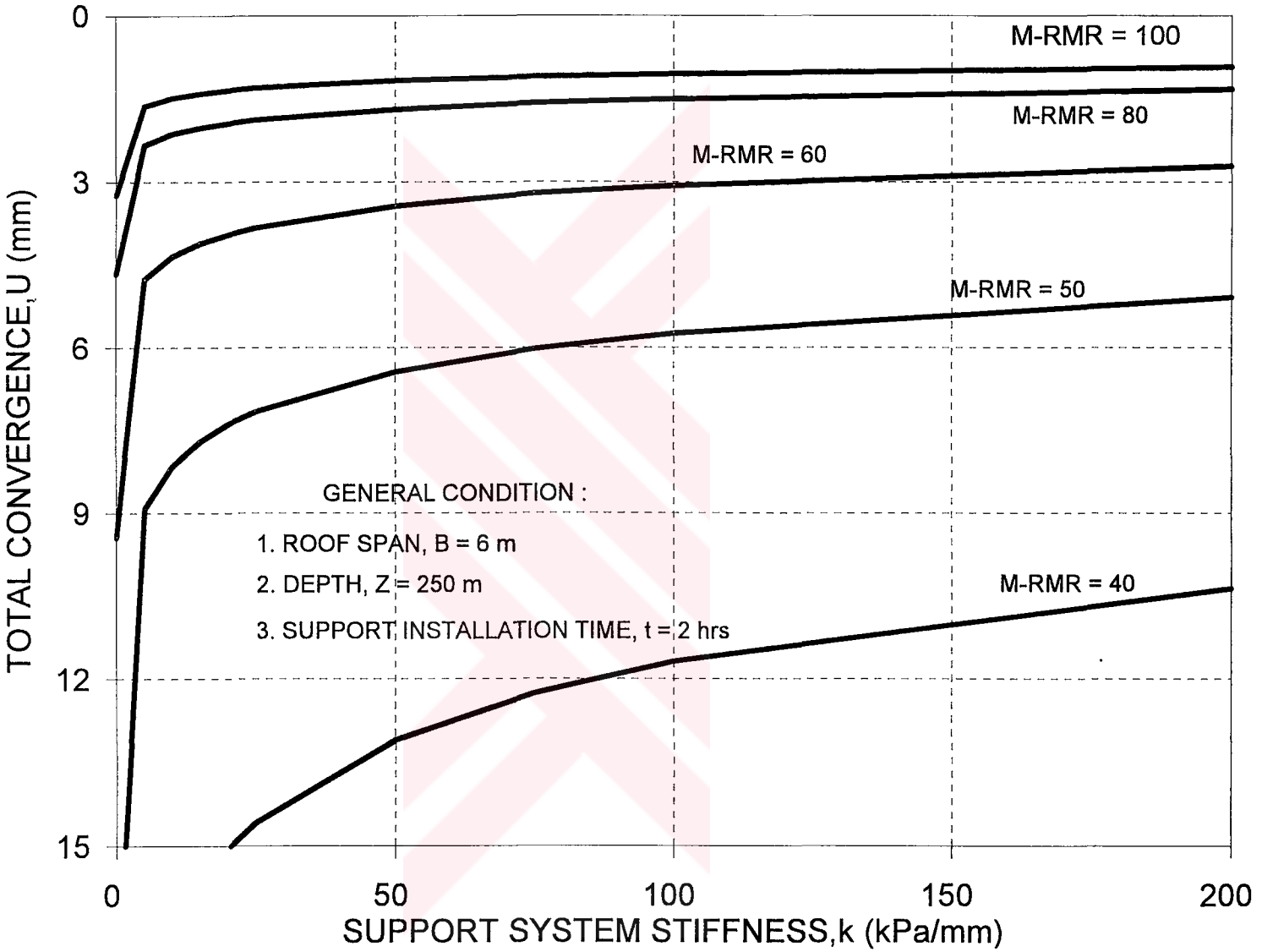

Figure 8.4 The effect of support system stiffness, *k*, for various M-RMR values

Effect of Support Installation Time

Stresses and displacements in the rock mass surrounding tunnels or roadways develop due to excavation. In order to control the deformation in underground openings and provide stability, various support types are used. Support installation time is very significant because the amount of deformation developing with time might become too high if the support was installed too late. Once the movement starts in the roof it will be very difficult to control. That is why the supports must be installed as early as possible. The effect of support installation time is included in Equation 8.13 that will be presented in Section 8.3.3. The effect of installation time is depicted in Figure 8.5. The support installation time may not be important for M-RMR=100 but it becomes very significant if the rock mass rating is low (i.e., M-RMR=40).

Equation 8.11 can be assumed as a general deformation equation for different regions in underground openings. However, the difficult problem is how to estimate or calculate the parameter e^A.

8.3.3 Effect of Rock Mass Quality, Roof Span and Depth

The importance of roof span (B), Rock Mass Quality (i.e. RMR), and stress (Z) were emphasized by Panet (1993) and Ladanyi (1993). In this study, the effects the above mentioned parameters were included in parameter e^A as shown in Equations 8.12a and 8.12b.

$$e^A = e^{f(M\text{-}RMR)} e^{f(B)} e^{f(Z)} \quad \text{or} \tag{8.12a}$$

$$e^A = e^{f(M\text{-}RMR)+f(B)+f(Z)} \tag{8.12b}$$

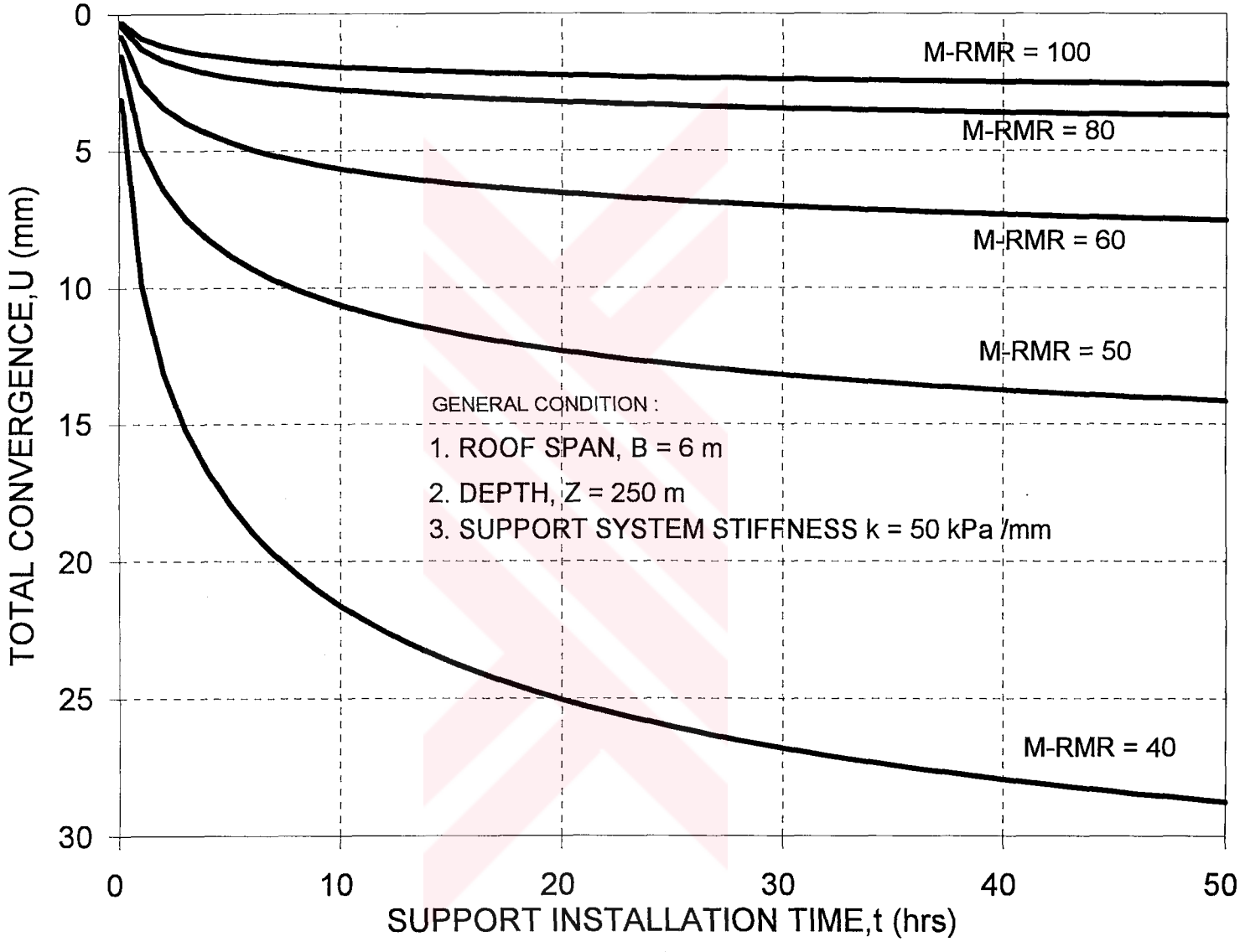

Figure 8.5 Effect of the support installation time for various M-RMR values

where,

$$f(M-RMR)=\frac{100-(M-RMR)}{(M-RMR)}$$

$$f(B)=\frac{B_{\min}}{B_{\max}}\cdot B \qquad (B_{min} \text{ and } B_{max} \text{ are defined by the output of the RMR system for the selected M-RMR value})$$

$$f(Z)=0.06\,\gamma\,H$$

The parameter e^A can now be put into Equation 8.10 to obtain the maximum deformation expressed in Equation 8.11.

$$U=\left[e^{\left[f(M-RMR)+f(B)+f(Z)\right]-\ln\left(\frac{k^{0.25}}{\rho^{0.60}}+1\right)}\right]\left[e^{0.025-\frac{B}{\left(B^2+x\right)}}\right]\left[1-e^{-\frac{Z}{B}}\right] \qquad (8.13)$$

The effects of the factors, shown in Equation 8.13 will be discussed in the following sections.

Effect of Modified Rock Mass Rating (M-RMR)

The effect of this parameter for original RMR (Bieniawski, 1979) has been introduced by Ünal (1983). In this study, the effect of M-RMR is included in constant *f(M-RMR)* and shown in Table 8.2. As can be seen from this table, when the rock is competent (M-RMR=100), the values of the constant *b* becomes unity.

Figure 8.6 shows a family of deformation curves for various M-RMR values. The variation of in situ convergence as a function of rock mass quality was presented by Giles (1984) as shown in Figure 8.7. As it can be realized in Figures 8.6 and 8.7, the curves show the same trend.

Table 8.2 Effect of constant C for various values of modified rock mass rating (M-RMR) (after Ünal, 1983)

M-RMR	$e^C = e^{\left(\frac{100}{M-RMR}-1\right)}$
100	1.00
80	1.25
60	1.95
40	4.48
30	10.81
20	54.60

Effect of Roof Span (B)

It is clear from Figure 8.1, presented earlier, that within the applicability limits of the Geomechanics Classification System, for a particular value of RMR, the roof spans (B) changes between two limits. The upper limit is the maximum roof span (B_{max}) above which an immediate collapse would occur if excavated, and the lower limit (B_{min}) is the minimum roof span below which no support is required. Within the upper and lower limits, the stand-up times of the smaller roof spans are longer than that of the larger ones. This situation shows the definite effect of the roof span width (B) on the ground behavior. The effect of roof span on convergence is also presented by Figure 8.8.

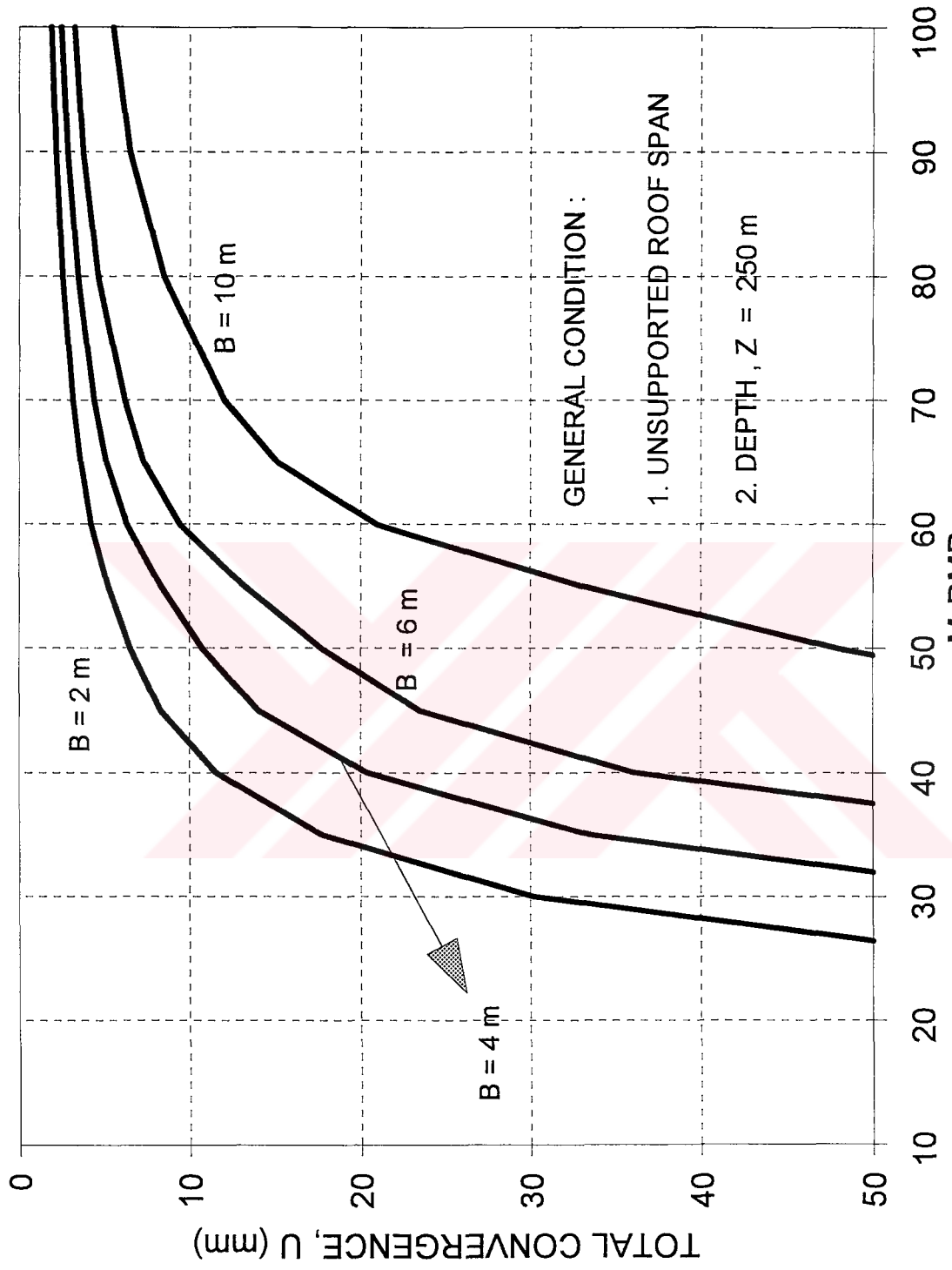

Figure 8.6 M-RMR versus convergence characteristic curves for various unsupported roof span

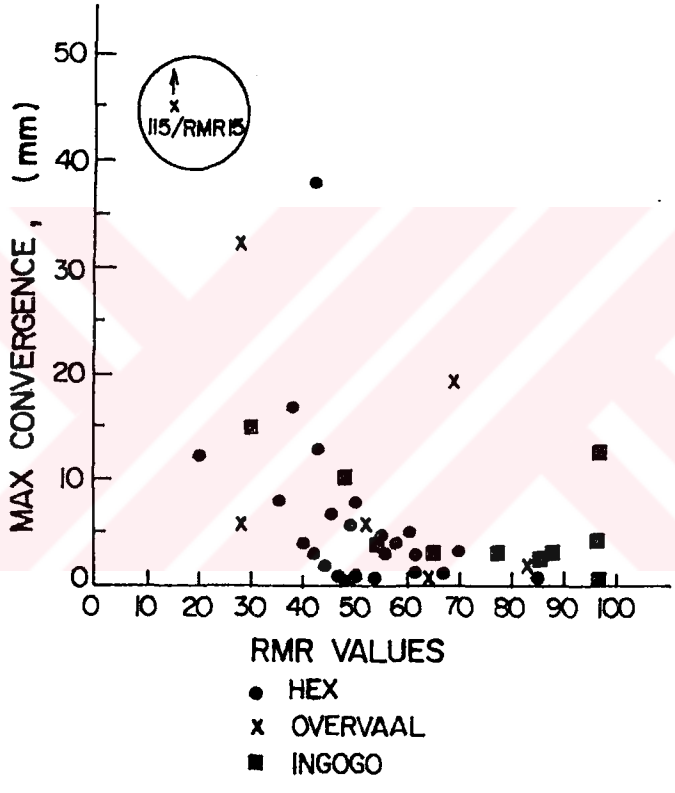

Figure 8.7 Maximum convergence and RMR values for various tunnels (after Giles, 1984)

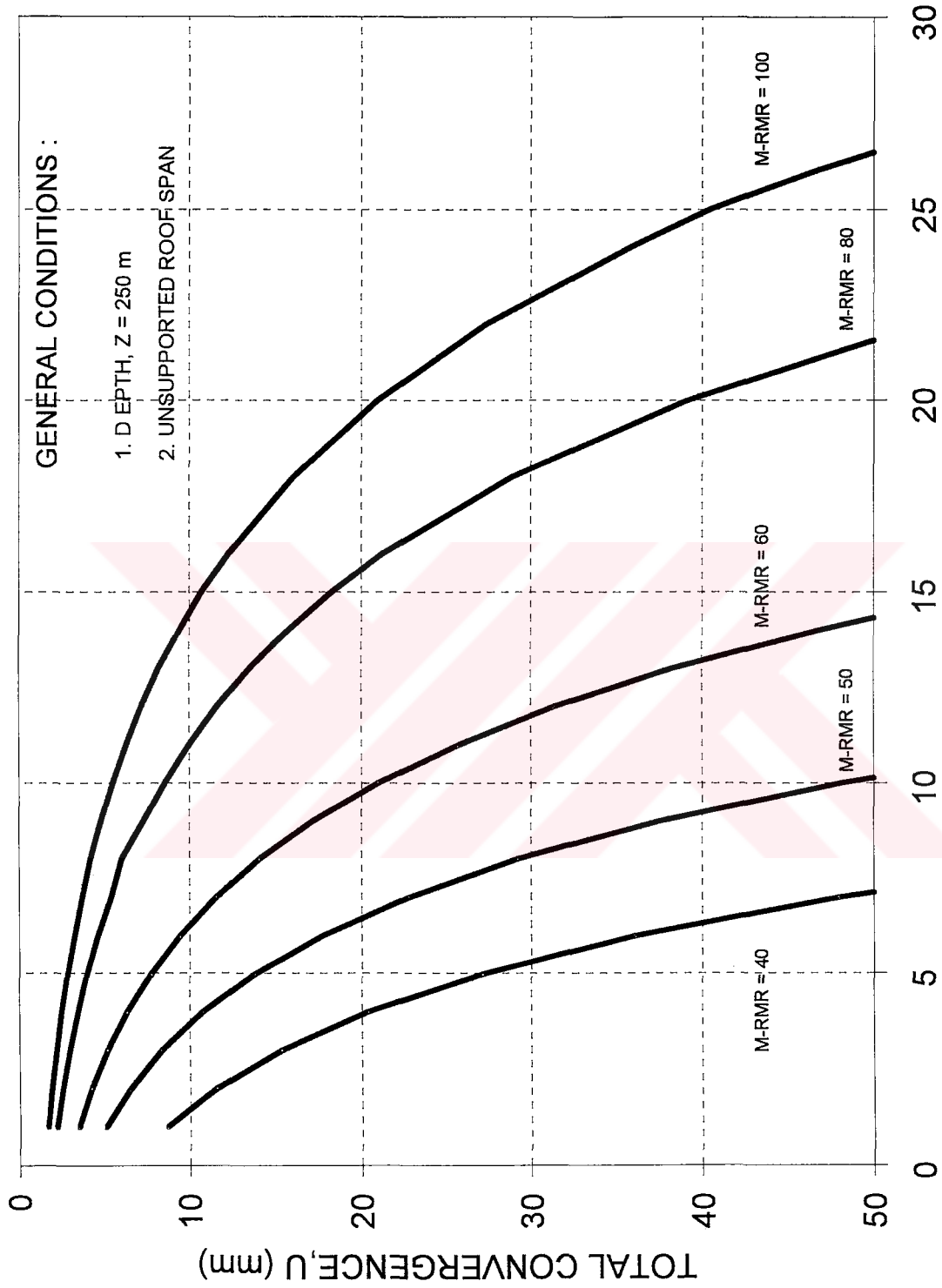

Figure 8.8 Roof span versus convergence characteristic curves for various M-RMR values

Effect of Stress Based on Depth (Z)

The stress distribution surrounding an underground opening has a significant effect on stability. Therefore, this effect has been included in the general convergence equation (Equation 8.13). The effect of stress can be determined by overburden thickness and unit weight of the overburden. The effect of depth on convergence was presented by Kammer (1975) as shown in Figure 8.9. According to some other investigators, however, depth does not have any effect on convergence. The results obtained from Equation 8.13 are plotted in Figure 8.10. The graphs obtained in Figures 8.9 and 8.10 show similar characteristics.

8.3.4 Worked Examples

The following examples illustrate the effects of M-RMR, the roof span, the depth, the support stiffness, and its installation time and also the effect of face advance rate. In these examples, the following data are used.

Example - 1

Unsupported Roof Span	: 6 m (arbitrarily selected)
Depth	: 250 m (arbitrarily selected)
Face advance rate	: 8 m/day

Under these conditions and for various M-RMR values, the deformations were calculated as a function of time and face advance and the results are plotted as shown in Figure 8.11.

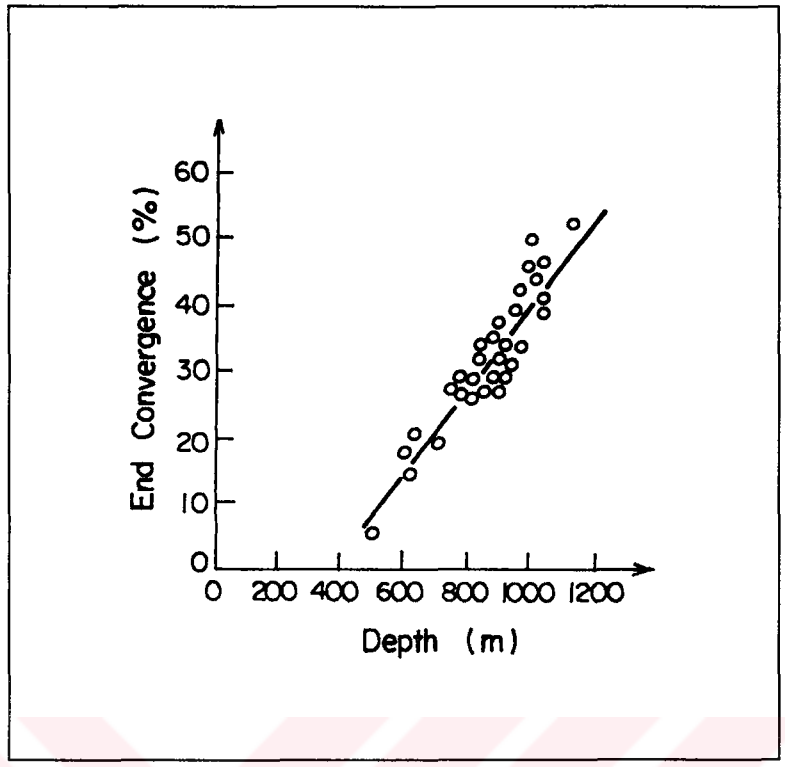

Figure 8.9 Effect of depth on convergence (after Kammer, 1975)

Example - 2

Modified Rock Mass Rating (M-RMR)	: 50 (arbitrarily selected)
Depth	: 250 m
Face advance rate	: 8 m/day

The deformations were calculated for the various unsupported roof spans. The results were presented in Figure 8.12.

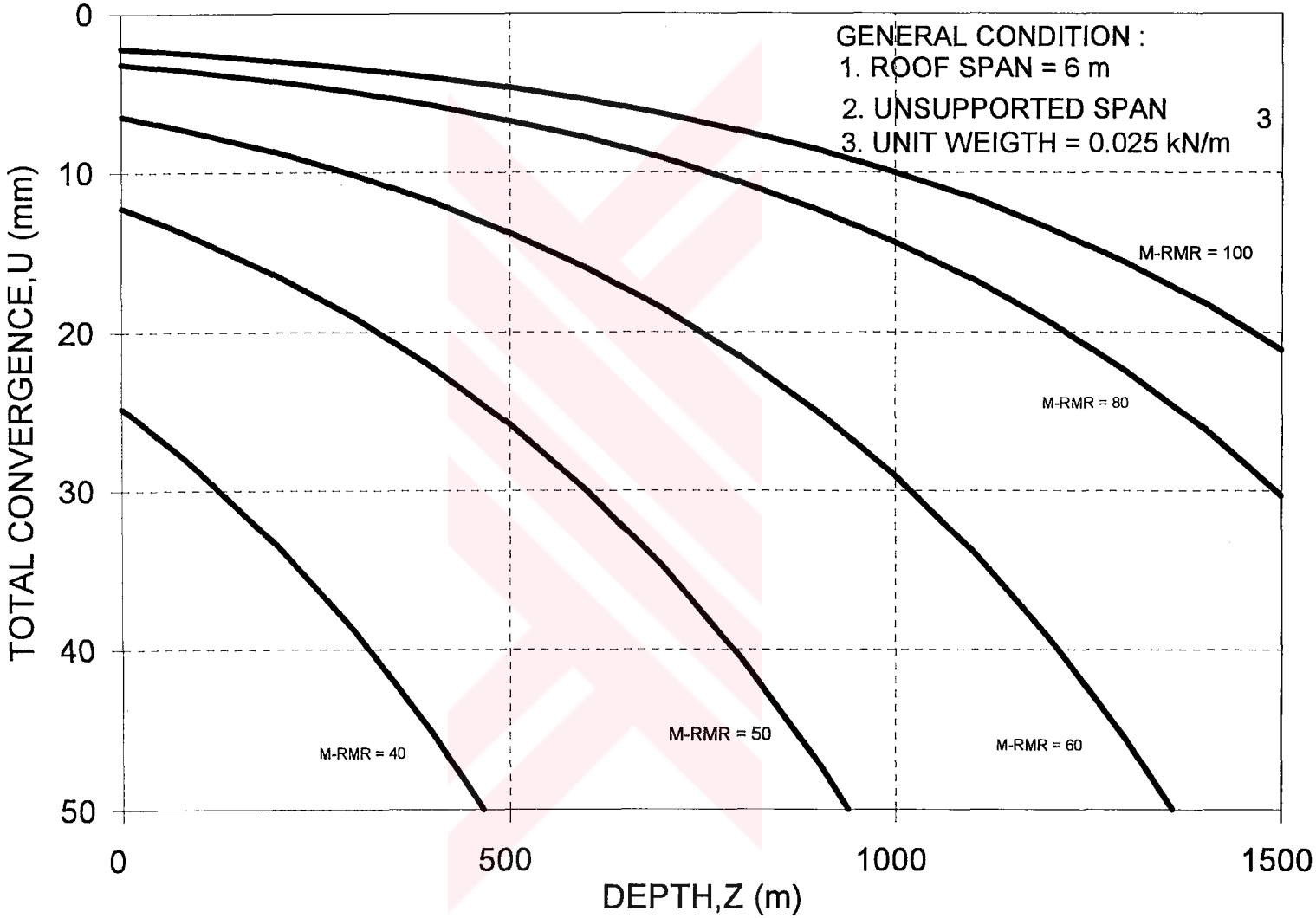

Figure 8.10 Effect of depth on convergence based on Equation 8.13

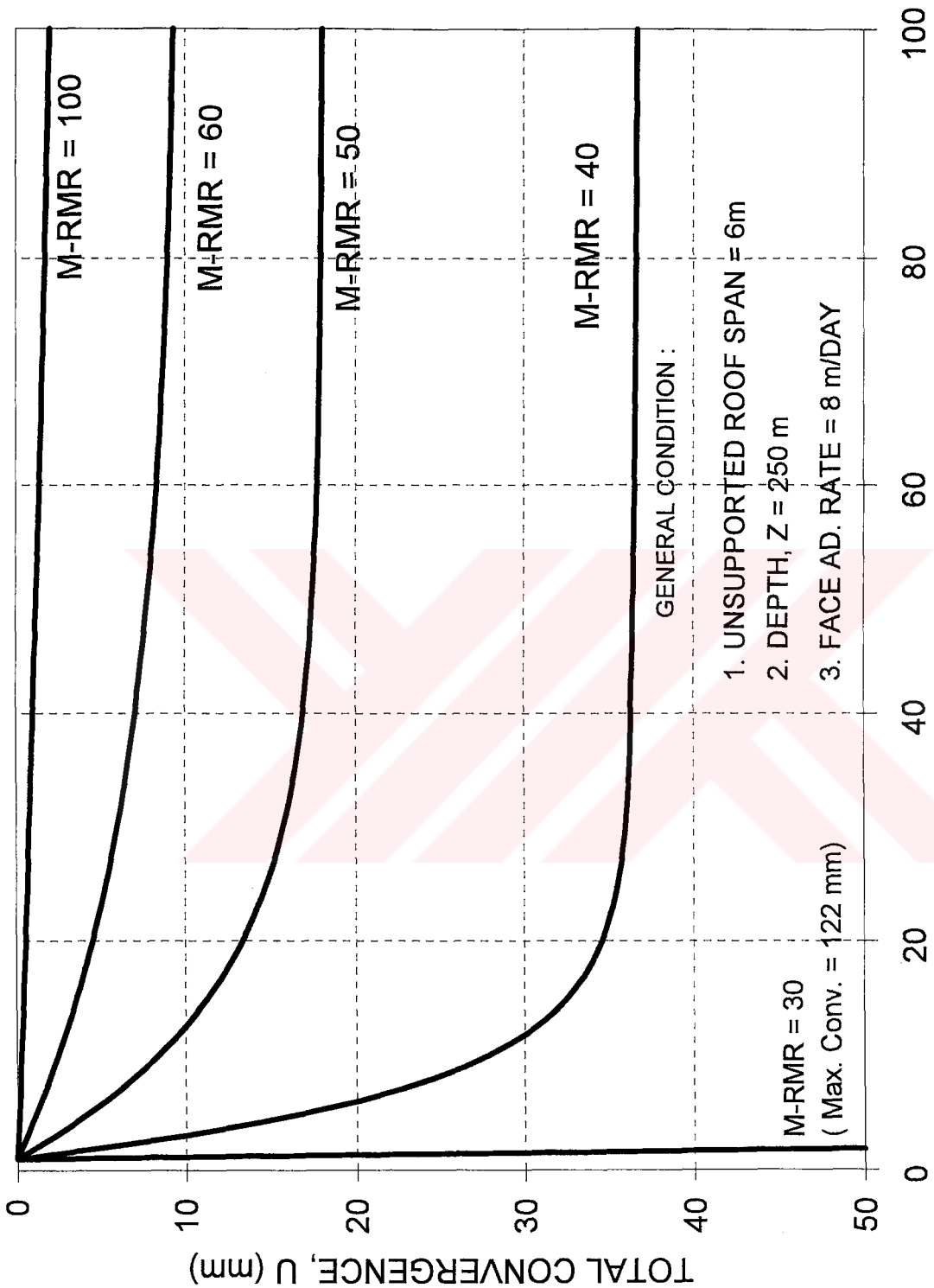

Figure 8.11 Time versus deformation characteristic curves for various M-RMR values

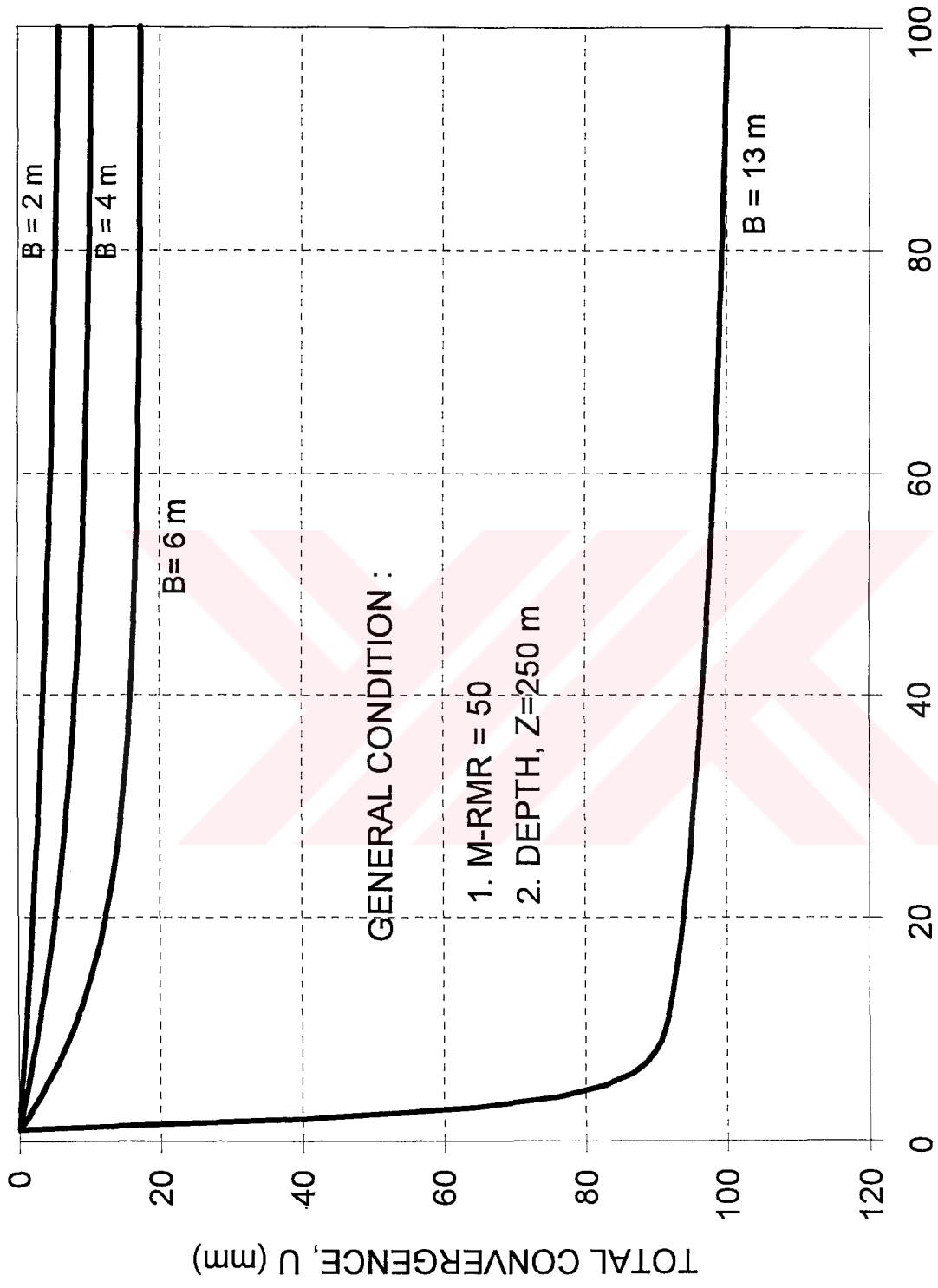

Figure 8.12 Effect of span on time and face advance dependent deformations

Example - 3

Modified Rock Mass Rating (M-RMR)	: 50 (arbitrarily selected)
Depth	: 250 m
Face advance rate	: 8 m/day

The calculated deformations were plotted in Figure 8.13 as a function of time and face advance, for all possible combination of various spans, (i.e. B_{max}=10 m, B=6 m, B_{min}=2.5 m) and for support system stiffness of k=50 kPa/mm.

Example - 4

Roof span	: 6 m (arbitrarily selected)
Depth	: 250 m

Under these conditions, the deformations were calculated for various M-RMR and face advance-velocity values. The results are given in Figure 8.14.

Example - 5

Modified Rock Mass Rating (M-RMR)	: 40 (arbitrarily selected)
Roof span	: 6 m
Depth	: 250 m
Support installation time	: 3 hours

Deformations for above given conditions were calculated for the various support system stiffnesses utilizing Equation 8.13 and the results plotted as shown in Figure 8.15.

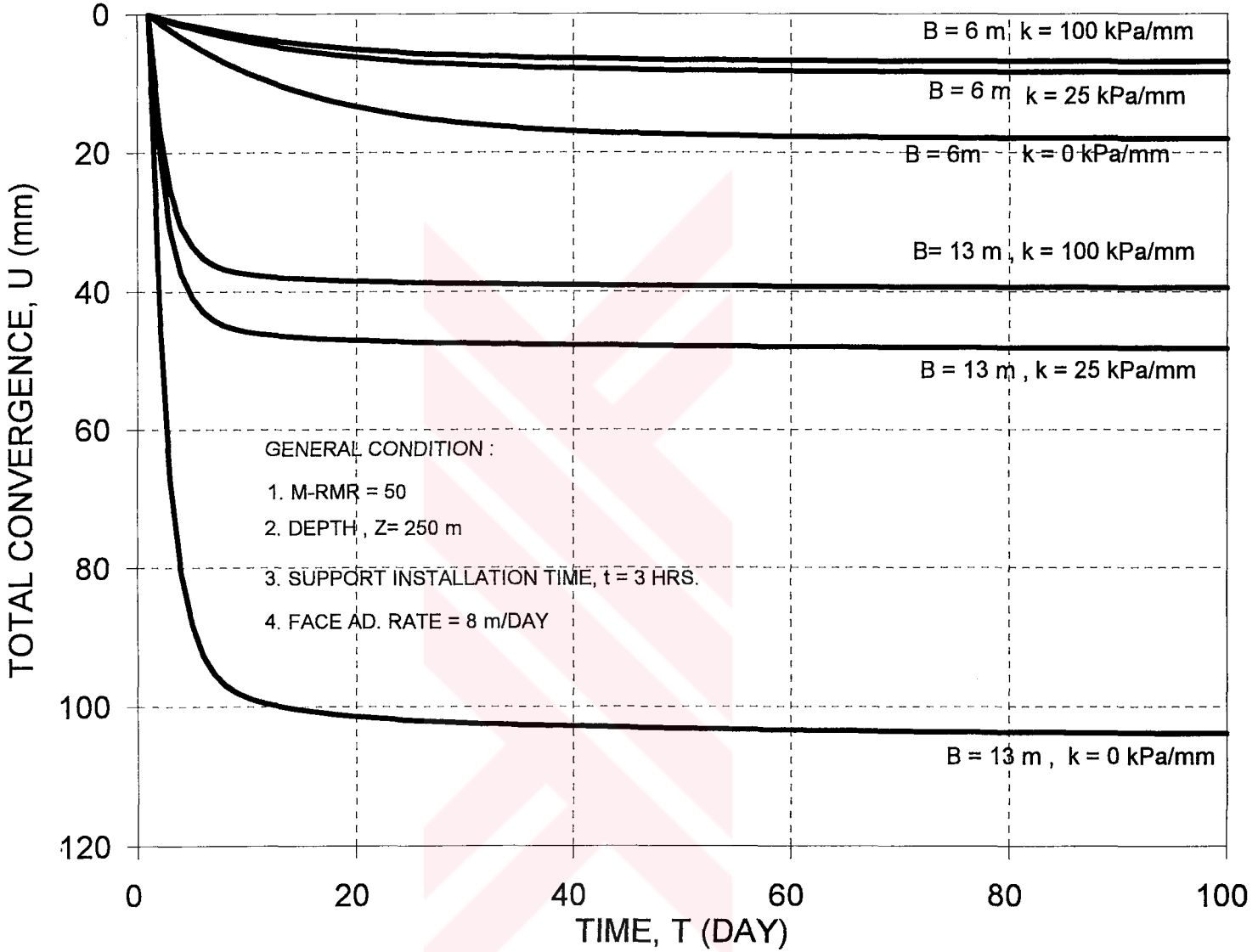

Figure 8.13 The combined effect of the support system stiffness (k) and the span on time and face advance dependent deformations for RMR=50

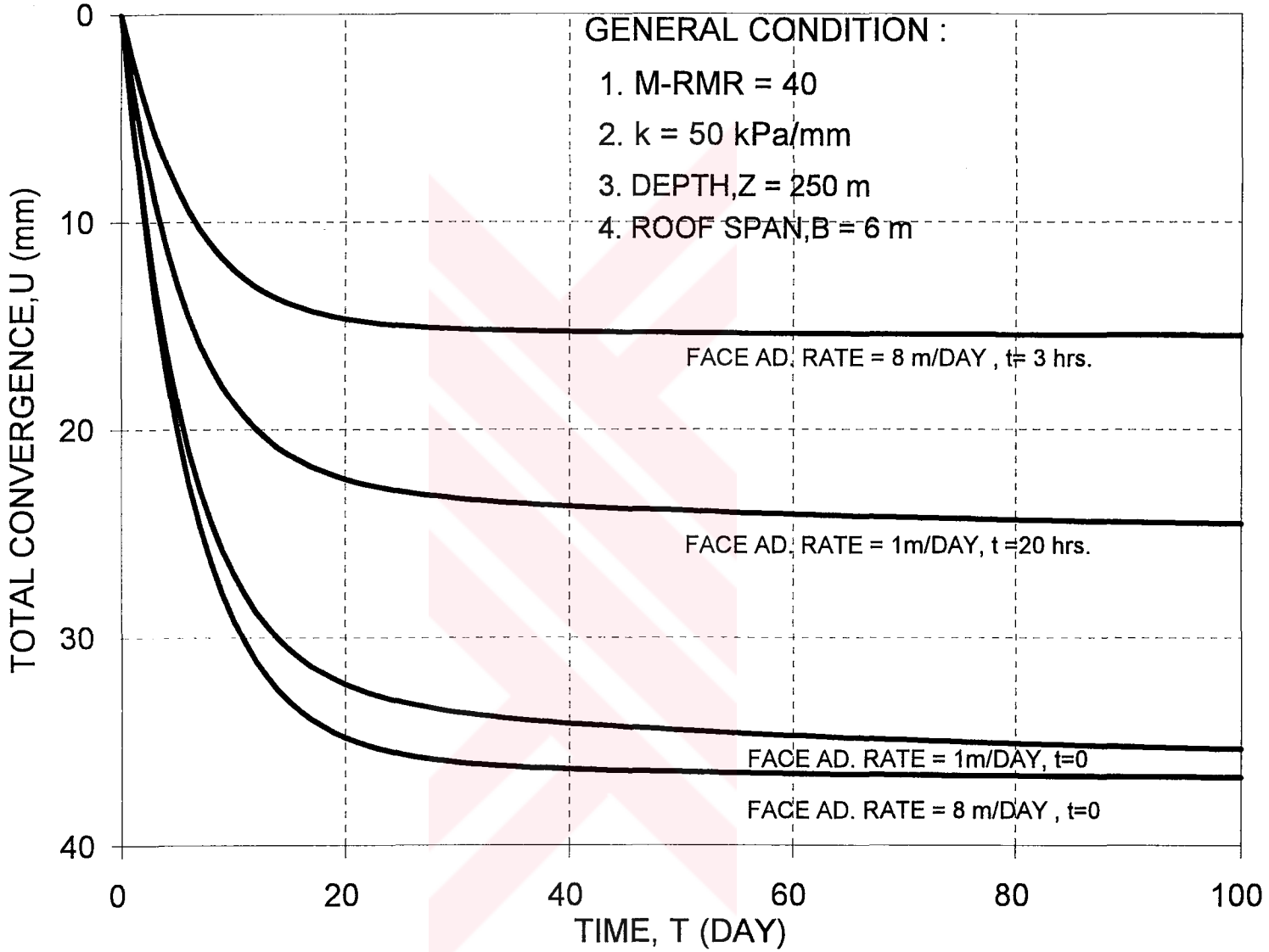

Figure 8.14 The combined effect of face advance rate and M-RMR on time and face advance dependent deformations

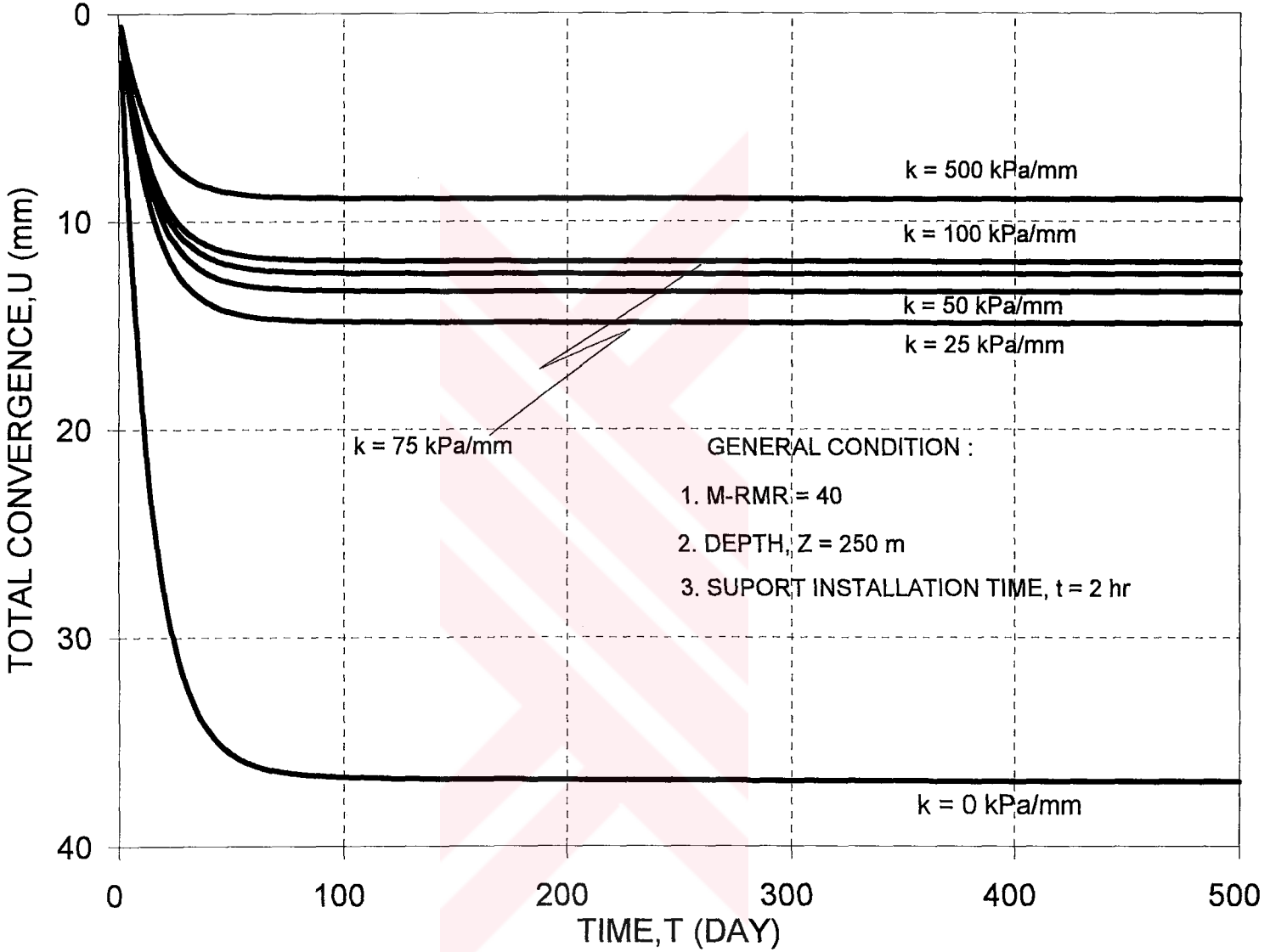

Figure 8.15 Effect of support stiffness (for M-RMR=40) on time and face advance dependent deformations

Example - 6

Modified Rock Mass Rating (M-RMR)	: 40 (arbitrarily selected)
Roof span	: 6 m
Depth	: 250 m
Support system stiffness	: 50 kPa/mm

Deformations were calculated as a function of time and face advance for two different face advance-rates (i.e. 8 m/day and 1 m/day) and three different support installation times (i.e. t= 3 hrs, 9 hrs, and 20 hrs). The results are presented in Figure 8.16.

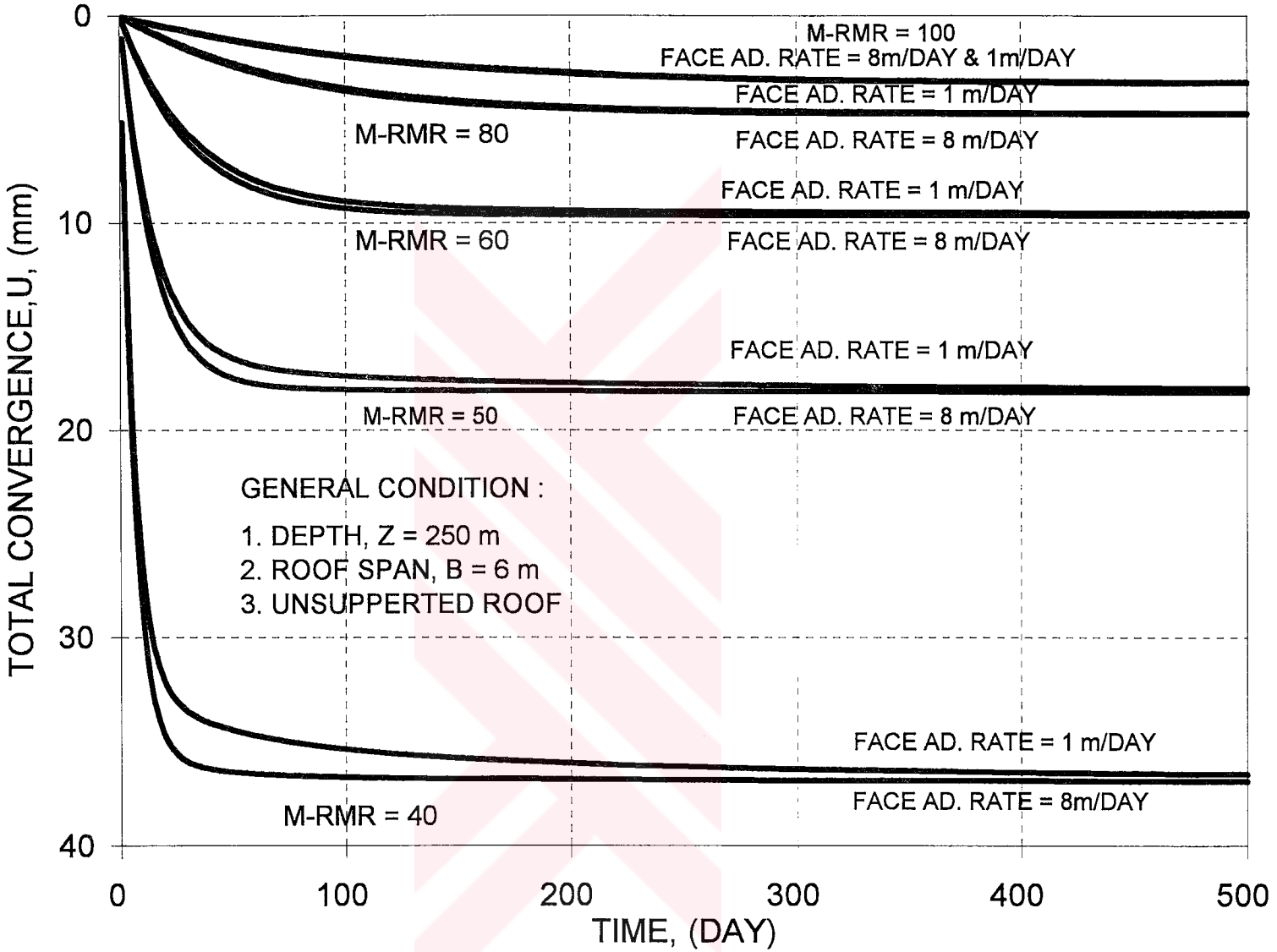

Figure 8.16 The combined effect of face advance rate and the support installation time on time and face advance deformation for M-RMR=40, 50, 60, 80 and 100

CHAPTER IX

CONCLUSIONS AND RECOMMENDATIONS

9.1 Conclusions

The two main objectives of this study were as follows:

1) Characterization of weak, stratified and clay-bearing rock mass, and development of a Modified Rock Mass Rating System (M-RMR)

2) Development of an empirical model for characterization of strata behavior in mine roadways.

Main conclusions derived from this study are as follows:

1) The M-RMR System sufficiently characterizes the weak, stratified and clay-bearing rock mass; therefore, engineering applications that would be carried out according to this system could be adequate for making design decisions.

2) Ratings associated with compressive strength, point load index, RQD, discontinuity spacing, inflow of ground water and joint orientation index were suggested respectively with the following equations:

$$R = 0.856\,\sigma_c^{0.515}$$

$$R = 3.5\, I_{s(50)}^{0.62}$$

$$R = 2.7 + 0.173\, RQD$$

$$R = 3.93\, I_{JS}^{0.187}$$

$$R = 15\, e^{-0.03W}$$

$$R = \begin{cases} \text{if } ICR \le 5 & R = -12 \\ \text{if } 5 < ICR \le 25 & R = 0.35\, ICR - 13.75 \\ \text{if } ICR > 25 & R = -5 \end{cases}$$

3) The suggested Modified RMR (M-RMR) index can be calculated by using the equation given below:

$$M - RMR = F_c \left[I_{PLT} + I_{RQD} + I_{JC} \right] + I_{JS} + I_{GW} + I_{JO}$$

4) Based on statistical evaluation of the results obtained from diametral and axial point-load tests, and considering the anisotropy index (I_a) as well as Young's Modulus and Poisson's Ratio of rocks the following regression equation was obtained:

$$E/\nu = 732\, I_a^{-5.54}$$

5) Utilizing the slake-durability test results, it was found that, only uniaxial compressive strength, RQD and condition of joints are affected by weathering. The suggested weathering coefficient for weatherability can be obtained from the following regression equation:

$$F_C = 0.7\, e^{0.005 I_{d2}}$$

6) In order to evaluate the classification data, a computer program called "ROCK MASS V2.0" was developed. Using this software, the logs of

the input parameters, the associated ratings and the final classification index values can be efficiently determined, in a short period of time for each length of drill-run or structural region.

7) Based on statistical evaluation of the in situ data, it was found that both the convergence and roof strata displacements are "time" and "face advance" dependent and can be characterized by following exponential equations:

   i) time dependent convergence:

$$U = a\left[1 - e^{-t/b}\right]$$

   ii) face advance-dependent convergence:

$$U = a\left[1 - e^{-x/b}\right]$$

   iii) total convergence:

$$U = a\left[e^{0.025 - B/(B^2+x)}\right]\left[1 - e^{-t/b}\right]$$

   Constant a in this equation is defined as follows:

$$a = e^{f(M-RMR)+f(B)+f(Z)}$$

8) Convergence versus time graphs (convergence curves), rate of convergence versus time graphs (convergence-velocity curves) and the rate of convergence-velocity versus time graphs (convergence acceleration curves) provide significant information on the stability of openings, the interaction between support and rock mass and the performances of different support systems.

9) Based on the interpretation of the convergence curves, the following conclusions can be drawn:

i) In all cases, convergence curve reaches to an asymptotical value indicating that the opening has been stabilized in all of the supported sections. This can also be interpreted as the success of the support design method used.

ii) The maximum total convergence occurs in the yielding steel arch region (14.20 mm) where station K16 is located. The maximum total convergence readings obtained in other regions are as follows: Split-Set (10.50 mm), Sis-resin (7.0 mm), yielding super swellex (6.5 mm), Fosroc-resin (6.35 mm) and the mixed support region (4.62 mm) in which yielding super swellex and yielding steel arches were used together.

iii) The lowest maximum convergence obtained in almost all mixed support (bolts and steel arch) regions may reflect an overdesign, but it is a good indicator for proper design in regions where rock bolts are used as the sole means of support.

iv) In the region supported by yielding steel arches, the total maximum convergence has the highest value but this asymptotical value was reached much earlier (100 days) than the other types. The opposite fact is true for the mixed support region (150 days).

v) The slopes of convergence curves provide information on relative quality of the interaction and also on performance of the

support types used. The lower the slope, the better the interaction and/or performance is.

vi) The decrease in slope of the initial convergence curve reflects initiation of an interaction. The approach of the convergence curve towards an asymptotical value is an indication of full stability or completion of the interaction between rock mass and support.

vii) It is difficult to determine the time of initiation and completion of interaction by looking at convergence curves. However, it is possible to obtain this information from rate of convergence and rate of convergence-velocity graphs.

10) The convergence-velocity curves were plotted by utilizing the differential equation obtained by taking the first partial derivative of the convergence equation (U). Based on the results of these analyses, the following conclusions can be drawn:

i) The curves representing the total rate of convergence of rock bolts are between curves representing the yielding steel arches and mixed support.

ii) The plots associated with the rate of maximum total convergence follow the same pattern for all supported sections as in the case of the maximum total convergence plots.

iii) The rate of strata convergence is different in each area stabilized by different type of support and decreases with time.

iv) When the value of the total convergence is high, then the initial rate of convergence is also high. However, in these cases, the rate of convergence approaches to zero (an indication of full stability) earlier (i.e., 90 days for yielding arch) than the other types. The opposite is also true for the mixed support region (150 days). However, interaction is completed in 90 and 50 days in regions stabilized by yielding arches and mixed support (arches and bolts) respectively.

v) In the graphs of "rate of convergence versus time" sudden increases and decreases in rates can easily be observed. This may be due to irregular rate of tunnel face advance. When excavation starts after a period of stoppage, then convergence increases suddenly reaching to a maximum value and then drops down to its initial rates.

vi) The other important phenomena observed in these analyses is that these sudden increases and decreases in instant convergence rates (i.e., amplitudes) are high when the tunnel face is close to the station and decreases gradually and disappears finally when stability is fully reached. Frequency of the rate-changes also decreases with time.

vii) Lower amplitudes and frequencies in rate of convergence are an indication of better control of strata and better interaction between support and rock mass. It should be noticed however that this situation could be an indication of an overdesign.

11) The convergence-acceleration curves were plotted by utilizing the partial differential equation obtained by taking the second partial derivative of the time and face-advance dependent convergence equation (U). Based on the results of these analyses, the following conclusions can be drawn:

i) The rate of convergence-velocity (acceleration) is different in each area stabilized by different type of supports and decreases with time.

ii) The point where the rate of convergence-velocity becomes constant, in other words, the time at which full interaction is achieved, is different at each supported section.

iii) As the acceleration approaches to zero, it fluctuates up and down between positive and negative values depending on the rate of face advance. These amplitude and frequency of those fluctuations are high when the area is close to the tunnel face; however, they cease as the tunnel face goes away.

iv) If the interaction is not sufficiently adequate or the rate of tunnel face advance is irregular, initially the acceleration is negative, and the amplitude and frequency of the activity (fluctuation) is high. If the interaction is better, then the initial values of the acceleration is closer to zero and fluctuations of the acceleration will be relatively low.

9.2 Recommendation for Future Work

Based on this study, the author's recommendations for future research are as follows:

1) The Modified Rock Mass Rating System is being currently used in Çayeli Bakır Mine in Turkey and in a copper-zinc mine in Tunisia. The M-RMR System should be tried in a number of other mines so that more feedback can be obtained in classifying weak, stratified and clay-bearing rock mass.

2) The output of M-RMR System should be evaluated with more field observations.

3) In this study, the convergence and roof displacement measurements were carried out in a gate roadway during its initial drivage. The behavior of this opening was similar to a tunnel, a main haulageway or an undisturbed roadway in underground. Further investigations should be carried out in this opening in order to evaluate the dynamic effects of the retreating longwall faces and the response of the six different support types which were used to stabilize this roadway.

4) The effects of depth, roof span, and M-RMR index should be investigated in other mines and locations, so that, the suggested empirical model would be further justified.

REFERENCES

Aghai, N., 1991. "A Model for Shaft Location Selection and Ground Control Approach to Shaft Design", M.Sc. Thesis, Middle East Technical University, 167p.

Amadei, B. and Curran, C.H., 1980. "Creep Behavior of Rock Joints", 13th Canadian Rock Mech. Symp., Undeground Rock Eng., CIM, Vol. 22, The Canadian Inst. of Min. and Metal., Toronto, Ontario, May, pp. 146-150.

Barton, N., Lien, R. and Lunde, J., 1974. "Engineering Classification of Rock Masses for the Design of Tunnel Support", Rock Mech., 6, pp. 183-236.

Bhasin, R., 1994. "Technical Note: Rock Mass Characterization for Large Caverns in India and Norway Using a New Method of Recording and Presenting Engineering Geological Data", Int. J. Rock Mech. Min. Sci. and Geomech. Abstr., Vol. 31, No. 1, pp. 87-91.

Bieniawski, Z.T., 1973. "Engineering Classification of Jointed Rock Masses", Trans. S. Afr. Inst. Civ. Eng., 15, pp. 335-344.

Bieniawski, Z.T., 1976. "Rock Mass Classifications in Rock Engineering", Exploration for Rock Engineering, A.A. Balkema, Johannesburg, pp. 97-106..

Bieniawski, Z.T., 1978. "Determining Rock Mass Deformability: Experience from Case Histories", Int. J. Rock Mech. Min. Sci., Vol. 15, pp. 237-247.

Bieniawski, Z.T., 1979. "The Geomechanics Classification in Rock Engineering Applications", Proc. 4th Int. Congr. Rock Mech., ISRM, Vol. 2, Montreux, pp. 4-48.

Bieniawski, Z.T., 1984. Rock Mechanics Design in Mining and Tunneling, Rotterdam, Balkema, 272p.

Bieniawski, Z.T., 1989. Engineering Rock Mass Classifications, Wiley, New York, 251p.

Bieniawski, Z.T., 1993. "Classification of Rock Masses for Engineering: The RMR System and Future Trends", Comprehensive Rock Engineering, Vol. 3, Pergamon Press, pp. 553-575.

Bishop, A.W., 1955. "The Use of the Slip Circle in the Stability Analysis of Slopes", Geotechnique, Vol. 5, pp. 7-17.

Blair, G.W.S., 1969. "Elementary Rheology, Academic Press, New York.

Boisen, B.P., 1977. "A Hand Portable Point Load Tester for Field Measurements", Proc. Eighteenth U.S. Symp. on Rock Mech., Keystone, Colorado, pp. 40-45.

Broch and Franklin, 1972. "The Point Load Strength Test", Int. J. of Rock Mech. Min. Sci. and Geom. Abstract, Vol. 9, pp. 669-697.

Brook, N. and Dharmaratne, G.R., 1985. "Simplified Rock Mass Rating System for Mine Tunnel Support", Trans. Inst. Min. Metall. 94, pp. A148-A154.

Brown, E.T., Braw, J.W., Ladanyi, B. and Hoek, E., 1983. "Ground Response Curves for Rock Tunnels", Journal of Geotechnical Engineering Division, ASCE 109, pp. 15-39.

Butler, A.G. and Franklin, J.A., 1990. "Classex: An Expert System for Rock Mass Classification", Static and Dynamic Considerations in Rock Eng., Brummer (ed.), Balkema, Rotterdam, pp. 73-80.

Can, Y., 1987. "Drift Support Techniques in weak Rock and Measurement of Displacement Around Rock Excavations", Inst. of Mining and Met. Trans., Sect. A, Vol. 96, pp. A47-A50.

Carter, N.L. and Kirby, S.H., 1978. "Transient Creep and Semibrittle Behavior of Crystalline Rocks", Pageoph, Vol. 116, pp. 807-839.

Cording, E.J., and Deere, D.U., 1972. "Rock Tunnel Supports and Field Measurements", Proc. Rapid Excav. Tunneling Confr., AIME, New York, pp. 601-622.

Cummings, R.A., Kendorski, F.S. and Bieniawski, Z.T., 1982. "Caving Rock Mass Classification and Support Estimation", U.S. Bureau of Mines Contract Report # J0100103, Engineers International, Inc., Chicago, 195p.

Daemen, J.J. and Fairhurst, C., 1971. "Influence of Failed Rock Properties on Tunnel Stability", Dynamic Rock Mechanics, Amer. Inst. of Min., Metal. and Petroleum Engineers, New York, pp. 855-875.

Deere, D.U., Hendron, A.J., Patton, F.D. and Cording, E.J., 1967. "Design of Surface and Near Surface Construction in Rock," Proc. 8th U.S. Symp. Rock Mech., AIME, New york, pp. 237-302.

Deere, D.U., and Deere, D.W., 1988. "The RQD Index in Practice", Proc. Symp. Rock Classif. Eng. Purp., ASTM Special Technical Publication 984, Philadelphia, pp. 91-101.

Deere, D.U., 1989. "Rock Quality Designation (RQD) after Twenty Years", U.S. Army Corps of Engineers Contract Report GL-89-1, Walterways Experiment Station, Vicksburg, MS, 67p.

Dietrich, J.H., 1972. "Time Dependent Friction in Rocks", J. Geophysical Research, Vol. 77, No. 20, pp. 3690-3697.

Dong, F., Song, H. and Gou, Z., 1988. "The Broken Rock zone Around Tunnels and Its Support Theory", 7th Int. Confr. on Ground Control in Mining, West Virginia Univ., Morgantown, 3-5 August, pp. 336-343.

Dusseault, M.B. and Fordham, C.J., 1993. "Time Dependent Behavior of Rocks", Comprehensive Rock Engineering, ed. J.A. Hudson, Vol.3, pp. 120-147.

Farmer, I., 1983. Engineering Behaviour of Rocks, 2nd Edn., Chapman and Hall Ltd., London.

Filcek, H. and Kwasniewski, M.A., 1993. "Fundamentals of Mine Roadway Support Design: Rock-Support Interaction Analysis", Comprehensive Rock Engineering, ed. J.A. Hudson, Vol.2, pp. 671-695.

Franklin, J.A., 1975. "Safety and Economy in Tunneling", Proc. 10th Can. Rock Mech. Symp., Queens Univ., Kinston, Canada, pp. 27-53.

Genevois, R. and Prestininzi, A., 1979. "Time-Dependent Behavior of Granitic Rocks Related to Their Alteration Grade", Proc. 4th Int. Cong. on Rock Mech., ISRM, Montreaux, Switzerland, Vol. 1, pp. 153-159.

Ghosh, C.N. and Ghose, A.K., 1992. "Estimation of Critical Convergence and Rock Load Mine Roadways - an Approach Based on Rock Mass Rating", Geotechnical and Geological Engineering, Vol. 10, pp. 185-202.

Giles, E.L., 1984. "The Merits of Tunnel Instrumentation in South African Rock Conditions", Symp. on Monitoring for Safety in Geotechnical Engineering, South Africa.

Goodman, R.E., 1980. Introduction to Rock Mechanics, Wiley, New york, 478p.

Gökay, K., 1988. "Bearing Capacity Analysis of Layered Rock for an Underground Mine", M.Sc. Thesis, Dept. of Mining Engineering, Middle East Technical University, 135p.

Griggs, D.T., 1939. "Creep of Rock", Jour. of Geology, Vol. 47, 225p.

Griggs, D.T., 1940. "Experimental Flow of Rocks Under Conditions Favoring Recrystallization", Geol. Soc. America Bull., Vol. 51, 1001p.

Guadin, B., Falacci, J.P., Panet, M. and Salva, L., 1981. "Soutene d'une galeria dans les marnes du Cénomanien", Proc. 10th Confr. on Soil Mech. and Foundation Engr., Stockholm, pp. 293-296.

Guenot, A., Panet, M. and Sulem, J.A., 1985. "A New Aspect in Tunnel Closure Interpretation", Proc. 26th U.S. Symp. On Rock Mech., pp. 455-460.

Hassani, F.P., Whittaket, B.N. and Scoble, M.J., 1981. "Application of the Point Load Index Test to Strength Determination of Rock and Proposals for a New Size Correction Chart", Proc 21st US Rock Mech. Symp., Rolla, pp. 543-553.

Hobbs, D.W., 1970. "Stress-Strain-Time Behavior of a Number of Coal Measure Rocks", Int. J. Rock Mech. Min. Sci., Vol. 7, pp. 149-170.

Hoek, E. and Brown, E.T., 1980. Underground Excavations in Rock, London, U.K., 527p.

Hoek, E. and Brown, E.T., 1988. "The Hoek-Brown Failure Criterion - a 1988 Update", Proc. 15th Con. Rock Mech. Symp., University of Toronto, October, pp. 31-38.

Inyang, H.I. and Pitt, J.M., 1990. "Standardisation of a Percussive Drill for Measurement of the Compressive Strength of Rocks", Proc. of the Thirty First U.S. Symp. on Rock Mech., Denver, pp. 489-496.

Inyang, H.I., 1991. "Development of a Preliminary Rock Mass Classification Scheme for Near-Surface Excavation", Int. J. of Surface Min. and Rec., Vol. 5, pp. 65-74.

ISRM, 1979. "Commission on Standardization of Laboratory and Field Tests, Suggested Methods for the Quantitative Description of Discontinuity in Rock Masses", Int. J. Rock Mech. Sci. and Geomech. Abstr., Vol. 15, pp. 319-368.

ISRM, 1981. "Rock Characterization, Testing and Monitoring - ISRM Suggested Method", Pergamon, Oxford, 211p.

İstanbulluoğlu, S., 1995. "Strata Control Aspects at the Gate Roadways of OAL Underground Mine", Ph.D. Thesis, Department of Mining Engineering, Middle East Technical University, 202 p (unpublished).

Jethwa, J.L., Dube, A.K, Singh, B. and Mithal, R.S., 1982. "Evaluation of Methods for Tunnel Support Design in Squeezing Rock Conditions", Proc. 4th Int. Congr., Int. Assoc. Eng. Geol., Vol. 5, Delhi, pp.125-134.

Kammer, W., 1975. "Einflüsse auf die Querschnitts und Aubauverformung in Abbaustrecken, Untersuchungsbericht".

Kazi, A. and Şen, Z., 1985. "Volumetric RQD : An Index of Rock Quality", Proc. of the Int. Symp. on Fundementals of Rock Joints, Bjorkliden, pp. 15-20.

Kendorski, F.S., Cummings, A., Bieniawski, Z.T. and Skinner, F., 1983. "A Rock Mass Classification Scheme for the Planning of Caving Mine Drift Supports", Proc. Rapid Excav. Tunneling Conf., AIME, New York, pp. 193-223.

Kester, W.M. and Chugh, Y.P., 1980. "Pre-Mining Investigations and Their Use in Planning Ground Control in the Illinois Coal Basin", Proc of the 1st. Confr. on Ground Control Problems in the Illinois Coal Basin, June, pp. 33-34.

Ladanyi, B., 1974. "Use of the Long-Term Strength Concept in the Determination of Ground Pressure on Tunnel Lining", Advances in Rock Mech., Proc. of the 3rd. Congr. of the ISRM, Denver, pp. 1150-1156.

Ladanyi, B., 1980. "Direct Determination of Ground Pressure on Tunnel Lining in a Non-Linear Visco-Elastic Rock", Proc. Symp. 13th Canadian Rock Mech., Underground Rock Eng., CIM Special Vol. 22, The Canadian Inst. of Min. and Metal., Toronto, pp. 126-132.

Ladanyi, B., 1993. "Time Dependent Response of Rock around Tunnels", Comprehensive Rock Engineering, ed. J.A. Hudson, Vol. 2, pp. 78-109.

Laubscher, D.H., 1977. "Geomechanics Classification of Jointed Rock Masses - Mining Applications", IMM Transactions., Vol. 86, pp. A1-A7.

Laubscher, D.H., 1984. "Design Aspects and Effectiveness of Support Systems in Different Mining Conditions", Transactions of IMM, Vol. 93, pp. A70-A81.

Laubscher, D.H., 1990. "A Geomechanics Classification System for the Rating of Rock Mass in Mine Design", J.S. Afr. Inst. Min. Metall., Vol. 90, No. 10, Oct., pp. 257-273.

Laubscher, D.H., 1993. "Planning Mass Mining Operations", Compressive Rock Engineering, ed. J.A. Hudson, Vol.2, pp. 547-575.

Lauffer, H., 1958. "Gebirgklasslfizierung für den Stollenbau." Geol. Bauwesen, 74, pp. 46-51.

Lauffer, H., 1988. "Zur Gebirgsklassifizierung bei Frasvortrieben", Felsbau, 6(3), pp. 137-149.

Lee, C.H., and Chen, S.T., 1989. "Estimation of Rock Mass Modulus", Int. J. of Min. and Geo. Eng., Vol.7, pp. 175-181.

Majdi, A., Hassani, F.P. and Cain, P., 1986. "The Influence of Design Parameters on Tunnel Closure in the Sydney Coal Field", Proc. of the 88th Annual General Meeting of CIM, Montreal, 36p.

Majdi, A. and Hassani, F.P., 1989. "Access Tunnel Convergence Prediction in Longwall Coal Mining", Int. J. of Mining and Geological Engineering, Vol. 7, pp. 283-300.

Mark, C. and Chase, F.E., 1993. "Gate Entry Design for Longwalls Using the Coal Mine Roof Rating", Proc. of the 12th Int. Confr. on Ground Control in Mining, Morgantown, WV, pp. 76-83.

Mathews, K.E., Hoek, E., Wyllie, D.C. and Stewart, S.B.V., 1980. "Prediction of Stable Excavations for Mining at Depths Below 1000 meters in Hard Rock", CANMET Report 802-1571.

Mendes, F.M., Gama, C.D., Santos, M.C., Arrais, C.M., Gaspar, A.F. and Silva P.B., 1993. "Geomechanics and Mine Support Investigation in the Germunde Coal Mine", EUROCK'93, Portugal, pp. 637-642.

Merritt, A.H., 1972. "Geologic Prediction for Underground Excavations", Proc. Rapid Excav. Tunneling Conf., AIME, New York, pp. 115-132.

Milne, D. and Potvin, Y., 1992. "Measurement of Rock Mass Properties for Mine Design", EUROCK'92, London, pp. 245-250.

Moebs, N.N. and Stateham, R.M., 1986. "Coal Mine Roof Stability : Categories and Causes", USBM IC 9076, 15p.

Molinda, G.M. and Mark, C., 1993. "The Total Mine Roof Rating (CMRR) A Practical Rock Mass Classification for Coal Mines", Proc. 12th Confr. on Ground Control in Mining, West Virginia Univ., Morgantown, pp. 92-103.

Murell, S.A.F., 1967. "An Experimental Study of the Effect of Temperature and Stress on the Creep of Rocks", Geophys, J.R. Astr. Soc., Vol. 14, pp. 51-55.

Murell, S.A.F., 1969. "Micromechanical Basis of the Deformation and Fracture of Rocks", Proc. Int. Conf. Struct. Solid Mech., Southampton, Vol. 1, pp. 271-275.

Nair, K. and Boresi, A.P., 1970. "Stress Analysis of Time Dependent Problems in Rock Mechanics", Proc. 2nd Congr., ISRM, Beograd, Vol. 2, pp. 531-536.

Newman, D.A., and Bieniawski, Z.T., 1985. "Modified Version of the Geomechanics Classification for Entry Design in Underground Coal Mines", Trans. Soc. Min. Eng., AIME 280, pp. 2134-2138.

Nicholson, G.A. and Bieniawski, Z.T., 1990. "A Non-Linear Deformation Modulus Based on Rock Mass Classification", Int. J. of Min. and Geological Engineering, Vol.8, pp. 181-202.

Nieble, C.M., Brito, S.N.A., Fujimura, F. and Hennies, W.T., 1993. "Rock Mechanics as a Support to Safety in Underground Mining", EUROCK'93, pp. 643-649.

Ode, H., 1968. "Review of Mechanical Properties of Salt Relating to Salt Dome Genesis", In Saline Deposits, Spec. Pap. - Geol. Soc. Am. 88, pp. 543-595.

O'Rourke, J.E., 1989. "Rock Index Properties for Geoengineering in Undeground Development", Mining Engineering, February, pp. 106-110.

Ojo, O. and Brook, N., 1990. "The Effect of Moisture on Some Mechanical Properties of Rock", Mining Science and Technology, Vol. 10, pp. 145-156.

Özel, R., 1988. "Load and Convergence Measurements in Longwall Faces at Bigadiç-Simav Mine and Recommendations for Hydraulic Face Props", M.Sc. Thesis, Dept. of Mining Engineering, Middle East Technical University, 160p.

Özel, R., 1995. "Development of Guidelines for Selection of Longwall Shield Supports", Ph.D. Thesis, Dept. of Mining Engineering, Middle East Technical University, 245p.

Özkan, İ., 1989. "Determination of Classification Parameters for Weak and Stratified Rocks Based on RMR and Q-Systems", M.Sc. Thesis, Dept. of Mining Engineering, Middle East Technical University, 156p.

Pacher, F., Rabcewicz L. and Golser, J., 1964. "Zum der seitigen Stand der Gebirgsklassifizierung in Stollen und Tunnelbau", Proc. XXII Geomech. Colloq., Salzburg, pp. 51-58.

Palmstrom, A., 1982. "The Volumetric Joint Count - a Useful and simple Measure of the Degree of rock jointing", Proc. 4th Int. Congr., Int. Assoc. Eng. Geol., Vol. 5, Delhi, pp. 221-228.

Pan, Y.W. and Dong, J.J., 1991a. "Time Dependent Tunnel Convergence I. Formulation of the Model", Int. J. Rock Mech. Min. Sci. and Geomech. Abstr., Vol. 28, No. 6, pp. 469-475.

Pan, Y.W. and Dong, J.J., 1991b. "Time Dependent Tunnel Convergence II. Advance Rate and Tunnel Support Interaction", Int. J. Rock Mech. Min. Sci. and Geomech. Abstr., Vol. 28, No. 6, pp. 477-488.

Panek, L.A., 1962a. "The Effect of Suspension in Bolting Bedded Mine Roof', USBM RI5156, 25p.

Panek, L.A., 1962ba. "The Combined Effects of Friction and Suspension in Bolting Bedded Mine Roof", USBM RI6139, 31p.

Panet, M., 1979. "Time Dependent Deformations in Underground", Proc. 4th Confr. ISRM, Vol. 3, pp. 279-290.

Panet, M. and Guenot, A., 1982. "Analysis of Convergence Behind the of a Tunnel", Tunnelling 82, IMM, Brighton, pp. 197-204.

Panet, M., 1993. "Understanding Deformations in Tunnels", Comprehensive Rock Engineering, ed. J.A. Hudson, Vol.1, pp. 663-689.

Parsons, R.C. and Hedley, D.G.F, 1966. "The Analysis of Viscous Property of Rocks for Classification", Int. J. Rock Mech. Min. Sci., Vol. 3, pp. 325-335.

Paşamehmetoğlu, A.G., Ünal, E. and Tutluoğlu, L., 1988. Rock Mechanics Investigations in Simav Underground Mine, Final Report, 361p..

Paşamehmetoğlu, A.G., Ünal, E. and Tutluoğlu, L., 1989. "Investigations into Strata Control Systems for Weak Strata in a Borax Mine", Proc. 8th Int. Strata Control Conf., Düsseldorf, Germany, May 22-26, paper D-5.

Potvin, Y., Hudyma, H. and Miller, H., 1988. "The Stability Graph Method for Open Stope Design", Proc. 90th CIM AGM, Edmanton, Alberta.

Priest, S.D. and Hudson, J.A., 1976. "Discontinuity Spacing in Rock", Inst. J. Rock Mech. and Min. Sci., Vol. 13, pp. 135-198.

Priest, S.D. and Brown, E.T., 1983. "Probabilistic Stability Analysis of Variable Rock Slopes", Trans. Inst. Min. Metall., London, Sec. A, Vol. 92, pp. A1-A12.

Rafia, F., 1980. "An Assessment of Room and Pillar Coal Mine Roof Conditions by Means of Engineering Rock Mass Classifications", M.Sc. Thesis, Penn State University, 123p.

Serafim, J.L. and Pereira, J.P., 1983. "Considerations of the Geomechanics Classification of Bieniawski", Proc. Int. Symp. Eng. Geol. Underground Constr., LNEC, Lisbon, Vol. 1, pp. II,33-II,42.

Shelton, P.D., 1982. "Relation Between Closure and Support in Deep Mine Excavations", Symp. on Strata Mechanics, Univ. of Newcastle upon Tyne, 5-7 April, pp. 230-233.

Sheorey, P.R., 1984. "Use of Rock Classification to Estimate Roof Caving Span in Oblong Workings", Int. Journal of Mining Engineering, Vol.2, pp. 133-140.

Sheorey, P.R., 1985. "Support Pressure Estimation in Failed Rock Conditions", Eng. Geol., Vol. 22, pp. 127-140.

Sheorey, P.R., 1991. "Experience with Application of the NGI Classification to Coal Measures", Int. J. Rock Mech. Min. Sci. and Geomech. Abstr., Vol. 28, No. 1, pp. 27-33.

Sheorey, P.R., 1993. "Experience with the Application of Modern Rock Classifications in Coal Mine Roadways", Comprehensive Rock Engineering, ed. J.A. Hudson, Vol. 4, pp. 411-431.

Sickler, R.A., 1986. "Engineering Classification of Shales", Proc. of the 5th Confr. on Ground Control in Mining, June 11-13, Morgantown, WV, pp. 221-233.

Singh, R.N., Hassani, F.P. and Elkington, P.A.S., 1983. "The Application of Strength and Deformation Index Testing to the Stability Assessment of Coal Measures Excavations", Proc. 24th US Symp. on Rock Mechanics, June, pp. 599-609.

Singh, K.B., Singh, T.N., Singh, D.P. and Jethwa, J.L., 1994. "Effect of Discontinuities on Strata - Movement Problems in Collieries: A Review", Geotechnical and Geological Engineering, Vol. 12, pp. 43-62.

Solberg, P.H., Lanchner, D.A., Summers, R.S. and Weeks, J.D., 1978. "Experimental Fault Creep Under Constant Differential Stress and High Confining Pressure", Proc. 19th U.S. Symp. on Rock Mech., Stateline, Nevada, pp. 118-120.

Stille, H., Groth, T. and Fredriksson, A., 1982. "FEM-Analysis of Rock Mechanics Problems by JOBFEM", Swedish Rock Engineering Research Foundation and Institution for Soil and Rock Mechanics, Royal Institute of Technology, Stockholm, Nr. 307:1/82.

Sulem, J., Panet, M. and Guenot, A., 1987a. "Closure Analysis in Deep Tunnels", Int. J. Rock Mech. Min. Sci. and Geomech. Abstr., Vol. 24, No. 3, pp. 145-154.

Sulem, J., Panet, M. and Guenot, A., 1987b. "An Analytical Solution for Time-Dependent Displacements in a Circular Tunnel", Int. J. Rock Mech. Min. Sci. and Geomech. Abstr., Vol. 24, No. 3, pp. 155-164.

STSC, Inc., 1991. "Statgraphics: Statistical Procedures Reference Manual V5.0", 1750p.

Şen, Z., 1990. "Cumulative Core Index for Rock Quality Evaluations", Int. J. Rock Mech. Min. Sci. and Geomech. Abstr., Vol. 27, No. 2, pp. 87-94.

Tallon, E.M., 1982. "Comparison and Application of Geomechanics Classification Schemes in Tunnel Construction", Tunnelling'82, The Inst. of Mining and Metallurgy, pp. 241-246.

Tan, T.K. and Kang, W.F., 1980. Locked in Stress, Creep and Dilatancy of Rocks and Constitutive Equations", Rock Mechanics, Vol. 13, No. 1, pp. 5-22.

Terzaghi, K., 1946. "Rock Defects and Loads on Tunnel Support. Rock Tunneling with steel Supports", ed. R. V. Proctor and T. White, Commercial Shearing Co., Youngstown, OH, pp. 15-99.

Tincelin, M., 1978. "Analysis of Stability by the Convergence-Confinement Method", Discussions at the end of the paper, Proc. Paris Conference, October 26, Published in Underground Space, May/June, 1980, Vol. 4, No. 6, pp. 301-402.

Tsidzi, K.E.N., 1991. "Point Load Uniaxial Compressive Strength Correlation", Int. Society for Rock Mech. Symp., Aachen, Deutschland, Vol. 1, pp. 637-639.

Ulusay, R., 1991. "Geotechnical Evaluations and Deterministic Design Considerations for Pitwall Slopes at Eskihisar (Yatağan-Muğla) Strip Coal Mine", Ph.D. Thesis, Dept. of Geological Engineering, Middle East Technical University, 340p.

Ulusay, R., Özkan, İ. and Ünal, E., 1992. "Characterization of Weak, Stratified and Clay-Bearing Rock Masses for Engineering Applications and Jointed Rock Masses", Granlibakken Conference Center, Lake Tahoe, California, June 3-5, pp. 233-240.

Ünal, E., 1983. "Design Guidelines and Roof Control Standards for Coal Mine Roofs", Ph. D. Thesis, Pennsylvania State University, University Park, 355p.

Ünal, E., 1986a. "Empirical Approach to Calculate Rock Loads in Coal Mine Roadways", 5th Conf. on Ground Control in Mining, W.V. Univ., Morgantown, pp. 234-241.

Ünal, E., 1986b. "Tünel Tasarımında Bütünleme Yaklaşımı", Tünellerin Projelendirilmesi ve İnşası Semineri, DSİ, 5-9 Mayıs, Cilt 11-12, Adana.

Ünal, E., 1988. "Strata Control Lecture Notes", Middle East Technical University, Ankara.

Ünal, E. and Akçakoca, H., 1988. "Dimensioning of Support Systems", Internal Report, METU MUG-10, Dept. of Mining Eng., Middle East Technical University.

Ünal, E., 1989. "Support Selection of Mine Roadways by Means of a Computer Program", Rock Mech. as a Guide for Efficient Utilization of Natural Resources, Proc. 30th U.S. Symp. on Rock Mech., pp. 943-952.

Ünal, E. and Ergür, K.M., 1990. "PC Based Modeling of Rock Reinforcement Requirements in Mine Roadways", Proc. 31st Symp. on Rock Mech., CSM Golden, Colorado, pp. 761-768.

Ünal, E. and Özkan, İ., 1990. "Determination of Classification Parameters for Clay-Bearing and Stratified Rock Mass", 9th Int. Conf. on Ground Control in Mining, WV Univ., Morgantown, pp. 250-259.

Ünal, E. and Özkan, İ, 1992. "Flexible Support Design for Gate-Roads of Retreating Longwall Panels", Proc. 12th Conf. on Ground Control in Mining, WV Univ, Mrgantown, pp. 133-143.

Ünal, E., Ulusay, R. and Özkan, İ., 1992. "Characterization of Weak, Stratified and Clay-Bearing Rock Masses", EUROCK'92 - Int. Symp. on Rock Characterization, Chester, UK, September, pp. 330-335.

Ünal, E., Özkan, İ. and Ergür, K.M., 1994. Türkiye Madencilik Endüstrisinde İleri Teknoloji Uygulamaları - Bölüm I: Kaya Saplamaları ile Tahkimat Teknolojisinin Geliştirilmesi, Final Report, Project No: TÜBİTAK MAG-987/YBAG-0028, 226p.

Venkateswarlu, V., 1986. "Geomechanics Classification of Coal Measure Rocks vis - a- vis Roof Support", Ph.D. Thesis, Indian School of Mines, Dhanbad, 251p.

Venkateswarlu, V., Ghose, A.K. and Raju, N.M., 1989. "Rock-Mass Classification for Design of Roof Supports - A Statistical Evaluation of Parameters", Mining Science and Technology, Vol. 8, pp. 97-107.

Wells, B.T., and Singh, R.N., 1985. "Statistical Interpretation of Gate Roadways Deformation Data in the UK", Int. J. of Mining Engineering, Vol. 3, pp. 261-270.

Whittaker, B.N., Hassani, F.P. and White, M.J., 1983. "Instrumentation for Stability Evaluation of Coal Mine Tunnels and Excavation", Proc. of the Int. Symp. on Field Measurements in Geomech., Vol. 2, pp. 1257-1266.

Wickham, G.E., Tiedemann, H.R. and Skinner, E.H., 1972. "Support Determination based on Geologic Predictions", Proc. Rapid Excav. Tunnelling Conf., AIME, New York, pp. 43-64.

Williamson, D.A., 1984. "Unified Rock Classification System", Bull. Assoc. Engr. Geol., Vol. 2, No. 3, pp. 345-354.

Wilson, A.H., 1980. "A Method of Estimating the Closure and Strength of Lining Required in Drivages Surrounded by a Yield Zone", Int. J. Rock Mech. Min. Sci. and Geomech. Abstr., Vol. 17, pp. 349-355.

APPENDIX A

RECENT DEVELOPMENTS ON ROCK MASS CLASSIFICATION SYSTEMS AND MINE ROOF BEHAVIOR

A.1 General

In this Section, a literature review on rock mass classification systems and mine roof behavior were presented in detail.

A.2 Rock Mass Classification Systems

The design engineer and engineering geologist are confronted with rock as an assemblage of blocks of rock material separated by various types of discontinuities, such as joints, faults, bedding planes, and so on. This assemblage constitutes a rock mass. They must therefore consider the characteristics of both the intact material and the discontinuities.

The question immediately arises as to how the rock material is related to the rock mass. In answering this question, first of all, the importance of the properties of intact material will be generally overshadowed by the properties of the discontinuities in the rock masses. However, this does not mean that the properties of the intact rock material should be disregarded when considering the behavior of jointed rock masses. After all, if discontinuities are widely spaced or if the intact rock

is weak and altered, the properties of the intact rock may strongly influence the gross behavior of the rock mass. Furthermore, a sample of a rock material sometimes represents a small-scale model of the rock mass, since they both have gone through the same geological cycle. Nevertheless, in general, the properties of the discontinuities are of greater importance than the properties of the intact rock material.

An important issue in rock classifications is the selection of the parameters of greatest significance. There appears to be no single parameter or index that can fully and quantitatively describe a jointed rock mass for engineering purposes. Various parameters have different significance, and only if taken together can they describe a rock mass satisfactorily (Bieniawski, 1989).

In the case of surface excavations and those near-surface underground rock excavations that are controlled by the structural geological features, the following classification parameters are important: strength of intact rock material, spacing of discontinuities, condition of discontinuities, orientation of discontinuities, and groundwater conditions. In the case of deep underground excavations where the behavior of rock masses is stress-controlled, knowledge of the virgin stress field or the changes in stress can be of greater significance than the geological parameters.

Consequently, if certain conditions are fulfilled, rock mass classification can effectively combine the findings from observation, experience, and engineering judgment to provide information for a quantitative assessment of rock mass conditions, prediction of roof behavior and determining support requirements.

Rock masses are classified for the following purposes (Bieniawski, 1993):

1. to identify the most significant parameters influencing the behavior of rock mass;
2. to divide a particular rock mass unit into a number of rock mass classes of varying quality;
3. to provide a basis for understanding the characteristics of each rock mass class;
4. to derive quantitative data for engineering design;
5. to recommend support guidelines for tunnels and mines;
6. to provide a common basis for communication between engineers and geologists; and
7. to relate the experience on rock conditions at one site to the conditions and experience encountered at others.

The above items suggest three main benefits of rock mass classifications:

1. improving the quality of site investigations by calling for the minimum input data as classification parameters;
2. providing quantitative information for design purposes; and
3. enabling better engineering judgment and more effective communication on a project.

A.2.1 Basic and Commonly Used Rock Mass Classification Systems

Many rock mass classification systems have been developed by a number of researchers in various countries. However, six of these classification systems should be mentioned, because they are most commonly and widely used in the past, namely, those proposed by Terzaghi (1946), Lauffer (1958), Deere et al. (1967), Wickham et al. (1972), Bieniawski (1973) and Barton et al. (1974).

The rock load classification of Terzaghi, in 1946, was the first practical classification system introduced and has been dominant in the USA for many years, proving many successful for tunneling with steel supports (Terzaghi, 1946). Lauffer's classification (1958) was a considerable step forward in the art of tunneling in 1958 since it introduced the concept of the stand-up time of an unsupported span in a tunnel, which is highly relevant in determining the type and amount of tunnel support (Lauffer, 1958). Deere's classification of 1967 introduced the rock quality designation (RQD) index - a simple and practical method of describing and classifying the quality of rock core recovered from boreholes (Deere et al., 1967). The concept of rock structure rating (RSR) was the first system featuring classification ratings for weighing the relative importance of classification parameters (Wickham et al., 1972). The RMR system was proposed by Bieniawski (1973), and the Q system by Barton et al. (1974). All of the last three systems include different parameter ratings and provide quantitative data for the selection of modern tunnel reinforcement measures such as rock bolts and shotcrete. The original classification systems are listed in Table 2.1.

A.2.2 Contributions to the Original Rock Mass Classification Systems

The original rock mass classification systems presented in Table A.1 have found wide applications in various types of engineering projects. Most of the applications have been in the field of tunneling. The RMR and Q systems have also been used widely in mine applications. After and/or during these applications, new contributions to the original rock mass classification systems were made. These contributions are summarized in the following sections.

Table A.1 Major engineering Rock Mass Classifications currently in use (after Bieniawski, 1989).

Name of Classification	*Originator and Date*	*Country of Origin*	*Applications*
Rock loads	Terzaghi, 1946	USA	Tunnels with steel support
Stand-up time	Lauffer, 1958	Austria	Tunneling
NATM	Pacher, Rabcewicz and Müller, 1964	Austria	Tunneling
Rock quality designation	Deere et al., 1967	USA	Core logging, tunneling
RSR concept	Wickham et al., 1972	USA	Tunneling
RMR system (Geomechanics Classification)	Bieniawski, 1973 (last modified, 1979, USA)	South Africa	Tunnels, mines, slopes, foundations
Q system	Barton et al., 1974	Norway	Tunnels, chambers, mines
Strength-Size	Franklin, 1975	Canada	Tunneling
Basic geotechnical description	International Society for Rock Mechanics, 1981		General, communication

Contributions to Rock Quality Designation

The RQD calculations are based on the actual drilling-run length used in the field, preferably no greater than 1.5 m. The core length is measured along the centerline (see Figure A.1). The optional core diameters are the NX size (54 mm) and

NQ size (47.5 mm), but sizes between BQ and PQ with core diameters of 36.5 mm and 85 mm may be used provided careful drilling that does not cause core breakage by itself is utilized.

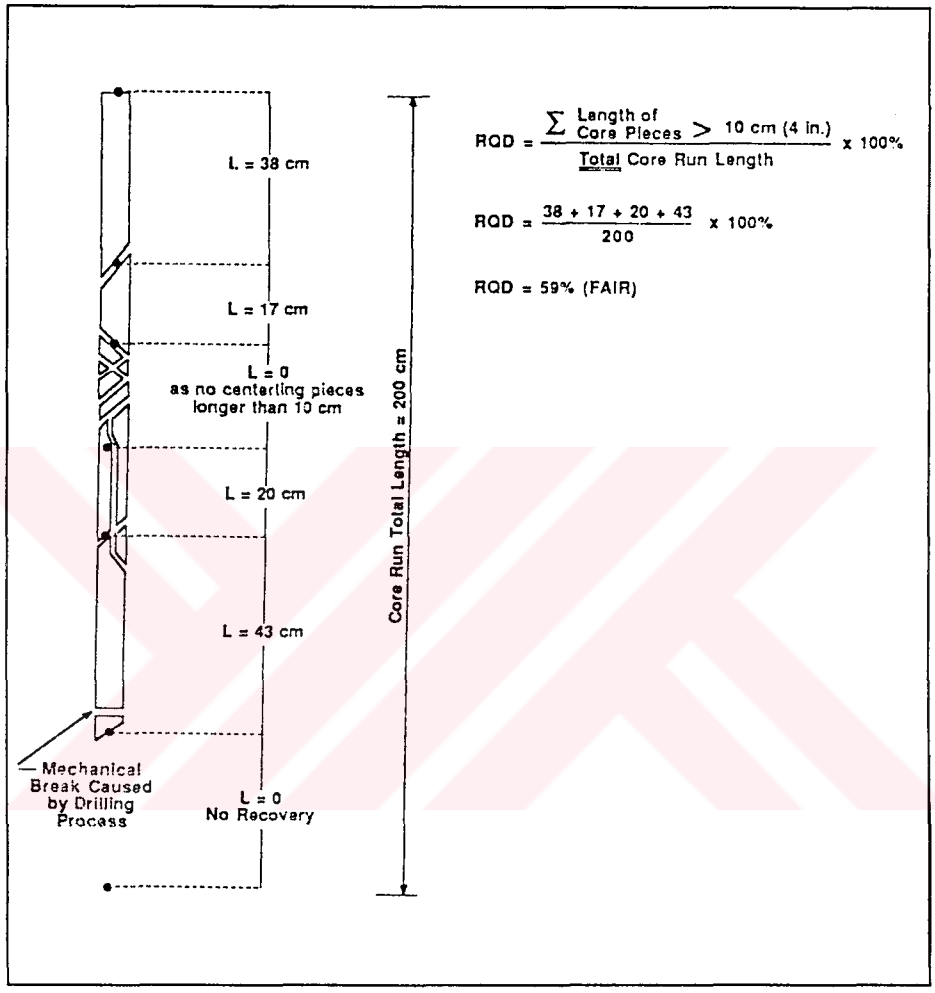

Figure A.1 Procedure for measurement and calculation of rock quality designation (after Deere, 1989)

Cording and Deere (1972) attempted to relate the RQD index to Terzaghi's rock load factors and presented tables relating tunnel support and RQD. They found that Terzaghi's rock load concept should be limited to tunnels supported by steel sets, as it does not apply well to openings supported by rock bolts.

Merritt (1972) found that the RQD could be of considerable value in estimating rock support requirements for rock tunnels. He compared the support criteria based on his improved version, as a function of tunnel width and RQD with those proposed by others. Merritt's (1972) suggestions were compiled by Deere and Deere (1988).

Priest and Hudson (1976) established a relation between the Rock Quality Designation (RQD) and mean discontinuity frequency per meter (λ). The equation proposed indicates a negative exponential distribution and theoretical RQD* can be calculated as follows:

$$RQD^* = 100 \cdot e^{-0.1\lambda} \cdot (0.1\lambda + 1) \qquad \text{(A.1)}$$

Palmstrom (1982) has suggested that when core is unavailable the *RQD* may be estimated from the number of joints (discontinuities) per unit volume, in which the number of joints per meter for each joint set is added. The conversion for clay-free rock masses is

$$RQD = 115 - 3.3 \cdot J_v \qquad \text{(A.2)}$$

where, J_v is the total number of joints per cubic meter.

These methods given for RQD calculation are based on establishing the statistical relationship between the RQD and mean discontinuity spacing or fracture frequency, measured along a line through a rock mass. The new equation for Volumetric RQD (V. RQD) based on matrix rock blocks was suggested by Kazi and Şen (1985).

$$V \cdot RQD = 100 \cdot e^{-0.001 \cdot n_b} \cdot (0.001 \cdot n_b + 1) \qquad \text{(A.3)}$$

where n_b is frequency of matrix blocks per m^3. A matrix block depends on volumetric fracture frequency per cubic meter.

Another equation for broken core zones and core loss was established by Şen (1990). Cumulative Core Index (CCI) is included into Priest and Hudson's equation (Equation A.1).

$$E(CCI) = 100 - 100 \cdot c \cdot e^{-0.1\lambda} \cdot (1 + 0.1\lambda) + 100 \cdot \lambda \cdot f \qquad \text{(A.4)}$$

where,

c : core loss factor, in the range of 0 and 1

λ : mean discontinuity frequency per meter

f : weakness weighing factor

The measured and theoretical RQD values examined by Priest and Hudson (1976) (Equation A.1) were further evaluated by Farmer (1983). According to Farmer, at high RQD values the correlation is good but at low RQD, the theoretical RQD values tend to be unrealistically high. The reason for this is that, at low values the condition of the rock and the width of discontinuity opening have a significant effect on measures of RQD.

Lee and Chen (1989) have suggested that when the discontinuity spacings have regular intervals, S, the modulus of elasticity of rock mass can be expressed as

$$E_m = \frac{1}{\left(\frac{1}{E_r} + \frac{1}{S \cdot K_n}\right)} \qquad \text{(A.5)}$$

where

E_r : modulus of intact rock, in MPa

K_n : normal stiffness of the discontinuity, in MPa/m

S : discontinuity spacing (assume $S = 1/\lambda$; λ is the mean discontinuity frequency per meter)

Nevertheless, the correlation of the RQD with the in-situ modulus of deformation has not been used much in recent years (Deere and Deere, 1988).

The maximum roof span of a longwall or depillaring panel at the time of nether roof collapse was shown to have a direct relation with RQD by Sheorey (1984). The variation of the equivalent face advance or ultimate stable span Q_{eq} with RQD was suggested by Sheorey as following equation:

$$Q_{eq} = 0.59 \cdot RQD + 5.2 \quad \text{(m)} \qquad \text{(A.6)}$$

According to Sheorey (1984), Equation A.6 is applicable to longwall panels employing conventional supports and to those depillaring panels where the coal left as remnants is not more than 20 %. With powered supports, the rate of advance is high and time effects may tend to increase the span. It may not be applicable to wet roofs and to those strata which have slickensided or clay-filled joints and distinct joint sets (not random joints) beside bedding planes.

Today, the RQD is used as a standard parameter in drill core logging and forms a basic element of the two major rock mass classification systems: the RMR and Q systems.

Contributions to Geomechanics Classification System - RMR

Rock mass rating (RMR) system, otherwise known as the Geomechanics Classification was modified over the years as more case histories became available and to conform with international standards and procedures. Over the past 20 years, the RMR system has stood the test of time and benefited from extensions and applications by many authors throughout the world. These varied applications amounting to 351 case histories (Bieniawski, 1989), involved tunnels, chambers, mines, slopes and foundations. Nevertheless, it is important that the RMR system is used for the purpose for which it was developed, and not as a "cookbook" for empirical design (Bieniawski, 1993).

Significant contributions to hard rock mining, coal mining, rippability, dam foundation, tunneling and slope stability were made by various researchers in different countries.

Bieniawski's Basic RMR value was last modified based on Laubscher's (1977) studies. Laubscher suggested adjustment on basic RMR index regarding blasting, in-situ stresses, and major faults and fracture as shown in Figure A.2.

According to Bieniawski (1989), if infilling is present in a joint, rating of joint condition may not be determined due to the influence of the gouge. That is why guidelines for classification of discontinuity conditions given in Table A.2 should be used.

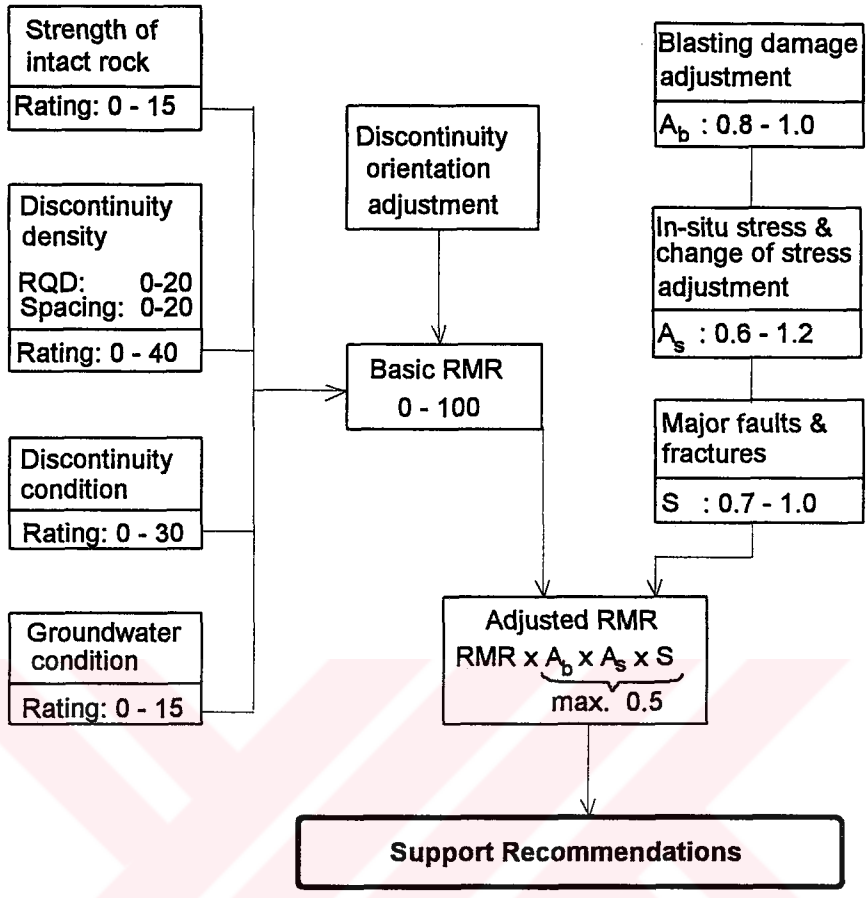

Figure A.2 Adjustments to the Rock Mass Rating System for mining applications (after Bieniawski, 1979)

The output of the RMR System, namely the stand-up time versus roof span plots in relation to the RMR assessment based on case history data by Bieniawski (1984) is given in Figure A.3. Lauffer (1988) presented a revised stand-up time diagram specially for tunnel boring machine (TBM) excavation as shown in Figure A.4.

Table A.2 Guidelines for classification of discontinuity conditions (after Bieniawski, 1989)

Parameter	Ratings				
Discontinuity length	<1 m	1 - 3 m	3 - 10 m	10 - 20 m	>20 m
(persistence / continuity)	6	4	2	1	0
Separation (aperture)	None	<0.1 mm	0.1 - 1.0 mm	1 - 5 mm	>5 mm
	6	5	4	1	0
Roughness	Very rough	Rough	Slightly rough	Smooth	Slickensided
	6	5	3	1	0
			Hard filling	Soft filling	
Infilling (gouge)	None	<5 mm	>5 mm	<5 mm	>5 mm
	6	4	2	2	0
Weathering	Unweathered	Slightly weathered	Moderately weathered	Highly weathered	Decomposed
	6	5	3	1	0

Support load can be determined using Equation A.7a proposed by Ünal and Ergür (1990). This equation is a modified form of the original Equation A.7b sugggested by Ünal (1983, 1986a), and Ünal and Ergür (1990).

$$P = S \cdot \left(\frac{100 - RMR}{100} \right) \cdot \gamma \cdot B = \gamma \cdot h_t \qquad \text{(A.7a)}$$

$$P = \left(\frac{100 - RMR}{100} \right) \cdot \gamma \cdot B = \gamma \cdot h_t \qquad \text{(A.7b)}$$

where,

P : support load, kN

B : tunnel width, m

γ : rock density, kN/m³

h_t : rock load height, m

S : stress constant

This equation has been cross referenced and/or used by various authors.

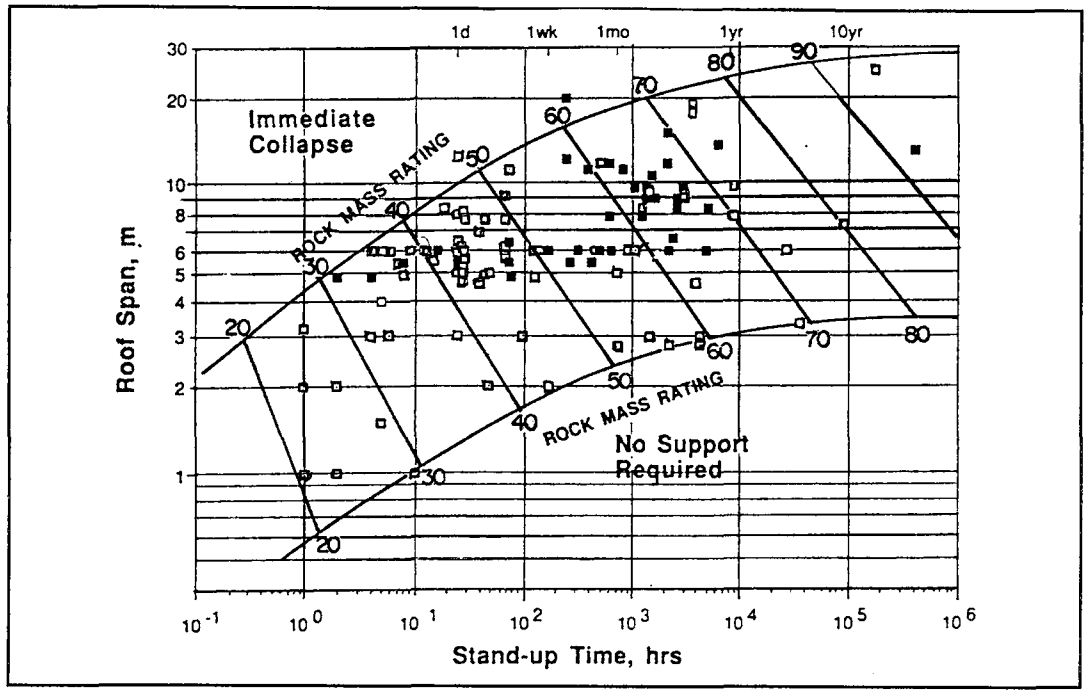

Figure A.3 Relationship between the stand-up time and span for various rock mass classes, according to the Geomechanics Classification (after Bieniawski, 1989).

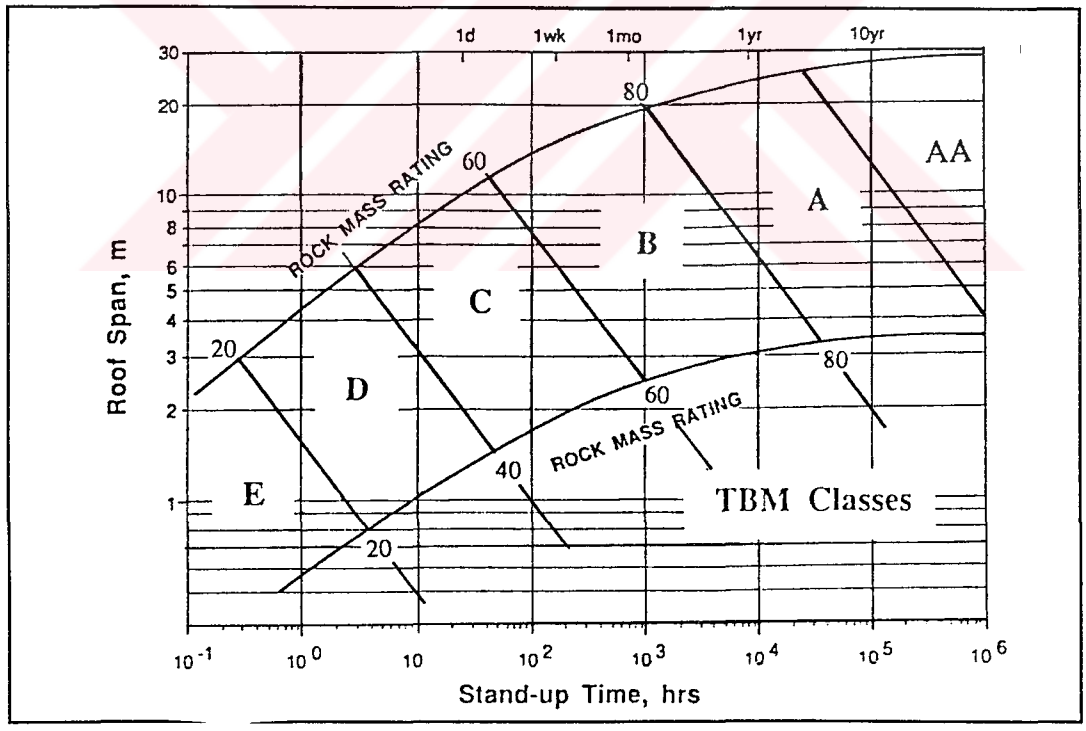

Figure A.4 Modified 1988 Lauffer diagram depicting boundaries of rock mass classes for TBM applications (after Lauffer, 1988).

The variation of rock pressure, P, as a function of roof span for different RMR values is illustrated in Figure A.5.

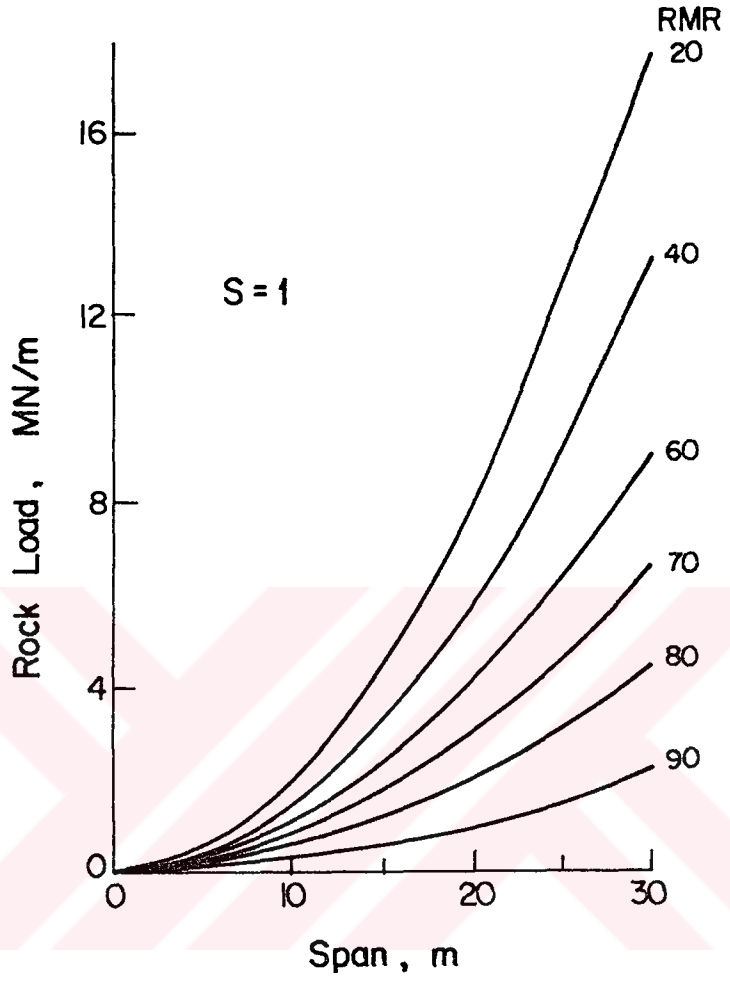

Figure A.5 Rock load related to roof span for various RMR values (after Ünal, 1983)

The Geomechanics Classification proved to be a useful method for estimating approximate value of the in-situ deformability of rock masses. The following correlation was suggested by Bieniawski (1978).

$$E_m = 2 \cdot RMR - 100 \qquad \text{(A.8)}$$

where, E_m is the in-situ modulus of deformation in GPa and $RMR > 50$. More recently, Serafim and Pereira (1983) provided many results in the range $RMR < 50$ and proposed a new correlation:

$$E_m = 10^{\left(\frac{RMR-10}{40}\right)} \tag{A.9}$$

The correlation between the in situ modulus of deformation and RMR suggested by Bieniawski, and Serafim and Pereira is presented in Figure A.6.

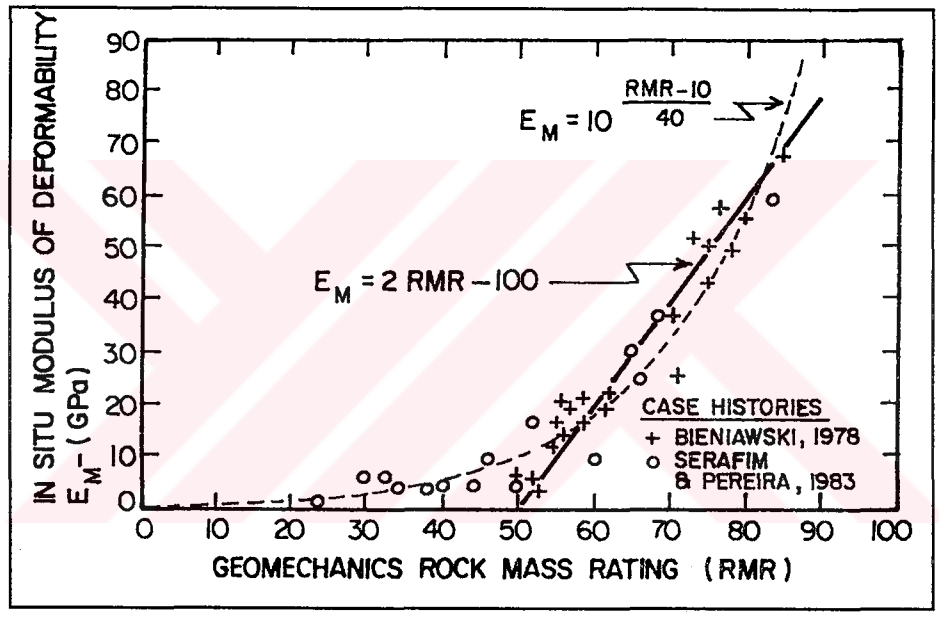

Figure A.6 Correlation between the in-situ modulus of deformation and RMR (after Serafim and Pereira, 1983; Bieniawski, 1978)

According to Nicholson and Bieniawski (1990), a rock mass deformation modulus comparable to the scale of a plate bearing test may be expressed as

$$E'_d = E_{dc} \cdot (RF) \tag{A.10}$$

where,

E_{dc} : modulus determined from unconfined compression test on intact specimens ($E_{dc} = \sigma_c / \varepsilon_{1c}$)

RF : a reduction factor comparable to a plate bearing test scale in per cent.

It is also assumed that RF has the same general distribution with respect to RMR for the case of zero minor principal stress (an assumption used to calculate modulus values from plate load tests) as suggested by Serafim and Pereira (1983).

The RMR data in Serafim and Pereira's correlation (including Bieniawski's 1978 data) ranged from approximately 25 to 85. The correlation line best fitting the range in data expressed the deformation modulus (GPa) as an inverse log function of RMR (Figure A.7). Extension of the correlation beyond the range of supporting data requires considerable speculation. Recognizing the approximate nature of the RF distribution assumption (due to the range in available data and assumptions involved) and the need to express the RF as a percentage (0 to 100 %) the following approximate expression is suggested.

$$RF = 0.0028 \cdot (RMR)^2 + 0.9 \cdot e^{\left(\frac{RMR}{22.82}\right)} \qquad \text{(A.11)}$$

This reduction factor, as shown in Figure A.7, varies from 100 % for (RMR)=100 to 0.9 % for (RMR)=0.0.

Also a new empirical relation has been established to estimate the in-situ modulus of deformation (Nieble et al., 1993).

$$E_m = E_i \cdot \left[(RMR - 8) \cdot 10^{-2} \right]^2 \qquad \text{(A.12)}$$

where, E_i is modulus of deformation for intact rock and E_i is equal to $K \cdot \sigma_{ci}$. K is a parameter based on softer or harder rocks and σ_{ci} is the uniaxial compressive strength of the intact rock.

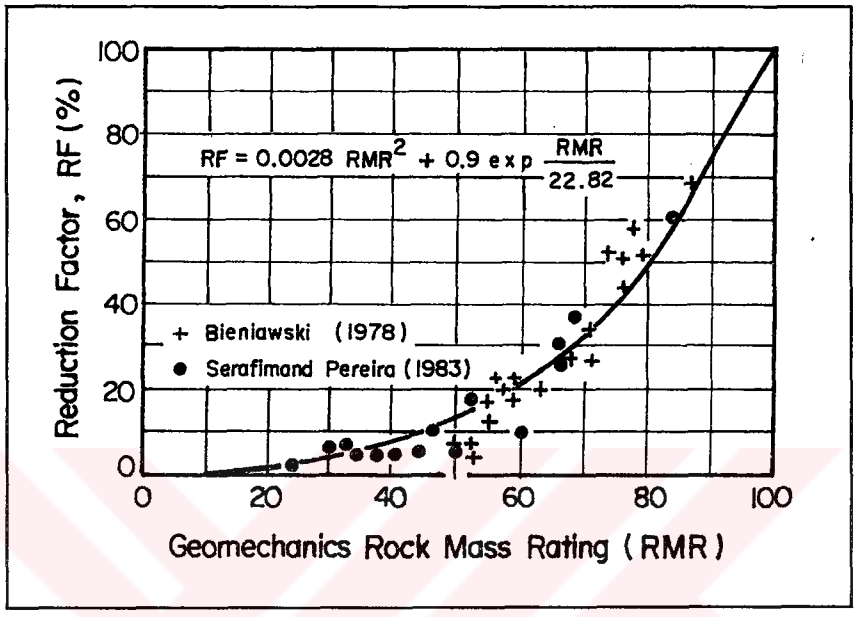

Figure A.7 Reduction factor against RMR (after Nicholson and Bieniawski, 1990)

15 years ago, Hoek and Brown (1980) proposed a method for estimating rock mass strength which makes use of the RMR classification. The criterion for rock mass strength is as follows:

$$\frac{\sigma_1}{\sigma_c} = \frac{\sigma_3}{\sigma_c} + \sqrt{m \cdot \frac{\sigma_3}{\sigma_c} + s} \qquad \text{(A.13)}$$

where

σ_1 : the major principal stress at failure,

σ_3 : the applied minor principal stress,

σ_c : the uniaxial compressive strength of the rock material,

m and s : constants dependent on the properties of the rock and the extent to which it has been fractured by being subjected to σ_1 and σ_3.

For intact rock, $m = m_i$, which is determined from a fit of the above equation to triaxial test data from laboratory specimens, taking s = 1 for rock material. For rock masses, the constants m and s are related to the basic (unadjusted) RMR as follows (Hoek and Brown, 1988):

For Undisturbed Rock Masses (smooth-blasted or machine-bored excavations):

$$m = m_i \cdot e^{\left(\frac{RMR-100}{28}\right)} \tag{A.14}$$

$$s = e^{\left(\frac{RMR-100}{9}\right)} \tag{A.15}$$

For Disturbed Rock Masses (slopes or blast-damaged excavations):

$$m = m_i \cdot e^{\left(\frac{RMR-100}{14}\right)} \tag{A.16}$$

$$s = e^{\left(\frac{RMR-100}{6}\right)} \tag{A.17}$$

Sheorey (1985) suggested that Bieniawski's (1979) suggestions about friction angle values of rock mass, for peak friction angle can be used. Also, the results of the direct shear test and the results obtained from RMR and Q-systems were compared by Özkan (1989). According to Özkan, internal friction angle values predicted from Bieniawski's RMR suggestions were comparable with the peak friction angle results obtained from direct shear tests.

Contributions to Q System

The new contributions to the original Q-system are summarized below:

According to Sheorey (1984), Barton's equivalent dimension equation (1974) could be rewritten to estimate roof caving span in oblong workings as given in Equation A.18:

$$a = \frac{2 \cdot ESR \cdot Q^{0.40}}{\alpha(b/a)} \qquad \text{(A.18a)}$$

where, α is a function of b/a, b is face length (m) and a is face advance (m) in oblong workings. The simple nomogram presented in Figure A.8 can be used to predict the face advance required to cause roof collapse as given by Sheorey (1984). The safe unsupported span is a_{eq} which can be calculated by

$$a_{eq} = 2 \cdot ESR \cdot Q^{0.4} \qquad \text{(A.18b)}$$

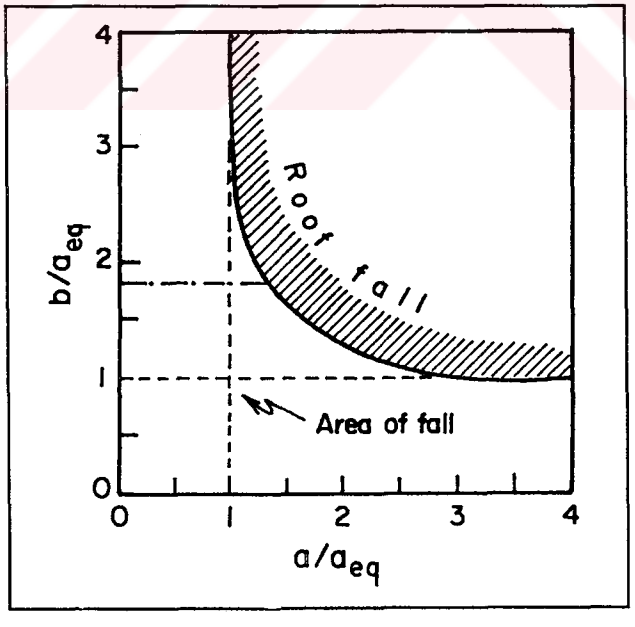

Figure A.8 Nomogram for estimation of roof collapse (after Sheorey, 1984)

Sheorey (1985) carried out analysis on the results of seven case studies in India. He found that support pressure (P - kg/cm^2) proposed by Barton et al (1974) for ultimate roof support pressure does not agree with practical observations if the values of the stress reduction factor (SRF) recommended by Barton et al. (1974) are used in calculating the rock quality index Q. The modified values of SRF, given in Table A.3, were suggested in order to obtain a good agreement between the calculated and observed values. This modification in SRF considers the rock mass rating RMR and the cover pressure to account for the effects of depth and broken zone size on support pressure.

Table A.3 Recommended values of stress reduction factor (SRF) for squeezing rock conditions (after Sheorey, 1985)

RMR x cover pressure p_0 (in MPa)	Recommended SRF
<150	1 - 2
150 - 200	2 - 4
200 - 250	2.5 - 5
250 - 300	3.5 - 6.5
300 - 350	4 - 8
350 - 400	5 - 10
400 - 450	7 - 12
450 - 500	9 - 17
500 - 550	13 - 22
550 - 600	18 - 28

The prerequisite of the semi-analytical method is that the radius of the broken zone must be known from in-situ observations. If such a measurement is carried out with buckling supports, the radius obtained will be larger and the ultimate support pressure calculated will be in error. No such measurement is required while using Barton's support pressure equation with the recommended SRF values and

therefore this becomes a simple formula giving reasonable estimates of the ultimate support pressure.

According to Sheorey (1985), the semi-analytical method proposed for stress analysis in the broken rock annulus also gives reasonable support pressure values. The method shows that Bieniawski's and Barton's rock classifications provide good estimates of the peak and residual angles of internal friction respectively.

Different correlations between the RMR and Q index values were proposed by various authors (Bieniawski, 1976; Jethwa et al., 1982). This general relationship between the RMR and Q-system is shown in Figure A.9.

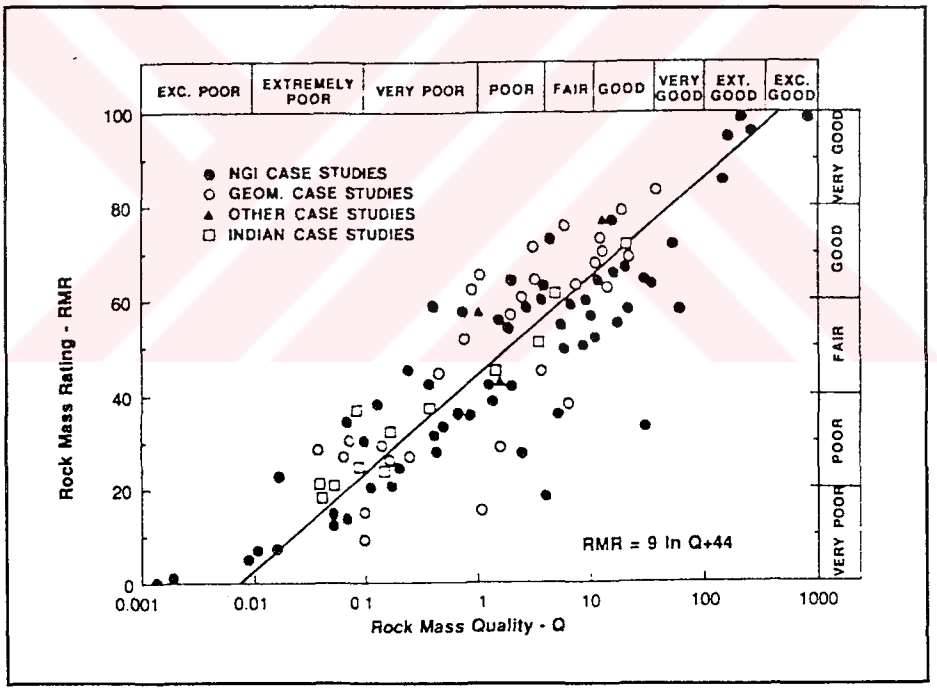

Figure A.9 Correlation between the RMR and the Q-index (after Bieniawski, 1976 and Jethwa et al., 1982)

A.2.3 Modified and Adapted Rock Mass Classification Systems

Although original rock mass classification systems, mentioned in Section A.2.1, have been widely used, they can not always adequately define the complex ground conditions and constitute a base for design approaches. Therefore, geotechnical engineers confront various working and design problems that are not addressed in existing classification systems, and then arises the need to adopt them for changes in original parameters by modifying already existing parameters or by equipping the system with new classification parameters. The modified and adopted classification systems are listed in Table A.4.

Mining Rock Mass Rating System - MRMR

Laubscher (1977, 1984, 1990, 1993) modified the Geomechanics Classification developed by Bieniawski (1976, 1979) for mining applications involving asbestos mines in southern Africa. The fundamental difference was the recognition that in situ Rock Mass Ratings (RMR) had to be adjusted according to the mining environment, so that the final ratings (MRMR), which is called Mining Rock Mass Rating, could be used for mine design. The system has been successfully used in mining projects in Canada, Chile, China, the Philippines, Sri Lanka, South Africa, the USA and Zimbabwe.

In order to decide how the rock mass will behave in a mining environment, the rock mass ratings index (RMR) is adjusted for weathering, mining induced stresses, joint orientation and blasting (Laubscher, 1977, 1984), and a new rating (FF) for RQD and joint spacing (JS) rating was suggested by Laubscher (1990, 1993).

Table A.4 Modified and adopted engineering Rock Mass Classification Systems

Name of Classification	**Originator and Date**	**Country of Origin**	**Applications**
MRMR	Laubscher, 1977	South Africa	Mining
MBR	Cummings et al., 1982	USA	Hard rock mining
RMS	Stille et al., 1982	Sweden	Metal mining
Simplified RMR	Brook and Dharmaratne, 1985	Sri Lanka	Mining
Modified RMR	Newman and Bieniawski, 1985	USA	Coal mining
R	Venkateswarlu, 1986	India	Coal mining
BRZ	Dong et al., 1988	China	Coal mining
RTR	Inyang, 1991	USA	Tunneling, mining, slopes, chambers
SGDM	Milne and Potvin, 1992	Canada	Mining
GC	Mendes et al., 1993	Portugal	Coal mining
CMRR	Molinda and Mark, 1993	USA	Coal mining
Modified RMR	Sheorey, 1993	India	Coal mining
Modified Q	Sheorey, 1993	India	Coal mining
RFI	Singh et al., 1994	India	Coal mining
M-RMR	Ünal and Özkan, 1990	Turkey	Metal and coal mining

The following parameters were suggested to be used in classifying the rock mass, using the in-situ RMR system.

i) Intact rock strength - IRS

ii) Fracture frequency - FF (for RQD plus JS)

iii) Joint condition and water

The in-situ rock mass rating (RMR) is the sum of the individual ratings. The in-situ RMR has to be multiplied by an adjustment percentage to give the MRMR index. The adjustment percentages are empirical, having been based on numerous observations in the field (Laubscher, 1993). The following input parameters require adjustment for the MRMR system:

i) Weathering

ii) Joint Orientation

iii) Mining-Induced Stresses

iv) Blasting Effects

The rock mass strength (RMS) is derived from the IRS which is given in the below equation:

$$RMS = \frac{A-B}{80} \times C \times \frac{80}{100} \qquad \text{(A.19)}$$

where, B is the IRS rating, A is in-situ RMR, and C is IRS value (MPa).

According to Laubscher, the design rock mass strength (DRMS) is the unconfined rock mass strength in a specific mining environment. A mining operation exposes the rock surface and the concern is with the stability of the zone that surrounds the excavation. The extent of this zone depends on the size of the excavation and, except with mass failure, instability propagates from the rock surface.

The size of the rock block will generally define the first zone of instability. Adjustments, which relate to that mining environment, are applied to the RMS to give the DRMS. As the DRMS is in MPa it can be related to the mining-induced stresses, therefore, the adjustments used are weathering, orientation and blasting. The support guidelines for tunnels using MRMR System is also given by Laubscher (1990).

Modified Basic-RMR-System

Cummings et al. (1982) and Kendorski et al. (1983) also modified the Geomechanics Classification (Bieniawski, 1979) for mining applications in US block caving copper mines. The MBR (modified basic RMR) system uses the basic RMR approach of Bieniawski (1979) with some of the concepts of Laubscher (1977).

The basic input parameters of MBR system are the same of those of RMR system which are strength of intact rock, discontinuity density (RQD and joint spacing), discontinuity condition, and ground water condition.

The MBR system has six adjustment factors as listed below:

i) Blasting damage (A_B), ii) Induced stresses (A_S), iii) Fracture orientation (A_O), iv) Major structures (S), v) Distance to cave line (DC), vi) Block/panel size (PS)

For production drifts the MBR permanent support chart given in Figure A.10 is recommended by Cummings et al. (1982).

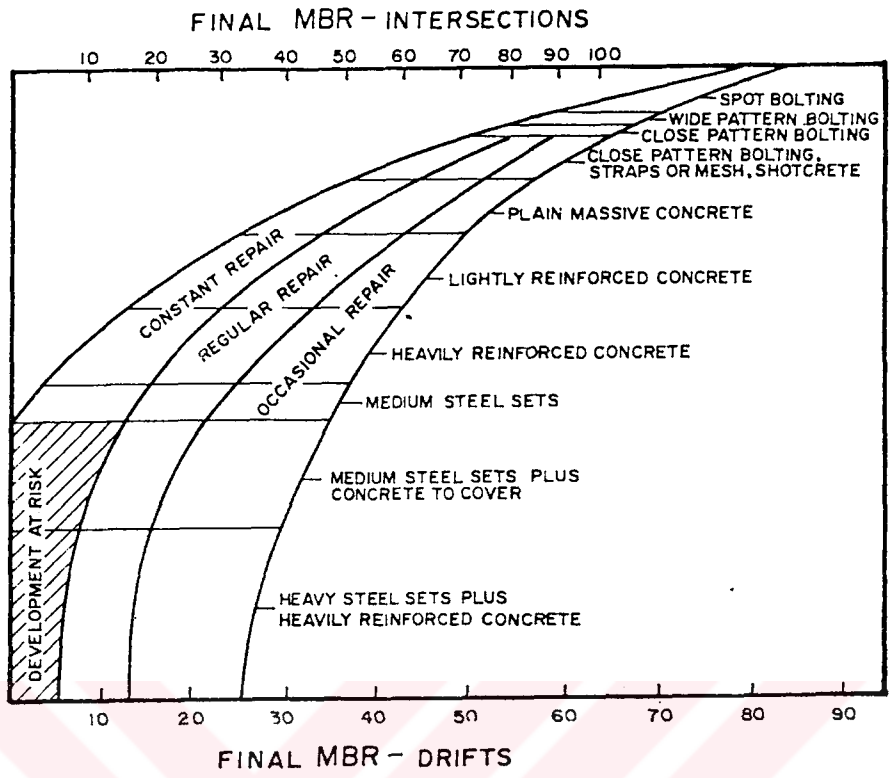

Explanation of the Support Types

Spot Bolting: *Bolting to restrain limited areas or individual blocks of loose rock, primarily for safety.*

Wide Pattern Bolting: *Bolts on spaced 1.2–1.8 m. May be wider in very large openings, when longer bolts are used.*

Close Pattern Bolting: *Bolts spaced less than 0.9–1.2 m (practical limit 0.6 m).*

Close Pattern Bolting, Mesh, or Straps, Shotcrete: *Close pattern bolts with welded mesh or chain link in raveling ground, and nominal 100 mm of shotcrete.*

Plain Massive Concrete: *Cast-in-place massive concrete lining, 0.3–0.45 m thick, may be applied over bolts or bolts and mesh when necessary. Prior shotcrete, if not damaged, may be considered part of this concrete thickness. Concrete should have a* minimum as-placed *28-d compressive strength of 21 MPa (3000 lb/in.^{2}.*

Lightly Reinforced Concrete: *Massive, cast-in-place concrete lining 0.3–0.45 m thick as above, lightly reinforced with rebars on 0.6-m centers or continuous heavy chain link. Reinforcement mainly in brows, crown, corners, and intersections.*

Heavily Reinforced Concrete: *Massive, cast-in-place concrete lining as above, heavily reinforced with rebars on 0.6-m centers or less, on ribs and crown.*

Medium Steel Sets: *Medium wide-flange steel sets on 1.2-m centers, fully lagged on the crown and ribs.*

Medium Steel Sets Plus Plain Concrete to Cover: *Medium wide-flange steel sets on 1.2-m centers, with plain, cast-in-place concrete (min strength 21 MPa) of sufficient thickness to cover the sets.*

Heavy Steel Sets Plus Heavily Reinforced Concrete: *Heavy wide-flange steel sets on 1.2-m centers, with minimum 0.3-m-thick heavily reinforced concrete throughout.*

General: *Concrete: it is assumed that proper concrete practice is observed: negligible aggregate segregation, full rock–concrete contact, adequate curing time.*

Chain link or steel sets, from development support, are considered reinforcement if the concrete between the sets is also reinforced.

Figure A.10 MBR permanent support chart for production drifts (after Cummings et al., 1982)

Rock Mass Strength - RMS

The classification system suggested by Stille et al. (1982) is a modification of the RMR System suggested by Bieniawski (1979). Stille et al. aims at determining rock mass strength (RMS); loading conditions and initial stress field are, therefore, not considered. The first five parameters, of the original RMR System, namely: strength, RQD, joint spacing, joint condition, and groundwater remain unchanged. Beyond that every combination of three different types of joint sets and two types of joints are rated according to Table A.5. From the sum of the ratings obtained from the table of original ratings (Bieniawski, 1979) and Table A.5 rock mass strength is determined according to Table A.6.

Table A.5 Rating of joint sets (after Stille et al., 1982)

Type of joint system/joint	1 or 2 joint systems			More than 2 joint systems
	Single distinct joint	Strength along joint direction	Others	
Pervasive	-15	-15	0	-15
Not pervasive	-5	-5	0	-10

Table A.6 Relationship between rating and rock mass strength (after Stille, 1982)

RMS-value		100-81	80-61	60-41	40-21	<20
σ_{cm}, MPa		30	12	5	2.5	0.5
Mohr – Coulomb Parameters	ϕ	55°	45°	35°	25°	15°
	c, MPa	4.7	2.5	1.3	0.8	0.2

Simplified Rock Mass Rating - Simplified RMR

The geotechnical parameters required for the assessment of support requirements have been discussed by Brook and Dharmaratne (1985). The support systems suggested by the three systems, namely RMR, Q and MRMR, were also compared by these authors.

The simplified system for derivation of the necessary input parameters is proposed, which has three major components - the intact rock strength, normally measured by point load testing; the joint spacing, obtained by scan line surveys; and the joint type, determined from the observed expression, separation and gouge condition. The omission of the usually recorded rock quality designation (RQD) value is shown to be justified and not to affect the final rating, expressed as a percentage, R, which is obtained by modification of the in-situ components with adjustment factors to allow for environmental considerations (Table A.7).

The in-situ rating as obtained above relates to a description of the rock mass with no consideration of other factors that may affect the stability and support requirements of an excavation. Environmental conditions that are not included in the classification may considered to affect the three major component rating percentages and can be allowed for by multiplying these percentages by suitable adjustment factors. The conditions that are considered sufficiently important to require such an adjustment are weathering, joint orientation and effects of stress and blasting. These do not all affect all the parameters. The adjustment procedure is detailed in Table A.8.

Table A.7 Simplified rock mass rating (after Brook and Dharmaratne, 1985)

Parameter	Maximum rating, %	In-situ values Quantity	Rating				
Intact rock strength IRS	30	Compressive strength, MPA, usually from point load test	30 % IRS 200,		(= 30 % (I_S (50)9)		
Joint spacing (JS)	30	Spacing relative to excavation size	> 0.3	0.3-0.1	0.1-0.03	0.03-0.01	< 0.01
		One point set	30 %	25-30 %	20-25 %	15-20 %	10-15 %
		Two joint sets	25-30 %	20-25 %	15-20 %	10-15 %	5-10 %
		Three joint sets	20-25 %	15-20 %	10-15 %	5-10 %	0-5 %
Joint type (JT)	30		Exact value interpolated if necessary. 30 % x Adjustment factor				
			Adjustment			Adjustment factor	
		Expression and continuity	Discontinuous			1.0	
			Wavy			0.75-1.0	
			Straight			0.5-0.75	
		Surface if in contact	Rough			1.0	
			Slightly rough			0.75-1.0	
			Smooth to polished			0.5-0.75	
		Separation	< 1 mm			0.9-1.0	
			2-1 mm			0.8-0.9	
			5-2 mm			0.7-0.8	
			10-5 mm			0.6-0.7	
			>10 mm			0.5-0.6	
		Gouge properties	Hard packed			1.0	
			Sheared			0.75-1.0	
			Soft, clay			0.5-0.75	
Groundwater (GW)	10		Dry	Most	Wet	Moderate pressure	High pressure
			10 %	8 %	5 %	2 %	0

Table A.8 Adjustment factors for in-situ rating components in simplified method (after Brook and Dharmaratne, 1985)

	IRS	JS	JT
Weathering			
Slight	0.9	-	0.9
Moderate	0.75	-	0.75
Slightly unfavorable	0.5	-	0.5
Orientation of excavation			
Slightly unfavorable	-	0.9	0.9
Moderately unfavorable	-	0.75	0.75
Highly unfavorable	-	0.5	0.5
In-situ or induced stress compared with IRS			
Causing slight failure	0.9	-	0.9
Moderate failure	0.75	-	0.75
General failure	0.5	-	0.5
Blasting			
Smooth	-	0.9	0.9
Moderately rough	-	0.75	0.75
Rough	-	0.5	0.5

IRS : Intact Rock Strength
JS : Joint Spacing
JT : Joint Type

The support types suggested by Brook and Dharmaratne (1985) can be summarized as follows: Rock masses with an adjusted rating in excess of 70 % will seldom require any support, and those in the range 50-70 % should require only occasional support at some joint intersections or other identifiable local trouble spots. A rock mass with a rating of 40-50 % will generally require some light, systematic support, but in the range 30-40 % systematic support will be necessary, with additional lagging or shotcreting to reduce the tendency of the rock mass to loosen.

The 20-30 % range will call for increased levels of systematic support and lagging, typically by the application of shotcrete reinforced by steel mesh or by closely set timber supports with complete lagging. Rock masses with an adjusted rating in the range 10-20 % usually require extensive support by steel support members and lagging, and it is possible that extensive repair work will be required as stress effects become more pronounced. If the adjusted rating is less than 10 %, it will generally be very difficult to maintain an adequate tunnel profile, but the possibility of increasing the effective rating by reducing the size of the excavation should be noted.

Modified Rock Mass Rating - Modified RMR

The Geomechanics classification (Bieniawski, 1979) was modified for roadway (entry) and roof support design in underground room-and-pillar coal mines (Newman and Bieniawski, 1985). Adjustment multipliers were introduced to incorporate the influence of strata weatherability, high horizontal stress, and the roof support reinforcement factor into the existing classification system.

The table of original rating (Bieniawski, 1979) was unchanged but the new calculation of final adjustment RMR was recommended by the following equation:

$$Modified\ RMR = \left[Slake\ Multiplier \times (\sigma_c + RQD + JS + JC) + GW - O\right] \times HS \times RF \quad \text{(A.20)}$$

where, Slake Multiplier, *HS* and *RF* are adjustment for weatherability, horizontal stress and roof support reinforcement, respectively. These adjustment values were also given in Figure A.11 through A.13.

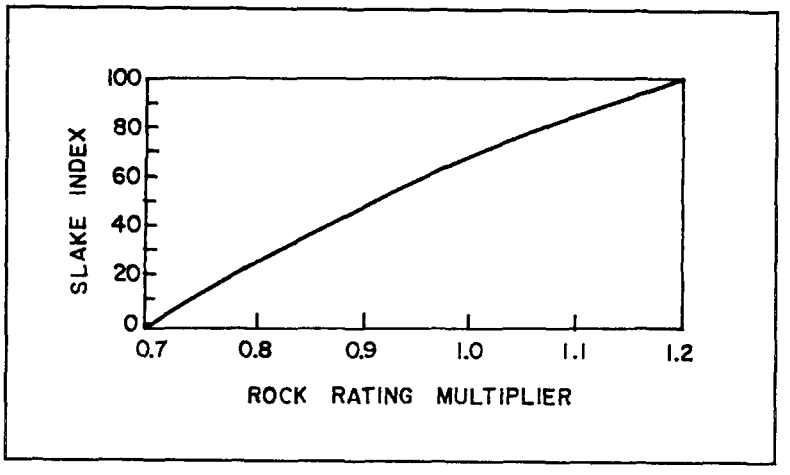

Figure A.11 Slake durability index versus rock rating multiplier (after Newman and Bieniawski, 1985)

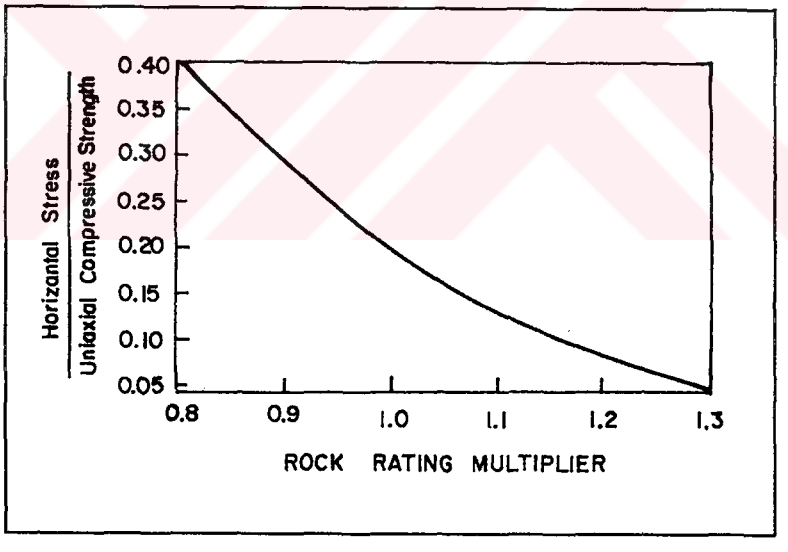

Figure A.12 Horizontal stress/weighted compressive strength versus rock rating multiplier (after Newman and Bieniawski, 1985)

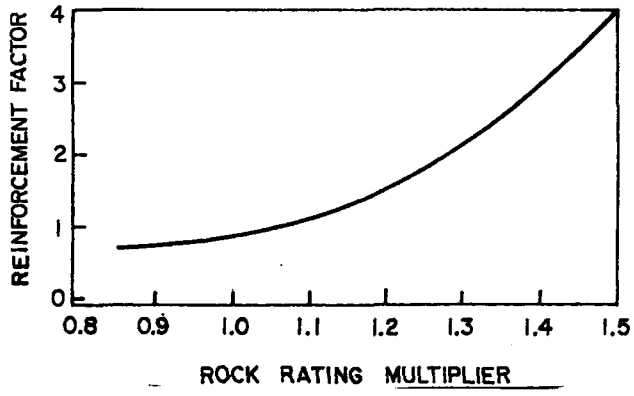

Figure A.13 Roof support reinforcement factor versus rock rating multiplier (after Newman and Bieniawski, 1985)

The New Geomechanics Classification Rating - R

Venkateswarlu (1986) of the Central Mining Research Station (CMRS) of India, modified the Geomechanics Classification (Bieniawski, 1979) for estimating roof conditions and determining the required support types for Indian coal mines.

The new geomechanics classification used in India is a simple and practical method of estimating roof condition in a mine. The five classification parameters and their importance ratings are given in Table A.9 (After Venkateswarlu et al., 1989).

The New Geomechanics Classification Rating is called the "R" by Ghosh and Ghose (1992).

The following empirical relation has been established to estimate the rock load (Venkateswarlu, 1986).

$$Rock\ Load = Roof\ Span \times Rock\ Density \times \left[1.7 - 0.037 \cdot R + 0.0002 \cdot R^2\right] \quad (A.21)$$

Table A.9 The new geomechanics classification ratings for parameter values (after Venkateswarlu et al., 1989)

Parameter		Range of values				
1) Layer thickness	(cm)	< 2.5	2.5-7.5	7.5-20	20-50	> 50
	Rating	0-5	6-12	13-19	20-25	26-30
2) Structural features	(Structural index)	> 14	14-11	11-7	7-4	4-0
	Rating	0-4	5-10	11-16	17-21	22-25
3) Weatherability (I_{sd-1})	(%)	< 60	60-85	85-97	97-99	> 99
	Rating	0-3	4-8	9-13	14-17	18-20
4) Strength of the rock	(kg/cm^2)	< 100	100-300	300-600	600-900	> 900
	Rating	0-2	3-6	7-10	11-13	14-15
5) Groundwater flow	(ml/min)	> 2000	2000-200	200-20	20-0	Dry
	Rating	0-1	2-4	5-7	8-9	10

Also, at the same Research Station in India, a new empirical relation has been presented by Ghosh and Ghose (1992) based on R.

$$Rock\ Load = 5 \times Roof\ Span^{0.3} \times Density \times [1 - R/100]^2 \qquad (A.22)$$

44 case studies obtained from coal mine roadways in India were evaluated by Sheorey (1991, 1993). As a result of his analysis, the performance of Rock Load equation (Venkateswarlu, 1986; Eq. A.21) developed based on R system was found perfectly fitting the in situ data. Nevertheless, Sheorey (1993) proposed an adjustment to R system for inclusion of stress factor as shown in Equation A.23.

$$R_{mod} = R(Without\ Strength\ Rating) - 20.7 \log SRF + Strength\ Index \qquad (A.23)$$

where *SRF* is stress reduction factor which is a parameter in Q-system (Barton et al., 1974) and *Strength Index* is obtained from R-System.

The Broken Rock Zone - BRZ

The virgin rock mass is in a state of static equilibrium attained after surviving many events in the long period of geologic past. The process of excavation within the rock mass disturbs the state of the equilibrium and a new set of forces are brought into existence. The magnitude of the radial stress decreases while the tangential stress increases at the circumference of the tunnels. While the stress concentration are developing, the rock mass moves towards the opening. The state of stress changes from triaxial into biaxial one in the vicinity of the tunnel. These reduce the strength of the rock mass. So, when the stresses exceed the strength of rock mass, failures occur, and the stresses redistribute again, and more fractures develop. Failures extend deep into the rock mass. When the stresses are equal to or smaller than the strength of the rock mass, they stop extending further and the stresses come into a new equilibrium state. The failed area surrounding the opening is called the BRZ (Dong et al., 1988) and the radial distance that failure extends into the rock mass is called the thickness of the BRZ.

The following regression equation has been suggested by Dong et al. (1988) to determine the thickness of the broken rock zone (L_p):

$$L_p = 2.22 \times B^{2.94} \times R_a^{-1.05} \times H^{4.30} \times 10^{-11} \qquad \text{(A.24)}$$

where, L_p (cm) is the thickness of the BRZ, B (m) is the width, R_a (MPa) is the compressive strength of rock, and H (m) is the depth.

The authors have also developed a new avenue for support guidelines based on the thickness of the BRZ, as shown in Table A.10.

Table A.10 The classification and support guidelines based on BRZ (after Dong et al., 1988)

BRZ (Lp-cm)	Classification	Support Guidelines
0 - 40	Small	Usually the thickness of the shotcrete is not more than 10 cm
40 - 150	Medium	Normally the bolts are 1.0 to 1.8 meters long and the shotcrete is less than 15 cm thick
> 150	Large	Bolt-shotcrete (if BRZ is more than 200 cm Bolt-shotcrete-wire mesh) or the three piece steel arches

Dong et al. (1988) have also developed the relationship presented in Equation A.25 to determined the maximum convergence (C_{max}) at the tunnel surface:

$$C_{max}/R_0 = 0.0121 \cdot \exp\left(1.53\, L_p/R_0\right) \qquad \text{(A.25)}$$

where, R_0 is the radius of circular tunnel, and L_p is the thickness of BRZ.

Rock Trenchability Classification - RTC

The laboratory tests on rocks are often conducted on small cores of reasonably intact material. Generally, rocks decrease in strength with increase in sample size because the probability of the presence of large strength controlling flaws increases with sample size. This is a plausible explanation for the disparity between laboratory and field specific energies often observed in rock excavation. Since the synergistic effects of discontinuity properties, scale of excavation and moisture condition can not be effectively evaluated using laboratory test results solely, it is

necessary to use judgment along with such results in rating rock masses. Such a rating may involve the formulation of a single numerical index which must account for the significant properties, weighted to incorporate their relative importance. In this report, a preliminary classification system was formulated by Inyang (1991) which is called the Rock Trenchability Classification (RTC). Consideration is given to rock material strength; rock brittleness; discontinuity spacing; orientations and linkage; and the scale of excavation. Results of decades of investigations by many workers on various aspects of rock mass strength are taken into consideration

To determine the Rock Trenchability Classification, RTC, of each in situ rock mass, the Rock Trenchability Rating, RTR, must first be determined. RTR is summation of the ratings for various rock mass parameters that are significant in mechanical trenching. Its magnitude approximates the ratio of the rock mass strength to intact rock strength. An intact rock has a RTR of 100. The presence of significant discontinuities and moisture reduces RTR to values less than 100. The general formulation and the parameters considered were given below and presented in Table A.11.

$$RTR = A_R + B_R + C_R + D_R + E_R \qquad \text{(A.26)}$$

where,

RTR :Rock trenchability rating

A_R :Rating for flaw spacing relative to trench depth

B_R :Rating for the number of discontinuity sets

C_R : Rating for the orientation of dominant discontinuities relative to cutter alignment

D_R :Rating for the degree of linkage of discontinuities

E_R :Rating for moisture condition

Table A.11 The rock trenchability rating (RTR) chart (after Inyang, 1991)

PARAMETER		CLASS AND RATING						
A	FLAW SPACING (> 1cm) TRENCH DEPTH	IA .8	IIA .8-.3	IIIA .3-.08	IVA .08-.05	VA .05-.03	VIA .03-.01	VIIA .01-.004
	Rating, A_R	100	40	30	25	16	12	7
B	NUMBER OF DISCONTINUITY SETS	IB one	IIB two	IIIB three	IVB random	VB one plus random	VIB two plus random	VIIB three plus random
	Rating, B_R	18	15	8	5	3	2	0
C	ORIENTATION OF THE MOST DOMINANT DISCONTINUITIES	Range of Dip Angles		IC	IIIC & VIIC	IIC & VIIIC	IVC & VIC	VC
		0° → 10°		25	25	25	25	25
		10° → 20°		23	22	23	22	20
		20° → 40°		21	17	19	16	15
		40° → 60°		20	17	18	12	10
	Rating, C_R	60° → 80°		19	20	17	18	17
		80° → 90°		18	21	16	20	18
D	DEGREE OF LINKAGE OF DISCONTINUITIES	ID isolated	IID continuous (one directions)		IIID continuous (two directions)	IVD continuous (one directions)		VD continuous (two directions)
	Rating, D_R	7	5		3	3		0
E	MOISTURE CONDITION	IE dry	IIE moist		IIIE very wet	IVE dripping		VE flowing
	Rating, E_R	0	-8		-12	-13		-15

$$y = RTR/100$$

y : Strength reduction coefficient = the factor by which the rock material strength can be multiplied to obtain the rock mass strength.

$$RTC = [yt_0][yR_0] = y^2 t_0 R_0 \qquad \text{(A.27)}$$

$$RTC = 0.0001(RTR)^2 t_0 R_0 \quad \text{(MPa)} \qquad \text{(A.28)}$$

RTR : Rock trenchability classification

t_0 : Intact rock tensile strength

R_0 : Brittleness index = t_0 / C_0

C_0 : Intact rock compressive strength

As indicated by Equation A.28, RTC comprises RTR (a measure of discontinuity, moisture and scale effects), intact rock strength and a brittleness index. Rock brittleness is very important in the action of tools on rock surfaces. It controls the ease with which cracks can propagate through rocks. Inyang and Pitt (1990) described a situation in which rock brittleness may have influenced drill bit penetration rates in hard but brittle rocks. A simple index of brittleness is R_0, the ratio of tensile to compressive strength of rock. The smaller the magnitude of R_0, the more brittle the rock.

The rock trenchability classification (RTC) scheme was given in Table A.12.

Table A.12 The rock trenchability classification (RTC) scheme (after Inyang, 1991)

$10^{-4}(RTR)^2 t_0 R_0$		QUALITATIVE	SUITABILITY
MPa	psi	DESCRIPTION OF ROCK	FOR TRENCHING
< 0.5	72.5	very weak rock	easily trenchable
0.5 - 1.0	72.5 - 145.0	fairly weak rock	fairly trenchable
1.1 - 1.5	145.0 - 217.5	moderately strong rock	moderately trenchable
1.6 - 2.0	217.5 - 290.0	fairly strong rock	barely trenchable
2.1 - 2.5	290.0 - 362.5	very strong rock	untrenchable
> 2.5	362.5	extremely strong rock	highly untrenchable

Stability Graph Design Method - SGDM

The estimation of the stability of a mining surface was developed by Mathews et al. (1980). This graphical design technique for estimating the stability of underground mining surface was modified by Potvin et al. (1988). In essence, this technique was based on the modified version of the Q system. The system differs from the standard NGI classification in that the stress reduction factor (SRF) is dropped. The rock quality index is therefore based on RQD, the number of joint sets and the roughness and alteration of joint surfaces. Little experience has been obtained with groundwater effects so the validity of the groundwater factor for this design technique cannot be assessed.

The stability graph design method takes into account most of the factors which are felt to influence of the stability of a mining surface. The x-axis of the graph (Figure A.14) is simply the shape factor or hydraulic radius of the surface analyzed. It is defined as the area of the surface divided by the perimeter. The y-axis of the graph consists of stability number N which is an assessment of the overall condition of the rock mass surface. The stability number is defined by the following equation:

$$N = Q' \times A \times B \times C \tag{A.29}$$

where,

Q' : modified NGI classification

A : stress factor $0.1 \leq A \leq 1.0$

B : joint orientation factor $0.2 \leq B \leq 1.0$

C : surface orientation factor $2 \leq C \leq 8$

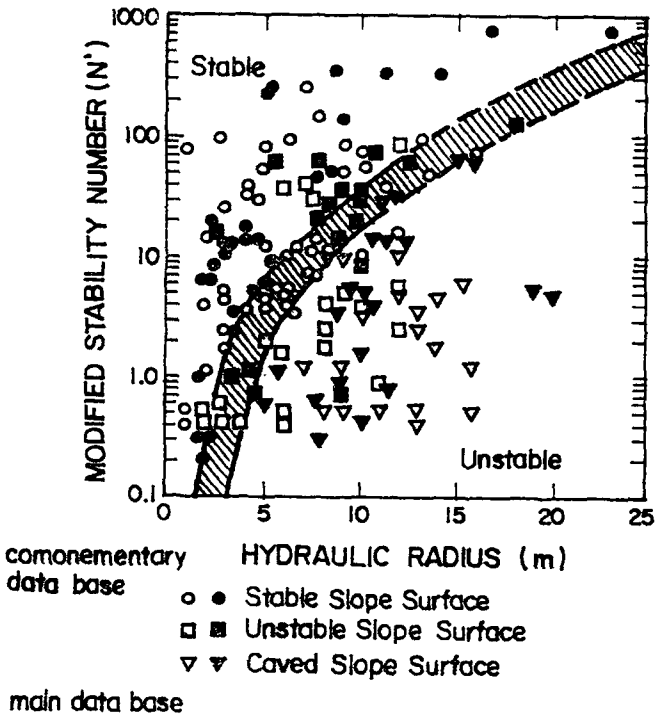

Figure A.14 Modified stability graph design technique showing the plotted case histories used to develop the system (after Potvin et al., 1988)

Geomechanical Classification - GC

The importance of discontinuities in the behavior of underground excavations justifies the increasing use of accurate methods for its characterization.

Geological discontinuities such as faults, joints, etc. control in a greater or lesser degree, the mechanical properties of rock masses, generally diminishing its strength and increasing its deformability. The properties of fractures that have more influence in the stability of excavations can be measured by using the scanline technique (Mendes et al., 1993).

The mean spacing of the dominant set of discontinuities allows us to distinguish the following situations presented in Tables A.13a, A.13b, A.13c and A.13d.

Table A.13 Descriptions for joint spacing, aperture, filling thickness and persistency (after Mendes et al., 1993)

a. Spacing	Description
< 20 cm	Crushed ground or small spacing
20 cm - 2 m	Moderate spacing
2 m - 10 m	Wide spacing
> 10 m	Very wide spacing

In the absence of filling material, the apertures were described according to the scheme below:

b. Aperture	Description
< 0.05 mm	Very tight
0.5 - 10 mm	Small aperture
> 10 mm	Wide opening

In the case of filled discontinuities they can be classified as:

c. Filling Thickness	Description
0.5 - 10 mm	Filled small aperture
> 10 mm	Wide aperture

The possibility of occurrence of incoherent filling material, which is not common unless the aperture is greater than 1 mm, was also considered. The persistence of the dominant set was classified as follows:

d. Persistency	Description
< 3 m	Small
> 3 m	Significant

As far as water transmissivity is concerned, there are possibilities of absence of water, presence of some moisture, or occurrence of significant water flow. The characterization of a certain sector of the rock mass is done by indicating the alternatives which are presented for each of the parameters described above. The result of the geomechanical classification is obtained by summing the points "P_i", which are determined according to an interactive process of improvement, so that their sum falls within the intervals that fulfill the correspondences listed in Table A.14.

Table A.14 Support recommendations in Geomechanical Classification (after Mendes et al., 1993)

Punctuation	Class	Type of Support
< 15	I	None
15 - 20	II	Rock bolts
20 - 35	III	Rock bolts with metallic mesh
35 - 50	IV	Steel arches TH-21, spaced 1.5 m
> 50	V	Steel arches TH-21, spaced 1.0 m, or TH-29 spaced 1.5 m

In this study, this rating intervals for each P_i are not given.

A simple statistical equation for the density of support was also developed by Mendes et al. (1993). This equation is based on the average vertical convergence rate and class number as shown in Equation A.30.

$$D = -0.12 + 4.84 \cdot C - 3.37 \cdot U' \qquad \text{(A.30)}$$

where, D is the support density (kg/m³), C is the class number (1 to 5) and U' is the average convergence rate (mm/day).

Coal Mine Roof Rating - CMRR

The U.S. Bureau of Mines has developed a rock mass classification system for coal mine roof control. The Coal Mine Roof Rating System (CMRR) evaluates the structural competence of mine roof using simple field tests and observations obtained from underground exposures in roof falls or overcasts (Molinda and Mark, 1993).

According to Molinda and Mark (1993), the geologic origin or nature of the discontinuity is not important. Shear planes, bedding, slickensides, and joints are all equivalent in their effect on the roof. It is the surface cohesion, frequency and persistence of the feature which makes it more or less damaging to roof strength. The CMRR provides guidelines for 1) the complete collection of data relevant to roof strength, and 2) the correct evaluation of the unit/discontinuity properties which affect the strength.

The CMRR employs the familiar format of Bieniawski's RMR, summing various individual ratings to obtain a final CMRR on a 0-100 scale. The CMRR is also designed so that the CMRR/unsupported span/standup time relationship is roughly comparable to the relationship determined for the RMR. Certain other features have been adopted from classification systems proposed by Moebs and Stateham (1986), Williamson (1984), Kester and Chugh (1980), and Sickler (1986). Much of the field data used in the development of the CMRR was obtained during a nationwide study of ground control in longwall mines (Mark and Chase, 1993).

There are three main elements of the CMRR: i) collection of the field data; ii) calculation of Unit Ratings (UR), and iii) interpretation of the results.

The field data collection were included the compressive strength, weatherability, discontinuities, cohesion, roughness, spacing-persistence and groundwater.

In calculating the CMRR, firstly, Unit Ratings (UR) were determined for each unit within the bolted interval which is based on "cohesion-roughness" and "spacing-persistence" of discontinuities, "multiple discontinuity set adjustment", "compressive strength" and "weatherability adjustment".

When the UR are combined by a weighted average, the roof adjustments are made to arrive at the final CMRR. The roof adjustments were included the strong bed, unit contacts and groundwater adjustments. The CMRR could be calculated as follows:

$$CMRR = RR_w + Strong\,bed\,adj. + Units\,Contact\,adj. + Groundwater\,adj. + Surcharge\,adj. \quad \text{(A.31)}$$

where,

$$RR_w = \frac{(UR_1 \times t_1) + (UR_2 \times t_2) + \ldots + (UR_n \times t_n)}{t_1 + t_2 + \ldots + t_n} \quad \text{(A.32)}$$

where,

t_i : unit thickness, and

$$UR_i = Individual\,discontinuity\,rating + Multiple\,discontinuity\,set\,adj. + Strength\,rating + Weatherability\,adj. \quad \text{(A.33)}$$

Based on the CMRR system, Equation A.34 given below, was developed to guide the design of longwall pillars and gate entries (Mark and Chase, 1993):

$$ALPS\ SF_R = 1.76 - 0.014 \cdot CMRR \qquad (A.34)$$

where, $ALPS\ SF_R$ is the Analysis of Longwall Pillar Stability Factor.

Modified Rock Mass Rating - Modified RMR

44 case studies in coal mine roadways in India based on RMR, Q and CMRS systems are evaluated by Sheorey (1991, 1993).

One important parameter lacking in RMR system is the stress. Sheorey calculated RMR and Q values by considering only parameters that are common to both systems and determined an adjustment factor to include the effect of stress to the RMR value ($20.7 \cdot \log SRF$). The modified RMR system developed by Sheorey (1993) is given in the following equation:

$$RMR_{\text{mod}} = \left[(RQD + JS + JC + GW) - 20.7 \cdot \log SRF\right] + Strength\ Index - JO \qquad (A.35)$$

Also support load given by Ünal (1983) (see Equation A.7b) for this classification is modified by Sheorey (1993). According to Sheorey, the new equation is:

$$P = \left[\frac{100 - RMR_{\text{mod}}}{a}\right]^b \cdot \gamma \cdot B \qquad (A.36)$$

where, a and b are constants which are defined as $a = 94.5$ and $b = 1.37$.

Modified Q - System

Some unstable roadway cases show that Q system is inadequate for certain geological features not covered by it and also when joint orientation is unfavorable. Sheorey (1991, 1993) many times had the feeling that it needed a change

for horizontally stratified formations. He suggested for both unfavorable joint orientation as well as horizontal bedding, which may be considered as very favorable orientation. The following proposed changes in rock quality, listed in Table A.15, were arrived at after a few trials.

Table A.15 Suggested changes in Q-Index for unfavorable joint orientation and horizontal bedding (after Sheorey, 1993)

Condition	Modified
1. Horizontally stratified rock	change J_n to $J_n^{2/3}$
2. Irregular bed thickness	change Q to Q/3
3. Ball coal in roof	change Q to Q/5
4. Stone/clay pockets, kettle bottoms	change Q to Q/3
5. Unfavorable joint orientation or horizontal stress direction	change Q to Q/4

In Q system, support pressure (P, kg/cm^2) is calculated with the Jr and Q rating values. The new equation for roof support pressure suggested by Sheorey includes rock density, roadway span and Q rating values as shown in Equation A.37:

$$P = 0.5 \cdot \gamma \cdot B \cdot (Q_{\text{mod}})^{-1/3} \qquad \text{(A.37)}$$

Roof Fall Index - RFI

The roof fall index (Table A.16) has been developed relating roof instability to the presence of geological discontinuities (Singh et al., 1994). According to Singh et al. (1994), the normal faults (when associated with high frequencies of joints and cleats in their influence zone), bedding faults, slips and slickensides

Table A.16 Roof fall index cause failure type and prevention of strata movement problems due to discontinuities (after Singh et al., 1994)

Discontinuity	Roof fall index	Cause	Failure type	Prevention
Faults	1			
a. Normal		Poor cohesion/adhesion along the fault planes and increased frequency of other discontinuities within the influence zone	Shear	1. Plan roadways at 30-90° to fault planes 2. Use supplementary props, roof bolts connected with steel channel and irongirder crossbars 3. Netting and iron sheet to avoid inflow of gouge material
b. Bedding		Poor cohesion/adhesion along the fault planes	Tension	1. Reduce roadway width 2. Use roof bolts and roof stitchings across the fault planes
c. Slips		Poor cohesion/adhesion along the fault planes	Shear	1. Use roof bolts and roof stitchings across the fault planes
d. Slickensides		Very little cohesion across slickensides	Shear	1. Vertical bolts for slickensides dipping up to 20-30° 2. Bolts at right angle to steeper slickensides

Table A.16 (continued)

Discontinuity	Roof fall index	Cause	Failure type	Prevention
Bedding Planes	2	Delamination in thinly bedded strata leading to roof falls due to poor bending strength	Tension	1. Reduce roadways width 2. Leave a band of coal against weak and laminated shale roof 3. Use roof bolts, full-column resin bolts, trusses, posts and crossbars 4. Use staggered bolts to avoid concentration of tensile stresses along one horizon
Joints	3	Roadways parallel to joint strike and increased frequencies of joints	Shear	1. Orient entries at 30-45° oblique to joints 2. Use netting and bolts across joints and steel arches
Cleats	4	Roadways parallel to strike and closely spaced cleats	Shear	1. Orient entries at 20-45° oblique to cleats 2. Use wooden props and crossbars

invariably cause roof falls. The immediate roof area, composed of thinly bedded strata such as shale and alternative bands of shale and coal, also caves in. These lithologies are frequently observed in the roofs of coal mines and they are important components of coal measure rocks. However, thick beds can bridge across an opening and remain intact. Joints, another decisive factor for roof fall, influence roof stability only when they run parallel to roadways. However, closely spaced joints can fail irrespective of

their orientation difference with respect to the roadways. Cleats also follow a similar trend, but shearing along the cleats is less common than in joints.

A.3 Behavior of Mine Roadways

The proper functioning of an underground mine depends on providing efficient transport for mine personnel, mined materials, and mine equipment, materials and supplies, creating proper conditions of ventilation and air conditioning, as well as ensuring work safety. These effective solution of these matters is made possible only by ensuring the stability of mine roadways.

Three approaches for design of support in underground excavations were developed by the rock mechanics engineers as follows (Bieniawski, 1993):

i) **Analytical Design Method:** Analytical or closed form solutions are often employed in design practice, as for particular importance convergence-confinement method for the analysis of deep tunnels, but their use is restricted to situation characterized by relatively simple geometry, boundary conditions and material behavior. In order to overcome this limitation the so-called numerical (computer oriented) methods are nowadays frequently adapted for analysis related to complex design problems.

ii) **Observational Design Method:** Observational methods call for the instrumentation of the excavation and the implementation of support as the design is developed. This is demonstrated in the New Australian Tunnelling Method (NATM) and the Ground Reaction Curve (GRC).

iii) **Empirical Design Method:** This approach assesses the stability of mines and tunnels by the use of statistical evaluation of underground observations. The most tunnel supports and linings were designed using empirical rules defining ground loads acting on the supporting structures. This approach is popular by the use of rock mass classification systems. Correlations between rock mass conditions and the type of supported used are based on case histories.

Goodman (1980) and Hoek and Brown (1980) believe that the engineering rock mass classifications constitute the best known empirical approach for assessing the stability of underground opening in rock. Butler and Franklin (1990) also indicate that empirical design methods have the singular advantage of improving with experienced gained and time. Singh et al. (1994) state that determination of RMR and Q values is necessary so that a reasonable assessment of the support requirements is possible during the design stage. However, this approach according to Panet (1993) perpetuates existing practice, even if overconservative or unsatisfactory.

In order to investigate the behavior of roadways and to evaluate the stability, in situ measurements and observations are necessary. This stage is also required for the feed-back cycle of the design process.

A.3.1 Time and Face Advance Dependent Response of Rock Around Gate-Roads

Stresses and displacements in the rock mass surrounding tunnels or mine roadways depend on (Panet, 1993):

i) the rock mass properties,

ii) the in-situ stress,

iii) the type of excavation,

iv) the size and shape of the excavated area,

v) the stiffness of the lining or support, and

vi) the timing of support installation.

The variation of the distance between two opposite fixed points in the tunnel or mine roadway is called as the convergence which is considered as the function of required support. Convergence is dependent on the six parameters listed above.

In order to predict convergence, there are two general approaches (Ünal, 1983 and 1986b):

i) utilization of the rheological time dependent functions, which are developed based upon models composed of assemblages of linear spring and dashpots, and

ii) utilization of the face advance and time dependent functions, which are developed based upon statistical evaluation of the underground openings and curve fitting.

Rheological Time-Dependent Functions

Rheological models are assembled to represent macroscopic stress-strain-time-yield behavior phenomenologically (Blair, 1969), using four elements that emulate basic aspects of material as follows:

i) elastic spring; ii) viscous dashpot; iii) plastic slider; and iv) brittle yield element.

Using elements in parallel, series or various combinations, and by varying element parameters, a wide range of rock behavior could be modeled. The simplest rheological models are Maxwell and Kelvin-Voight models in viscoelastic medium.

Rheological models were used by a number of researches to predict the creep behavior of the rock material in the laboratory as well as to predict mine roof behavior. A brief summary of these studies are given in the following paragraphs.

Creep test studies: Recently, Dusseault and Fordham (1993) performed creep tests on hardrock, carbonates, sandstones, shales, saltrock, and coal; and evaluated the rheological functions obtained based on the creep test results. Test specimens seldom were large enough to be representative, and often intact samples were unconsciously favored.

In-situ testing has a vital role in rock engineering (Dusseault and Fordham, 1993); however, the most serious disadvantages of in situ testing are that:

i) stress and strain state are rarely homogenous;

ii) stresses are seldom known accurately;

iii) creep may concentrate in a single material or interface, but measuring devices average displacements over a gauge length;

iv) the field test data may reflect behavior of damaged or nonrepresentative material;

v) few large scale tests may be possible because of cost; and

vi) a limited range of temperature (T), and stress (σ) states are available in the typical in situ test program.

Despite these disadvantages, development of a large mine or civil engineering structure susceptible to creep requires in situ tests, perhaps extended for several years into the construction phase.

According to Filcek and Kwasniewski (1993), the calculation of rock displacements towards the excavation, deformational rock pressures on the excavation supports, and parameters of the rock-support interaction etc., are possible only in the cases when the rheological properties of the rocks and the rock mass are known. The only way to learn of these properties is through laboratory tests and/or field measurements. Experimental studies of the creep and stress relaxation in rocks are, unfortunately, very time consuming. They also require special testing equipment (creep testing machines and relaxation meters) and sophisticated methods of measuring strain. They must be conducted under conditions of constant temperature and constant air humidity, on stands protected against vibrations and shocks. For these reasons, among others, it seems that experimental rheological investigations do

not keep pace with the development of more and more advanced methods and analytical and numerical solutions used to describe the behavior of the rock mass in the vicinity of mine excavations. Thus, the practical application of these solutions is very frequently rendered difficult or even impossible.

Panet (1993) suggested the application of rheological models to the analysis of time dependent deformations of spherical or cylindrical cavities. However, it must be acknowledged that their application to actual underground works meets serious difficulties; in situ measurements very rarely agree over a long period of time with the rheological parameters deduced from the data obtained in the laboratory tests.

Field studies: Panet (1993), in his analysis, used both the rheological models and the best fit curve equations based on convergence data measured on several sites (Panet, 1979; Guadin et al., 1981; and Sulem et al., 1987a). He believes that rock rheology is a complex process which depends on the type of rock, the temperature and the mean and deviatoric stress. According to Dusseault and Fordham (1993), on the other hand, rheological models have the following deficiencies: i) they provide no direct predictions unless calibrated; ii) they do not account for shear and normal stress, temperature or instinct structure; and iii) they do not provide insight into fundamental creep mechanisms.

Statistical Evaluation of Experimental Data

The equations representing the best-fit-curves have been derived based on experimental data obtained in laboratory or by in situ data obtained monitoring of the convergence during tunnel or mine roadway constructions.

Laboratory Studies. The first creep laws described extensional deformation of metals under constant tensile load. Philips (in Ode, 1968) presented a logarithmic creep law of the form

$$\dot{\varepsilon} = B \cdot t^{-1} \tag{A.38}$$

where $\dot{\varepsilon}$ is the strain rate in s^{-1}, B is a constant and t is time in seconds.

The earliest work on time dependent behavior of rock has been carried out by Griggs (1939, 1940) under constant stress. This work demonstrated that the time dependent deformation of rocks and minerals is possible without producing immediate failure of the specimen. Griggs termed the time strain observed for rock as elasto-viscous and described it as being made up of two parts, namely:

i) pseudo-viscous flow, deformation at a constant rate, given C_t; and

ii) elastic flow, deformation decreasing logarithmically with time, given by $B \cdot \log t$.

The total strain $\left(\frac{\Delta L}{L}\right)$ after time t is given by an equation of the form:

$$\varepsilon_t = A + B \cdot \log t + C_t \tag{A.39}$$

where, t is the time, and A, B and C are constants depending on type of material. On the basis of experimental results and physical reasoning, Tan and Kang (1980) proposed a three-dimensional generalization of the experimental Griggs equation. Substantial additional evidence for this type of function was provided by Parsons and Hedley (1966). They showed that a logarithmic time dependent (creep) curve provided a good fit for the majority of the data obtained from 20 different rock types.

Hobbs (1970) came out essentially with the same conclusions from tests of sedimentary rock and suggested the following logarithmic function:

$$\varepsilon_t = A + B_t + \log(t+1) \tag{A.40}$$

For very low stress at room temperature, a logarithmic creep, in the form shown in Equation A.41 is also very often observed in rocks, and is preferred on theoretical grounds by some investigators (Carter and Kirby, 1978; Murell, 1967 and 1969).

$$S \propto \log\left(1 + {}^{t}/_{t_0}\right) \tag{A.41}$$

Genovois and Prestinizi (1979) showed that even highly weathered rock follow a logarithmic time dependent law. Laboratory time dependent case tests have also been carried out on jointed rocks, Dietrich (1972) investigated the relationship between the duration of stationary contact and the static friction coefficient of "clean" and gouge-filled rock joints. Experiments by Dietrich (1972) on both rough and smoothly ground rock surfaces showed that the time dependency of the static coefficient of friction, μ_S, could be expressed as:

$$\mu_s = \mu_0 + A \cdot \log t \tag{A.42}$$

where, μ_0 is the initial friction coefficient and A is a constant. Solberg et al. (1978) simulated time-dependent behavior along a fault by testing cylindrical specimens incorporating an inclined saw cut separated by gouge material. Their test data showed a logarithmically decreasing function. The most significant implication from this work is that time dependent behavior of jointed rock has the same general character as that of the intact rock. This conclusion was also confirmed by Amadei and Curran (1980).

Field Studies: It seems from the review presented in this Section that logarithmic laws would fit the majority of data on the creep of rocks at least at the laboratory scale. According to Ladanyi (1980, 1993) there is still question, however, as to how these data would apply to the field situations. He states that:

> "Important differences that have often been found between the predicted and observed creep behavior of underground openings and mine pillars are considered to be mainly due to the following two causes: the size effect and the stress redistribution with time."

It was further stated by Ladanyi (1980) that a correct initial convergence response for an unlined tunnel, or the pressure build up for a lined tunnel, can only be determined by a numerical step-wise analysis. Nair and Boresi (1970) found that the majority portion of stress distribution occurs in the initial 24 hours and practically all of it is completed in about a month.

In addition to the deformations caused by the gravity action (e.g. bed separation), the deformation of rocks in the vicinity of many underground openings in coal measure rocks are undoubtedly time dependent and considered to be due to stress redistribution with time. According to Shelton (1982) typical time dependent deformation can be described as occurring in three stages:

i) the elastic response to excavation can be said to be 50 percent complete at the face and is therefore practically unsupportable (Daemen and Fairhurst, 1971),

ii) time dependent deformation characterized by initially high rates of closure which reduces to less significant portions as the face is further advanced, and

iii) minor time related deformations may then occur over a long period of time.

The above considerations lead to the conclusion that any method attempting to predict directly the time dependent behavior of strata in underground should take into account of the steps involved before, during, and after excavation. One cannot hope that closed form solutions, associated with time dependent response of rock around excavations, will be able to give a complete answer to the problem comparable to the finite-element method (Ladanyi, 1980). Analytical methods, on the other hand, use the criterion of yield zone formation and the description of the ductile behavior of rocks, with many idealizations, hence do little other than illustrate mechanics of deformation (Shelton, 1982).

Consequently, the approach associated with the analysis of strata behavior should also include an input from the actual field observations. According to Tincelin (1978), one such approach has been presented by Professor Schwartz (in Tincelin, 1978) of the Ecole des Mines of Nancy and the ground deformation (convergence) was presented by a logarithmic law, as shown in Equation

$$U = A \cdot \log\left(1 + \frac{t}{T}\right) \tag{A.43}$$

where, U is the convergence in cm, t is the time in hrs, and A and T are constants. According to Tincelin (1978), Equation A.43 was also verified by observations.

Tallon (1982) established a relationship between ground deformations and rock mass rating (RMR) of the Geomechanics Classification in the following form:

$$U = a + b \cdot \ln t \tag{A.44}$$

where, U is deformation in mm, t is the time elapsed since excavation in days, and a and b are defining parameters. Based on the convergence measurements carried out in Pando highway tunnel, Spain, Tallon (1982) showed that there was a regression of the logarithmic type between the b and RMR index with a correlation coefficient of 0.92 and the following equation:

$$b = 63.42 - 14.36 \cdot \ln RMR \tag{A.45}$$

Tallon (1982) also suggested further studies which would include establishment of a correlation between deformation and the following main variables: time, rock quality index, support factor, and initial state of stress. It is interesting to note that the results of Moreno Tallon's analyses substantiate the results of Schwart'z field observations in that, in both cases, the deformation was presented by a logarithmic law. Tallon's work also represented a new field of application for the Geomechanics Classification.

Wells and Singh (1985) developed a linear equation with the statistical interpretation of gate roadways deformation data in the UK. According to these researchers, gate roadways influenced by the stress distributions brought about by longwall mining. It was shown that the most highly correlated variables with the important measures of closure were extracted seam height, roof strength, depth of working, roadway initial height and width, and support spacing. Consequently, the vertical closure was expressed as given in Equation A.46. However, the effects of support spacing and roadways initial height or width were not included in this equation.

$$\begin{aligned} Vertical\ Closure = {} & a_0 + (a_1 \times depth) + (a_2 \times external\ seam\ height) + \\ & (a_3 \times roof\ index) + (a_4 \times floor\ index) + \\ & (a_5 \times \ln(rib\ width)) \end{aligned} \tag{A.46}$$

where, a_0, a_1, a_2, a_3, a_4 and a_5 are constants which were determined by statistical analyses.

In the case of elastic medium, Panet (1979) and Gaudin et al. (1981) proposed to analyze the convergence (U) versus the distance to the face with the following equation.

$$U(X) = U_{\infty} \cdot \left[1 - e^{\left(-\frac{x}{X}\right)}\right] \tag{A.47}$$

Panet and Guenot (1982) have considered 12 different cases for the elastoplastic behavior including a strain-softening behavior case. They have seen that Equation A.47 was valid for elastoplastic medium. Their major conclusion was that: the face advance effect for elastoplastic material can be fairly well represented by the function given in Equation A.48.

$$U(X) = U_{\infty} \cdot \left[1 - \left(\frac{X}{x+X}\right)^2\right] \tag{A.48}$$

where, X is the distance related to the plastic radius r_p around the tunnel far behind the face.

The roadway closure studies carried out by Sulem et al. (1987) have shown that neither an exponential nor a logarithmic function could fit correctly the experimental data. The authors have shown that a very good approximation could be obtained with the function shown in Equation A.49.

$$U(t) = A \cdot \left[1 - \left(\frac{T}{t+T}\right)^n\right] \tag{A.49}$$

where, T is the homogenous to a relation time and $n > 0$, t is time (days), and A is a constant value.

A general equation for the convergence was also developed by Sulem et al. (1987a):

$$U(x,t) = U_1(x) + U_2(t) \qquad \text{(A.50)}$$

where, U_1 is the convergence developing depending on the distance to the face x, and U_2 is the convergence being related to the time dependent properties of the ground. Consequently, the relationship shown in Equation A.51 was developed by Sulem et al. (1987a).

$$U(x,t) = U_{\infty x} \cdot \left\{1 - \left[X/(x+X)\right]^2\right\} \times \left\{1 + m \cdot \left[1 - \left(T/(t+T)\right)\right]^n\right\} \qquad \text{(A.51)}$$

This function depends on five parameters x, T, n, $C_{\infty x}$ and m, where,

x : distance to the face (m),

X : distance related to the distance of influence of the face,

t : time (days),

T : characteristic parameter of the time-dependent properties of the ground,

$U_{\infty x}$: "instantaneous closure" obtained in the case of an infinite rate of the face advance (no time dependent effect),

$U_{\infty x}$ (1+m) : final closure,

m : ratio to Equation A.48 of A in Equation A.49.

Sulem et al. (1987b) also developed a closed form solution based on the analysis of in situ measurement carried out for determination of ground pressure acting on the tunnel support.

It has been shown by Majdi et al. (1986) that the vertical convergence profile on tunnel closure, in the Sidney coal field, can be obtained as a function of distance from the face line by employing the function given in Equation A.52.

$$C = a \cdot \left[1 - e^{-\frac{x}{b}} \right] + c \qquad \text{(A.52)}$$

where, C is the vertical convergence in %, a, b and c are constants and x is the distance from the faceline. The constant a represents the total vertical convergence.

As a result of displacement measurements carried out around excavations driven in weak rocks Can (1987) have shown that for a supported drift driven in weak rock the wall displacement satisfies the relationship given in Equation A.53.

$$U = A \cdot \left(1 - B^{-k \cdot t} \right) \qquad \text{(A.53)}$$

where, A, B and k are empirically determined constants, and

$$\lim_{t \to \infty} \frac{dU}{dt} = U' \qquad \text{(A.54)}$$

where, U' is the slope of the deformation-time curve. If Equation A.54 equal to zero then the drift support is stable.

Based on theoretical and in situ studies of tunnel deformation in longwall coal mining, Majdi and Hassani (1989) have developed a method to predict tunnel convergence profiles from the faceline in longwall lining. The method accounts for i) the effect of panel width, ii) extracted seam height, iii) deformation moduli of the goaf material and coal pillar, iv) depth of cover, v) in situ structural defects, vi) tunnel shape and tunnel size, and vii) strength characteristics of surrounding strata. In order to reflect the effects of the time-dependent deformation and the face advance, this

method includes the exponential function of Majdi et al. (1986) and the time dependent displacement function developed by Panet (1979).

$$U = \left\{ A\left[1 - e^{\left(\frac{-4x}{9.2D + W_0} \right)} \right] + C_1 + C_2 \right\} (1 + C_c)(100) \qquad \text{(A.55)}$$

where, U is the vertical convergence, A is the constant that can be calculated by the analytical solution of Wilson (1980), D is depth of cover, W_0 is the average extracted panel width, C_1 is the function of Panet (1979), C_c is shape effect, x is the distance from the faceline and C_2 represents the vertical displacement.

Based on field instrumentation in eight different coal mines representing varying depths and strata conditions, a relation for obtaining the critical convergence value have been established by Ghosh and Ghose (1992). They observed that the maximum closure is a function of various parameters, like i) roadway span, ii) rock density, iii) depth, iv) geological features, v) ground water condition, vi) layers in roof rock, vii) weatherability of the rock, etc. As all the parameters except the first two were considered in calculating the rock mass rating (R), which was developed by Venkateswarlu (1986). Hence, it could be assumed that the maximum ground movement (C_m) is a function of three major parameters: rock mass rating (R), roadway span (B), and rock dry density (γ).

$$C_m = 40 \cdot B^{0.5} \cdot \gamma^{0.3} \cdot (1 - R/100)^3 \qquad \text{(A.56)}$$

where C_m is in millimeters, B is in meters and γ is in kN per cubic meters.

A.3.2 Integrated Approach

The tunnel or roadway deformations (U) and roof pressure (P) can be estimated by the integrated approach developed by Ünal (1983). This approach considers the effects of the roof span (B), the rock mass rating (RMR), and the support reinforcement factor (RF).

The engineering geological description of roof strata which are necessary to identify the geological structures, and other features affecting the stability of the mine openings are the basic information used as an input data at various steps of the integrated approach. These steps also shown in Figure A.15 can be briefly written as follows:

i) $P = f(RMR, B, \gamma)$, ii) $B = f(RMR, t)$, iii) $U = f(RMR, B, RF, t)$, and iv) $P = f(U, SS)$

where, t is the support installation time, SS is the system support stiffness.

In underground coal mines, it is not always possible to observe the behavior of the unsupported roof spans because leaving an unsupported area is not permitted or it is usually against the mining regulations. The best alternative is to make use of the analytical or empirical methods and, if possible, to cross check the findings with underground measurements. Therefore at this stage, the support characteristic curves and the ground reaction curves can be introduced to the analysis and they can be compared with the rock loads and allowable deformations, which constitutes the output of the fourth step of the integrated approach (Ünal, 1986b).

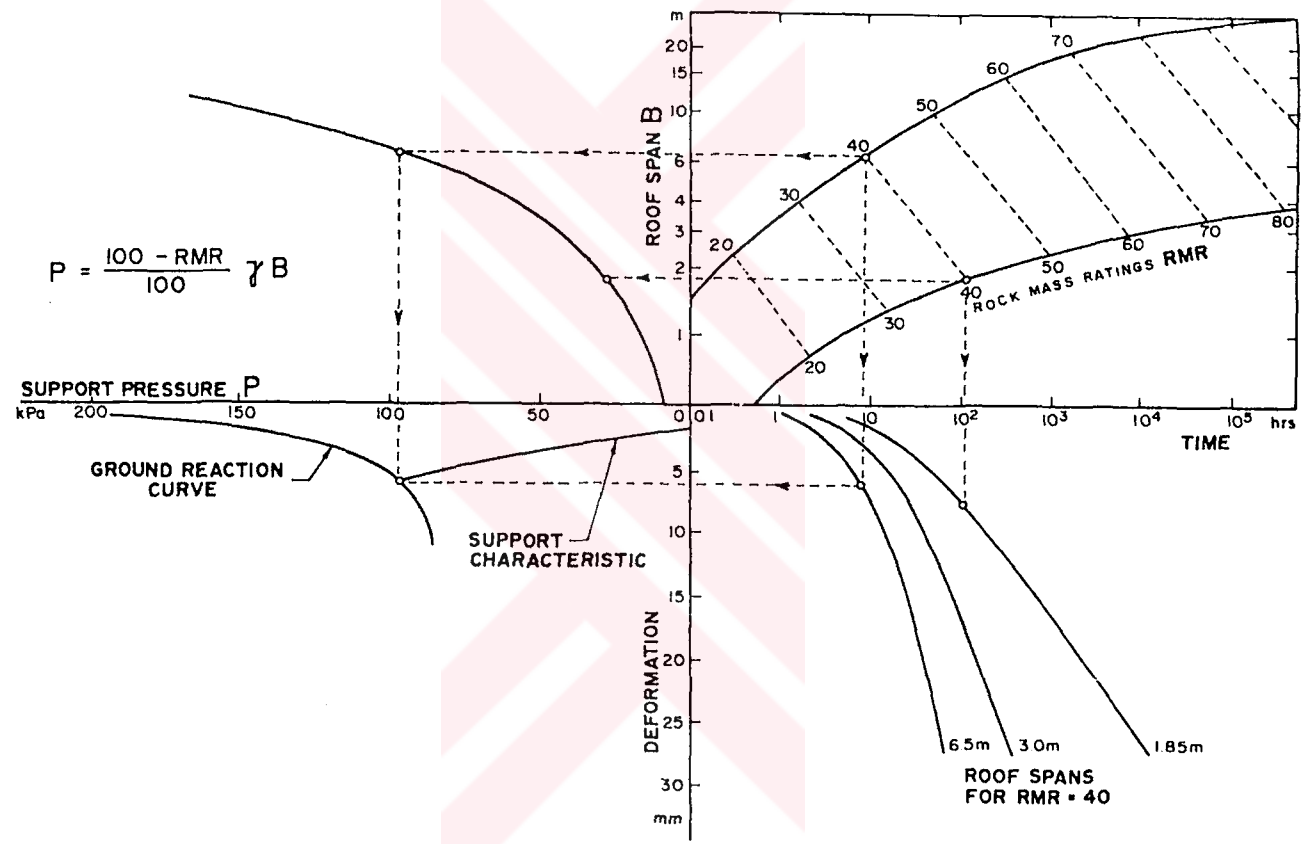

Figure A.15 Illustration of the integrated approach to tunnel stability (after Ünal, 1983)

In order to provide the required information for the third step of the integrated approach, the following basic procedures were followed:

i) the logarithmic law, presented by Schwartz and verified by his field observations, was assumed to apply, and thus deformation (u) expressed as a function of time (t), in the following form:

$$U = f(t) \tag{A.57}$$

ii) Equation A.57 was modified to include the effect of rock mass rating (RMR), the effect of roof span (B), and the reinforcement factor (RF) yielding the following general equation:

$$U = f(t, RMR, B, RF) \tag{A.58}$$

The effects of the factors, shown in Equation A.58 will be discussed in the following sections.

The basic deformation time function was expressed by a logarithmic law, e.g., as:

$$U = \log\left(1 + \frac{t}{t_0}\right) \tag{A.59}$$

where, t_0 is an arbitrary time unit. Since the major portion of the stress distribution, after excavation, was found to occur in the initial 24 hours (Nair and Boresi, 1970), the value of t_0 was taken as 24 throughout the analysis.

Effect of Rock Mass Rating (RMR):

The effect of *RMR* can be included in Equation A.58 as follows:

$$U = e^{\left(\frac{100}{RMR}-1\right)} \cdot \log\left(1+\frac{t}{24}\right) \qquad \text{(A.60)}$$

In Equation A.60, the time is expressed in hours and the deformation in centimeters (cm).

Effect of Roof Span (B):

In order to include the effect of B on roof deformation, the following parameter was introduced:

$$e^{h\cdot\left(\frac{B_{max}}{B}-1\right)}$$

where, h is a constant, B_{max} is the maximum roof span (for a particular *RMR*, within the range of applicability shown in Figure A.15), and B is the active roof span of the opening. Thus, the new equation of deformation will be as follows:

$$U = e^{h\cdot\left(\frac{B_{max}}{B}-1\right)} \cdot e^{\left(\frac{100}{RMR}-1\right)} \cdot \log\left(1+\frac{t}{24}\right) \qquad \text{(A.61)}$$

Effect of Reinforcement Factor (RF):

In order to express, mathematically, the behavior of the inadequately supported roof-span, a new term, reinforcement factor (*RF*) is introduced. A similar parameter has been introduced by Panek (1962a, 1962b) for stability studies of the stratified coal mine roofs.

The reinforcement factor in this study is defined as the ratio between the deformations of the unsupported roof and the supported roof, i.e.,

$$RF = \frac{(\ )_{\text{unsupported roof}}}{(U)_{\text{supported roof}}} = \frac{(U)_U}{(U)_s} \tag{A.62}$$

The following constants were developed to explain the effect of RF on time deformation characteristics:

$$a = \frac{2 - RF}{RF} \quad \& \quad d = \frac{2 \cdot RF - 2}{RF}$$

when $RF = 1 \rightarrow a = 1 \rightarrow d = 0$

when $RF = 2 \rightarrow a = 0 \rightarrow d = 1$

The total effect of the reinforcement factor on deformation can now be expressed as follows:

$$U = \left(\frac{2 - RF}{RF}\right) \cdot e^{\left(\frac{100}{RMR} - 1\right)} \cdot e^{h\left(\frac{B_{max}}{B} - 1\right)} \cdot \log\left(1 + \frac{t}{24}\right) + \left(\frac{2 \cdot RF - 2}{RF}\right) \cdot \log\left(1 + \frac{t}{24}\right) \tag{A.63}$$

or

$$U = \frac{1}{RF} \cdot \log\left(1 + \frac{t}{24}\right) \cdot \left[(2 - RF) \cdot e^{\left(\frac{100}{RMR} - 1\right)} \cdot e^{h\left(\frac{B_{max}}{B} - 1\right)} + 2 \cdot (RF - 1)\right] \tag{A.64}$$

As can be seen from Equation A.63, the deformation is a function of time (t), span (B), and reinforcement factor (RF), and can be shown in a simplified form as follows:

$$U = \left[a \cdot e^{b+c} + d\right] \cdot \log t \tag{A.65}$$

The following example illustrates the effects of the span and the reinforcement factor on time deformation characteristics curves:

Example: Consider the following:

$RMR = 40$ (arbitrarily selected)

$B_{max} = 6.5$ m (read from stand-up time versus span plots)

$\gamma = 25.14$ kN/m^3

$RF = 1$ (unsupported condition)

$B = 6.5$ m (arbitrarily selected)

The establishment of the integrated approach is concerned with the determination of the following:

i) rock loads as a function of rock load height (h_t) and roof span (B);

$$P = \left(\frac{100 - RMR}{100}\right) \cdot B \cdot \gamma \qquad \text{(A.7b)}$$

$P = 98.05$ kN / m^2

ii) a relationship between roof spans and stand-up times;

$$\left.\begin{array}{l} \text{RMR} = 40 \\ \text{B} \quad = 6.5 \text{ m} \end{array}\right\} \Rightarrow \text{unsupported stand - up time is 9 hrs (Figure A.15)}$$

iii) ground behavior characteristics in terms of roof deformation (U) as a function of time (t);

$$U = \left[a \cdot e^{b+c} + d\right] \cdot \log t \qquad \text{(A.65)}$$

where

$$a = \frac{2 - RF}{RF} = 1$$

$$d = \frac{2 \cdot RF - 2}{RF} = 0$$

$$b = \left(\frac{100 - RMR}{100} \right) = 1.5$$

$$c = h \cdot \left(\frac{B_{\max}}{B} - 1 \right)$$

where B_{max} = 6.5 m (for RMR = 40)

B = 6.5 m (arbitrarily selected)

h = -0.2665 (constant for RMR = 40)

Then $c = 0$

$\therefore$ $$U = e^{1.5} \cdot \log\left(\frac{t}{24} + 1 \right)$$

The solution of this problem is given with Figure A.15 which is also included the solutions of 3 and 1.85 meter spans under same conditions.

iv) The left lower quadrant (step 4) provides information on the rock load (support pressure) and the maximum allowable deformation. The significance of this output information lies on the fact that the adequate support systems can be prescribed based on this information. The point obtained in step 4 (i.e., d') can be interpreted as the intersection of the ground reaction curve (GRC) with the support characteristic curve (SCC)

for an equilibrium condition. For a stability condition, however, SCC should intersect the GRC before this point.

In conclusion, the integrated approach presented in this study and the ground reaction curve concept are in a conceptual form, therefore, may not be directly applicable to actual design cases. These concepts serve as useful guides to the understanding of ground and support behavior and the factors of influence that are likely to be encountered in practice. The concepts should be substantiated with more field investigations and any necessary modifications should be made based on the data obtained from underground measurements (Ünal, 1983).

APPENDIX B

CONVERGENCE VERSUS TIME PLOTS IN A-810

TIME (DAYS)
20 40 60 80 100 120 140 160 180 200 220 240 260 280 300 320 340 360 380 400 420 440 460 480 500
REINFORCEMENT REGION : SPLIT SET
STATION NO : K 1 O
K 2 O
CONVERGENCE (%)
1 2 3 4 5 6 7 8 9 10 11 12 13 14 15

TIME (DAYS)
CONVERGENCE (cm)
REINFORCEMENT REGION : YIELDING SUPER SWELLEX
STATION NO : K 4
K 5
K 6

TIME (DAYS)
CONVERGENCE (MM)
REINFORCEMENT REGION : SIS RESIN BOLT
STATION NO : K 8
K 9
K 10

TIME (DAYS)
20 40 60 80 100 120 140 160 180 200 220 240 260 280 300 320 340 360 380 400 420 440 460 480 500
CONVERGENCE (mm)
1 2 3 4 5 6 7 8 9 10 11 12 13 14 15
REINFORCEMENT REGION : FIBRIC RESIN BOLT
STATION NO : K 12
K 13
K 14

TIME (DAYS)
20 40 60 80 100 120 140 160 180 200 220 240 260 280 300 320 340 360 380 400 420 440 460 480 500
CONVERGENCE (cm)
1 2 3 4 5 6 7 8 9 10 11 12 13 14 15
SUPPORT REGION : YIELDING STEEL ARCH
STATION NO : K 16
SUPPORT REGION : RIGID STEEL ARCH
STATION NO K 17
K 18

APPENDIX C

ROOF STRATA MOVEMENT VERSUS TIME PLOTS IN A-810

TIME (DAYS)
20 40 60 80 100 120 140 160 180 200 220 240 260 280 300 320 340 360 380 400 420 440 460 480 500
ROOF STRATA MOVEMENT (cm)
1 2 3 4 5 6 7 8 9 10 11 12 13 14 15
REINFORCEMENT REGION : SPLIT SET
STATION NO : EL
R1
R2
R3
R4
R5
ROOF LINE

TIME (DAYS)
ROOF STRATA MOVEMENT (mm)
REINFORCEMENT REGION : YIELDING SUPER SVELLEX
STATION NO : E4
R1
R2
R3
R4
R5
ROOF LINE

TIME (DAYS)
ROOF STRATA MOVEMENT (mm)
REINFORCEMENT REGION : SIS RESIN BOLT
STATION NO : E10
— — ? — — MEASUREMENTS OMITTED
R1
R2
R3
R4
R5
ROOF LINE

TIME (DAYS)
ROOF STRATA MOVEMENT (mm)
SUPPORT REGION : YIELDING STEEL ARCH
STATION NO : E16
R1
R2
R3
R4
R5
ROOF LINE
MEASUREMENTS OMITTED

TIME (DAYS)
ROOF STRATA MOVEMENT (mm)
R1
R2
R3
R4
R5
ROOF LINE
REINFORCEMENT REGION : FOSROC RESIN BOLT
STATION NO : E14
MEASUREMENTS OMITTED

APPENDIX D

CONVERGENCE CURVES OBTAINED BASED ON

EMPIRICAL EQUATION DEVELOPED

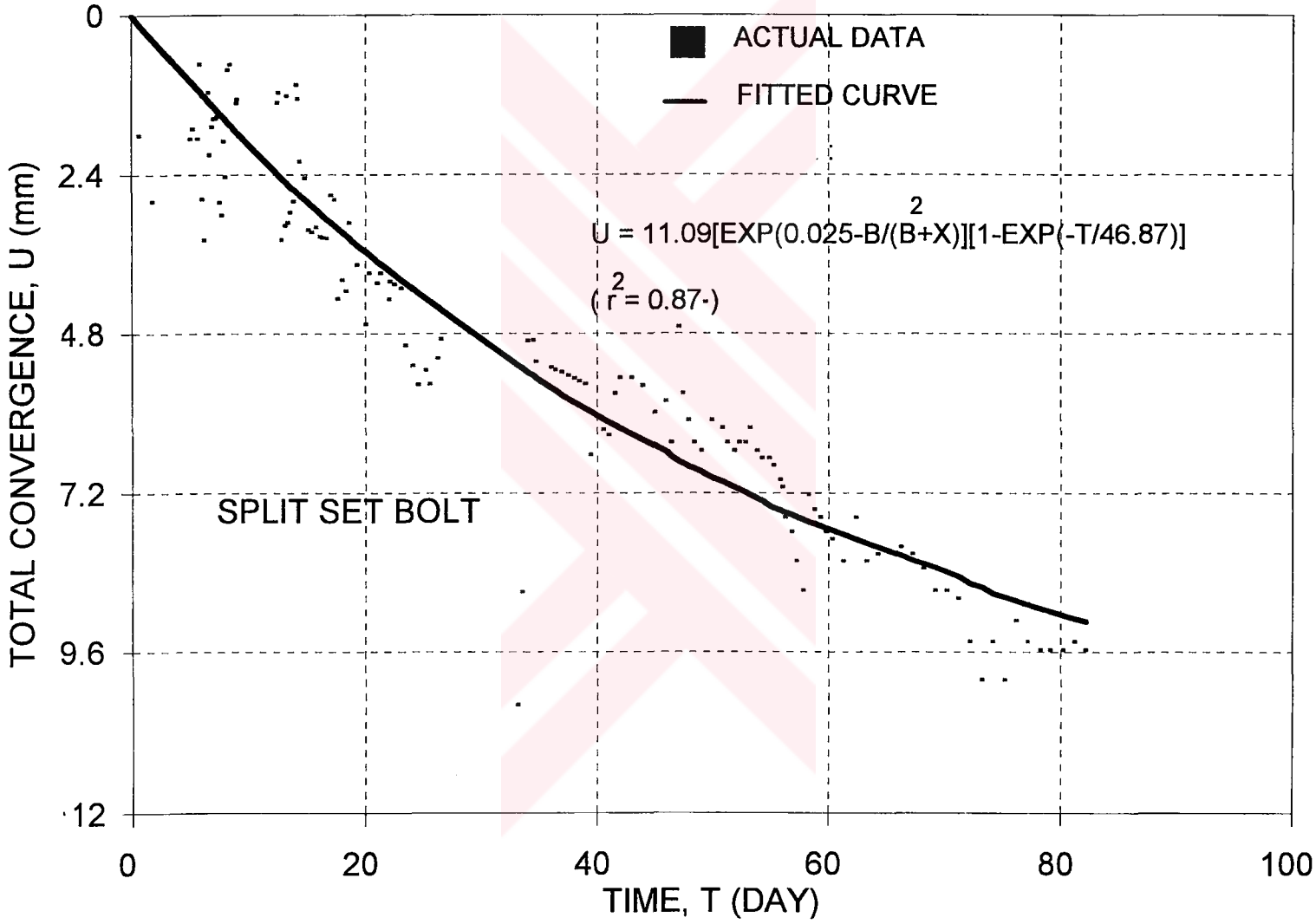
ACTUAL DATA
FITTED CURVE
U = 11.09[EXP(0.025-B/(B+X)][1-EXP(-T/46.87)]
2
(r = 0.87-)
2
SPLIT SET BOLT
TOTAL CONVERGENCE, U (mm)
0
2.4
4.8
7.2
9.6
12
0
20
40
60
80
100
TIME, T (DAY)

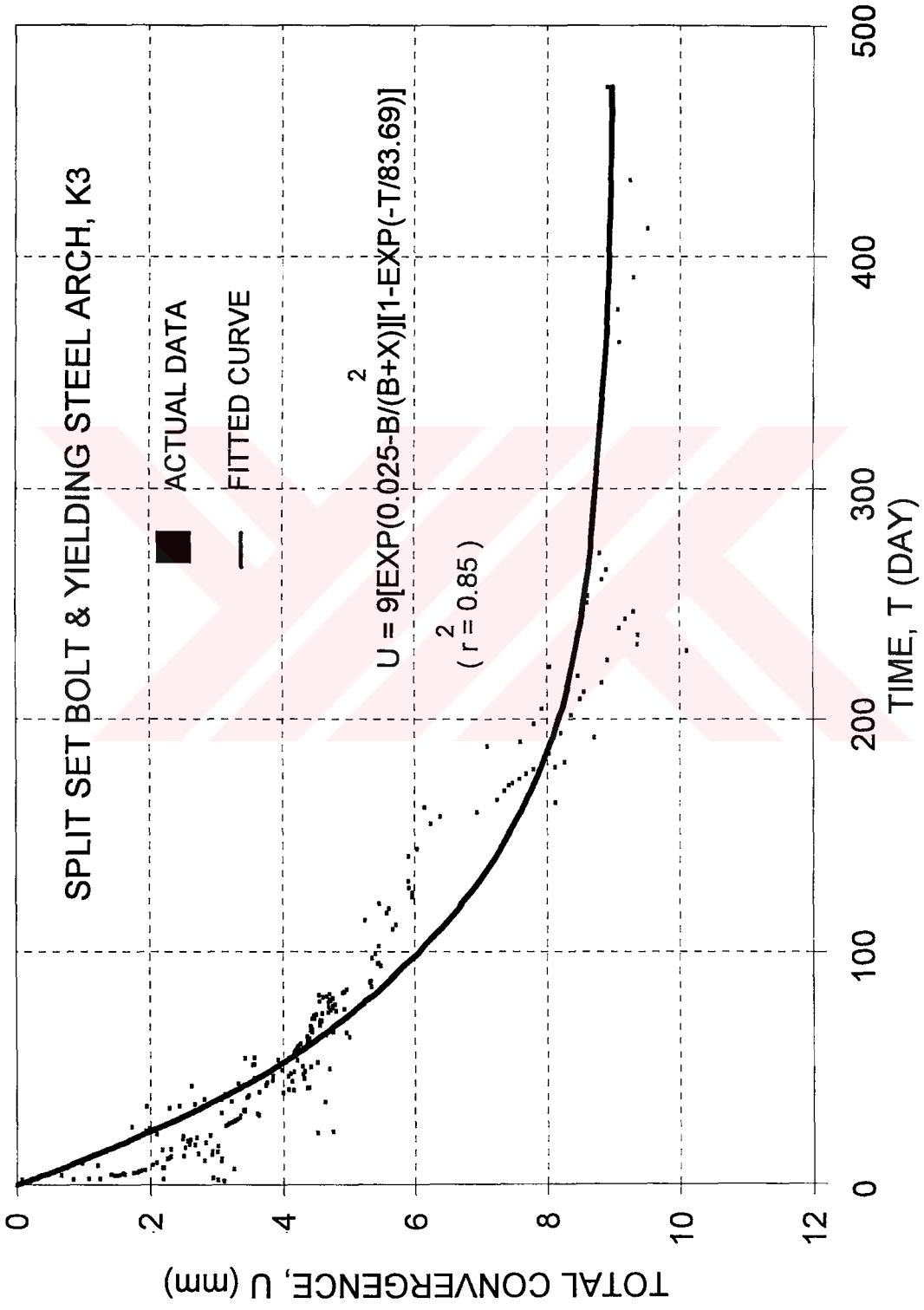
SPLIT SET BOLT & YIELDING STEEL ARCH, K3
ACTUAL DATA
FITTED CURVE
U = 9[EXP(0.025-B/(B+X))][1-EXP(-T/83.69)]
2
(r = 0.85)
2
TOTAL CONVERGENCE, U (mm)
TIME, T (DAY)
0
2
4
6
8
10
12
0
100
200
300
400
500

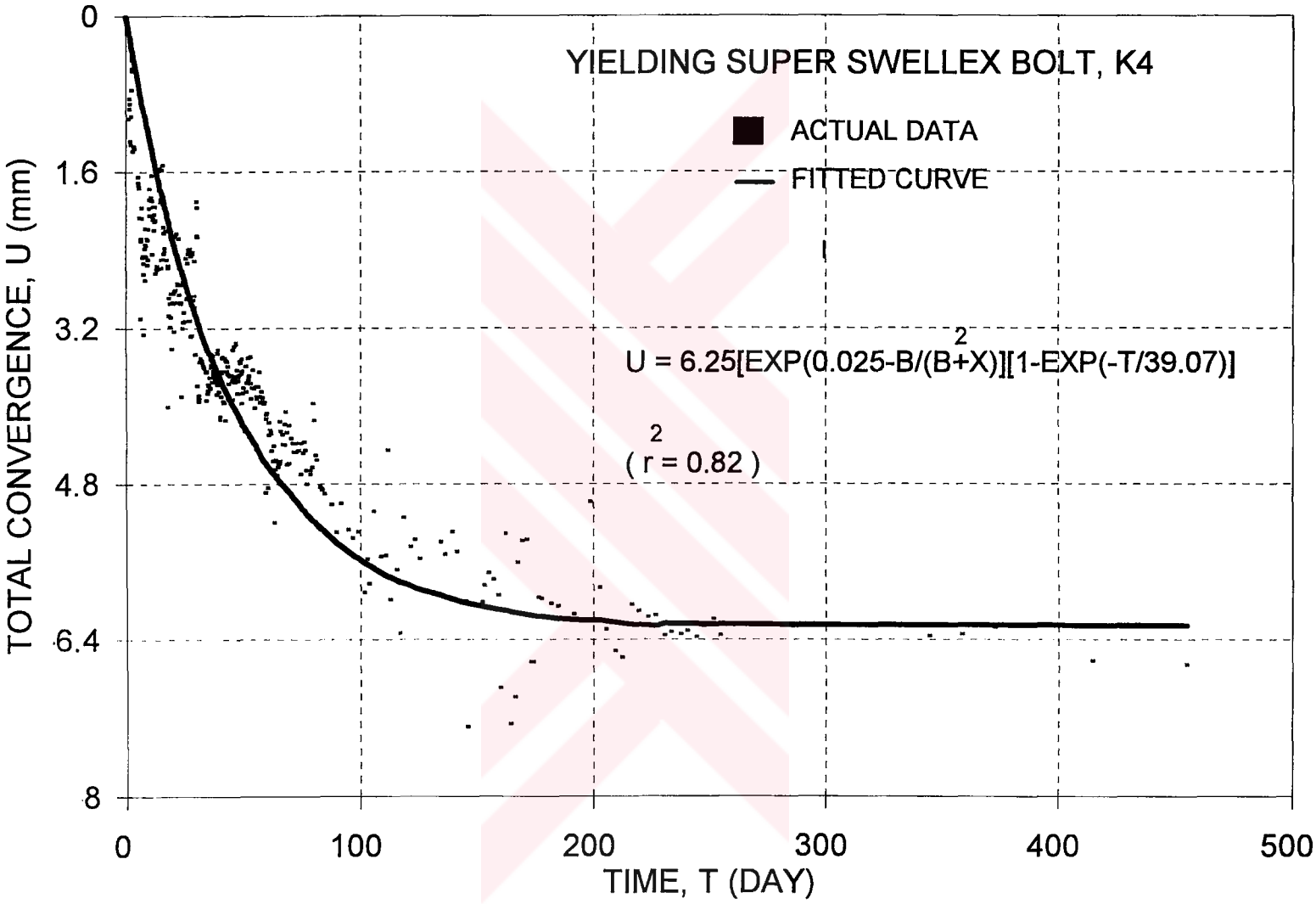
YIELDING SUPER SWELLEX BOLT, K4
ACTUAL DATA
FITTED CURVE
U = 6.25[EXP(0.025-B/(B+X)²)][1-EXP(-T/39.07)]
(r² = 0.82)
TOTAL CONVERGENCE, U (mm)
0
1.6
3.2
4.8
6.4
8
0
100
200
300
400
500
TIME, T (DAY)

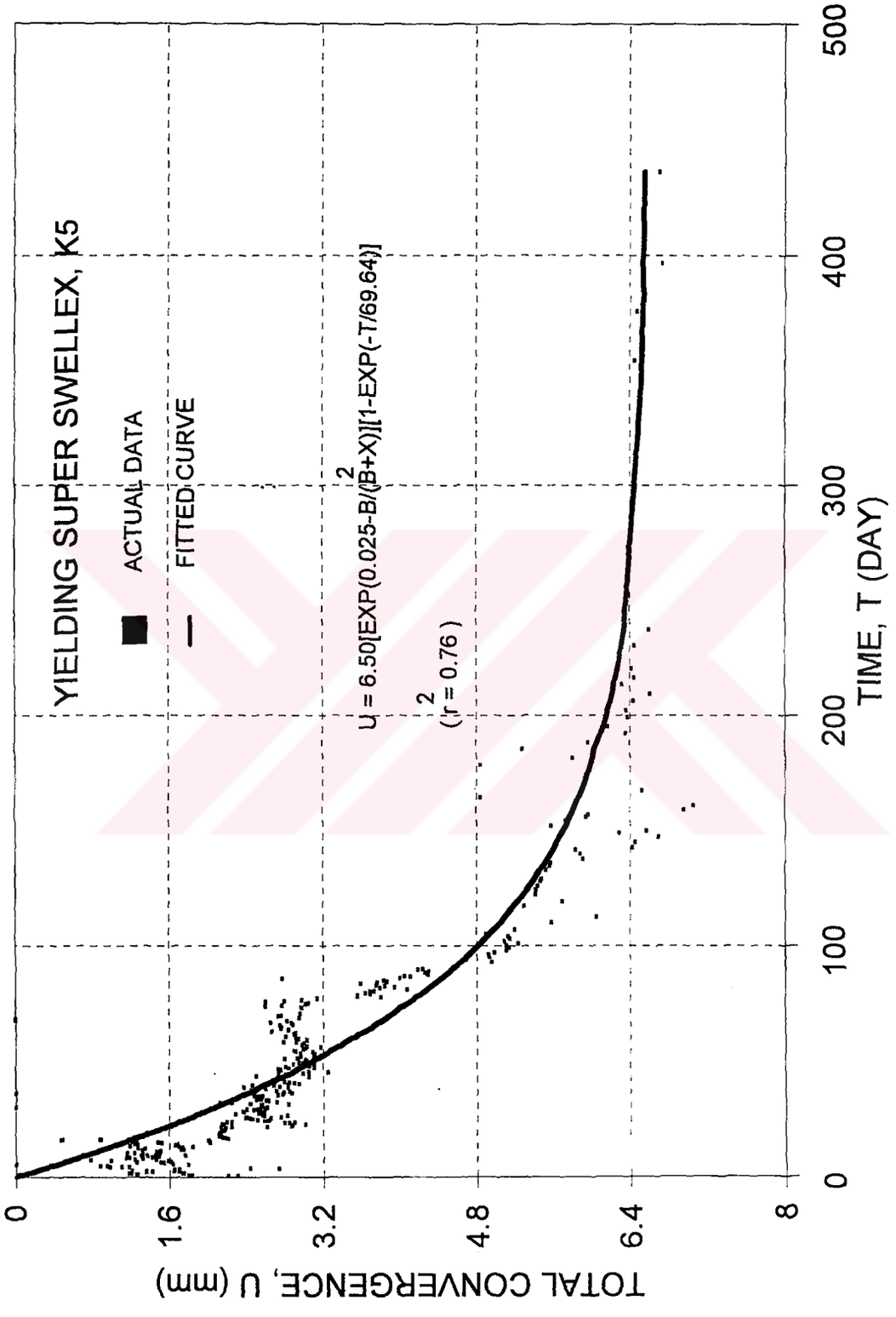
YIELDING SUPER SWELLEX, K5
ACTUAL DATA
FITTED CURVE
U = 6.50[EXP(0.025-B/(B+X))][1-EXP(-T/69.64)]
2
(r = 0.76)
2
TOTAL CONVERGENCE, U (mm)
TIME, T (DAY)
0
1.6
3.2
4.8
6.4
8
0
100
200
300
400
500

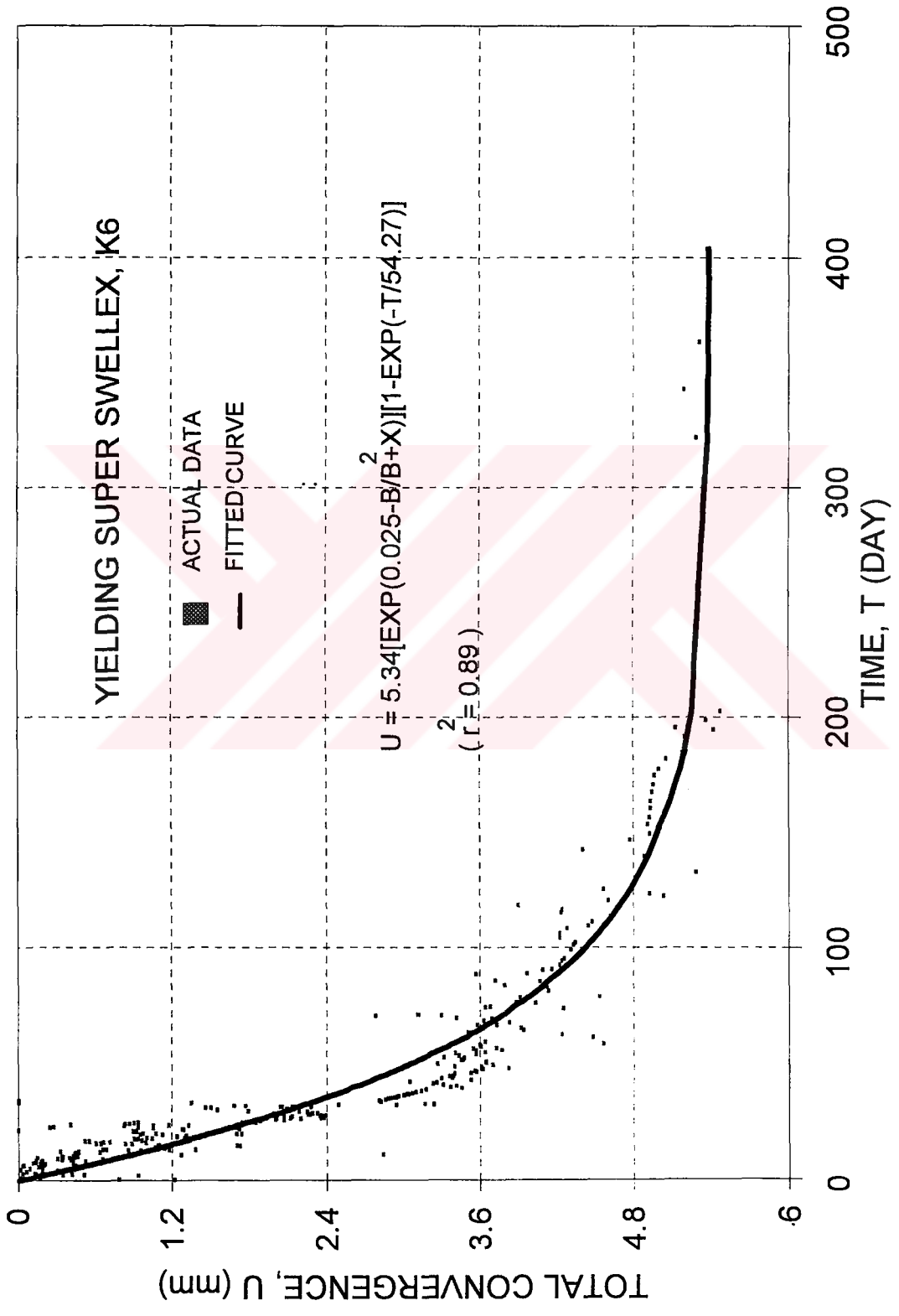
YIELDING SUPER SWELLEX, K6
ACTUAL DATA
FITTED CURVE
U = 5.34[EXP(0.025-B/B+X)][1-EXP(-T/54.27)]
2
(r = 0.89)
2
TOTAL CONVERGENCE, U (mm)
TIME, T (DAY)
0
1.2
2.4
3.6
4.8
.6
0
100
200
300
400
500

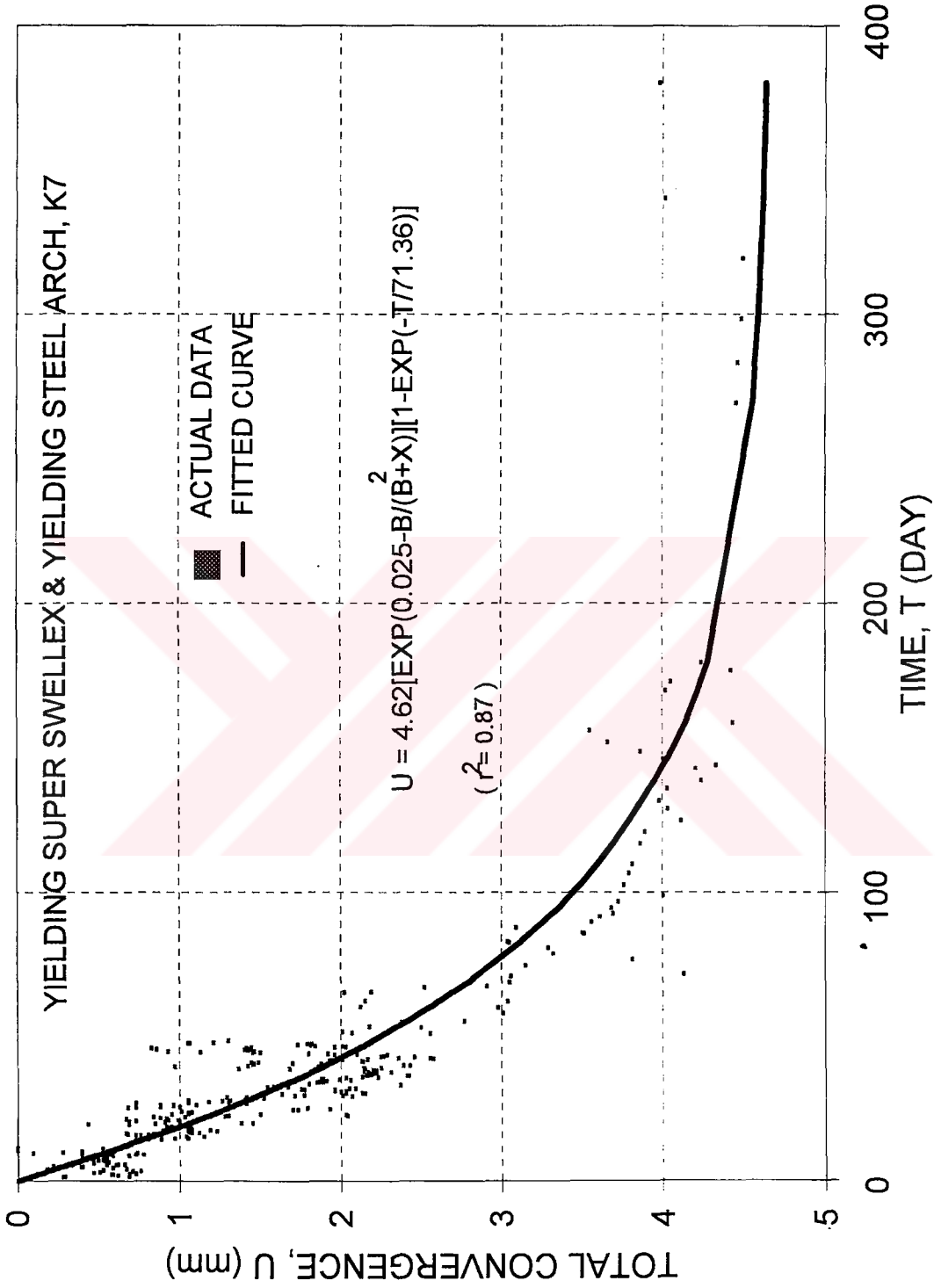
YIELDING SUPER SWELLEX & YIELDING STEEL ARCH, K7
ACTUAL DATA
FITTED CURVE
U = 4.62[EXP(0.025-B/(B+X)][1-EXP(-T/71.36)]
2
(r = 0.87)
TOTAL CONVERGENCE, U (mm)
TIME, T (DAY)
0
1
2
3
4
5
100
200
300
400

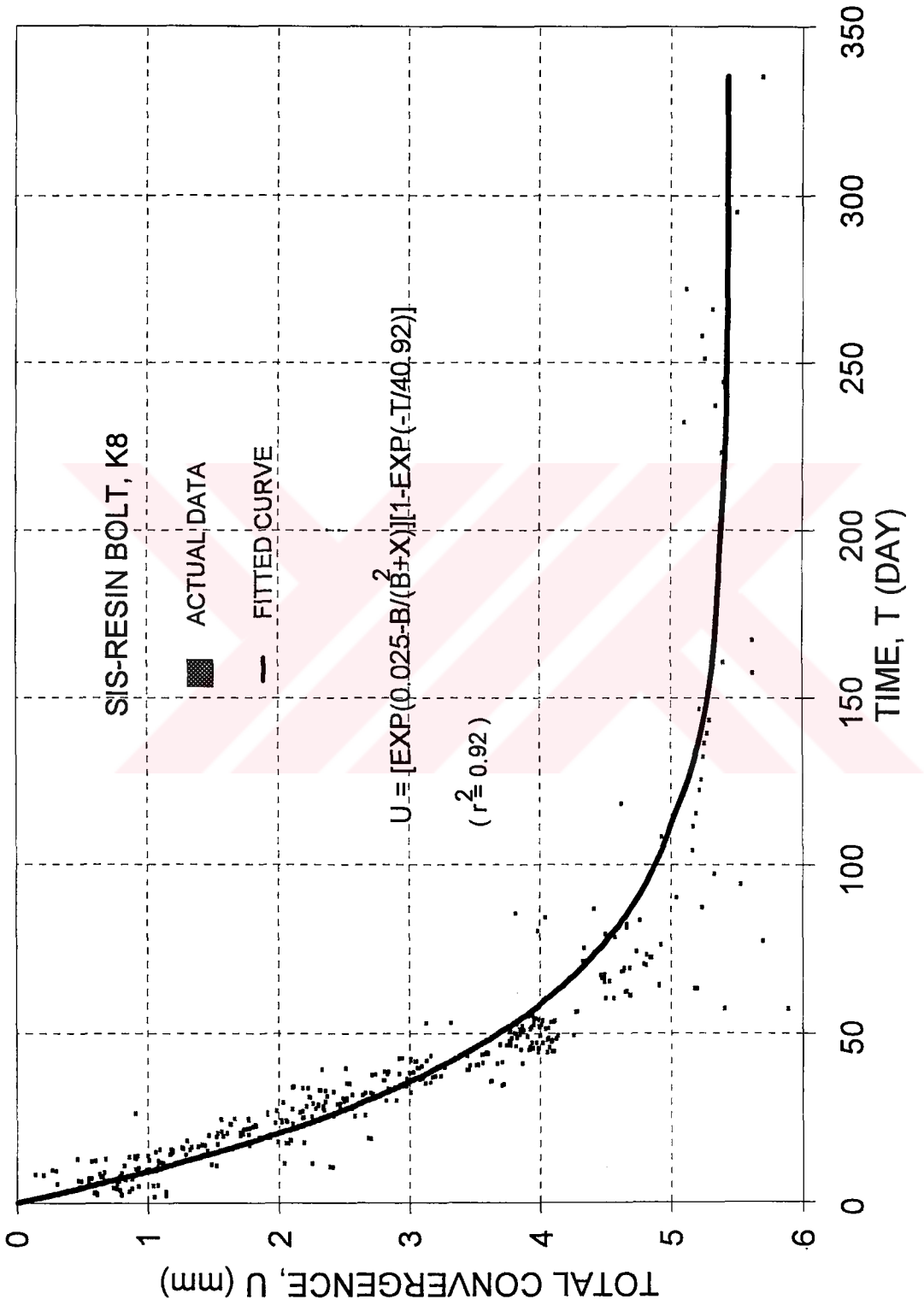
SIS-RESIN BOLT, K8
ACTUAL DATA
FITTED CURVE
U = [EXP(0.025-B/(B+X))][1-EXP(-T/40.92)]
(r2= 0.92)
TOTAL CONVERGENCE, U (mm)
TIME, T (DAY)
0
1
2
3
4
5
6
0
50
100
150
200
250
300
350

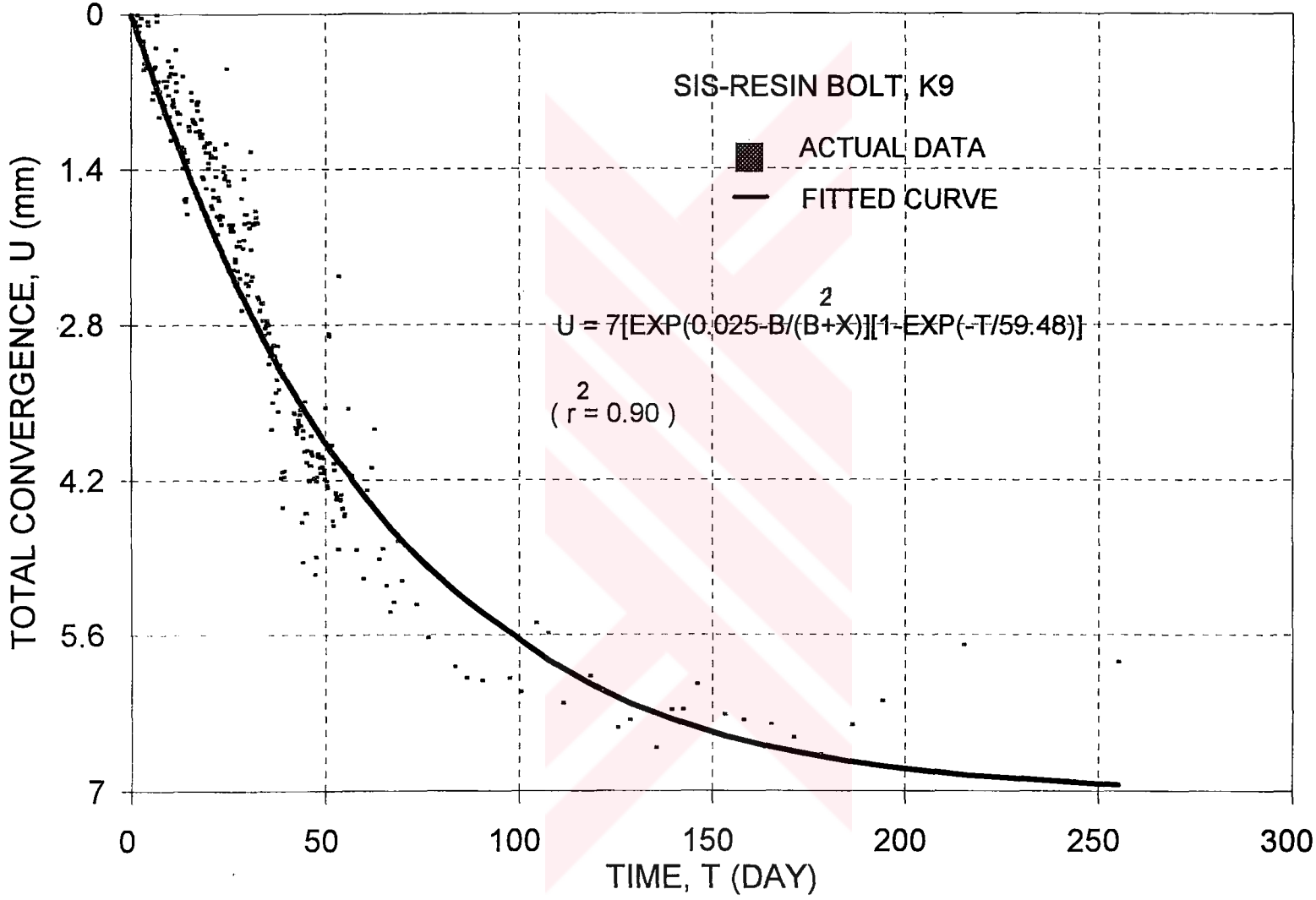
SIS-RESIN BOLT, K9
ACTUAL DATA
FITTED CURVE
U = 7[EXP(0.025-B/(B+X)][1-EXP(-T/59.48)]
2
(r = 0.90)
2
TOTAL CONVERGENCE, U (mm)
0
1.4
2.8
4.2
5.6
7
0
50
100
150
200
250
300
TIME, T (DAY)

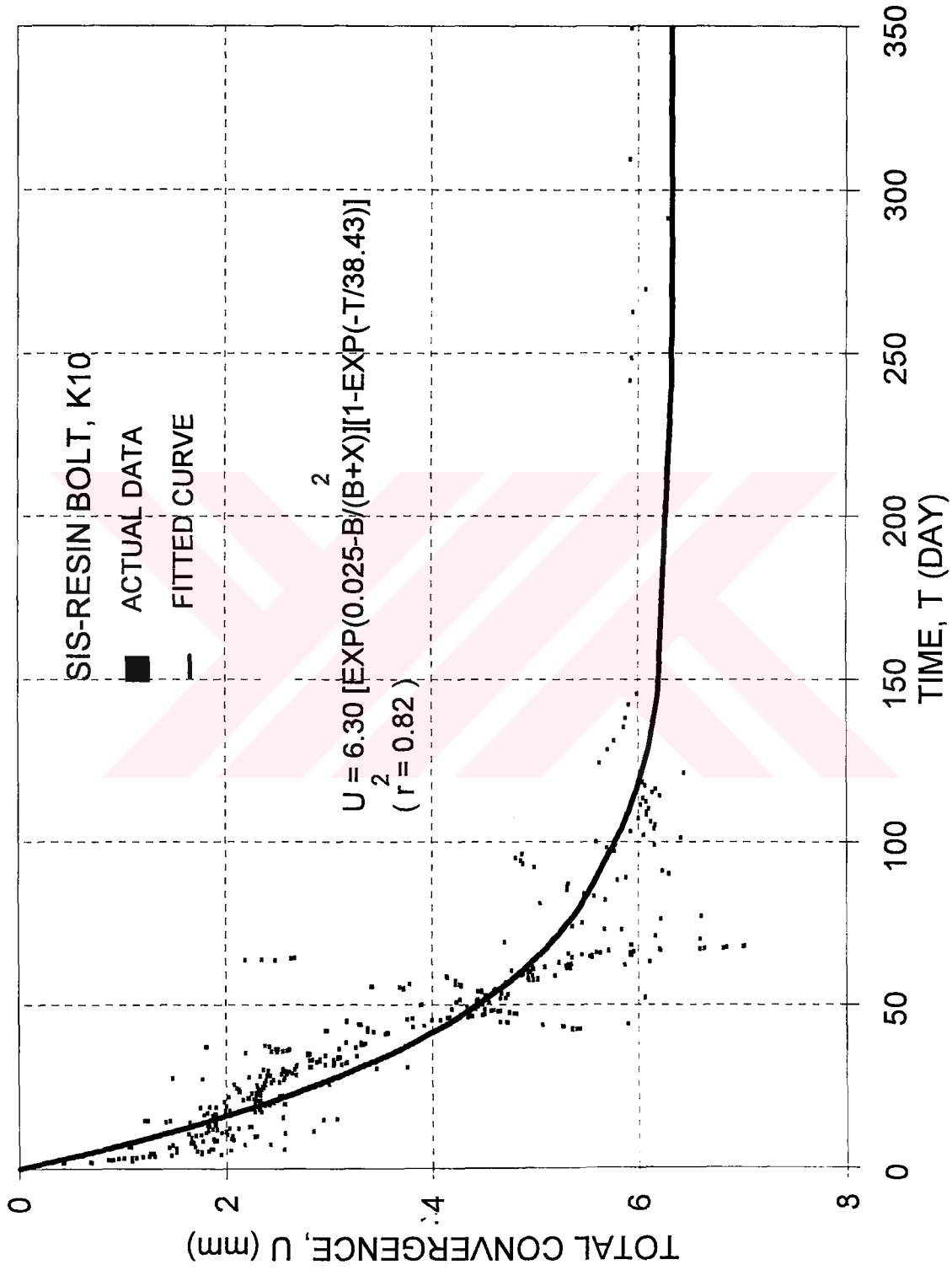
SIS-RESIN BOLT, K10
ACTUAL DATA
FITTED CURVE
U = 6.30 [EXP(0.025-B/(B+X))][1-EXP(-T/38.43)]
2
(r = 0.82)
2
TOTAL CONVERGENCE, U (mm)
TIME, T (DAY)
0
2
4
6
8
0
50
100
150
200
250
300
350

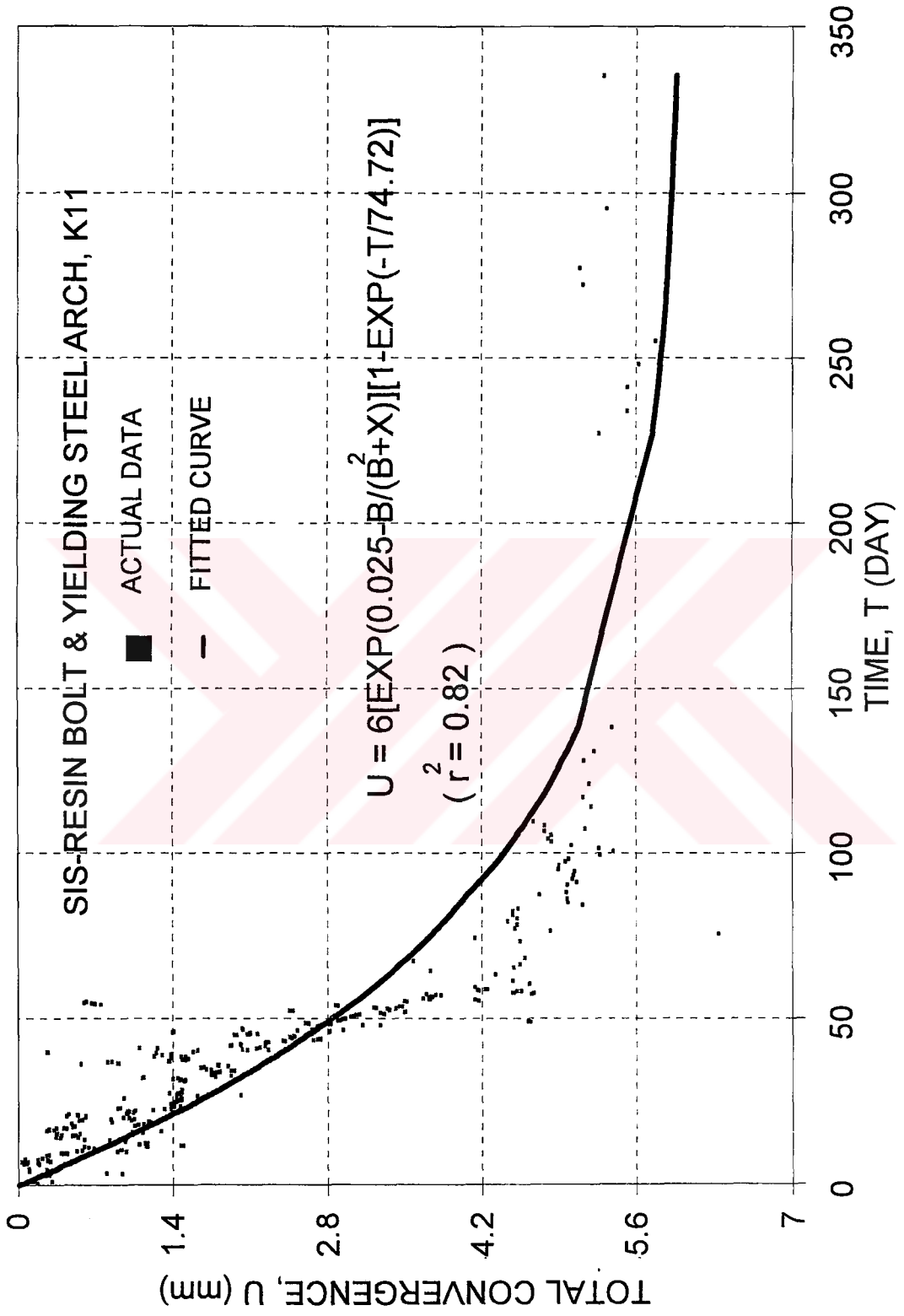
SIS-RESIN BOLT & YIELDING STEEL ARCH, K11
ACTUAL DATA
FITTED CURVE
U = 6[EXP(0.025-B/(B+X))][1-EXP(-T/74.72)]
(r = 0.82)
2
TOTAL CONVERGENCE, U (mm)
0
1.4
2.8
4.2
5.6
7
0
50
100
150
200
250
300
350
TIME, T (DAY)

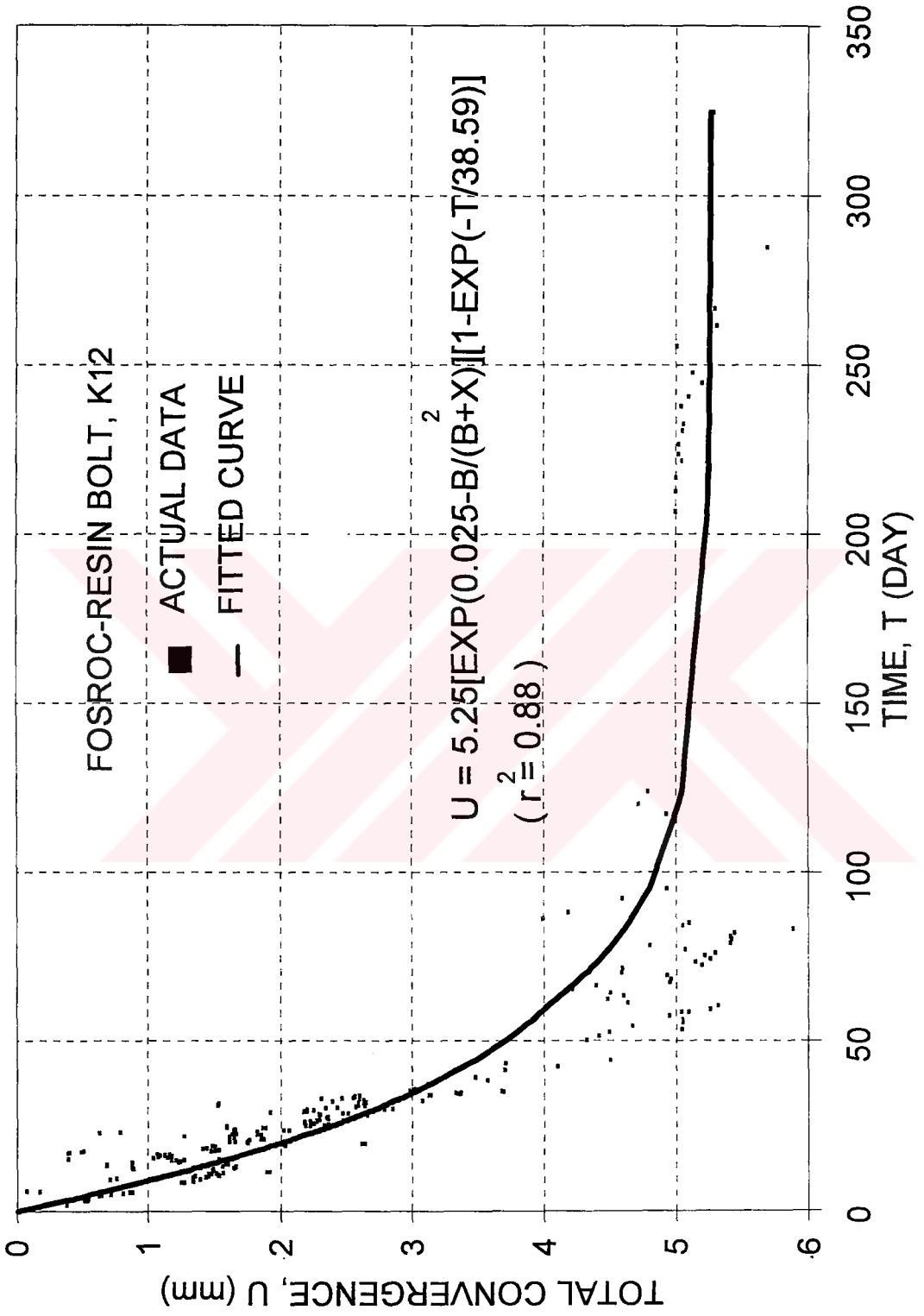
FOSROC-RESIN BOLT, K12
ACTUAL DATA
FITTED CURVE
U = 5.25[EXP(0.025-B/(B+X))][1-EXP(-T/38.59)]
2
(r = 0.88)
2
TOTAL CONVERGENCE, U (mm)
TIME, T (DAY)
0
1
2
3
4
5
6
0
50
100
150
200
250
300
350

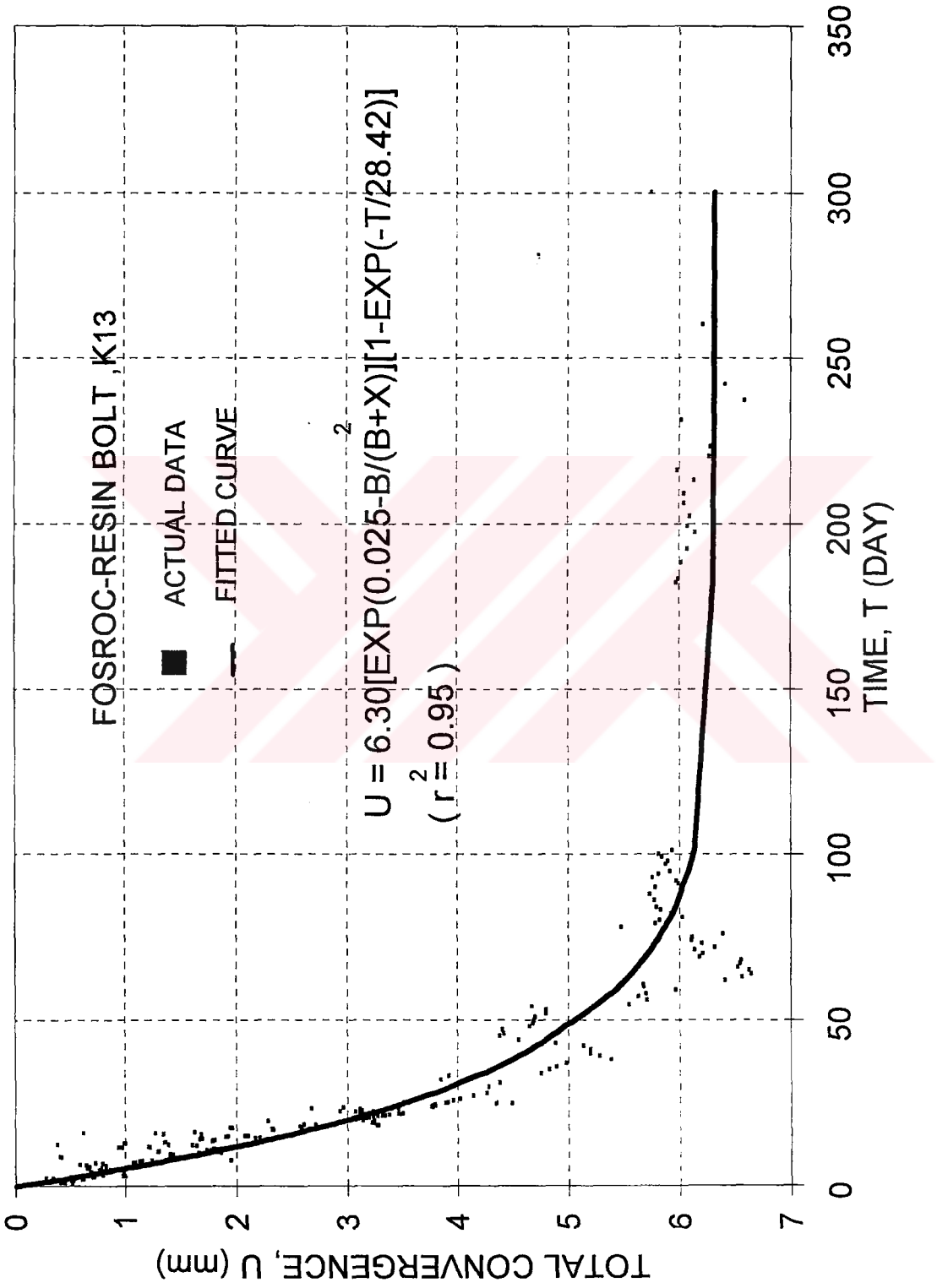
FOSROC-RESIN BOLT ,K13
ACTUAL DATA
FITTED CURVE
U = 6.30[EXP(0.025-B/(B+X))][1-EXP(-T/28.42)]
(r² = 0.95)
TOTAL CONVERGENCE, U (mm)
TIME, T (DAY)
0
1
2
3
4
5
6
7
0
50
100
150
200
250
300
350

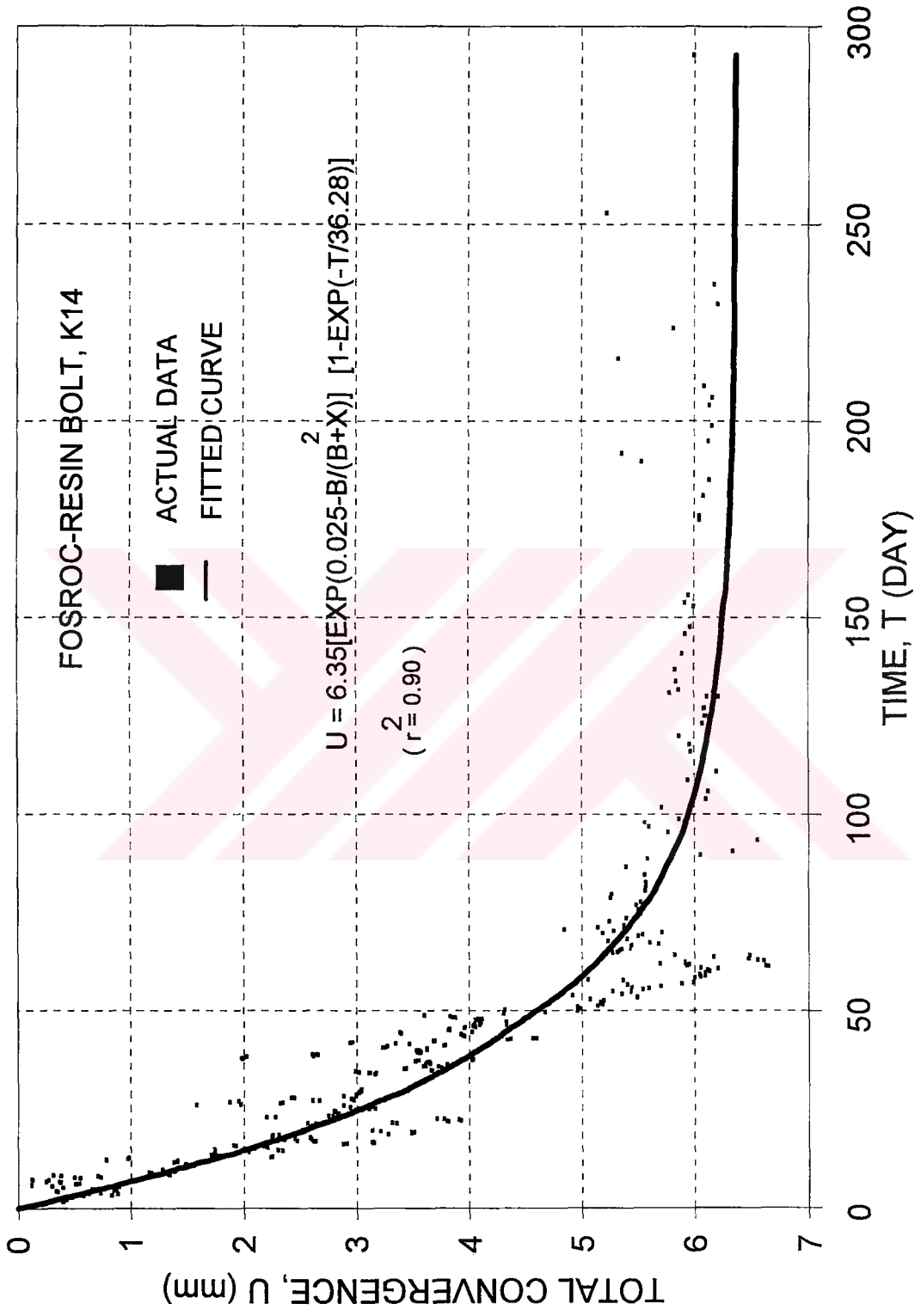
FOSROC-RESIN BOLT, K14
ACTUAL DATA
FITTED CURVE
U = 6.35[EXP(0.025-B/(B+X))]^2 [1-EXP(-T/36.28)]
(r^2 = 0.90)
TOTAL CONVERGENCE, U (mm)
TIME, T (DAY)
0
1
2
3
4
5
6
7
0
50
100
150
200
250
300

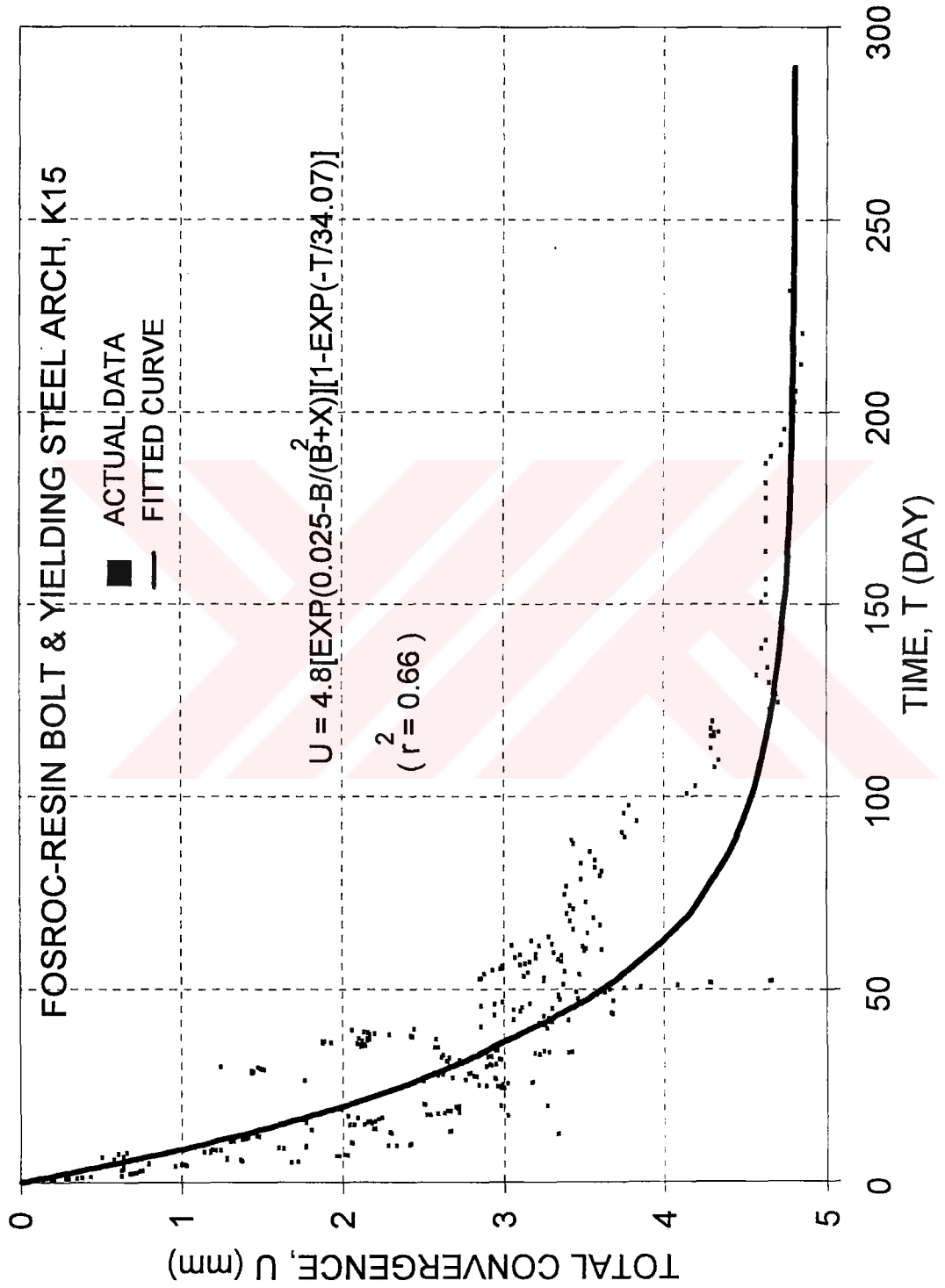
FOSROC-RESIN BOLT & YIELDING STEEL ARCH, K15
ACTUAL DATA
FITTED CURVE
U = 4.8[EXP(0.025-B/(B+X))][1-EXP(-T/34.07)]
(r = 0.66)
TOTAL CONVERGENCE, U (mm)
TIME, T (DAY)
0
1
2
3
4
5
0
50
100
150
200
250
300

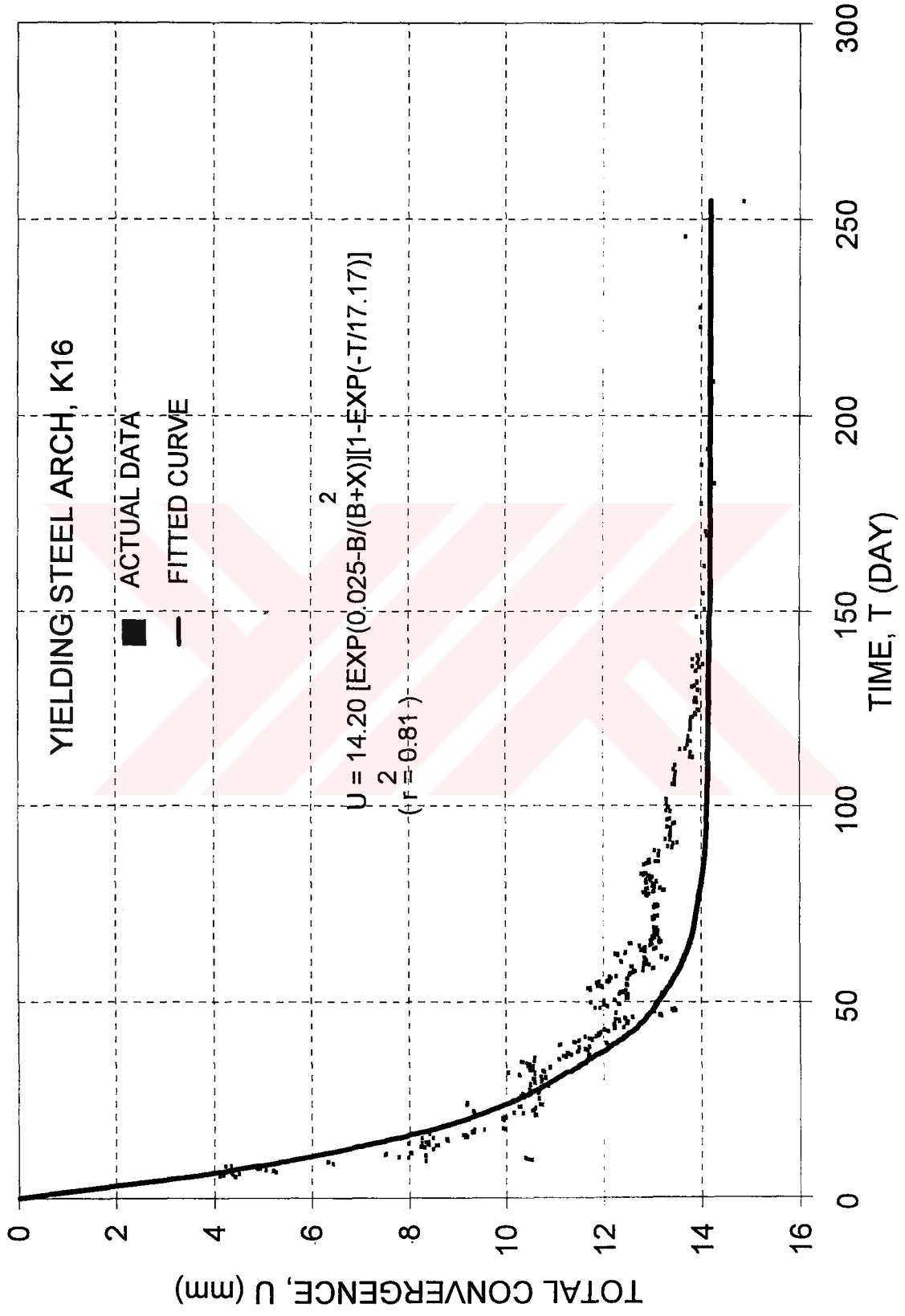
YIELDING STEEL ARCH, K16
ACTUAL DATA
FITTED CURVE
U = 14.20 [EXP(0.025-B/(B+X))][1-EXP(-T/17.17)]
2
(r = 0.81)
2
TOTAL CONVERGENCE, U (mm)
TIME, T (DAY)
0
2
4
6
8
10
12
14
16
0
50
100
150
200
250
300

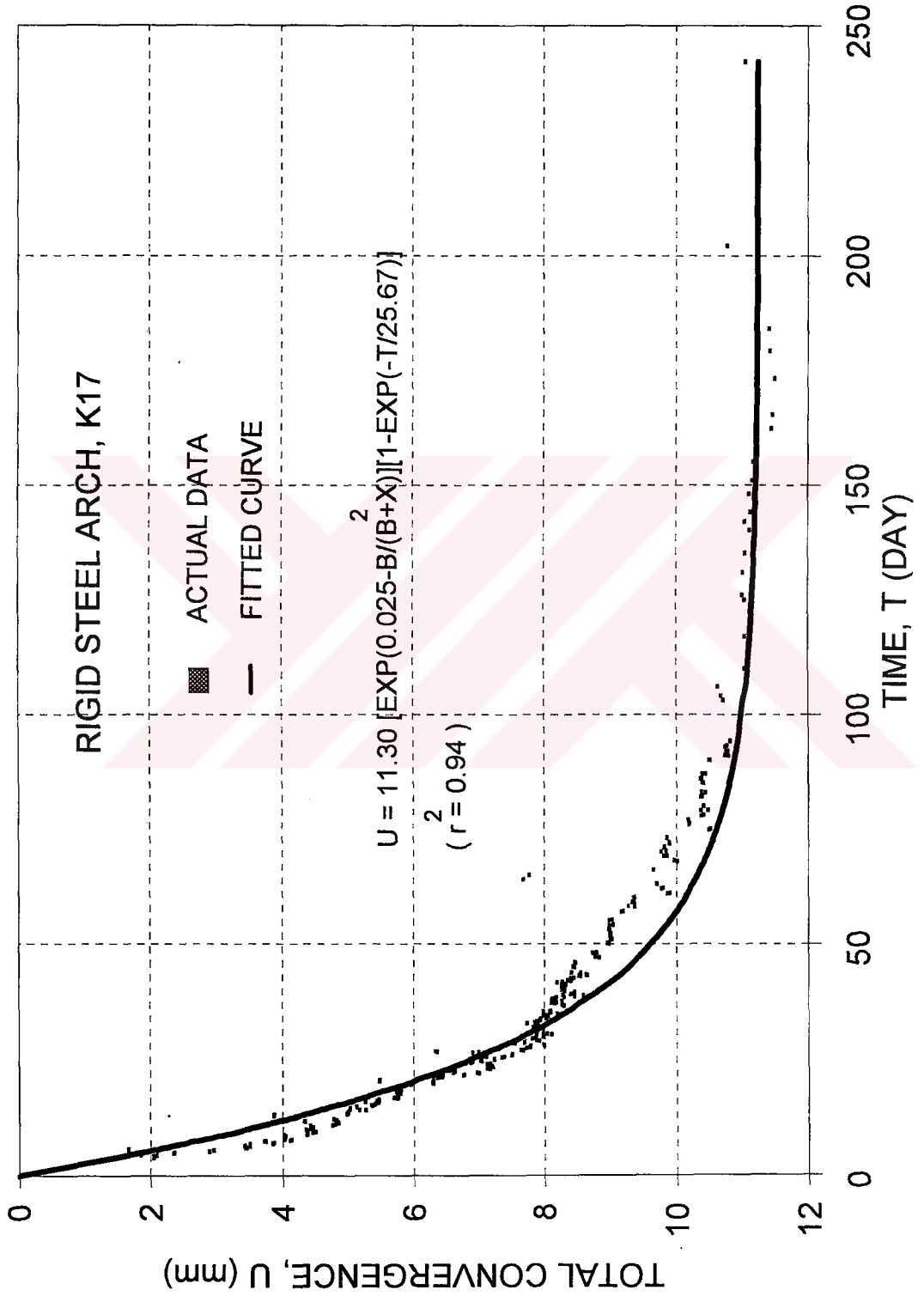
RIGID STEEL ARCH, K17
ACTUAL DATA
FITTED CURVE
U = 11.30 [EXP(0.025-B/(B+X))][1-EXP(-T/25.67)]
2
(r = 0.94)
2
TOTAL CONVERGENCE, U (mm)
TIME, T (DAY)
0
2
4
6
8
10
12
0
50
100
150
200
250

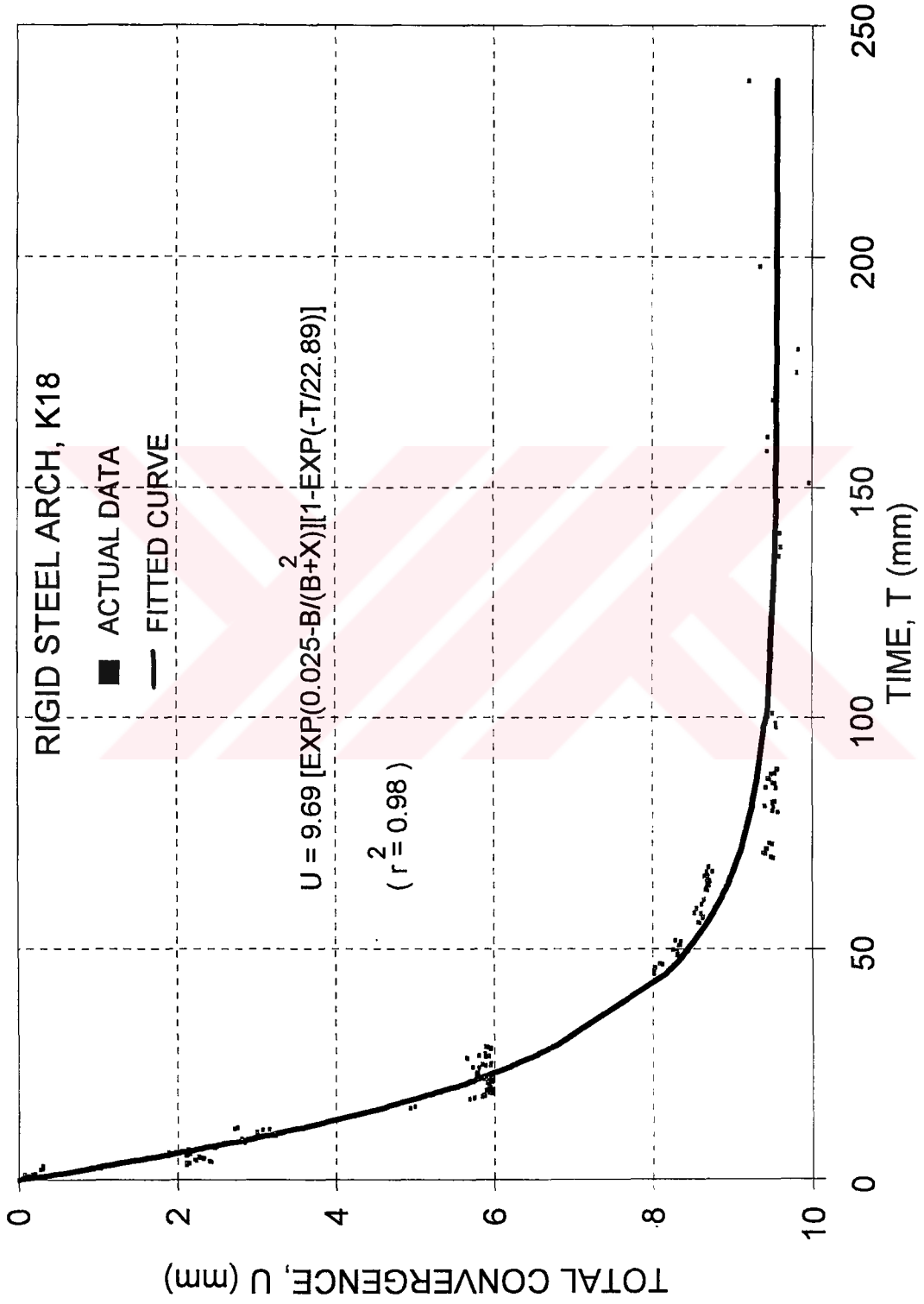
RIGID STEEL ARCH, K18
ACTUAL DATA
FITTED CURVE
U = 9.69 [EXP(0.025-B/(B+X)][1-EXP(-T/22.89)]
2
(r = 0.98)
TOTAL CONVERGENCE, U (mm)
TIME, T (mm)
0
2
4
6
8
10
0
50
100
150
200
250

APPENDIX E

CONVERGENCE-VELOCITY CURVES FOR

DIFFERENT SUPPORTED REGIONS

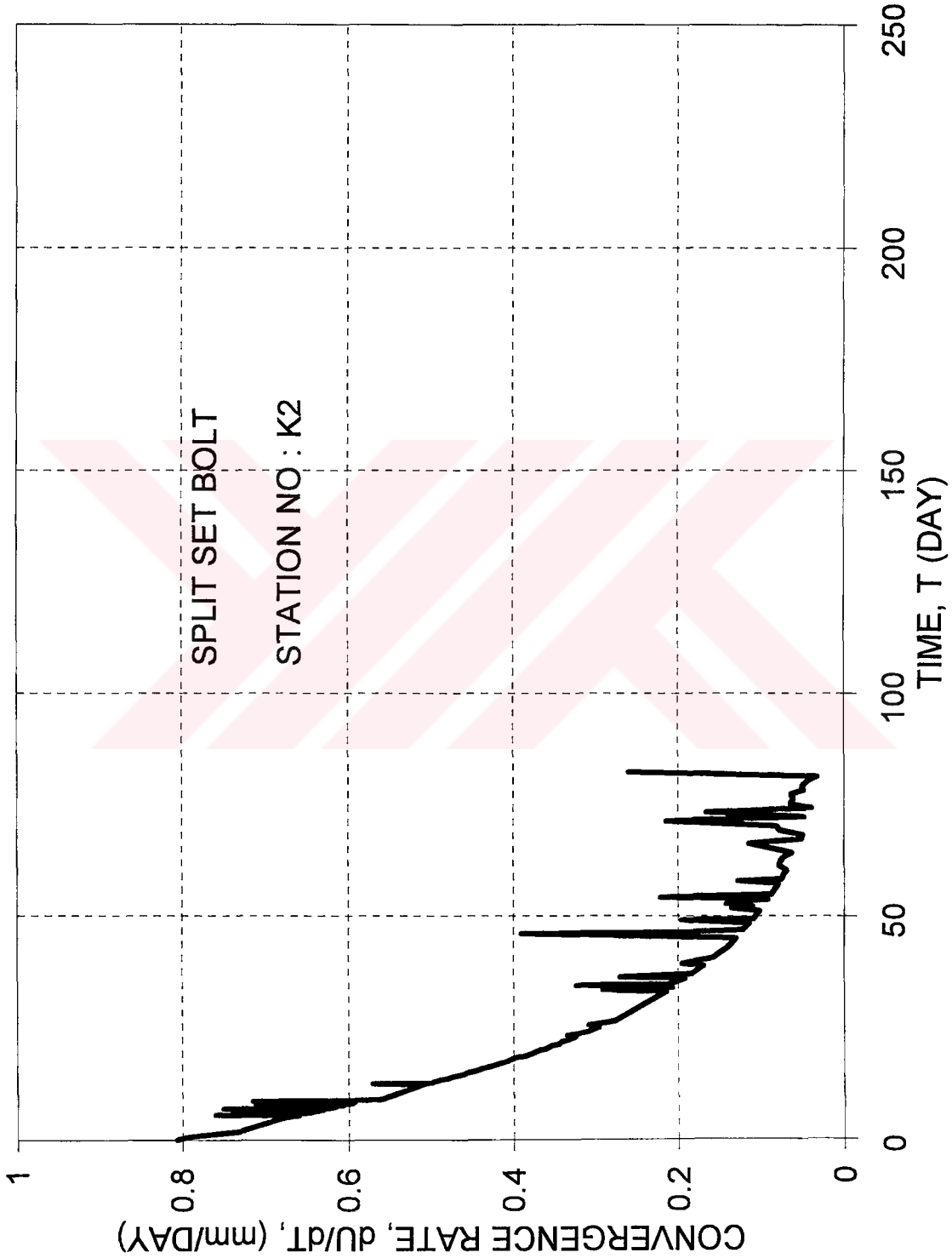
SPLIT SET BOLT
STATION NO : K2
CONVERGENCE RATE, dU/dT, (mm/DAY)
TIME, T (DAY)
0
0.2
0.4
0.6
0.8
1
0
50
100
150
200
250

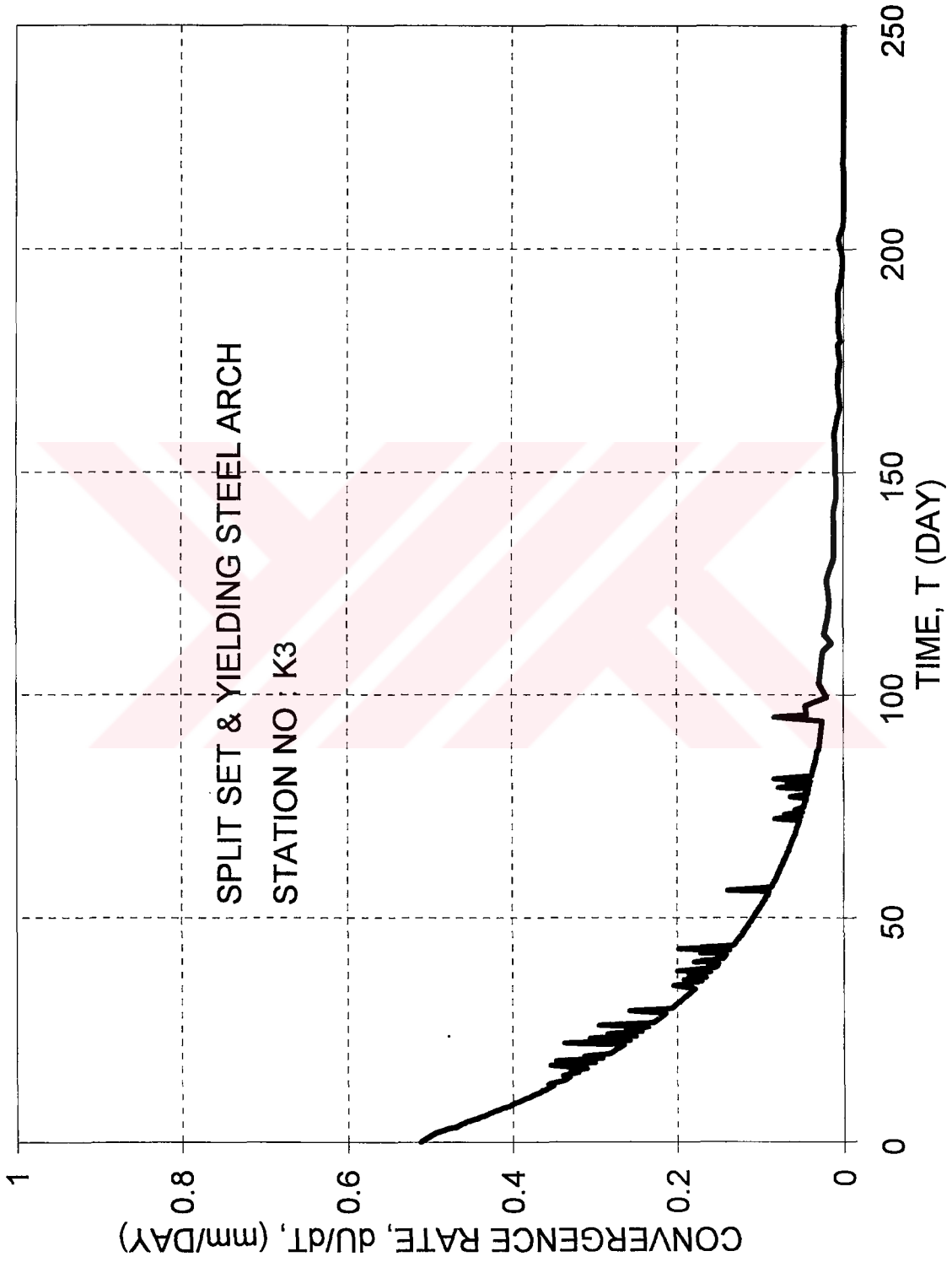
SPLIT SET & YIELDING STEEL ARCH
STATION NO : K3
CONVERGENCE RATE, dU/dT, (mm/DAY)
TIME, T (DAY)
0
0.2
0.4
0.6
0.8
1
0
50
100
150
200
250

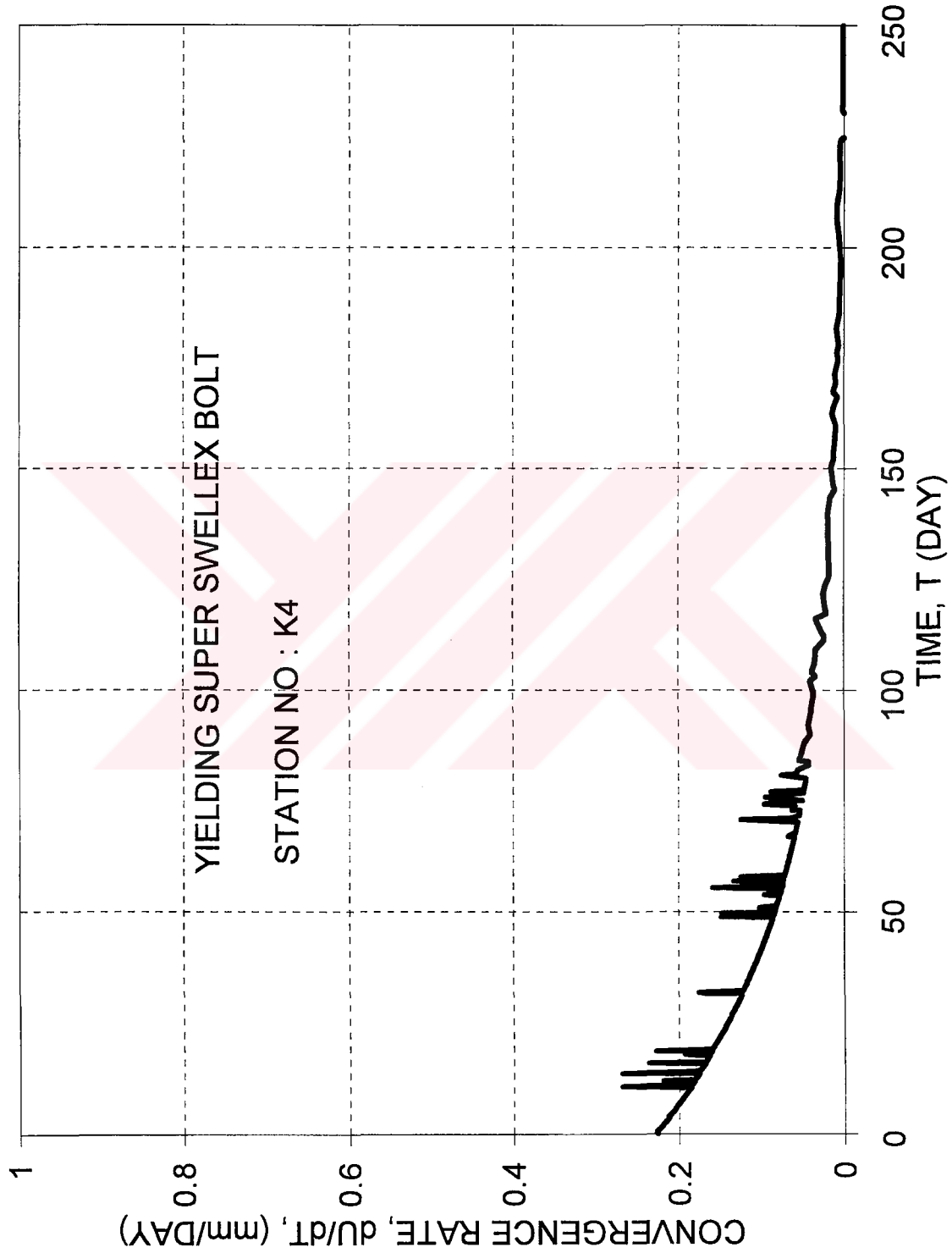
YIELDING SUPER SWELLEX BOLT
STATION NO : K4
CONVERGENCE RATE, dU/dT, (mm/DAY)
TIME, T (DAY)
0
0.2
0.4
0.6
0.8
1
0
50
100
150
200
250

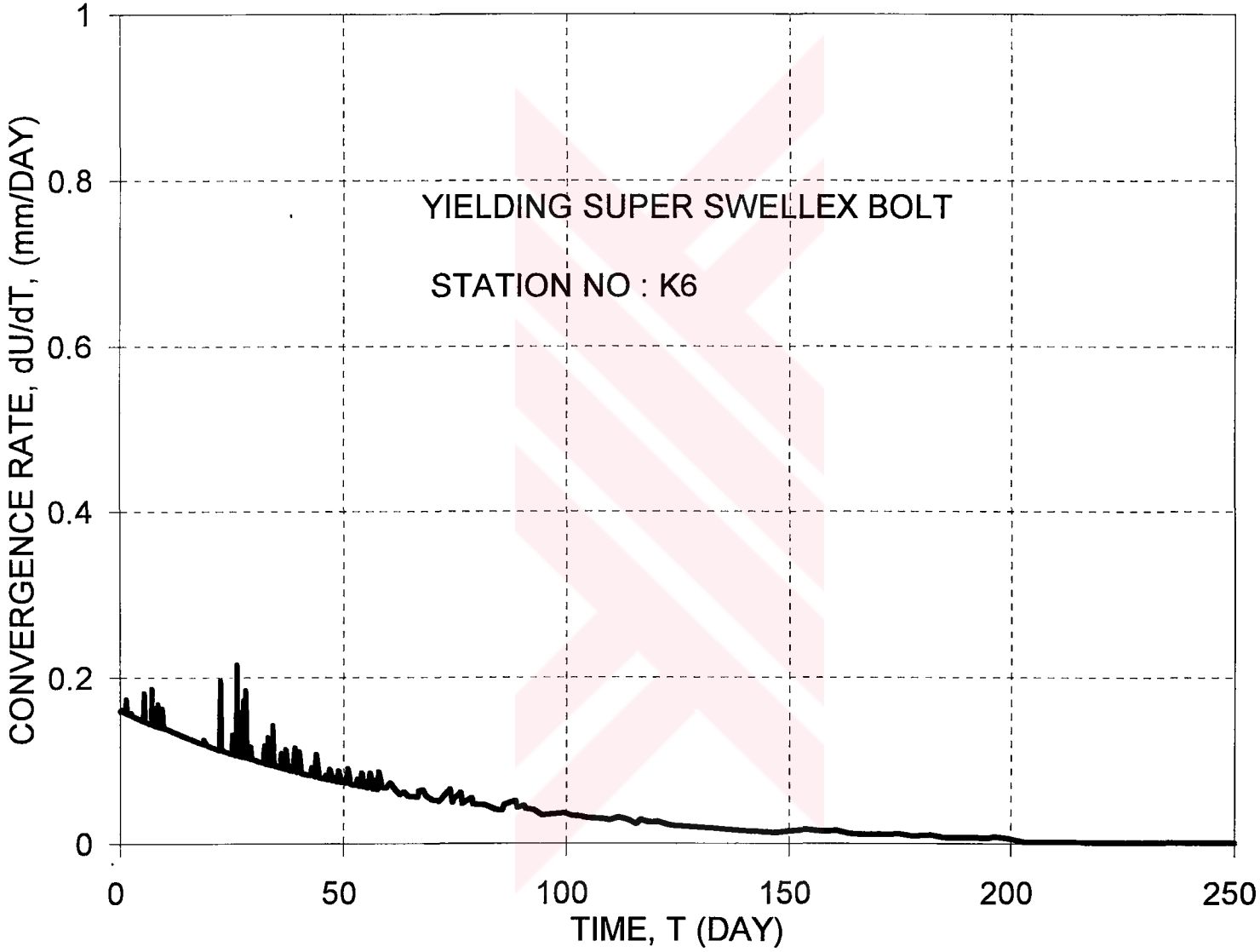
YIELDING SUPER SWELLEX BOLT
STATION NO : K6
CONVERGENCE RATE, dU/dT, (mm/DAY)
TIME, T (DAY)
1
0.8
0.6
0.4
0.2
0
0
50
100
150
200
250

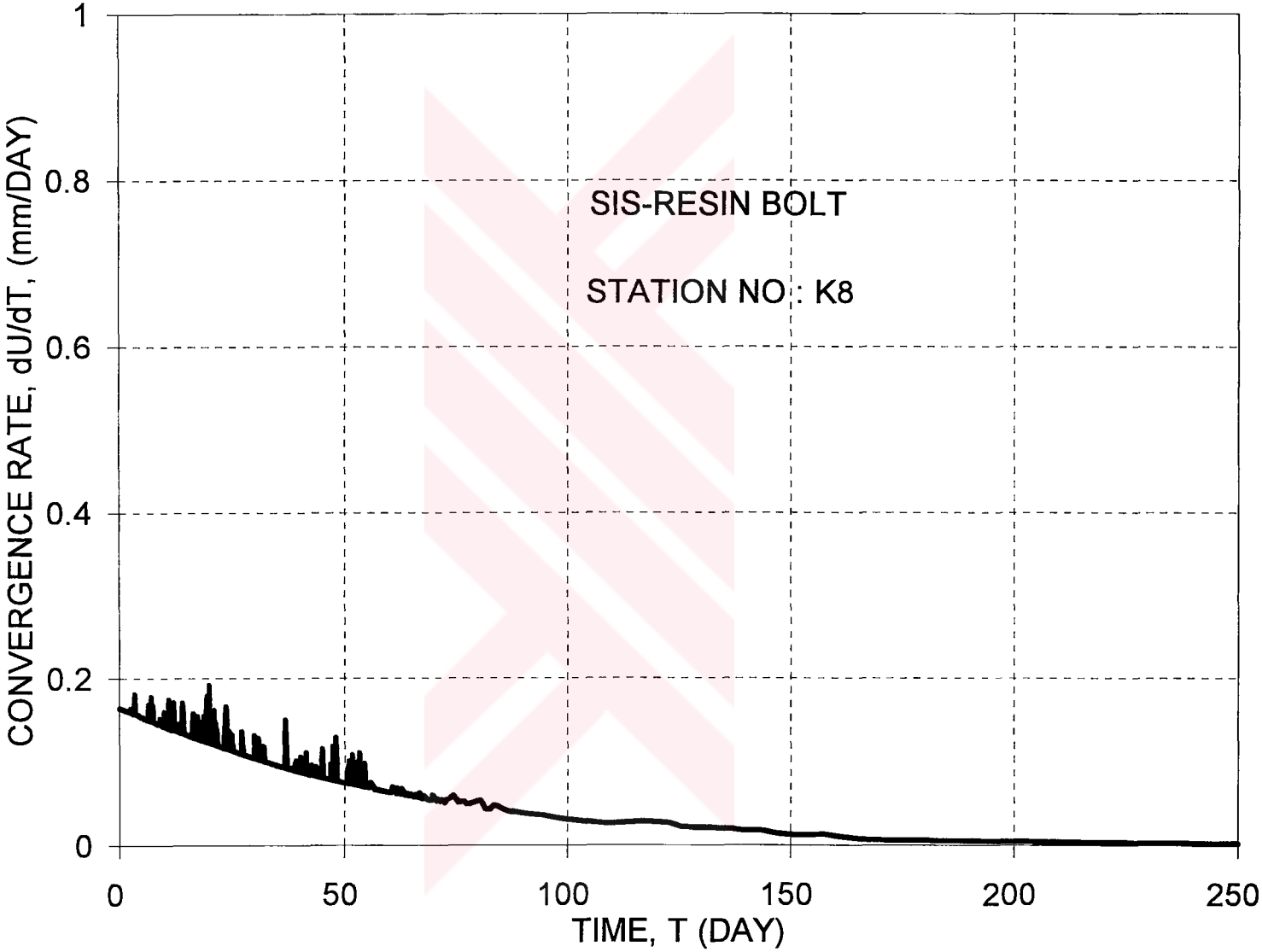
SIS-RESIN BOLT
STATION NO : K8
CONVERGENCE RATE, dU/dT, (mm/DAY)
TIME, T (DAY)
1
0.8
0.6
0.4
0.2
0
0
50
100
150
200
250

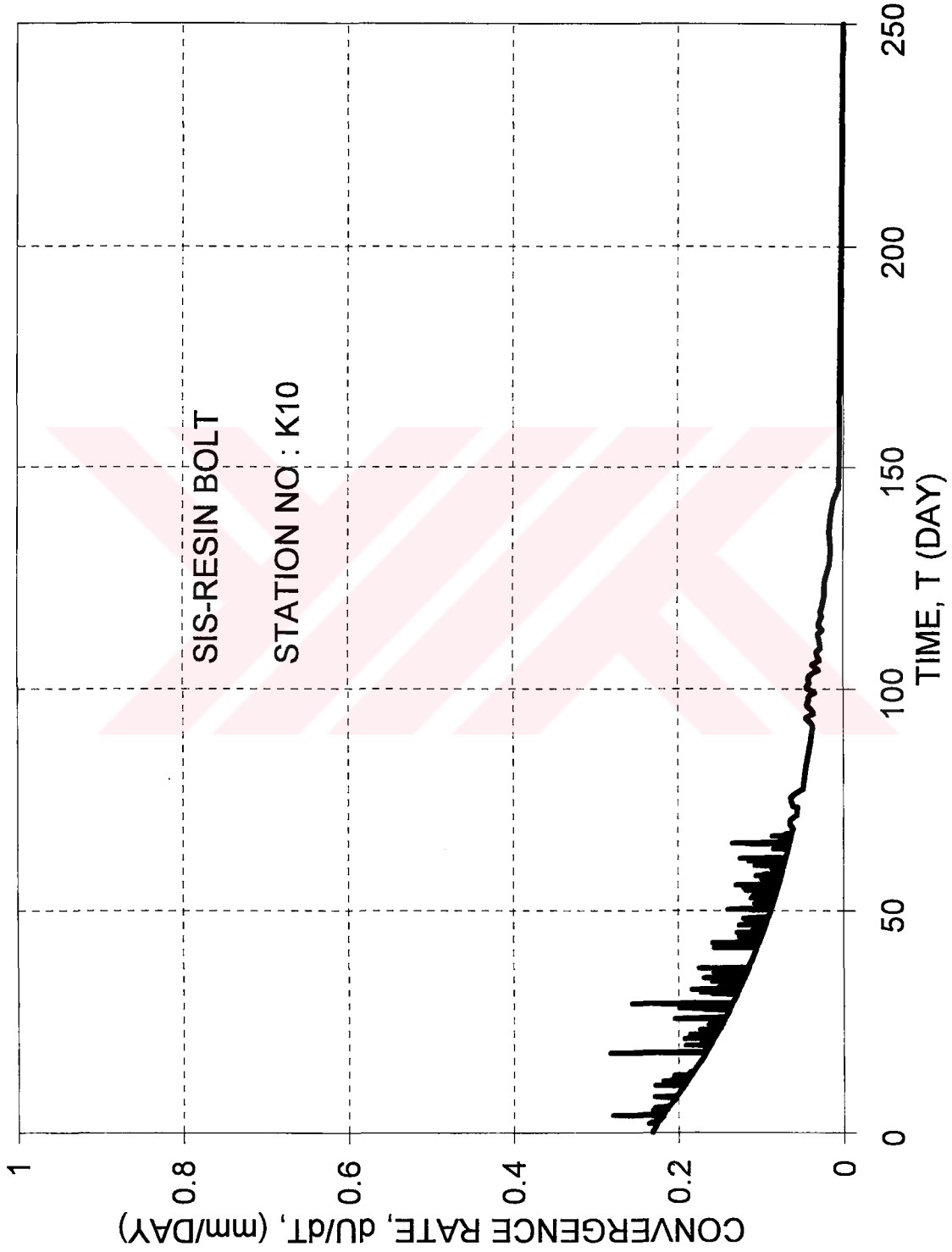
SIS-RESIN BOLT
STATION NO : K10
CONVERGENCE RATE, dU/dT, (mm/DAY)
TIME, T (DAY)
0
0.2
0.4
0.6
0.8
1
0
50
100
150
200
250

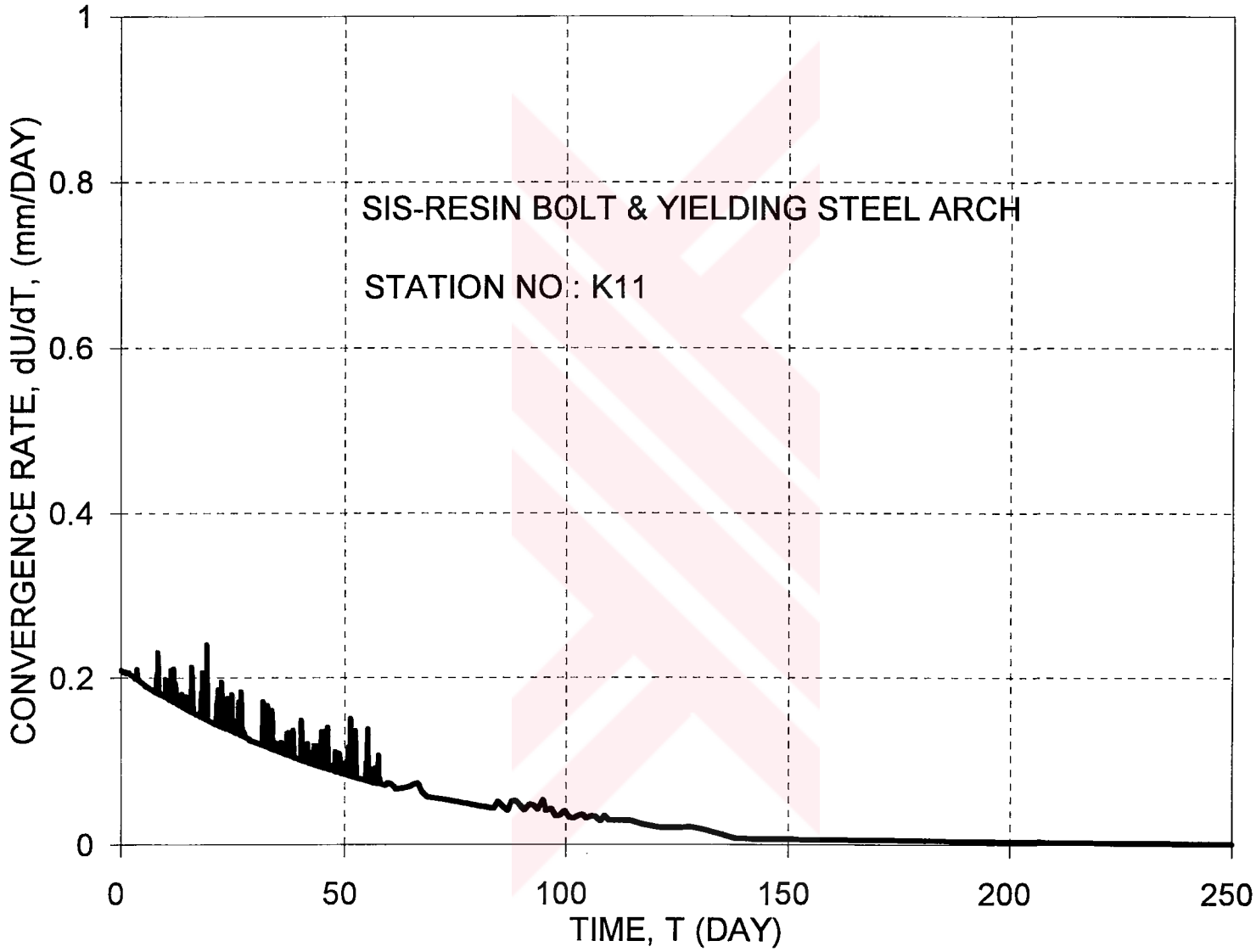
SIS-RESIN BOLT & YIELDING STEEL ARCH
STATION NO : K11
CONVERGENCE RATE, dU/dT, (mm/DAY)
TIME, T (DAY)
1
0.8
0.6
0.4
0.2
0
0
50
100
150
200
250

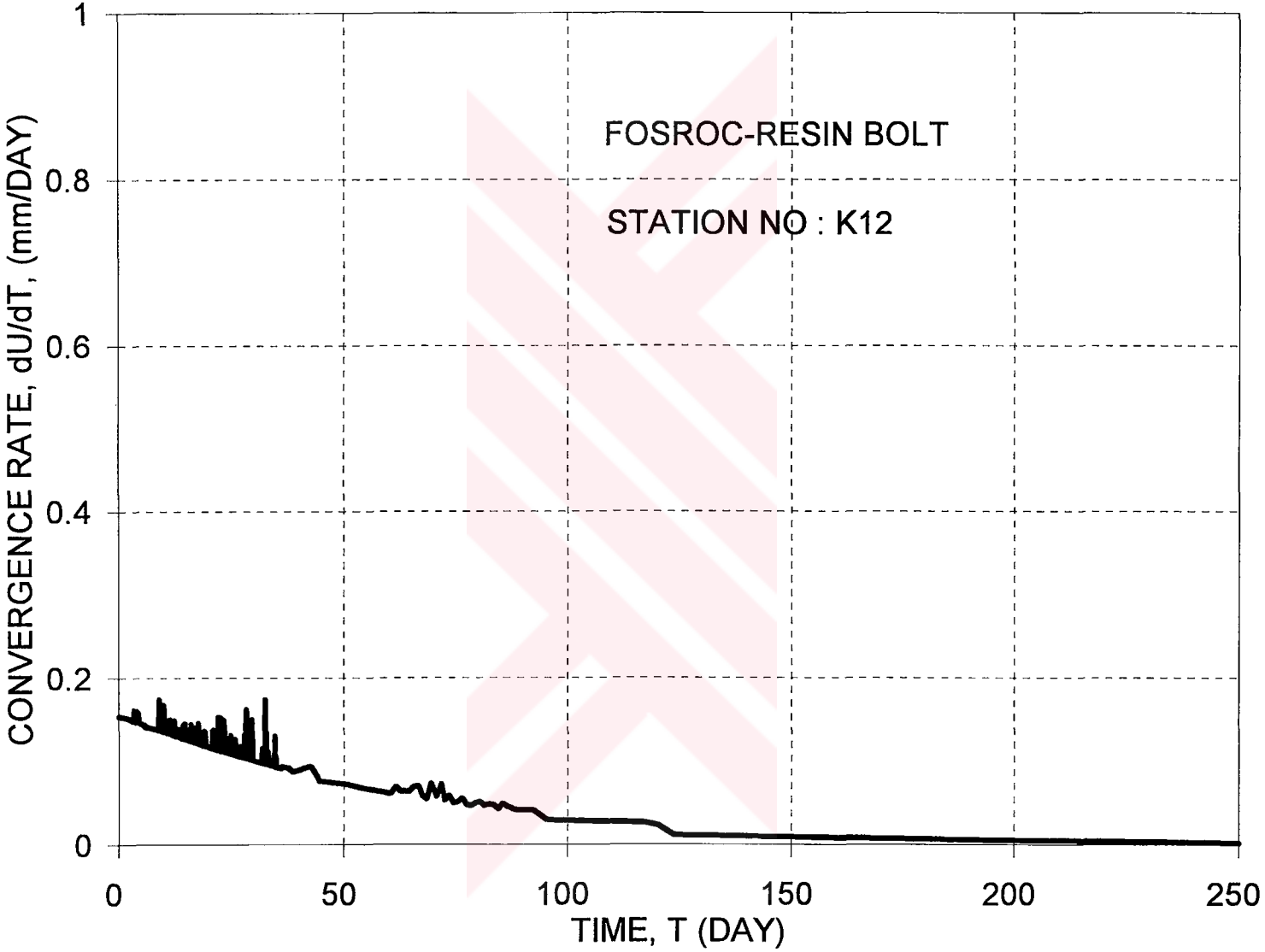
FOSROC-RESIN BOLT
STATION NO : K12
CONVERGENCE RATE, dU/dT, (mm/DAY)
TIME, T (DAY)
1
0.8
0.6
0.4
0.2
0
0
50
100
150
200
250

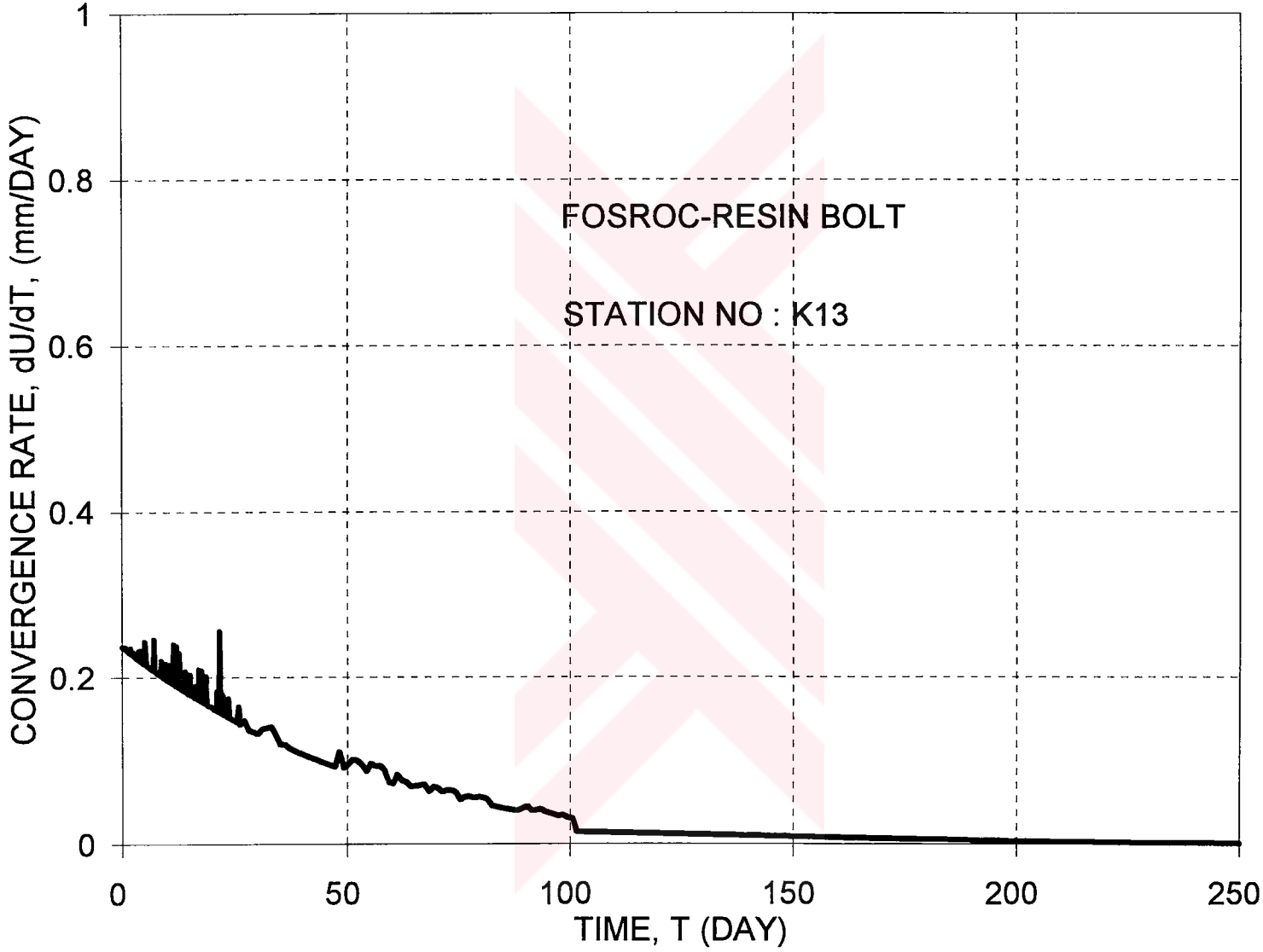
FOSROC-RESIN BOLT
STATION NO : K13
CONVERGENCE RATE, dU/dT, (mm/DAY)
TIME, T (DAY)
0
0.2
0.4
0.6
0.8
1
0
50
100
150
200
250

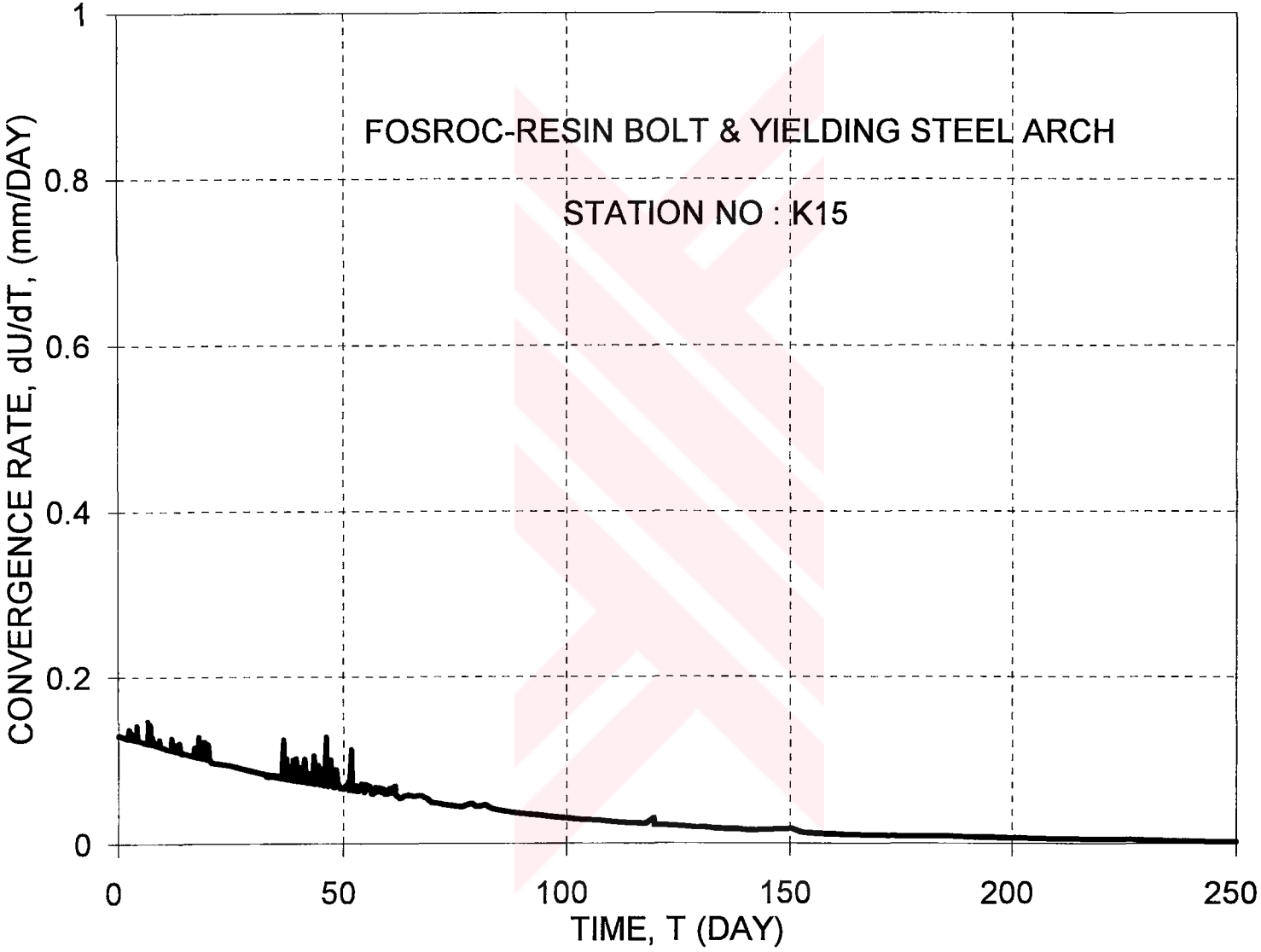
FOSROC-RESIN BOLT & YIELDING STEEL ARCH
STATION NO : K15
CONVERGENCE RATE, dU/dT, (mm/DAY)
1
0.8
0.6
0.4
0.2
0
0
50
100
150
200
250
TIME, T (DAY)

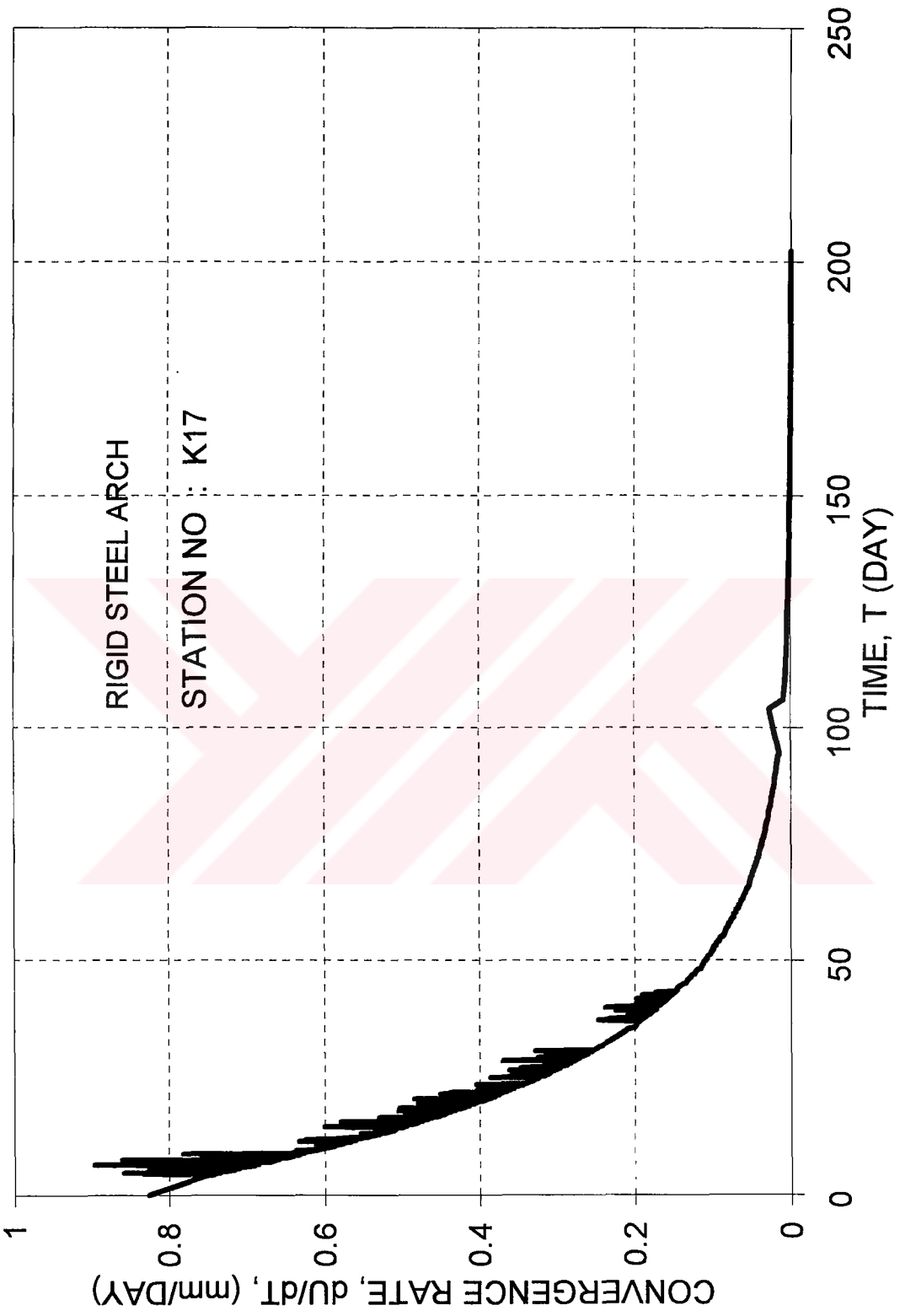
RIGID STEEL ARCH
STATION NO : K17
CONVERGENCE RATE, dU/dT, (mm/DAY)
TIME, T (DAY)
0
0.2
0.4
0.6
0.8
1
0
50
100
150
200
250

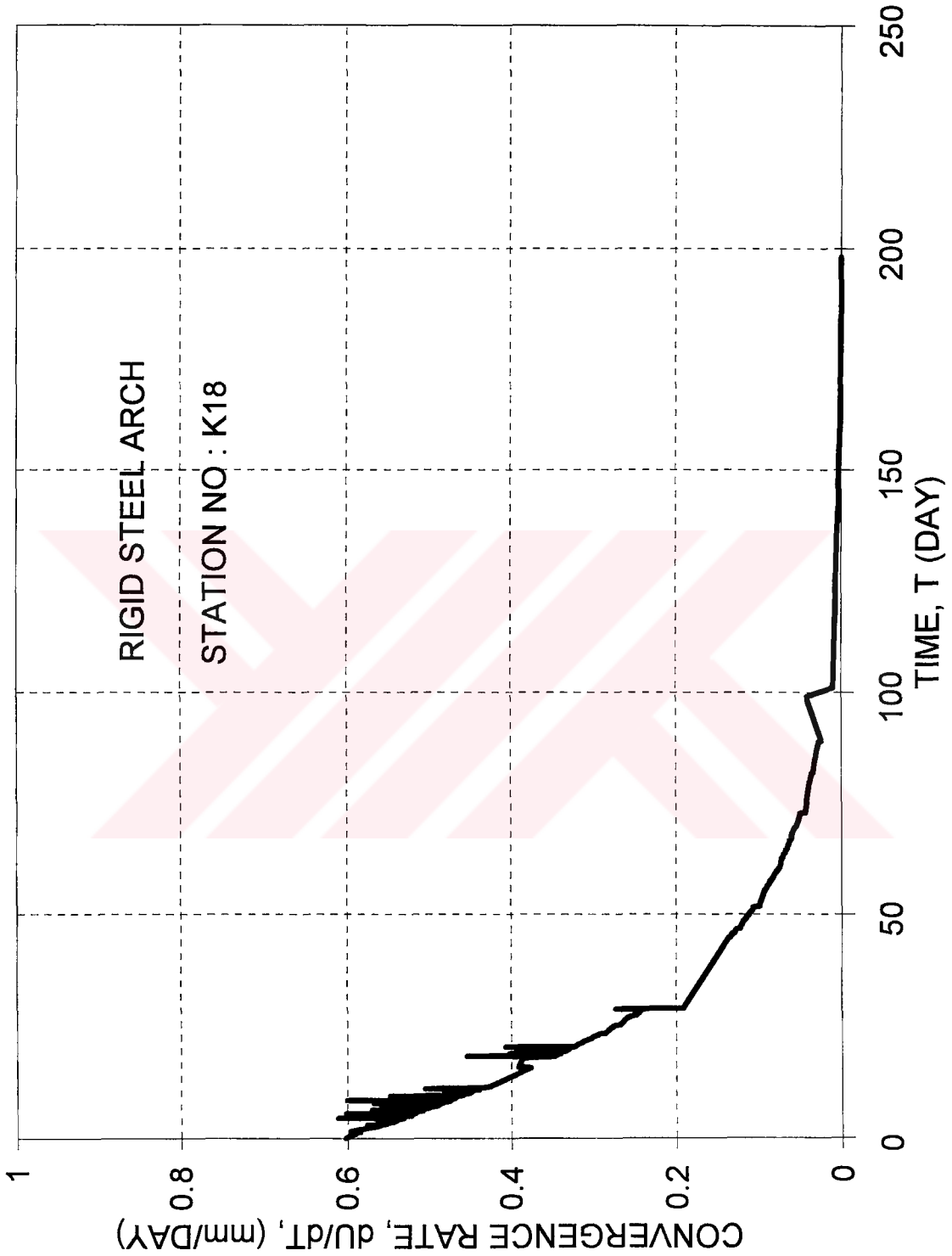
RIGID STEEL ARCH
STATION NO : K18
CONVERGENCE RATE, dU/dT, (mm/DAY)
TIME, T (DAY)
0
0.2
0.4
0.6
0.8
1
0
50
100
150
200
250

APPENDIX F

CONVERGENCE-ACCELERATION CURVES FOR DIFFERENT SUPPORTED REGIONS

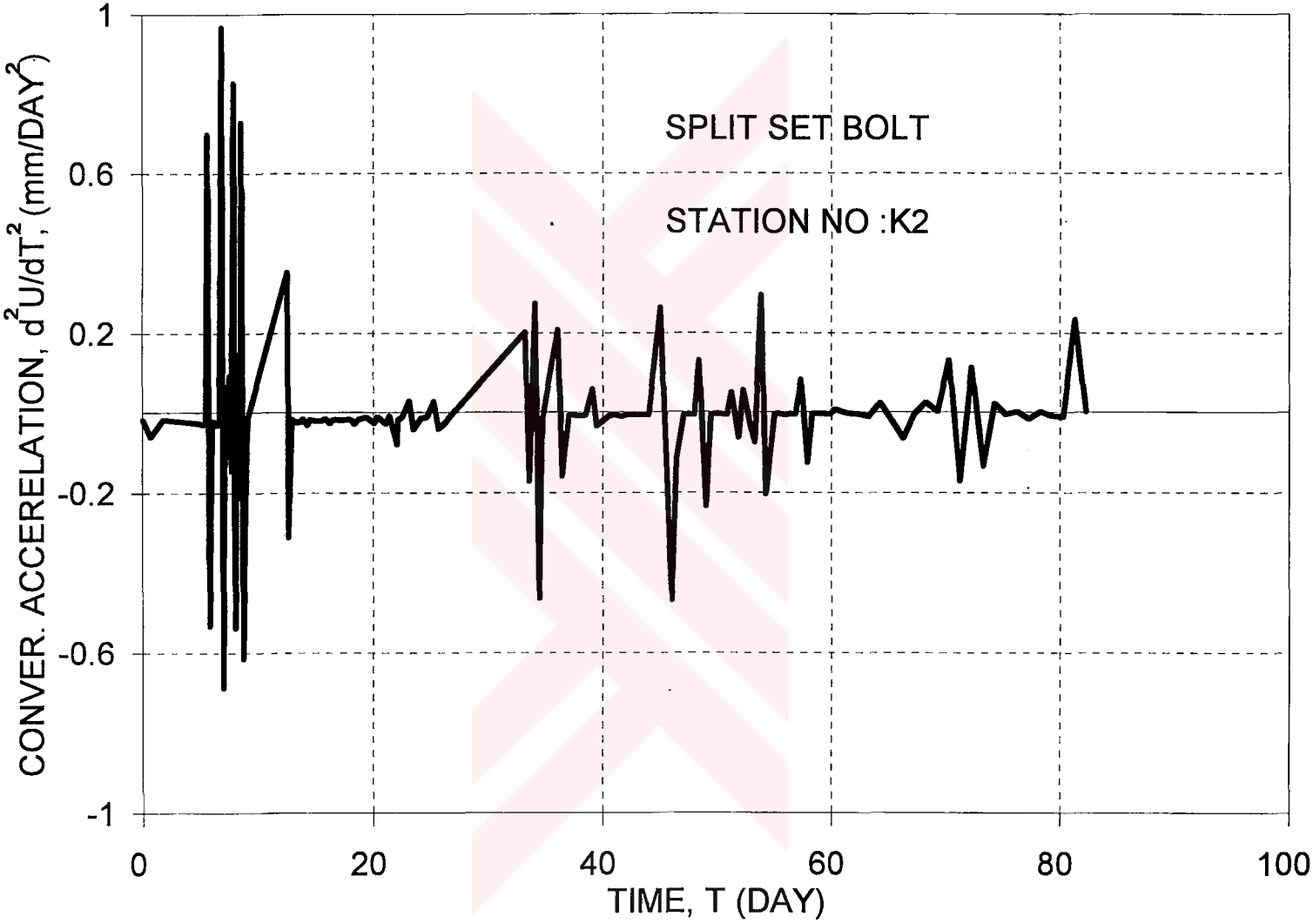
SPLIT SET BOLT
STATION NO :K2
CONVER. ACCERELATION, d²U/dT², (mm/DAY²)
1
0.6
0.2
-0.2
-0.6
-1
0
20
40
60
80
100
TIME, T (DAY)

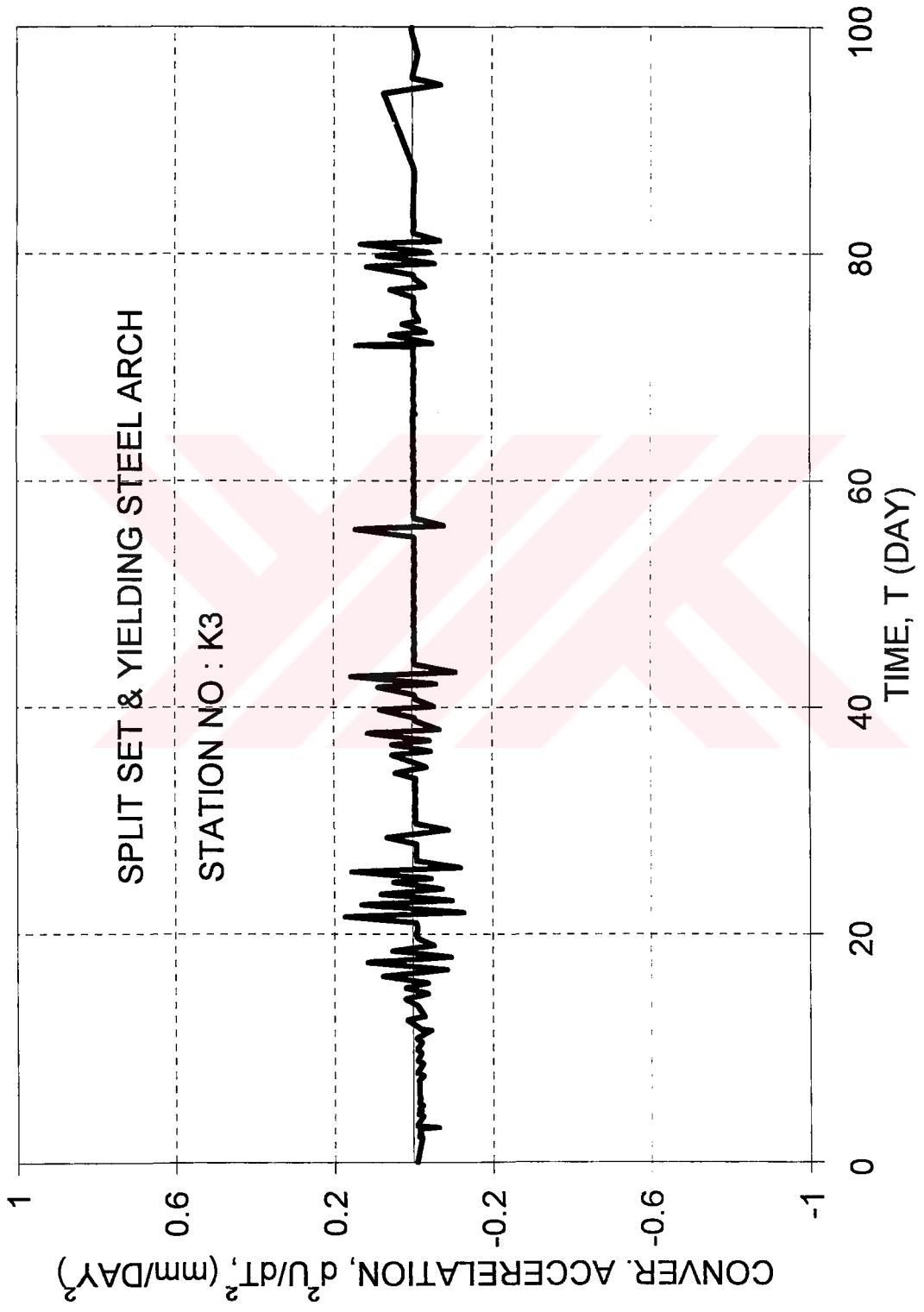
SPLIT SET & YIELDING STEEL ARCH
STATION NO : K3
CONVER. ACCERELATION, d²U/dT², (mm/DAY²)
1
0.6
0.2
-0.2
-0.6
-1
0
20
40
60
80
100
TIME, T (DAY)

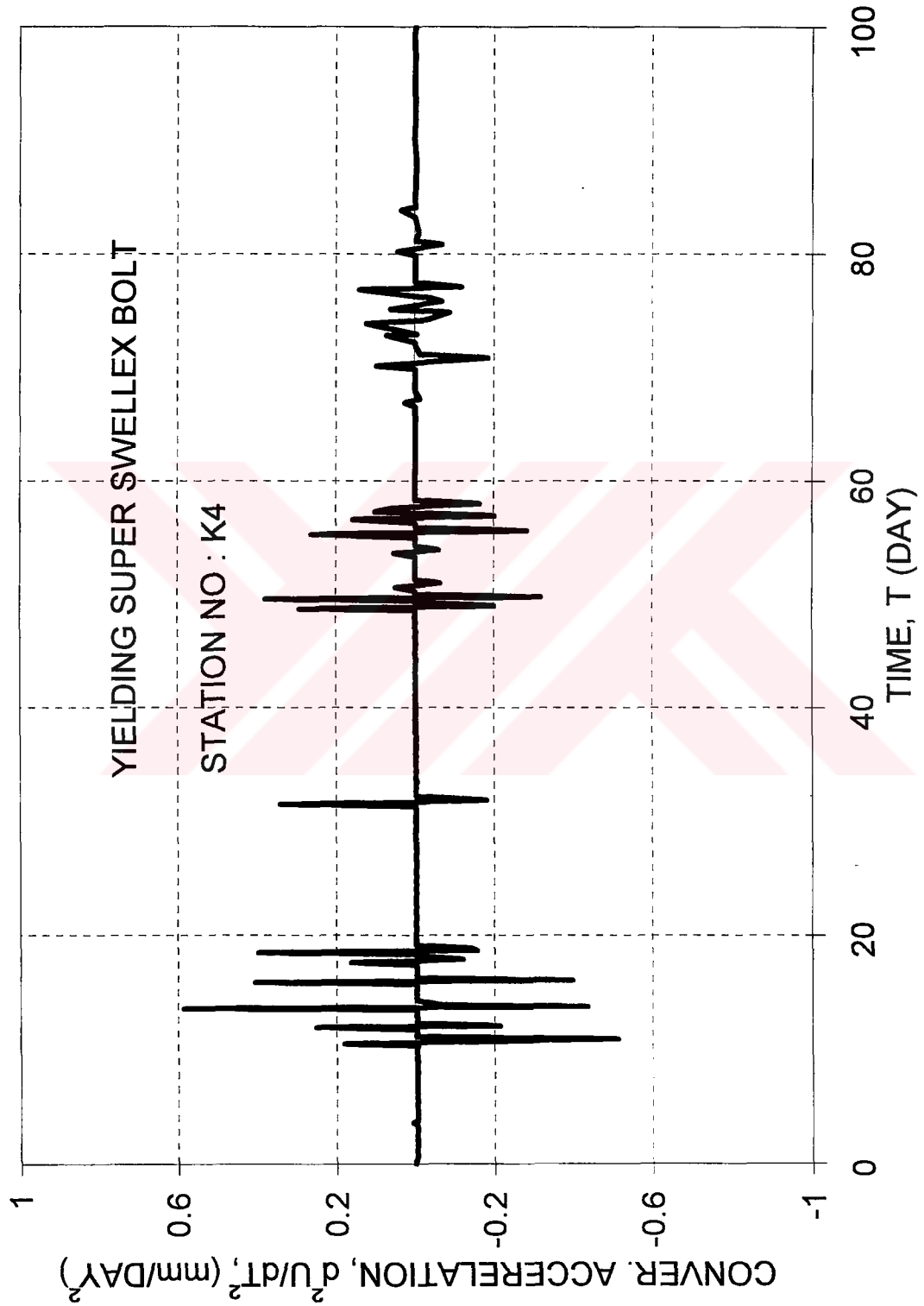
YIELDING SUPER SWELLEX BOLT
STATION NO : K4
CONVER. ACCERELATION, d²U/dT², (mm/DAY²)
TIME, T (DAY)
1
0.6
0.2
-0.2
-0.6
-1
0
20
40
60
80
100

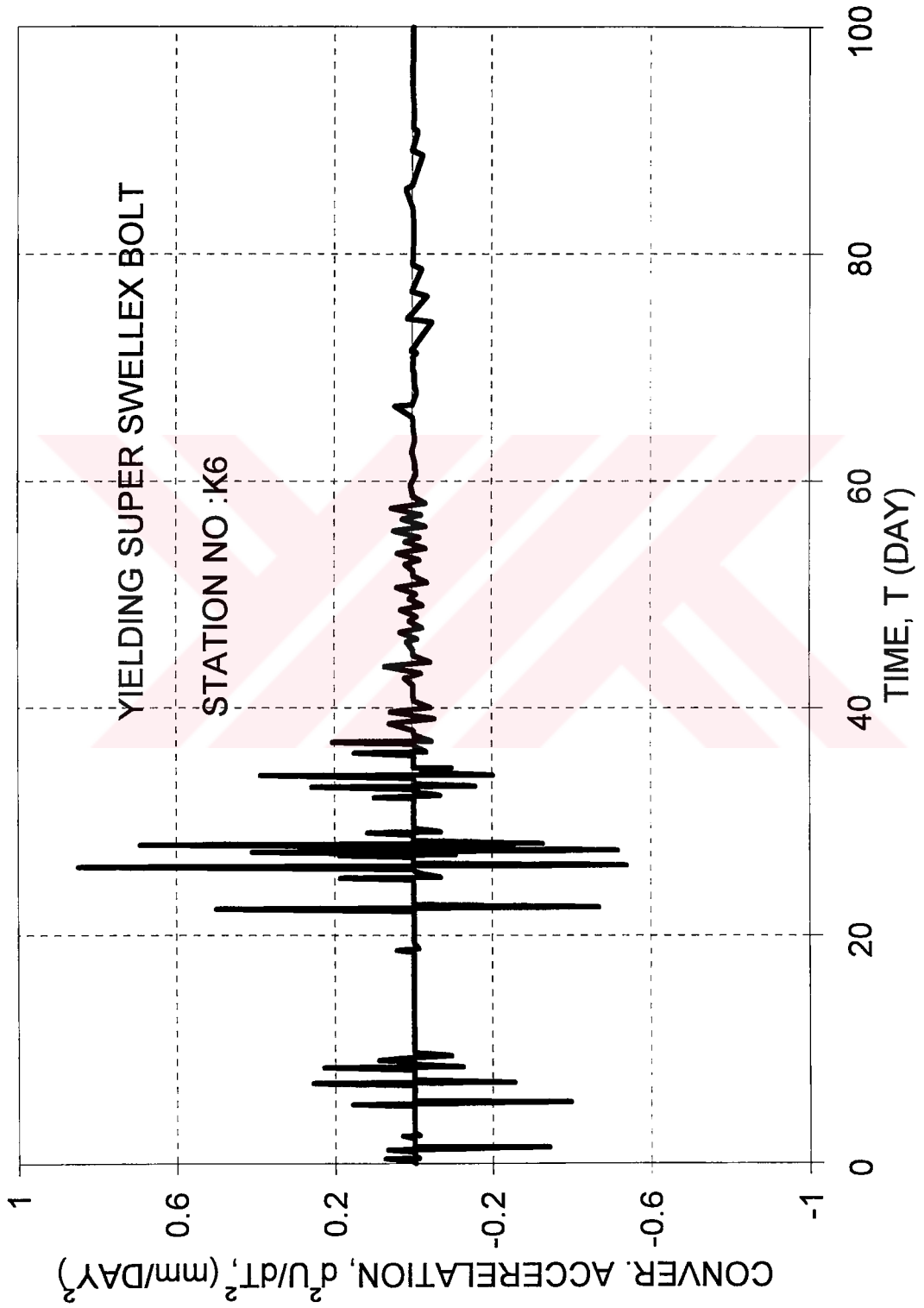
YIELDING SUPER SWELLEX BOLT
STATION NO :K6
CONVER. ACCERELATION, d²U/dT², (mm/DAY²)
1
0.6
0.2
-0.2
-0.6
-1
0
20
40
60
80
100
TIME, T (DAY)

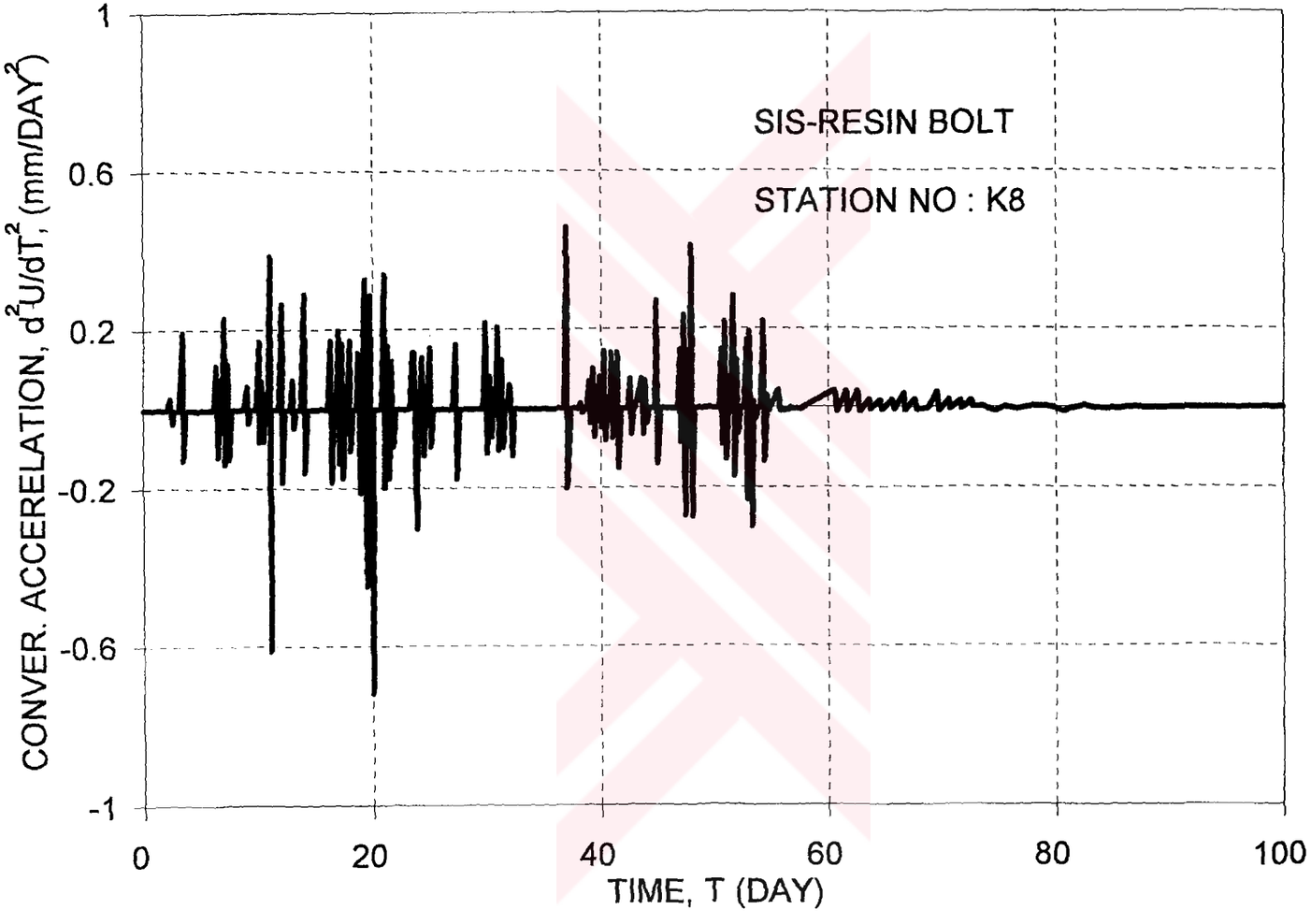
SIS-RESIN BOLT
STATION NO : K8
CONVER. ACCERELATION, d²U/dT², (mm/DAY²)
1
0.6
0.2
-0.2
-0.6
-1
0
20
40
60
80
100
TIME, T (DAY)

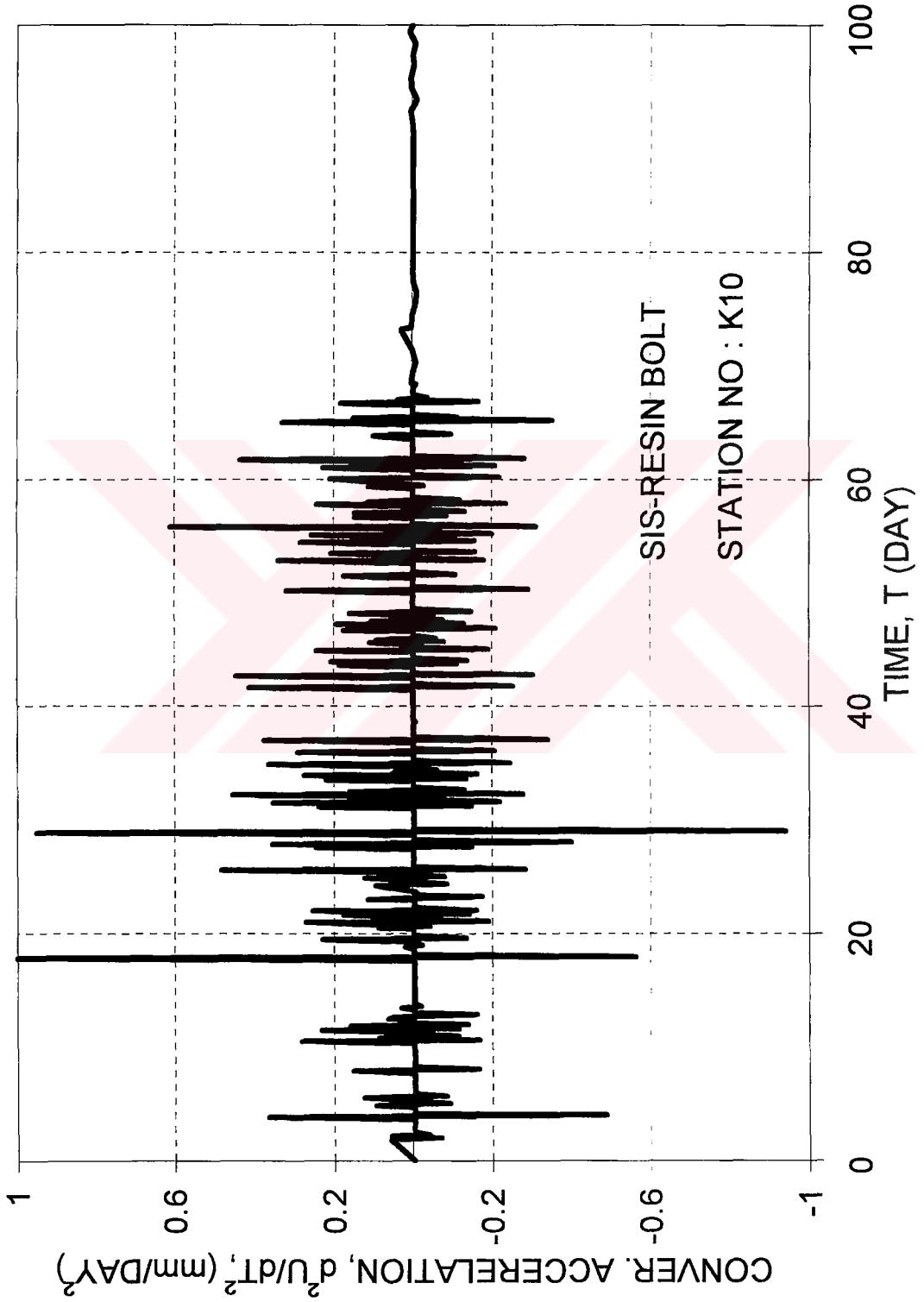
CONVER. ACCERELATION, d²U/dT², (mm/DAY²)
1
0.6
0.2
-0.2
-0.6
-1
0
20
40
60
80
100
TIME, T (DAY)
SIS-RESIN BOLT
STATION NO : K10

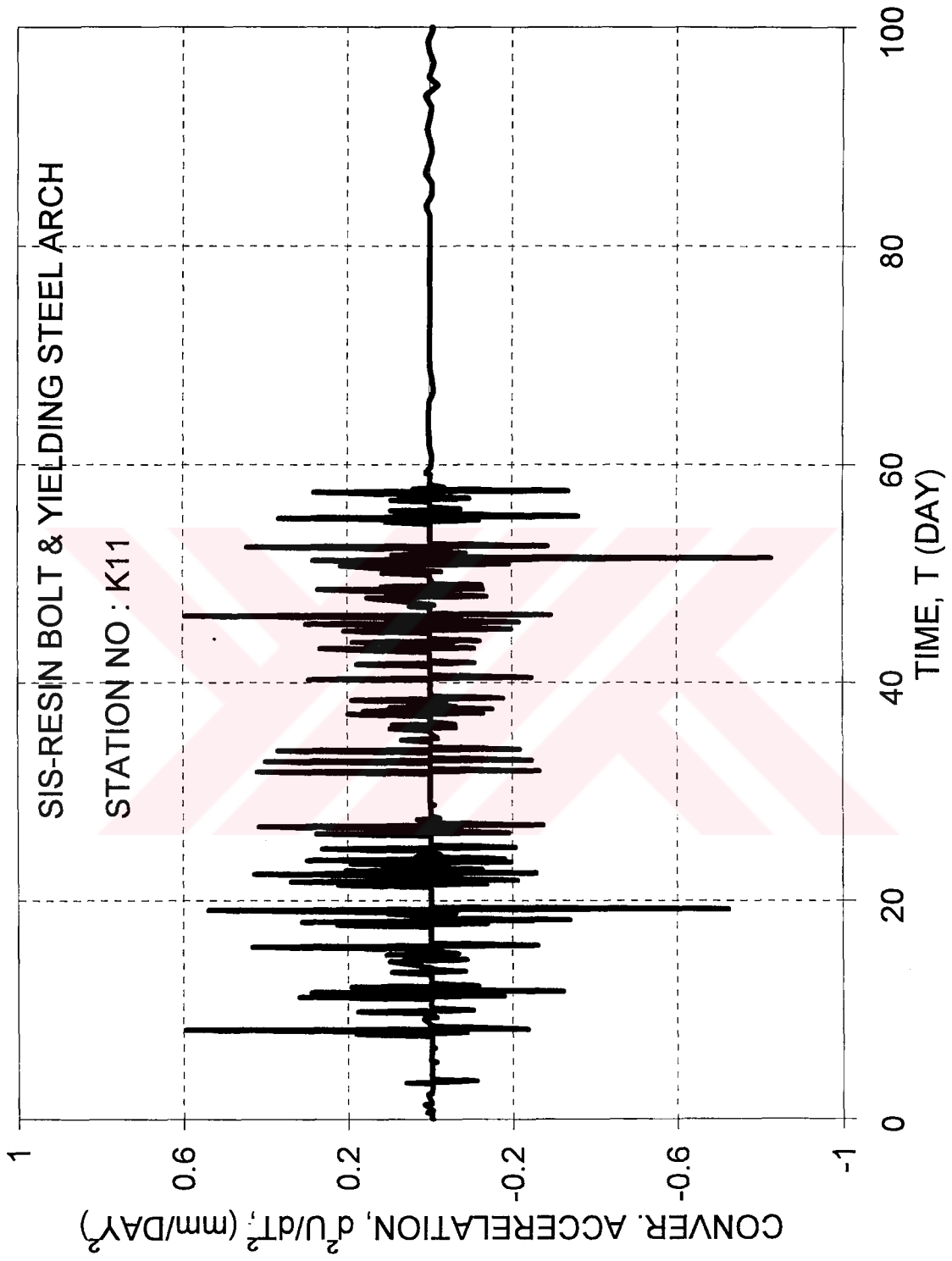
SIS-RESIN BOLT & YIELDING STEEL ARCH
STATION NO : K11
CONVER. ACCERELATION, d²U/dT² (mm/DAY²)
1
0.6
0.2
-0.2
-0.6
-1
0
20
40
60
80
100
TIME, T (DAY)

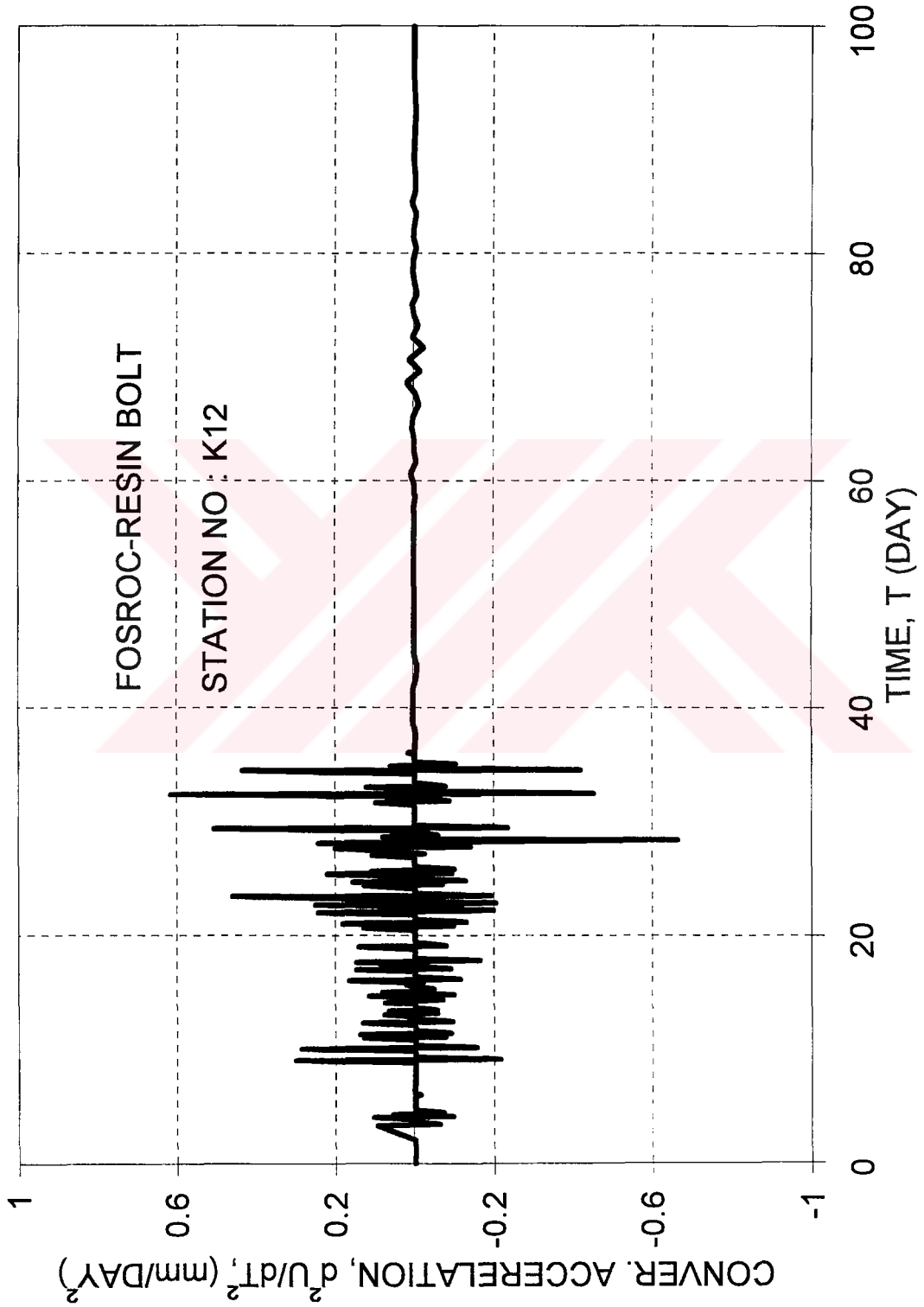
FOSROC-RESIN BOLT
STATION NO : K12
CONVER. ACCERELATION, d²U/dT² (mm/DAY²)
1
0.6
0.2
-0.2
-0.6
-1
0
20
40
60
80
100
TIME, T (DAY)

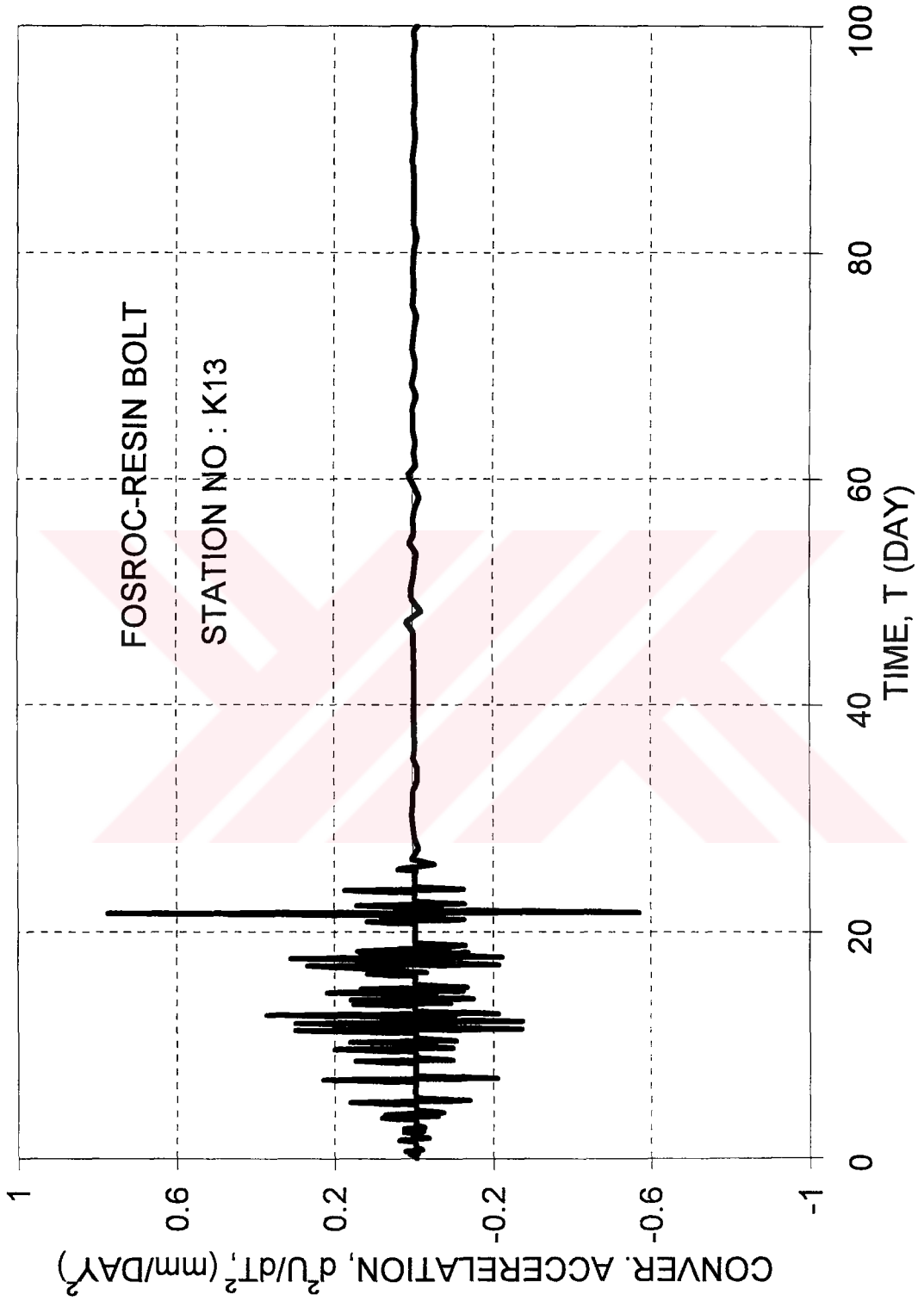
FOSROC-RESIN BOLT
STATION NO : K13
CONVER. ACCERELATION, d²U/dT², (mm/DAY²)
1
0.6
0.2
-0.2
-0.6
-1
0
20
40
60
80
100
TIME, T (DAY)

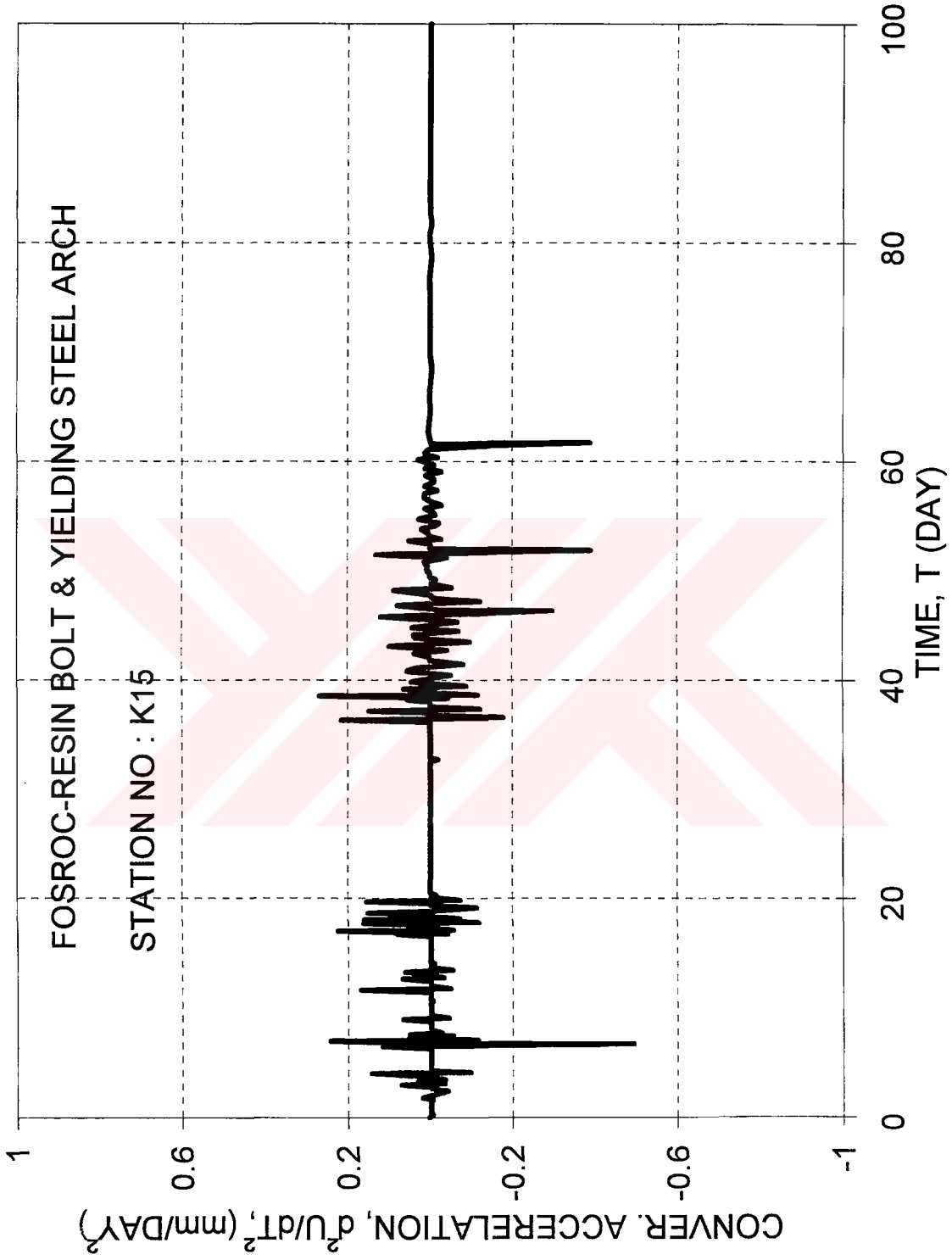
FOSROC-RESIN BOLT & YIELDING STEEL ARCH
STATION NO : K15
CONVER. ACCERELATION, d²U/dT², (mm/DAY²)
TIME, T (DAY)
1
0.6
0.2
-0.2
-0.6
-1
0
20
40
60
80
100

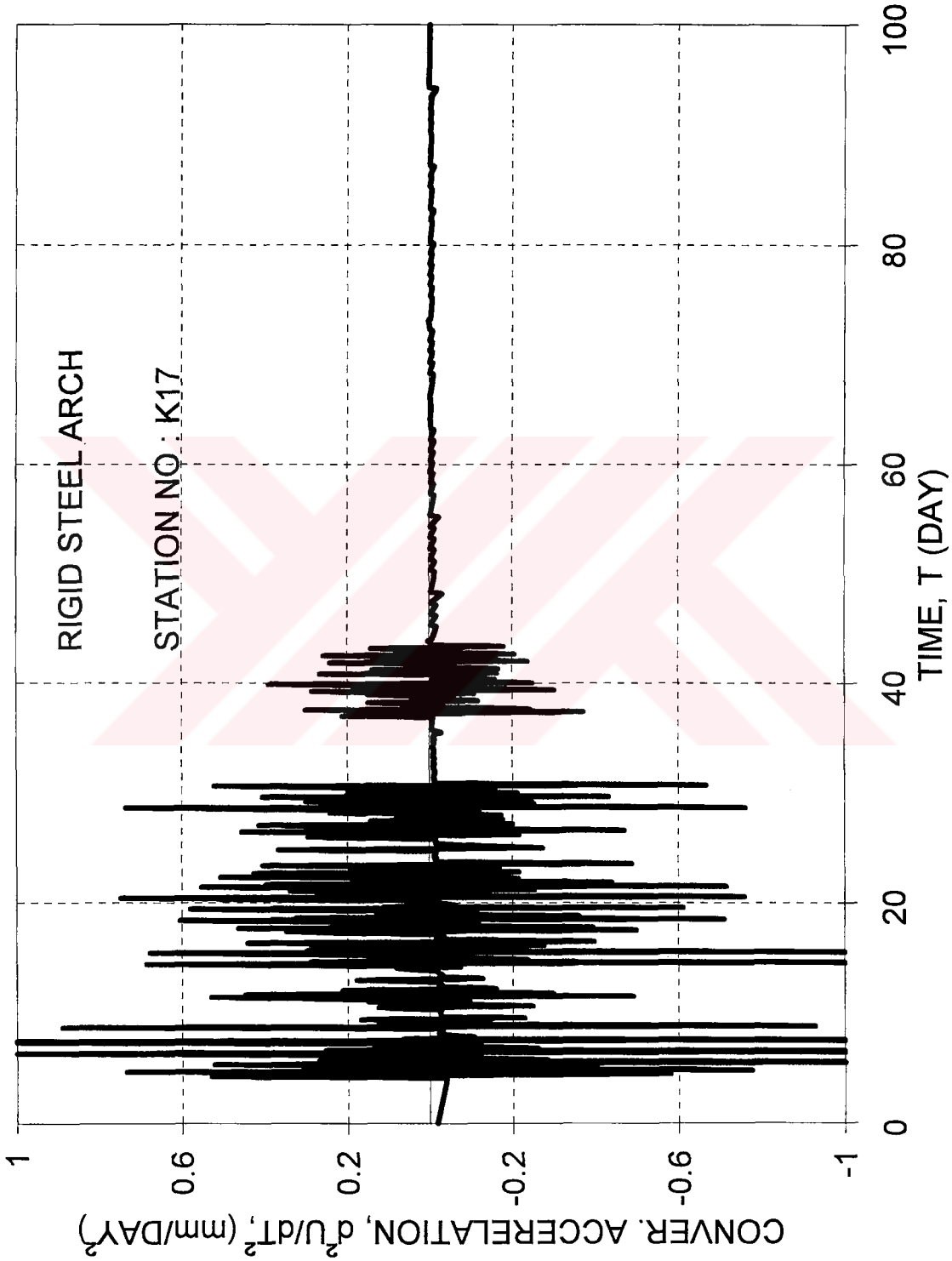
RIGID STEEL ARCH
STATION NO : K17
CONVER. ACCERELATION, d²U/dT², (mm/DAY²)
1
0.6
0.2
-0.2
-0.6
-1
0
20
40
60
80
100
TIME, T (DAY)

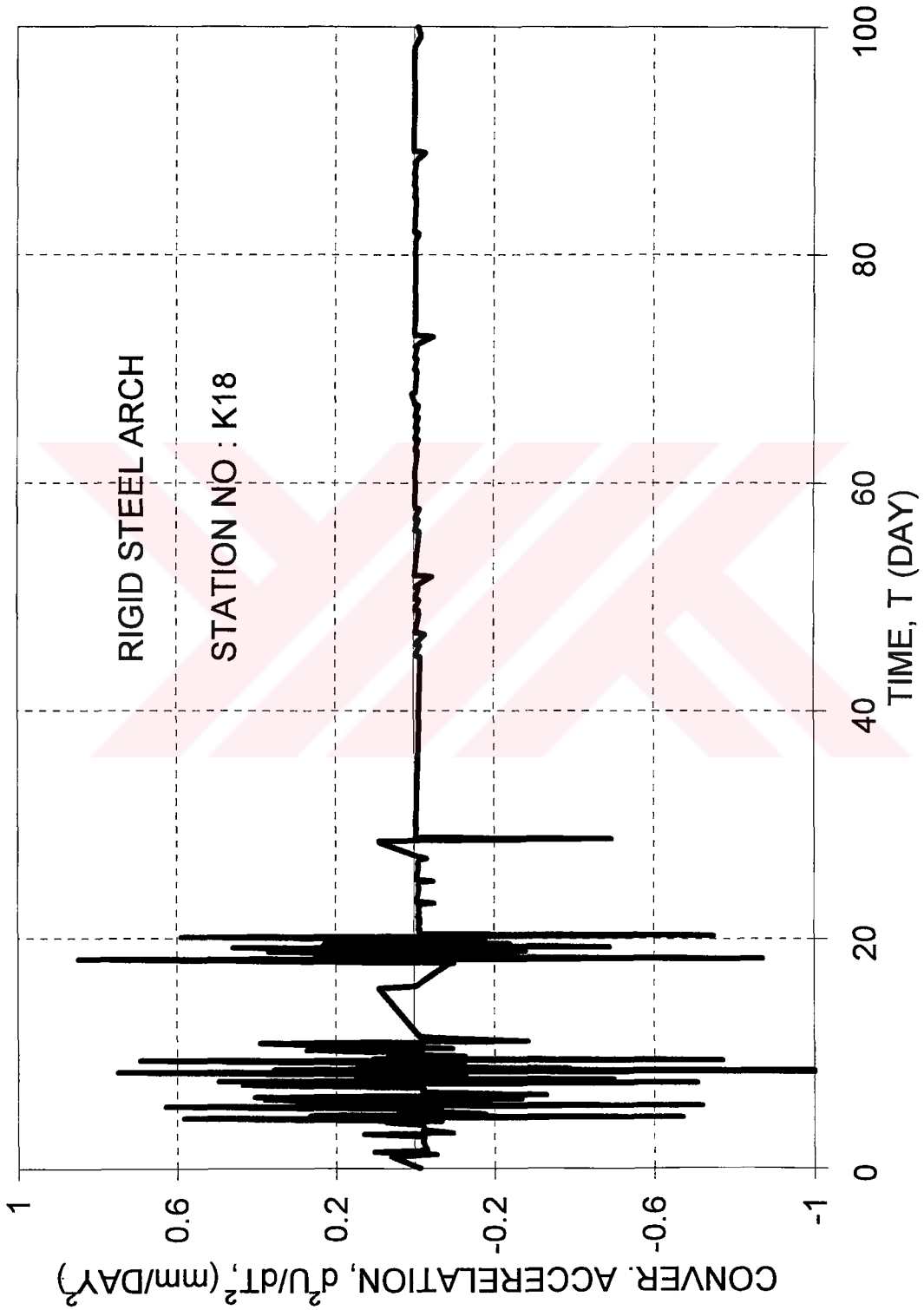
RIGID STEEL ARCH
STATION NO : K18
CONVER. ACCERELATION, d²U/dT², (mm/DAY²)
1
0.6
0.2
-0.2
-0.6
-1
0
20
40
60
80
100
TIME, T (DAY)

VITA

İhsan ÖZKAN was born in Eskişehir in 1963. He graduated from Dokuz Eylül University in 1985 with B.S. degree. He received M.Sc. from the Mining Engineering Department of the Middle East Technical University in 1989.

Currently he has been working as a research assistant in the Mining Engineering Department of Cumhuriyet University in Sivas since 1994.